Optimization of Isopropanol Production by Engineered *Escherichia coli*

DISSERTATION

In Partial Fulfillment of the Requirements

For the Academic Degree of Doctor rerum naturalium (Dr. rer. nat.)

Submitted to the Faculty of Sciences I – Life Sciences

Martin Luther University Halle-Wittenberg

By

Ramona Engelhardt, née Konrad, MSc

Born on January 15, 1982 in Buende, Germany

Halle (Saale) 2020

Examiners:

1. Prof. Dr. Markus Pietzsch, Martin Luther University Halle-Wittenberg
2. Prof. Dr. Bruno Bühler, Martin Luther University Halle-Wittenberg
3. Prof. Dr. Udo Rau, Technical University Braunschweig

Oral Defense: 03.11.2020

Declaration of Academic Honesty

I hereby declare and confirm with my signature that the present doctoral dissertation is solely the result of my own work, based on my research and without using any other resources than the ones indicated. All thoughts taken directly or indirectly from external sources are properly denoted as such.

I further declare that all persons and institutions that have assisted in the preparation of the thesis have been acknowledged and that this thesis has not been submitted, in part or wholly, as an examination document to any other authority.

Halle (Saale), 08.06.2020

(Signature)

Acknowledgement

I would like to express my sincere gratitude to my doctoral advisor Prof. Dr. Markus Pietzsch for his continuous support during my PhD studies, for his guidance, motivation and immense knowledge. Thank you for being a great teacher in every aspect of research.

I would particularly like to thank the Federal Ministry of Education and Research (*Bundesministerium für Bildung und Forschung*, BMBF) for the financial support and funding of the Leading-Edge Cluster "BioEconomy" and the Cluster project "TG 2 – Chemistry, VP 2.5, Energy-efficient synthesis of olefins from their corresponding alcohols".

I greatly appreciate the fruitful collaboration and constructive meetings with the project cooperation partners: Linde Engineering Dresden GmbH, CRI Catalyst Leuna GmbH, University of Leipzig (Institute of Technical Chemistry) and Fraunhofer Society (*Fraunhofer-Gesellschaft zur Förderung der angewandten Forschung e.V.*) - Center for Chemical-Biotechnological Processes (CBP) - Institute for Interfacial Engineering and Biotechnology (IGB) - Institute for Chemical Technology (ICT).

I am indebted to the Fraunhofer CBP for provision and analysis of the beech wood hydrolysate (BWH). I had the pleasure of meeting and working with many great Fraunhofer people: Dr. Daniela Pufky-Heinrich, Gerd Unkelbach, Tino Elter, Dr.-Ing. Katja Patzsch, Sandra Torkler, Anita May, Anja Hauffe, Holger Becker. Thank you also for giving me the opportunity to participate in the 35 L bioreactor scale cultivations of one of my isopropanol-producing strains.

I am very grateful to the examiners of my dissertation: Prof. Dr. Markus Pietzsch, Prof. Dr. Bruno Bühler and Prof. Dr. Udo Rau. Special thanks to the people who read parts of my thesis before submission and who provided me with valuable feedback: Anne Kind, Dr. Christian Marx and especially Dr. Bodo Moritz.

Profound thanks to Martina Anwand who taught me almost everything I know about bioreactor cultivation. Thank you for your advice and your friendship. I also thank Dr. Norbert Volk for his support in bioreactor cultivation planning. I would like to acknowledge the technical assistance of Martina Schreiber and Bal Mukund Sharma. Many thanks to Dr. Angelika Schierhorn who performed the peptide mass fingerprint analyses. I also wish to thank my former master students Joyshree Ganguly and Benjamin Schrank (now Böhme) for their dedicated work.

I cannot begin to express my thanks to my co-workers of the Department of Downstream Processing (*AG Aufarbeitung biotechnischer Produkte*). Thank you, not only for helpful advice, practical suggestions and insightful discussions, but also for making the lab my "second home".

I would like to thank my family and friends for their unwavering support and patience. I owe my deepest gratitude to my parents Gabi and Erwin Konrad for their love and encouragement. Thanks to my friend Carsten Struessmann for believing in me from the beginning. Heartfelt thanks to my husband Matthias Engelhardt. Thank you for your love, help, and your priceless computer tools. Special thanks to my cat Julie who was always by my side, while I was writing this thesis. Last, but not least, I would like to thank my daughter Isabelle Aurélie for being the light of my life.

The scientific man does not aim at an immediate result.

He does not expect that his advanced ideas will be readily taken up.

His work is like that of the planter - for the future.

His duty is to lay the foundation for those who are to come, and point the way.

He lives and labors and hopes.

Nikola Tesla

The Problem of Increasing Human Energy - (The Century Magazine, June 1900)

~

This thesis is dedicated to my parents.

~

In loving memory of my grandmother Alma and my grandfather Edmund.

Table of Contents

Declaration of Academic Honesty **2**
Acknowledgement **3**
Table of Contents **5**
List of Abbreviations **8**
List of Figures **12**
List of Tables **15**
1 Introduction **18**
2 State of the Art **21**
2.1 Isopropanol - Basic Facts **21**
2.2 Isopropanol Production by Chemical Processes **22**
2.3 Isopropanol Production by Microorganisms **22**
2.3.1 Natural Isopropanol Producers 22
2.3.2 Recombinant Isopropanol Producers 25
2.3.3 Enzymes of the Isopropanol Pathway 29
2.4 Lignocellulose Hydrolysates as Feedstock for Microorganisms **31**
3 Aims and Objectives **36**
4 Material and Methods **37**
4.1 Material **37**
4.1.1 Chemicals 37
4.1.2 Buffers and Solutions 39
4.1.3 Lignocellulose Hydrolysate 40
4.1.4 Bacterial Strains 41
4.1.5 Bacterial Growth Media, Antibiotics and Supplements 41
4.1.6 Plasmid DNA 42
4.1.7 Primer Oligonucleotides 43
4.1.8 Enzymes and Molecular Biology Reagents 44
4.1.9 Antibodies 45
4.1.10 Markers 45
4.1.11 Kits 46
4.1.12 Instruments, Devices, Laboratory Equipment and Consumables 46
4.1.13 Computer Programs and Online Tools 49
4.2 Methods **49**
4.2.1 Microbiological Methods 49
4.2.1.1 Cultivation of Bacterial Cells in Shake Flask Scale 49
4.2.1.2 Cultivation of Bacterial Cells in Bioreactor Scale 50
4.2.1.3 Adaptation of *Escherichia coli* to Minimal Medium 51

4.2.1.4 Long-term Storage of Bacteria (Preparation of Glycerol Stocks) ... 52
4.2.2 Molecular Biology Techniques ... 52
4.2.2.1 Agarose Gel Electrophoresis (AGE) ... 52
4.2.2.2 Purification of PCR Products ... 52
4.2.2.3 Preparation of Chemically Competent Cells ... 52
4.2.2.4 Transformation by Chemical Reagents ... 53
4.2.2.5 Plasmid Amplification and Isolation ... 53
4.2.2.6 Determination of DNA Concentration ... 53
4.2.2.7 Sequencing of Plasmid DNA ... 54
4.2.2.8 Metabolic Engineering by Red®/ET® Recombination ... 54
4.2.3 Analytical Methods ... 59
4.2.3.1 Determination of Cell Concentration ... 59
4.2.3.2 Soluble-Insoluble Partitioning of Proteins ... 60
4.2.3.3 Sodium Dodecyl Sulfate Polyacrylamide Gel Electrophoresis (SDS-PAGE) ... 60
4.2.3.4 Western Blot Analysis ... 61
4.2.3.5 Quantification of Glucose by YSI ... 61
4.2.3.6 Quantification of Acetate and Lactate by Enzymatic Test Kits ... 61
4.2.3.7 Quantification of Isopropanol, Acetone and Ethanol by Gas Chromatography ... 62
4.2.3.8 Quantification of O_2 Consumption, CO_2 Generation and Respiratory Quotient ... 64
4.2.3.9 Peptide Mass Fingerprint Analysis by MALDI-TOF/TOF Mass Spectrometry ... 65
4.2.4 Calculations and Equations ... 66
4.2.4.1 Lambert-Beer Law in Spectrophotometry ... 66
4.2.4.2 Gas Chromatography Calibration ... 66
4.2.4.3 Parameters for Evaluation of Bacterial Cultivations and Product Formation ... 66

5 Results ... 70

5.1 Construction of Isopropanol-Producing *E. coli* Strains ... 70
5.1.1 The Production Host ... 70
5.1.2 The Expression Vector and Isopropanol Pathway Genes ... 71
5.1.3 Engineered *E. coli* Strains for Isopropanol Production ... 75

5.2 Isopropanol Production from Glucose by Engineered *E. coli* in Shake Flask Scale ... 76
5.2.1 The Isopropanol Pathway Plasmid pRK_ISO_1E2e3c4c in *E. coli* DH5α and JM109 ... 77
5.2.2 The Isopropanol Pathway Plasmid pRK_ISO_1C2e3c4c in *E. coli* DH5α and JM109 ... 81

5.3 Isopropanol Production from Beech Wood Hydrolysate by Engineered *E. coli* in Shake Flask Scale ... 86

5.4 Isopropanol Production by Engineered *E. coli* in Bioreactor Scale ... 91
5.4.1 Glucose as Carbon Source for Isopropanol Production in Bioreactor Scale ... 92
5.4.2 Detection of Act Degradation by Mass Spectrometry ... 98
5.4.3 Beech Wood Hydrolysate as Carbon Source for Isopropanol Production in Bioreactor Scale ... 99

5.5 Isopropanol Separation and Recovery by Gasstripping ... 104
5.5.1 Gasstripping with Gas Washing Bottles ... 104
5.5.2 Gasstripping with Condensation Trap and Liquid Nitrogen ... 107

5.6 Optimization of Isopropanol Production by Minimization of Acetate Production ... 109

5.6.1 Knockout of Phosphotransacetylase in *E. coli* and Verification of Gene Disruption 109
5.6.2 Influence of Phosphotransacetylase Knockout on Isopropanol Production by Engineered *E. coli* in Bioreactor Scale 112
6 Discussion 119
6.1 Comparison of Isopropanol-Producing *E. coli* Strains in Shake Flask Scale 119
6.2 Beech Wood Hydrolysate as Carbon Source for Isopropanol-Producing *E. coli* in Shake Flask Scale 128
6.3 Isopropanol Production from Glucose and Beech Wood Hydrolysate by Engineered *E. coli* in Bioreactor Scale 132
6.4 *In Situ* Product Separation and Recovery by Gasstripping 141
6.5 Optimization of Isopropanol Production by Minimization of Acetate Production via Phosphotransacetylase Knockout in *E. coli* 144
6.6 Thermodynamic and Kinetic Considerations on Isopropanol Production by Engineered *E. coli* 151
7 Summary 154
8 Outlook 156
References 159
A Appendix 176
A.1 DNA Sequences and Plasmid Maps 176
A.2 Amino Acid Sequences and Enzyme Parameters 187
A.3 Additional Result Figures 192
Curriculum Vitae 196

List of Abbreviations

Table: List of abbreviations.
Abbreviations are listed in alphabetical order. Numbers and special characters are listed first. Abbreviations of genes are denoted with a small first letter, while the respective enzymes are indicated with a capital first letter. Parameters for evaluation of bacterial cultivations are not listed, but can be found in Table 4-27 on page 67.

Abbreviation	Meaning
3D	Three-dimensional
6PGDH	6-phosphogluconate dehydrogenase
$\Delta_rG'°$	Standard transformed Gibbs energy of a reaction
A	Absorbance
aa	Amino acid(s)
ABE	Acetone-butanol-ethanol
Acc	Acetyl-CoA carboxylase (*S. elongatus* PCC 7942)
Acct	Acetate CoA-transferase
Acetyl-CoA	Acetyl-Coenzyme A
Ack	Acetate kinase
acs	Acetyl-CoA synthetase gene
Acs	Acetyl-CoA synthetase
Act	Acetyl-CoA acetyltransferase
adc	Acetoacetate decarboxylase gene
Adc	Acetoacetate decarboxylase
adh	Alcohol dehydrogenase (secondary) gene
ADP	Adenosine diphosphate
AGE	Agarose gel electrophoresis
a.k.a.	Also known as
APS	Ammonium persulfate
AS	GenBank® accession number
ATCC	American Type Culture Collection
atoB	Acetyl-CoA acetyltransferase gene (*E. coli*)
atoDA	Acetate CoA-transferase genes (*E. coli*)
ATP	Adenosine triphosphate
AUC	Area under the curve
bar	Unit of pressure (100 kPa)
BCIP	5-bromo-4-chloro-3-indolyl phosphate
BMBF	*Bundesministerium für Bildung und Forschung* (Federal Ministry of Education and Research)
bp	Base pair(s)
BRENDA	Braunschweig Enzyme Database
BSA	Bovine serum albumin
BWH	Beech wood hydrolysate (glucose fraction)
Cas9	CRISPR-associated (protein)
CBP	Fraunhofer Center for Chemical-Biotechnological Processes
CCR	Carbon catabolite repression
CO	CO_2 production

Abbreviation	Meaning
CoA (or CoASH)	Coenzyme A (reduced)
CPR	Carbon dioxide production rate
CREATE	CRISPR EnAbled Trackable genome Engineering
CRISPR	Clustered Regularly Interspaced Short Palindromic Repeats
CS	Citrate synthase
CT	Condensation trap
ctfAB	Acetate CoA-transferase genes (*C. acetobutylicum*)
dATP	Deoxyadenosine triphosphate
dCTP	Deoxycytidine triphosphate
ddH_2O	Double-distilled water
dGTP	Deoxyguanosine triphosphate
dH_2O	Deionized water
D-LDH	D-lactate dehydrogenase
DMSO	Dimethyl sulfoxide
DNA	Deoxyribonucleic acid
dNTP	Deoxynucleotide triphosphate(s)
DSBR	Double-stranded break repair
dsDNA	Double-stranded deoxyribonucleic acid
DSM	DSMZ accession number
DSMZ	*Deutsche Sammlung von Mikroorganismen und Zellkulturen* (German Collection of Microorganisms and Cell Cultures)
dTTP	Deoxythymidine triphosphate
EC	Enzyme Commission
EDTA	Ethylenediamine tetraacetic acid
EMBL-EBI	European Bioinformatics Institute
Fed_{ox}	Ferredoxin (oxidized)
Fed_{red}	Ferredoxin (reduced)
FID	Flame ionization detector
FLP(e)	Flippase recombinase
FRT	FLP recombinase target
G6PDH	Glucose-6-phosphate dehydrogenase
G°	Gibbs free energy
GC	Gas chromatography
GHG	Greenhouse gas
GOx	Glucose oxidase
GPT	Glutamate-pyruvate transaminase
GRAVY	Grand average of hydropathicity
GST	Glutathione S-transferase
GWB	Gas washing bottle(s)
HCl	Hydrochloric acid
HF	High-Fidelity
HMF	5-(Hydroxymethyl)furfural
HPLC	High performance liquid chromatography
IB	Inclusion bodies (insoluble fraction)
IBE	Isopropanol-butanol-ethanol
Icl	Isocitrate lyase
ID	UniProt accession number
Idh	Alcohol dehydrogenase (secondary)

Abbreviation	Meaning
IDH	Isocitrate dehydrogenase
IEA	International Energy Agency
IPK	*Leibniz-Institut für Pflanzengenetik und Kulturpflanzenforschung* (Leibniz Institute of Plant Genetics and Crop Plant Research)
IPTG	Isopropyl β-D-1-thiogalactopyranoside
IRENA	International Renewable Energy Agency
IUPAC	International Union of Pure and Applied Chemistry
k	Mass transfer coefficient
K_c'	Apparent equilibrium constant (concentration-based)
k_{cat}	Turnover number
k_{cat}/K_M	Catalytic efficiency
K_M	Michaelis constant
lacI	Lac repressor gene
LacI	Lac repressor
LB	Lysogeny broth
L-LDH	L-lactate dehydrogenase
L-MDH	L-malate dehydrogenase
M	Marker
MALDI	Matrix-Assisted Laser Desorption/Ionization
MalS	Malate synthase
MFA	Metabolic flux analysis
MM	Minimal medium
mRNA	Messenger ribonucleic acid
MS	Mass spectrometry
MW	Molecular mass
NAD^+	Nicotinamide adenine dinucleotide (oxidized)
NADH	Nicotinamide adenine dinucleotide (reduced)
$NADP^+$	Nicotinamide adenine dinucleotide phosphate (oxidized)
NADPH	Nicotinamide adenine dinucleotide phosphate (reduced)
NBT	Nitroblue tetrazolium
NCM	Nitrocellulose membrane
n.d.	Not determined
n.m.	Not measurable
NphT7	Acetoacetyl-CoA synthase (*Streptomyces* sp. strain CL190)
n.s.	Not stated
nt	Non-transformed
OC	O_2 consumption
OD	Optical density
OPEC	Organization of the Petroleum Exporting Countries
ori	Origin of replication
OTR	Oxygen transfer rate
OUR	Oxygen uptake rate
p	Vapor pressure
PA	Polyacrylamide
PCR	Polymerase chain reaction
Pdh	Pyruvate dehydrogenase
Pfl	Pyruvate formate lyase
pH	Potential of hydrogen

Abbreviation	Meaning
PHB	Poly-3-hydroxybutyrate
phbA	Acetyl-CoA acetyltransferase gene (*C. necator*)
P_i	Phosphate (inorganic)
pI	Isoelectric point
pK_a	$-\log_{10}$ of the acid dissociation constant (K_a)
PMF	Peptide mass fingerprint analysis
PntAB	Transhydrogenase (*E. coli*)
pO_2	Oxygen partial pressure
poxB	Pyruvate oxidase gene
PoxB	Pyruvate oxidase
Pt	Platinum electrode
pta	Phosphotransacetylase gene (*E. coli*)
Pta	Phosphotransacetylase
PTS	Phosphotransferase system
R^2	Coefficient of determination
RBS (or rbs)	Ribosome binding site
RNA	Ribonucleic acid
rpm	Revolutions per minute
RQ	Respiratory quotient
RRF	Relative response factor
S	Soluble fraction
SDS	Sodium dodecyl sulfate
SDS-PAGE	Sodium dodecyl sulfate polyacrylamide gel electrophoresis
SUMO	Small ubiquitin-like modifier
t	Time
TAE	Tris-acetate-EDTA
TBS	Tris-buffered saline
TBS-TT	Tris-buffered saline with Tween® 20 and Triton X® 100
TCA	Tricarboxylic acid
TEMED	Tetramethylethylenediamine
TES	Trace element solution
thlA (or thl)	Acetyl-CoA acetyltransferase (thiolase) gene (*C. acetobutylicum*)
T_M	Oligonucleotide melting temperature
TOF	Time of Flight
TRIS (or Tris)	Tris(hydroxymethyl)aminomethane
tRNA	Transfer ribonucleic acid
TRX	Thioredoxin
U	Enzyme units (µmol min^{-1})
UNFCCC	United Nations Framework Convention on Climate Change
UV	Ultraviolet
VIS	Visible light
V_{max}	Maximum velocity
vs.	Versus
vvm	Vessel volumes per minute (aeration rate)
WB	Western Blot
YSI	Yellow Springs Instrument

List of Figures

Figure 1-1: Production cascade of the BioEconomy Cluster project "TG 2 – Chemistry, VP 2.5, Energy-efficient synthesis of olefins from their corresponding alcohols" 20
Figure 2-1: Structural formula of isopropanol. 21
Figure 2-2: Dehydration reaction of isopropanol to propene. 22
Figure 2-3: Hydration of propene to isopropanol. 22
Figure 2-4: Hydrogenation of acetone to isopropanol. 22
Figure 2-5: Schematic solvent production in *C. beijerinckii*. 23
Figure 2-6: Enzymatic reaction catalyzed by the acetyl-CoA acetyltransferase (Act) – EC 2.3.1.9. 29
Figure 2-7: Enzymatic reaction catalyzed by the acetate CoA-transferase (Acct) - EC 2.8.3.8. 30
Figure 2-8: Enzymatic reaction catalyzed by the acetoacetate decarboxylase (Adc) - EC 4.1.1.4. 30
Figure 2-9: Enzymatic reaction catalyzed by the isopropanol dehydrogenase (Idh) - EC 1.1.1.80. 31
Figure 2-10: Schematic presentation of plant cell wall structure and microfibril cross-section. 32
Figure 4-1: Mechanism of Red®/ET® recombination. 55
Figure 4-2: Experimental scheme for targeted disruption of genes in the *E. coli* genome by Red®/ET® recombination. 56
Figure 4-3: RRF calibration curves of isopropanol, acetone and ethanol. 64
Figure 5-1: Schematic presentation of the expression construct for isopropanol production in *E. coli*. 74
Figure 5-2: Influence of induction temperature on growth and isopropanol, acetate and lactate production of *E. coli* DH5α_1E and *E. coli* JM109_1E. 77
Figure 5-3: Influence of induction temperature on production of Act-StrepII (1E) in *E. coli* DH5α_1E (A, B) and *E. coli* JM109_1E (C, D). 79
Figure 5-4: Influence of induction temperature on production of Acct-His_{10} (2e), Adc-FLAG (3c) & Idh-c-Myc (4c) in *E. coli* DH5α_1E (A, B) and *E. coli* JM109_1E (C, D). 80
Figure 5-5: Influence of induction temperature on growth and isopropanol production of *E. coli* DH5α_1C and *E. coli* JM109_1C. 81
Figure 5-6: Influence of induction temperature on acetone, ethanol, acetate and lactate production of *E. coli* DH5α_1C and *E. coli* JM109_1C. 83
Figure 5-7: Influence of induction temperature on production of Act-StrepII (1C) in *E. coli* DH5α_1C (A) and *E. coli* JM109_1C (B). 84
Figure 5-8: Influence of induction temperature on production of Acct-His_{10} (2e), Adc-FLAG (3c) & Idh-c-Myc (4c) in *E. coli* DH5α_1C (A) and *E. coli* JM109_1C (B). 85
Figure 5-9: Comparison of BWH and glucose as carbon source for *E. coli* DH5α_1C in MM. 87
Figure 5-10: Growth, glucose consumption and acetone production using BWH as a carbon source for *E. coli* DH5α_1C in LB. 88
Figure 5-11: Influence of different BWH concentrations on growth of *E. coli* DH5α_1C. 89
Figure 5-12: Influence of different BWH concentrations on isopropanol and acetone production of *E. coli* DH5α_1C. 89
Figure 5-13: Acetate concentration in the cultivation medium of *E. coli* DH5α_1C grown with different BWH concentrations. 90

Figure 5-14: Growth, glucose consumption and product formation of *E. coli* DH5α_1C in LB plus glucose feed in 10 L bioreactor scale. 92
Figure 5-15: Time course of control variables and base addition for *E. coli* DH5α_1C in LB plus glucose feed in 10 L bioreactor scale. 93
Figure 5-16: Production of Act-StrepII (1C) (A), Acct-His_{10} (2e), Adc-FLAG (3c) & Idh-c-Myc (4c) (B) in *E. coli* DH5α_1C in LB plus glucose feed in 10 L bioreactor scale. 94
Figure 5-17: Growth, glucose consumption and product formation of *E. coli* DH5α_1E in LB plus glucose feed in 10 L bioreactor scale. 95
Figure 5-18: Time course of control variables and base addition for *E. coli* DH5α_1E in LB plus glucose feed in 10 L bioreactor scale. 96
Figure 5-19: Production of Act-StrepII (1E) (A) and Idh-c-Myc (4c) (B) in *E. coli* DH5α_1E in LB plus glucose feed in 10 L bioreactor scale. 97
Figure 5-20: Spatial congruencies of detected peptides and amino acid sequences of Act-StrepII (1C) or Act-StrepII (1E). 98
Figure 5-21: Growth, glucose consumption and product formation of *E. coli* DH5α_1E in LB plus 50% BWH/50% glucose feed in 10 L bioreactor scale. 99
Figure 5-22: Production of Acct-His_{10} (2e), Adc-FLAG (3c) & Idh-c-Myc (4c) in *E. coli* DH5α_1E in LB plus 50% BWH/50% glucose feed in 10 L bioreactor scale. 101
Figure 5-23: Growth, glucose consumption and product formation of *E. coli* DH5α_1E in LB plus 100% BWH feed in 10 L bioreactor scale. 102
Figure 5-24: Production of Act-StrepII (1E) (A), Acct-His_{10} (2e), Adc-FLAG (3c) & Idh-c-Myc (4c) (B) in *E. coli* DH5α_1E in LB plus 100% BWH feed in 10 L bioreactor scale. 103
Figure 5-25: Setup of gasstripping device with 2 gas washing bottles in 10 L bioreactor scale. 104
Figure 5-26: Gasstripping with model solution - Isopropanol concentration in 10 L bioreactor and 2 gas washing bottles - Isopropanol transfer from bioreactor to gas washing bottles. 105
Figure 5-27: Amount of volatile metabolic products in 10 L bioreactor and 2 gas washing bottles during cultivation of *E. coli* DH5α_1E in LB plus glucose feed with gasstripping. 106
Figure 5-28: Setup of gasstripping device with a condensation trap and liquid nitrogen in 10 L bioreactor scale. 107
Figure 5-29: Amount of volatile metabolic products in 10 L bioreactor and condensation trap during cultivation of *E. coli* DH5α_1E in LB plus 100% BWH feed with gasstripping. 108
Figure 5-30: Generation of a linear functional homology cassette for targeted disruption of the pta gene in *E. coli* 109
Figure 5-31: Verification of targeted pta gene disruption in *E. coli* DH5α on DNA level. 110
Figure 5-32: Verification of targeted pta gene disruption in *E. coli* DH5α on metabolic product level. 111
Figure 5-33: Growth, glucose consumption and product formation of *E. coli* DH5αΔpta_1E in LB plus glucose feed in 10 L bioreactor scale. 112
Figure 5-34: Influence of pta disruption on production of Act-StrepII (1E) (A), Acct-His_{10} (2e), Adc-FLAG (3c) & Idh-c-Myc (4c) (B) in *E. coli* DH5αΔpta_1E in LB plus glucose feed in 10 L bioreactor scale. 113
Figure 5-35: Amount of volatile metabolic products in 10 L bioreactor and condensation trap during cultivation of *E. coli* DH5αΔpta_1E in LB plus glucose feed with gasstripping. 114
Figure 5-36: Carbon dioxide production rate, oxygen uptake rate and respiratory quotient of *E. coli* DH5αΔpta_1E in LB plus glucose feed in 10 L bioreactor scale. 115
Figure 5-37: Growth, glucose consumption and product formation of *E. coli* DH5αΔpta_1C in LB plus glucose feed in 10 L bioreactor scale. 116

Figure 5-38: Influence of pta disruption on production of Act-StrepII (1C) (A), Acct-His_{10} (2e), Adc-FLAG (3c) & Idh-c-Myc (4c) (B) in *E. coli* DH5αΔpta_1C in LB plus glucose feed in 10 L bioreactor scale. 118
Figure 6-1: Influence of different BWH concentrations on specific isopropanol and acetone productivities of *E. coli* DH5α_1C. 130
Figure 6-2: Comparison of isopropanol formation by and growth of *E. coli* DH5α_1E in LB plus feed with glucose or BWH in 10 L bioreactor scale. 138
Figure 6-3: Central carbon metabolism of *E. coli*. 145
Figure 6-4: Carbon mass balances – Conversion efficiencies of *E. coli* DH5α_1E (A), *E. coli* DH5αΔpta_1E (B), *E. coli* DH5α_1C (C) and *E. coli* DH5αΔpta_1C (D) after 24 h in LB plus feed with glucose in 10 L bioreactor scale. 149
Figure A-1: Plasmid map of pHSG299. 177
Figure A-2: Plasmid map of pRK_ISO_1E2e3c4c. 181
Figure A-3: Plasmid map of pRK_ISO_1C2e3c4c. 185
Figure A-4: Schematic presentation of FRT-PGK-gb2-neo-FRT cassette. 187
Figure A-5: Production of Act-StrepII (1C) (A), Acct-His_{10} (2e), Adc-FLAG (3c) and Idh-c-Myc (4c) (B) in *E. coli* DH5α_1C at 37 °C in 100 mL shake flask scale. 192
Figure A-6: Time course of control variables and base addition for *E. coli* DH5α_1E in LB plus 50% BWH/50% glucose feed in 10 L bioreactor scale. 193
Figure A-7: Production of Act-StrepII (1E) in *E. coli* DH5α_1E in LB plus 50% BWH/50% glucose feed in 10 L bioreactor scale. 193
Figure A-8: Time course of control variables and base addition for *E. coli* DH5α_1E in LB plus 100% BWH feed in 10 L bioreactor scale. 194
Figure A-9: Time course of control variables and base addition for *E. coli* DH5αΔpta_1E in LB plus glucose feed in 10 L bioreactor scale. 194
Figure A-10: Time course of control variables and base addition for *E. coli* DH5αΔpta_1C in LB plus glucose feed in 10 L bioreactor scale. 195

List of Tables

Table 2-1: Selected properties of isopropanol. 21
Table 2-2: Typical solvent concentrations produced by *C. acetobutylicum* and *C. beijerinckii* 24
Table 2-3: Metabolic engineering of *C. acetobutylicum* for isopropanol production. 26
Table 2-4: Recombinant isopropanol-producing microorganisms. 27
Table 2-5: Summary of various pretreatment methods for lignocellulosic biomass. 34
Table 2-6: Lignocellulose-derived inhibitors, their origin and general inhibitory cellular mechanisms. 35
Table 4-1: List of chemicals. 37
Table 4-2: List of buffers and solutions. 39
Table 4-3: Content analysis of BWH – glucose fraction - batch no. K020/21 41
Table 4-4: List of bacterial strains 41
Table 4-5: List of bacterial (complex) growth media. 41
Table 4-6: List of antibiotics. 42
Table 4-7: List of supplements. 42
Table 4-8: List of acquired plasmid DNA. 42
Table 4-9: List of constructed plasmid DNA (this work). 43
Table 4-10: List of primer oligonucleotides. 43
Table 4-11: List of enzymes and molecular biology reagents. 44
Table 4-12: List of antibodies. 45
Table 4-13: List of markers and loading dyes. 45
Table 4-14: List of kits. 46
Table 4-15: List of instruments and devices. 46
Table 4-16: List of laboratory equipment. 47
Table 4-17: List of consumables. 48
Table 4-18: List of computer programs and online tools. 49
Table 4-19: Mimimal medium according to [Wilms et al., 2001]. 51
Table 4-20: Trace element solution (TES) for minimal medium according to [Wilms et al., 2001]. 51
Table 4-21: Additives for minimal medium according to [Wilms et al., 2001]. 52
Table 4-22: PCR mastermix (1×) for amplification of the linear functional homology cassette for Red®/ET® recombination. 57
Table 4-23: PCR program for amplification of the linear functional homology cassette for Red®/ET® recombination. 57
Table 4-24: PCR mastermix (1×) for verification of Red®/ET® recombination mutants. 58
Table 4-25: PCR program for verification of Red®/ET® recombination mutants. 59
Table 4-26: GC device, method and operation conditions. 63
Table 4-27: Parameters for evaluation of bacterial cultivations. 67
Table 5-1: Kinetic parameters of selected Act isoenzymes. 72
Table 5-2: Kinetic parameters of selected Acct isoenzymes. 73
Table 5-3: Kinetic parameters of selected Adc isoenzymes. 73
Table 5-4: Kinetic parameters of selected Idh isoenzymes. 74
Table 5-5: Engineered *E. coli* strains for isopropanol production. 75

Table 5-6: Influence of induction temperature on isopropanol production parameters of *E. coli* DH5α_1E and *E. coli* JM109_1E after 24 h. 78
Table 5-7: Influence of induction temperature on isopropanol production parameters of *E. coli* DH5α_1C and *E. coli* JM109_1C after 24 and 48 h. 82
Table 5-8: Influence of different BWH concentrations on isopropanol production parameters of *E. coli* DH5α_1C after 24 h. 90
Table 5-9: Influence of different BWH concentrations on acetate production parameters of *E. coli* DH5α_1C after 24 h. 91
Table 5-10: Product formation parameters of *E. coli* DH5α_1C after 24 h in LB plus glucose feed in 10 L bioreactor scale. 93
Table 5-11: Product formation parameters of *E. coli* DH5α_1E after 24 h in LB plus glucose feed in 10 L bioreactor scale. 96
Table 5-12: Product formation parameters of *E. coli* DH5α_1E after 24 h in LB plus 50% BWH/50% glucose feed in 10 L bioreactor scale. 100
Table 5-13: Product formation parameters of *E. coli* DH5α_1E after 24 h in LB plus 100% BWH feed in 10 L bioreactor scale. 102
Table 5-14: Influence of targeted pta gene disruption in *E. coli* DH5α on growth rate and acetate formation parameters after 8 h. 111
Table 5-15: Product formation parameters of *E. coli* DH5αΔpta_1E after 24 h in LB plus glucose feed in 10 L bioreactor scale. 113
Table 5-16: Product formation parameters of *E. coli* DH5αΔpta_1C after 24 h in LB plus glucose feed in 10 L bioreactor scale. 117
Table 6-1: Production of isopropanol pathway enzymes in *E. coli* DH5α_1E and JM109_1E at 24 °C and 37 °C in LB medium with 2% (w/v) glucose and 0.1 mM IPTG. 120
Table 6-2: Alternative isoenzymes for recombinant isopropanol production in *E. coli*. 124
Table 6-3: Comparison of expression construct designs for isopropanol (and acetone) production by *E. coli* in shake flask scale. 125
Table 6-4: Isopropanol production parameters of selected expression constructs in engineered *E. coli* on glucose. 128
Table 6-5: Lignocellulose-derived inhibitors and their critical concentrations for different *E. coli* strains. 132
Table 6-6: Growth, glucose consumption and isopropanol formation parameters of *E. coli* DH5α_1C and *E. coli* DH5α_1E after 24 h in LB plus feed with glucose in shake flask and bioreactor scale. 133
Table 6-7: Production of isopropanol pathway enzymes in *E. coli* DH5α_1C and *E. coli* DH5α_1E in LB with glucose as carbon source in 10 L bioreactor scale. 133
Table 6-8: Isopropanol production parameters of recombinant and natural isopropanol-producing organisms on pure carbon source in bioreactor scale. 136
Table 6-9: Growth, glucose consumption and isopropanol formation parameters of *E. coli* DH5α_1E after 24 h in LB plus feed with glucose or BWH in 10 L bioreactor scale. 138
Table 6-10: Comparison of isopropanol production parameters of recombinant and natural isopropanol-producing organisms on lignocellulose and other hydrolysates in bioreactor scale. 140
Table 6-11: Comparison of *in situ* product separation and recovery techniques for microbial solvent production. 143

Table 6-12: Growth, glucose consumption and isopropanol formation parameters of *E. coli* DH5α_1E, *E. coli* DH5αΔpta_1E, *E. coli* DH5α_1C and *E. coli* DH5αΔpta_1C after 24 h in LB plus feed with glucose in 10 L bioreactor scale. 147
Table 6-13: Production of isopropanol pathway enzymes in *E. coli* DH5α_1E, *E. coli* DH5αΔpta_1E, *E. coli* DH5α_1C and *E. coli* DH5αΔpta_1C in LB with glucose as carbon source in 10 L bioreactor scale. 148
Table 6-14: Thermodynamics of the isopropanol and acetate pathway reactions. 152
Table 6-15: Ideal stoichiometric balance of the recombinant isopropanol pathway in *E. coli* (aerobic).. 153
Table A-1: DNA sequence of pHSG299. 176
Table A-2: DNA sequence of pRK_ISO_1E2e3c4c. 178
Table A-3: DNA sequence of pRK_ISO_1C2e3c4c. 182
Table A-4: DNA sequence of the pta gene (*E. coli*). 186
Table A-5: Amino acid sequence of Act-StrepII (1E). 187
Table A-6: Parameters of Act-StrepII (1E) and Act (*E. coli)*. 187
Table A-7: Amino acid sequence of Act-StrepII (1C). 188
Table A-8: Parameters of Act-StrepII (1C) and Act (*C. acetobutylicum)*. 188
Table A-9: Amino acid sequence of Acct-His_{10} (2e) – subunit α & β. 189
Table A-10: Parameters of Acct-His_{10} (2e) – subunit α & β and Acct (*E. coli*) – subunit β. 189
Table A-11: Amino acid sequence of Adc-FLAG (3c). 190
Table A-12: Parameters of Adc-FLAG (3c) and Adc (*C. acetobutylicum)*. 190
Table A-13: Amino acid sequence of Idh-c-Myc (4c). 190
Table A-14: Parameters of Idh-c-Myc (4c) and Idh (*C. beijerinckii)*. 191

1 Introduction

Dependency on fossil resources for the production of energy, transportation fuels and chemicals has caused numerous economic, environmental and social problems, ranging from the depletion of non-renewable raw materials and ever rising greenhouse gas (GHG) emissions to the price fluctuations and reliance on trade agreements with countries harboring these resources. Fossil feedstocks comprise carbon- and energy-rich gaseous, liquid and solid substances that have been formed by decomposition of organic matter during processes that take millions of years to complete and require intense heat and pressure. The most common representatives are crude oil, natural gas and coal. Those are the base for an immense variety of products, of which fuel (for electricity and heat generation via combustion), gasoline and kerosene (transportation fuels), asphalt, rubber, fertilizers, solvents, adhesives, pesticides, pharmaceuticals and plastics are only a few examples.

The finite nature of fossil resources together with the surge in global energy consumption raises concern about the future availability of those commodities. Already in 1949, the geophysicist M. K. Hubbert published the theory of an event which was later called “peak oil”, the time point of maximal global oil (or coal/gas) production followed by terminal decline in the production rate. Hubbert linked the rates of production of coal, oil and natural gas to the growth of human population, the physical limits to expansion and the amount of fossil fuels (including oil shale) present on earth, concluding that “we may announce with certainty that the production curve of any given species of fossil fuel will rise, pass through one or several maxima, and then decline asymptotically to zero“ [Hubbert, 1949]. Despite significant disagreement and reporting bias on the amount of global fossil reserves (i.e. exploitable resources), even the most optimistic predictions state that peak has already occurred [Aleklett et al., 2010] or will occur in the near future [Miller and Sorrell, 2014; Owen et al., 2010]. Reserve-to-production ratios may be calculated for coal, natural gas or oil that globally range between 40 and 150 years [BP, 2016]. Closely related to the declining availability of those non-renewable resources is their fluctuating price on the world market [Qureshi and Blaschek, 2001]. Particularly the oil price does not reflect the production cost, but is influenced by supply and demand, trade agreements between the Organization of the Petroleum Exporting Countries (OPEC), other exporting and importing nations, politics, market strategies and other factors like wars or environmental disasters. The strong linkage between oil price and global economic activity marks oil price volatility as a source of uncertainty for investors and end consumers, especially when downward tendencies are involved. Considering peak oil, the International Energy Agency (IEA) forecasts an oil price of US$ 200 per barrel (~159 L) by 2030 [IEA, 2008].

Another concern regarding fossil commodities is the environmental impact of their production and utilization. The combustion of hydrocarbons for generation of energy and mobility causes release of carbon dioxide (CO_2) and other GHGs (e.g. sulfur dioxide, nitrogen oxides, carbon monoxide), the major cause for the global warming phenomenon. The largest share in anthropogenic CO_2 emissions (44% according to the International Renewable Energy Agency) is held by the burning of coal, which is also a leading cause for smog, acid rain and toxic air pollution [IRENA, 2014]. Extraction of crude oil and natural gas often requires the introduction of chemicals for well stimulation in a process termed hydraulic fracturing (“fracking”). Oil production causes pollution of sea and land by oil spills and adds its share to acidification of oceans and soils.

Due to the growing awareness on the plethora of adverse effects by utilization of fossil resources, extensive efforts have been made to stimulate research for alternative means, not only in the field of energy generation, but also in the production of various other fossil-derived goods and chemicals. Chemical products derived from fossil feedstocks are termed petrochemicals (petroleum = crude oil and refined crude oil products). The base building blocks of all petrochemicals can be divided into three classes: olefins (ethene, propene, butadiene), aromatics (benzene, toluene, xylenes) and syngas (derived from methane). Propene, also known as propylene, is the second most important petrochemical feedstock after ethene. It is gained mainly from oil and natural gas by steam or catalytic cracking or on-purpose methods like olefin metathesis or propane dehydrogenation and can be used as precursor for a variety of products, the plastic polypropene (polypropylene) comprising by far the biggest share. 2-Methyloxirane (propylene oxide), acrylonitrile, cumene, butyraldehyde, acrylic acid, acetone and isopropanol are further derivatives of propene. In 2013, 85 million tonnes of propene were processed worldwide [Ceresana, 2014].

Analogous to conventional oil refineries yielding several different products and as an alternative to fossil-based manufacturing, the concept of biorefineries has emerged during the last decades. The IEA Bioenergy Task 42 “Biorefinery” defines biorefining as “the sustainable processing of biomass into a spectrum of marketable products and energy” [IEA, 2014]. The idea is to develop and establish an environmentally and socially sustainable, safe, efficient and competitive production process for simultaneous manufacturing of biomass to marketable bio-based commodities like biofuels, bio-chemicals, bio-energy and bio-materials (non-food applications). The objectives of this concept are replacement of fossil-based products by their bio-based counterparts, minimization of material wastes by optimal and recycled use of production intermediates, independency from fossil feedstock-exporting countries, reduction of GHG emissions and stimulation of regional and rural development. Biorefineries can be classified and described by four main features: (a) platforms (e.g. core intermediates like C_5-C_6 carbohydrates, syngas, lignin, pyrolytic liquid), (b) products (e.g. energy, chemicals, materials), (c) feedstocks (e.g. biomass from forestry or agriculture residues) and (d) processes (e.g. biochemical or mechanical). According to Jungmeier et al., efficient combination and merging of platforms and processes including recycling could generate a variety of (value-added) products, reduce GHG emissions by 41-92% and save energy in the range of 24-42% compared to conventional reference systems based on fossil resources [Jungmeier, 2014]. Considering the Paris Agreement in late 2015 [UNFCCC, 2015] to limit global temperature rise to ~2 °C and to confine environmental harm by GHG emissions to tolerable levels, implementation of biorefineries could substantially contribute to reach this goal.

In conformity with the recently installed political frameworks and fundings for research on biorefineries in Germany, the work presented here is embedded in the Leading-Edge Cluster “BioEconomy” of the Federal Ministry of Education and Research (*Bundesministerium für Bildung und Forschung*, BMBF). The Cluster was initiated in 2012 and joins industrial and research partners in the pursuit of an economically viable and sustainable material and energetic use of non-food biomass. This work is part of the Cluster project “TG 2 – Chemistry, VP 2.5, Energy-efficient synthesis of olefins from their corresponding alcohols” (BMBF no. 031A072). The superordinate project aim is the theoretical and practical investigation of a biorefinery platform for the production of propene from the starting biomass beech wood (lignocellulosic biorefinery). Following optimization, the individual manufacturing steps should be scaled-up and integrated into an energy-efficient and economically viable corporate process. The schematic overview of the production cascade is depicted in Figure 1-1.

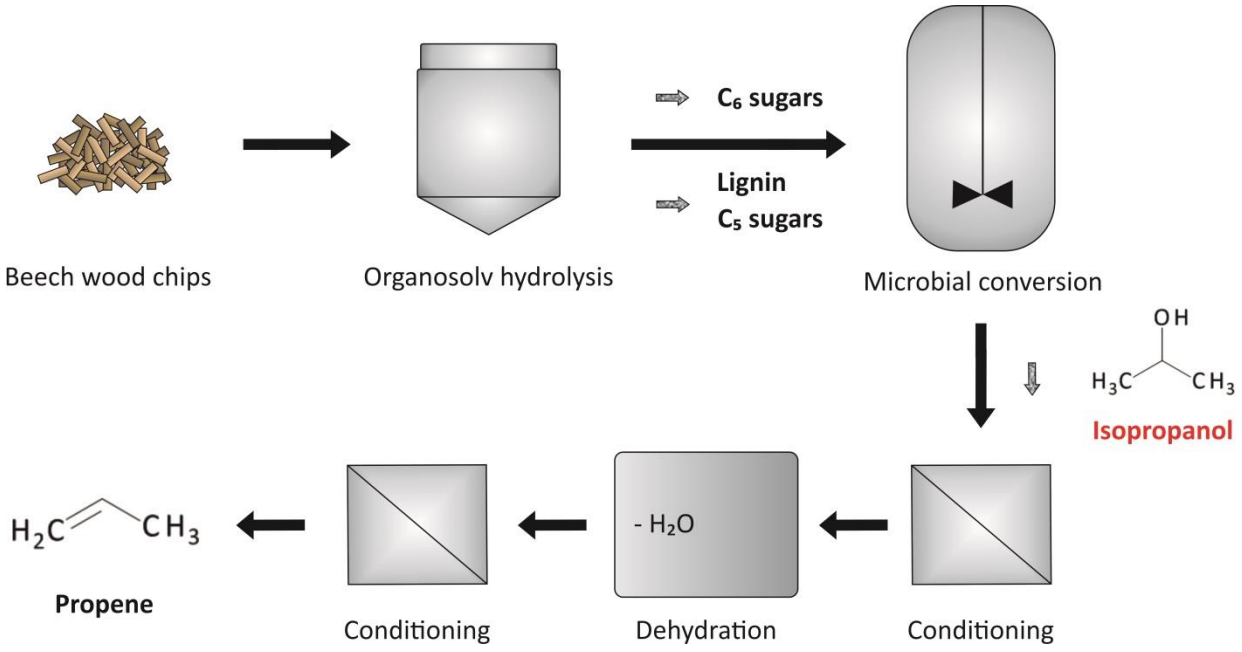

Figure 1-1: Production cascade of the BioEconomy Cluster project "TG 2 – Chemistry, VP 2.5, Energy-efficient synthesis of olefins from their corresponding alcohols".

In detail, the beech wood chips, remnants of the forestry and wood-processing industry, are subjected to an "Organosolv" hydrolysis, in which they are heated, pressurized and fractionated by an ethanol-water mixture. The gained product streams comprise the mother liquor, which can be further purified to yield lignin and C_5 sugars, and a fiber fraction, which is further enzymatically hydrolyzed to yield glucose. The glucose solution is utilized as a carbon source in the subsequent aerobic generation of isopropanol by engineered microorganisms. Isopropanol is further chemically converted to the final product propene in a dehydration reaction. Provision of sufficient quantities of the C_3 alcohol is a crucial step in the realization and assessment of the overall manufacturing process, therefore optimization of the microbial isopropanol production is the main topic of this work.

2 State of the Art

2.1 Isopropanol - Basic Facts

Isopropanol (IUPAC name: propan-2-ol; a.k.a. 2-propanol or isopropyl alcohol) is the smallest, non-cyclic secondary alcohol with the chemical formula C_3H_8O (structural formula depicted in Figure 2-1).

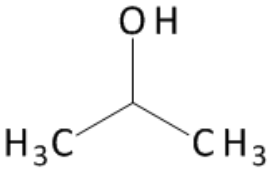

Figure 2-1: Structural formula of isopropanol.

It is a colorless, flammable liquid with a sweetish, pungent odor that evaporates quickly. Isopropanol is completely miscible with water in any ratio and forms an azeotropic mixture at 12.1 wt% water with a boiling point of 80.4 °C [Chemie.de]. Further properties of isopropanol are listed in Table 2-1.

Table 2-1: Selected properties of isopropanol.
Properties were compiled from [Chemie.de].

Properties	
Molecular mass	60.10 g mol^{-1}
Physical state at standard conditions	liquid
Density	0.78 g cm^{-3} (20 °C)
Melting point	-88 °C
Boiling point	82 °C
Ignition point	460 °C
Vapor pressure	4.2 kPa (20 °C)
Explosive limits	2 – 12.7 vol%
Specific thermal capacity	2.56 kJ kg^{-1} K^{-1}

Isopropanol is a bulk chemical and its applications are numerous. It is mainly used as a solvent for resins, lacquers and paints, in cosmetics, pharmaceuticals, adhesives, as an additive in antifreeze agents and as a cleaning agent and disinfectant in industry, medical care and households. It is applied in extraction and purification procedures of natural products like oils and fats and as a cleaning and drying agent in the manufacturing of electronic parts and metals. Further uses comprise its utilization as a defoaming agent, coolant, coupling agent, wetting agent, de-icing agent, preservative, polymerization modifier and precipitation agent. The secondary alcohol is also used as starting material in the production of various chemicals like acetone (via Meerwein-Ponndorf-Verley reduction), isopropylamine (e.g. used for glyphosate formulations) and isopropyl esters [ICIS]. Furthermore, isopropanol can be dehydrated to yield propene in an acid-catalyzed thermal process (Figure 2-2).

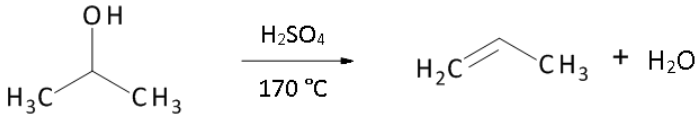

Figure 2-2: Dehydration reaction of isopropanol to propene.

With a global propene demand of ~50 million tones per year [IEA, 2014], the conversion of isopropanol could contribute a significant share to the production of the valuable polymer precursor.

2.2 Isopropanol Production by Chemical Processes

In 1920, isopropanol was the first industrial chemical synthesized from a petroleum-based product (propene). Nowadays, the secondary alcohol is still commercially manufactured by indirect or direct hydration of propene [Matar, 2001]. The indirect process involves reaction of refinery-grade propene with sulfuric acid to form an ester, isopropyl sulfate, which is then hydrolyzed with steam to the alcohol. The direct method requires high-quality (at least 90%) propene, which reacts directly with water, in liquid and/or gaseous phase, at high pressure in the presence of acidic catalysts (Figure 2-3).

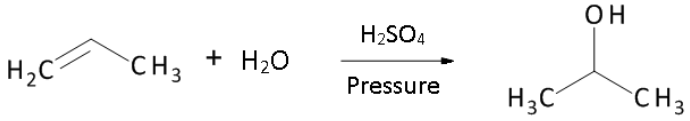

Figure 2-3: Hydration of propene to isopropanol.

Both techniques conclude with azeotropic distillation using either diisopropyl ether or cyclohexane as azeotropic agents. Only a small portion of isopropanol is generated by hydrogenation of crude acetone in liquid phase, which is suitable only if acetone is available in excess (Figure 2-4).

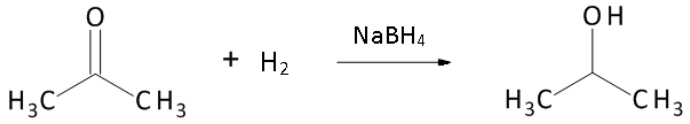

Figure 2-4: Hydrogenation of acetone to isopropanol.

2.3 Isopropanol Production by Microorganisms

2.3.1 Natural Isopropanol Producers

The bacterium *Clostridium beijerinckii* (*C. beijerinckii*), named after the Dutch microbiologist Martinus Beijerinck, has been known as a "solvent producer" since the beginning of the last century. Like the closely-related *Clostridium acetobutylicum* (*C. acetobutylicum*), most strains of C. *beijerinckii* (e.g. *C. beijerinckii* NRRL B592) can be utilized in the strictly anaerobic acetone-butanol-ethanol (ABE) fermentation, one of the first large-scale industrial fermentation processes (patent by [Weizmann, 1919]). But some strains are also able to generate isopropanol (e.g. *C. beijerinckii* NRRL B593 a.k.a.

DSM6423) from acetone (besides producing butanol and ethanol). Like most members of the class *Clostridia* (phylum/division Firmicutes, domain/kingdom Bacteria), *C. beijerinckii* is a gram-positive, obligate anaerobic, motile, rod-shaped, endospore-forming, ubiquitous bacterium.

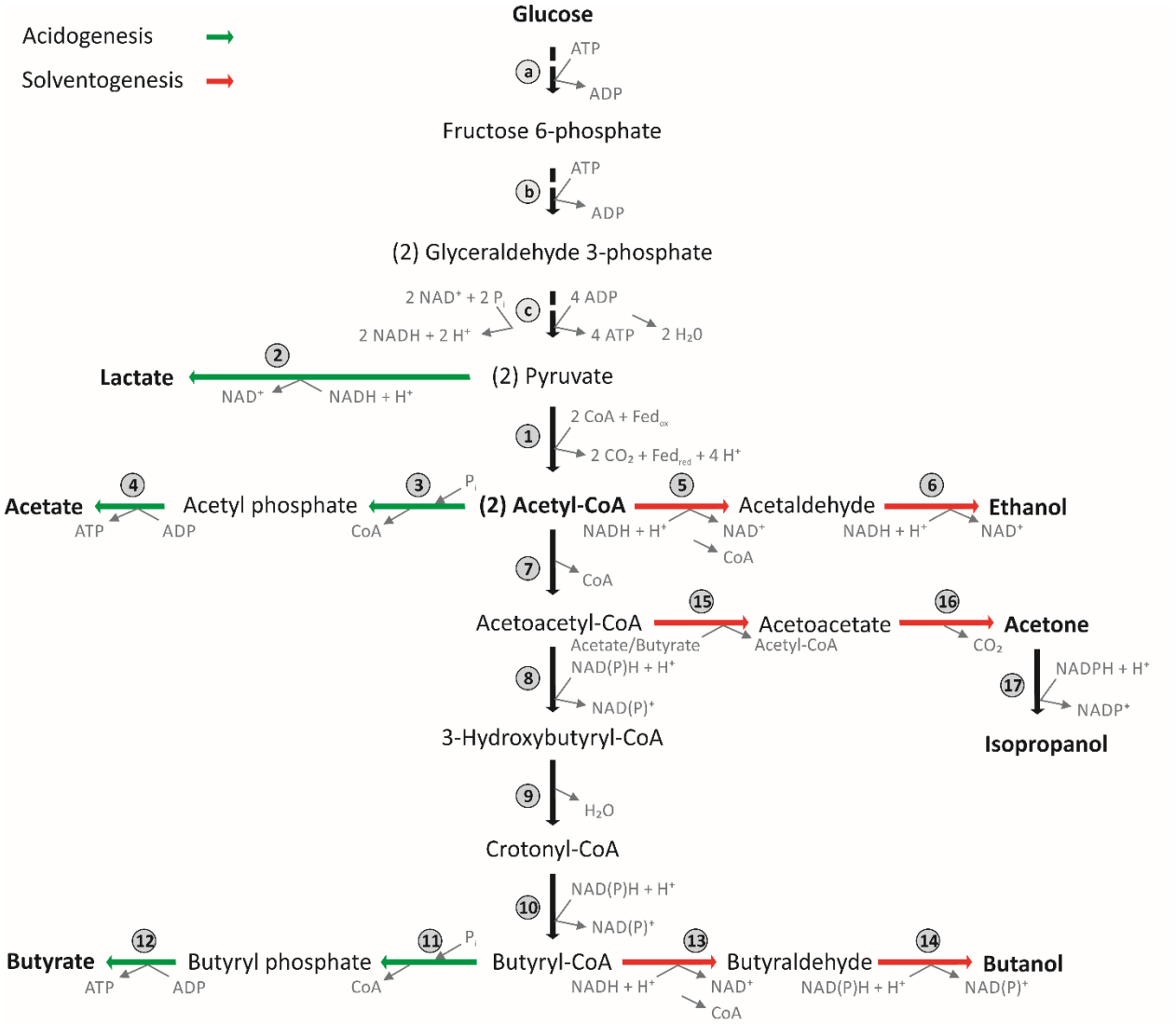

Figure 2-5: Schematic solvent production in *C. beijerinckii*.
Adapted from [Durre, 1998].
Circled numbers refer to the enzymes involved: **1** pyruvate:ferredoxin oxidoreductase, **2** L-lactate dehydrogenase, **3** phosphotransacetylase, **4** acetate kinase, **5** acetaldehyde dehydrogenase, **6** ethanol dehydrogenase, **7** thiolase, **8** 3-hydroxybutyryl-CoA dehydrogenase, **9** crotonase, **10** butyryl-CoA dehydrogenase, **11** phosphate butyryltransferase, **12** butyrate kinase, **13** aldehyde dehydrogenase, **14** alcohol dehydrogenase, **15** acetate CoA-transferase, **16** acetoacetate decarboxylase, **17** secondary alcohol dehydrogenase (only present in some *C. beijerinckii* species).
Substrate-to-product stoichiometry is not shown for reaction 2, 3, 5.
Glycolysis (metabolism of glucose to pyruvate) is not presented in detail, but consists of the following enzymes: **a** hexokinase and glucose-6-phosphate isomerase, **b** phosphofructokinase-1, fructose-bisphosphate aldolase and triose-phosphate isomerase, **c** glyceraldehyde 3-phosphate dehydrogenase, phosphoglycerate kinase, phosphoglycerate mutase, enolase and pyruvate kinase.
Fed_{ox}... ferredoxin (oxidized), Fed_{red}... ferredoxin (reduced)

It is capable of using a variety of sugar substrates like pentoses (e.g. xylose [Sun et al., 2015], arabinose [Forsberg et al., 1987]), hexoses (e.g. glucose, mannose [Essalem and Mitchell, 2016], fructose [Mitchell et al., 1995], galactose [Servinsky et al., 2010]), oligosaccharides (e.g. sucrose [Ahmed et al., 1988],

maltose [Mitchell et al., 1995], lactose [Servinsky et al., 2010], cellobiose [Ye et al., 2011]), starch [Ensley et al., 1975], certain acids (e.g. lactic acid [Forsberg et al., 1987], pectic acid [Nakajima et al., 1999]) and the polyol glycerol [Gonen et al., 2013] as carbon source. The sugars are metabolized to pyruvate via both, the pentose phosphate pathway and the Embden-Meyerhof-Parnas pathway, the most common type of glycolysis, generating the redox cofactor NADH and the „energy currency" ATP. The solvent production pathway in *C. beijerinckii* is illustrated in Figure 2-5 (page 23).

In *C. beijerinckii*, isopropanol is produced from the key metabolite acetyl-CoA by the catalytic action of four enzymes: a thiolase (**7**, a.k.a. acetyl-CoA:acetyl-CoA C-acetyltransferase, acetyl-CoA acetyltransferase or acetoacetyl-CoA synthase, EC 2.3.1.9), an acetate CoA-transferase (**15**, EC 2.8.3.8), an acetoacetate decarboxylase (**16**, EC 4.1.1.4) and an NADPH-dependent secondary alcohol dehydrogenase (**17**, EC 1.1.1.80) [Durre, 1998]. Similar to *C. acetobutylicum*, the products of *C. beijerinckii* are generated in an approximate ratio of 3:6:1 isopropanol/butanol/ethanol. Produced amounts of metabolic products are strain-, substrate-, medium- and cultivation-dependent, but are largely in the same range for both species (see Table 2-2). Generally, 15-18 g L^{-1} total solvents are generated within a period of 40-60 h [Woods, 1995].

Table 2-2: Typical solvent concentrations produced by *C. acetobutylicum* and *C. beijerinckii*.
Produced acids are not listed. Source: [Collas et al., 2012]. Cultivations were performed in a 1 L bioreactor with CM1 medium, 3 g L^{-1} ammonium acetate and 90 g L^{-1} glucose at pH 5 for 45 h.

Products [g L^{-1}]	***C. acetobutylicum* (ATCC 824)**	***C. beijerinckii* (NRRL B593)**
Acetone	5.7	0.2
Isopropanol	0.1	4.5
Butanol	10.0	8.4
Ethanol	1.1	0.1
Total solvents	16.9	13.2

In *C. acetobutylicum*, either acids or alcohols/ketones are produced, depending on the metabolic state of the cells. During the first metabolic phase, acidogenesis, the bacteria grow exponentially while generating acetate or butyrate together with molecular hydrogen, CO_2 and energy in the form of ATP. In stationary phase, the bacteria switch to solventogenesis by re-assimilation of the acids concomitantly with consumption of sugars, and subsequent production of acetone, butanol and ethanol, while NAD(P)H is regenerated to $NAD(P)^+$ [Girbal and Soucaille, 1998]. The acetone pathway-associated enzyme acetate CoA-transferase (CtfA and CtfB; **15** in Figure 2-5) is also responsible for reversion of the acids to acetyl- or butyryl-CoA [Hartmanis et al., 1984]. Although the molecular mechanisms behind the transition from acidogenesis to solventogenesis are largely unknown, several parameters involved in triggering the shift were identified. Drop of external pH from neutral to pH 5 due to accumulation of acids is considered to be one of the main factors for onset of solvent production as a detoxification response [Monot et al., 1984]. But also ATP availability [Meyer and Papoutsakis, 1989] and intracellular $NAD(P)H/NAD(P)^+$ ratio [Wietzke and Bahl, 2012] might play significant roles. In *C. beijerinckii*, the transition phenomenon was also observed, although George and Chen reported that acidogenesis can be circumvented by keeping a constant neutral pH [George and Chen, 1983]. Ahmed et al. suggested that in this species solventogenesis occurs in a growth rate-dependent manner. Also, sporulation in *C. beijerinckii* might not be as tightly connected to solventogenesis as in *C. acetobutylicum* [Ahmed et al., 1988]. It was observed

that an excess of carbon source (e.g. glucose) is essential for the onset and maintenance of solvent production [Jones and Woods, 1986].

Besides *C. beijerinckii*, other natural isopropanol producers have been identified throughout all domains of life. They all possess a secondary alcohol dehydrogenase that accepts acetone as a substrate and catalyzes the conversion to isopropanol. For example, Sutak et al. discovered such an enzyme in the protozoan parasite *Trichomonas vaginalis* (K_M for acetone: 0.09 mM, specific activity: 0.3 U mg^{-1} [Sutak et al., 2012]. Similar secondary alcohol dehydrogenases have been found in bacteria like *Methanofollis* [Bleicher and Winter, 1991], *Burkholderia* [Isobe and Wakao, 2003], *Thermoanaerobacter* [Burdette et al., 1996] and *Cupriavidus* [Jendrossek et al., 1990].

2.3.2 Recombinant Isopropanol Producers

During the last 25 years, a variety of genetic engineering tools, like shuttle vectors for transformation, gene downregulation by antisense RNA or gene disruption by homologous recombination, became available for the alteration and improvement of *Clostridia* properties [Desai and Papoutsakis, 1999; Heap et al., 2007; Mermelstein et al., 1992]. Focus was mainly on optimization of *C. acetobutylicum* with regard to increased butanol production [Harris et al., 2000; Nair and Papoutsakis, 1994]. But recently, implementation of isopropanol generation capability (instead of acetone) into the native ABE producer has gained much attention due to the potential utilization of isopropanol in an IBE fuel mixture. Collas et al. introduced the secondary alcohol dehydrogenase gene (adh) of *C. beijerinckii* NRRL B593 under control of the constitutive thiolase (thl) promoter into *C. acetobutylicum* ATCC 824 and overexpressed the acetate CoA-transferase (a.k.a. acetoacetyl-CoA:acetate/butyrate coenzyme-A transferase, ctfAB) and acetoacetate decarboxylase (adc) genes on a plasmid. Thus, a final isopropanol concentration of 8.8 g L^{-1} in 45 h was achieved, accompanied by only a minimal amount of acetone [Collas et al., 2012]. Several other research groups applied similar strategies, which resulted in isopropanol production by *C. acetobutylicum* and are listed in Table 2-3.

Table 2-3: Metabolic engineering of *C. acetobutylicum* for isopropanol production.

Reference	Introduced genes	Promoter	Deleted genes	Isopropanol [g L^{-1}]
[Collas et al., 2012]	ctfAB, adc of *C. acetobutylicum* ATCC 824 adh of *C. beijerinckii* NRRL B593	thl	-	8.8 (45 h)
[Lee et al., 2012a]	ctfAB, adc of *C. acetobutylicum* ATCC 824 adh of *C. beijerinckii* NRRL B593	adc	-	6.1 (43 h)
[Lee et al., 2012a]	ctfAB, adc of *C. acetobutylicum* ATCC 824 adh of *C. beijerinckii* NRRL B593	adc	butyrate kinase	4.4 (43 h)
[Dai et al., 2012]	adh of *C. beijerinckii* NRRL B593	thl	-[a]	7.6 (48 h)
[Dusseaux et al., 2013]	ctfAB, adc of *C. acetobutylicum* ATCC 824 adh of *C. beijerinckii* NRRL B593	thl	phosphate butyryltransferase, butyrate kinase	4.7 (30 h)
[Dusseaux et al., 2013]	ctfAB, adc of *C. acetobutylicum* ATCC 824 adh of *C. beijerinckii* NRRL B593	ptb[b]	phosphate butyryltransferase, butyrate kinase	4.2 (30 h)
[Jang et al., 2013]	adh, hydG[c] of *C. beijerinckii* NRRL B593	thl	butyrate kinase	3.6 (78 h)

ctfAB… acetate CoA-transferase gene, adc… acetoacetate decarboxylase gene, adh… (secondary) alcohol dehydrogenase gene, thl… thiolase gene, [a] butanol tolerant mutant of *C. acetobutylicum* Rh8, [b] phosphate butyryltransferase promoter, [c] hydG: putative electron transfer protein

Despite certain progress in increasing the isopropanol production capability of *Clostridia*, either by metabolic engineering or process design, this class of bacteria still has its drawbacks with regard to the selective generation of isopropanol. Knockout of solvent-related genes often resulted in unpredicted effects and unsuccessful re-direction of metabolic fluxes [Huang et al., 2010; Jiang et al., 2009; Lehmann et al., 2012]. Consequently, heterologous expression of the isopropanol pathway genes in different, non-butanol-producing and thus potentially more suitable microorganisms was considered and performed. Table 2-4 depicts an overview of recombinant microorganisms that have been engineered for selective isopropanol production.

Table 2-4: Recombinant isopropanol-producing microorganisms.
Recombinant *Clostridia* species are not listed (see Table 2-3). Volumetric isopropanol productivities (P_P) were calculated from the published concentrations and the cultivation times according to Equation 4-24, page 69.

Microorganism	Isopropanol [g L^{-1}]	P_P [g L^{-1} h^{-1}]	Features	Reference
Escherichia coli	4.9	0.161 (30.5 h)	Synthetic isopropanol pathway	[Hanai et al., 2007]
	40.1	0.668 (60 h)	pH control	[Inokuma et al., 2010]
	143.0[a]	**0.596 (240 h)**	**pH control & gasstripping**	
	13.6	0.389 (35 h)	Individual promoters	[Jojima et al., 2008]
	4.1	0.195 (21 h)	Cellobiose as carbon source	[Soma et al., 2012]
	3.1	0.052 (60 h)	Metabolic toggle switch	[Soma et al., 2014]
	3.9	0.093 (42 h)	Cell density-related switch	[Soma and Hanai, 2015]
	13.5	0.281 (48 h)	Optimization of codon bias, plasmid copy number, translation rates, pH control	[Liang et al., 2017]
	6.5	0.135 (48 h)	Genomic integration, RBS optimization	
Cupriavidus necator[c]	3.4	0.035 (96 h)	Fructose as carbon source, high biomass-related productivity	[Grousseau et al., 2014]
	9.1	0.111 (82 h)	GroESL[b] overexpression, fed-batch bioreactor cultivation	[Marc et al., 2017]
Candida utilis	9.5	0.183 (52 h)	Genomic integration, overexpression of precursor supply genes, pH control	[Tamakawa et al., 2013]
	27.2	0.139 (196 h)	Additional feed	
Synechococcus elongatus	0.0265	0.0001 (216 h)	Genomic integration, dark and anaerobic conditions (acetate from stored glycogen as carbon source), nitrogen/phosphate limitation	[Kusakabe et al., 2013]
	0.146 in 336 h (growth) plus 360 h (production)	0.0002 (696 h)	Switch from growth (light/aerobic) to production conditions (dark/anaerobic plus light/aerobic) and pH control	[Hirokawa et al., 2015]
Synechocystis sp.	0.227	0.0005 (480 h)	Genomic integration, photosynthetic conditions (aerobic/light)	[Zhou et al., 2016]

RBS… ribosome binding site, [a] cumulative sum of shake flask and recovery system, [b] chaperonin system, [c] PHB-deficient *C. necator* strain

In 2007, Hanai et al. tested gene combinations from *Clostridia*, *E. coli* and *Thermoanaerobacter brockii* (*T. brockii*) to establish a synthetic metabolic pathway in *E. coli* that generates isopropanol from glucose. With the most suitable combination of genes, a final isopropanol concentration of 4.9 g L^{-1} after 30.5 h could be achieved in aerobic shake flask experiments [Hanai et al., 2007]. In the same scale, but with

control of pH and intermittent glucose addition, the recombinant organism reached a maximum isopropanol concentration of 40.1 g L^{-1} after 60 h. By employing gasstripping as a recovery method, isopropanol generation could be increased to 143 g L^{-1} after 240 h (cumulative sum of shake flask and recovery system) [Inokuma et al., 2010]. Jojima et al. were able to engineer a strain with a ~2.4 times higher isopropanol productivity in shake flask scale compared to the strain of Hanai et al. by implementation of individual promoters for gene expression [Jojima et al., 2008]. Further investigations on isopropanol production by *E. coli* were performed by Soma et al., who were able to achieve 4.1 g L^{-1} isopropanol after 21 h directly from the substrate cellobiose. Cellobiose is a disaccharide of two glucose molecules and a degradation product of cellulose, a main component of lignocellulose hydrolysates. Cellobiose degradation was established in *E. coli* by anchoring of a β-glucosidase of *Thermobifida fusca* to the cell surface of the bacterium [Soma et al., 2012]. Soma et al. also fine-tuned isopropanol production by implementation of a conditional knockout ("metabolic toggle switch") that deviated the carbon flux from TCA cycle and thus increased the acetyl-CoA pool for the isopropanol pathway [Soma and Hanai, 2015; Soma et al., 2014]. Liang et al. were the first to apply optimization of codon usage, plasmid copy number and translation rates plus integration of the isopropanol pathway genes into the *E. coli* genome, which achieved an isopropanol concentration of 6.5 g L^{-1} within 48 h [Liang et al., 2017].

Besides *E. coli*, other organisms were investigated for recombinant isopropanol production. The gram-negative soil bacterium *Cupriavidus necator* is a facultative chemolithoautotroph, i.e. it can grow autotrophically (CO_2 fixation) on inorganic substances as well as heterotrophically on organic substances, both by using chemical reactions like H_2 oxidation (chemosynthesis). The bacterium is also able to store excess carbon in the form of poly-3-hydroxybutyrate (PHB) under nutrient limitation conditions. Introduction of a plasmid carrying homologous and *Clostridia* genes of the isopropanol pathway into a PHB-deficient *C. necator* strain, diverted the carbon flux from storage polymer formation to isopropanol generation and achieved a final concentration of 3.4 g L^{-1} after 96 h [Grousseau et al., 2014]. Overexpression of chaperones in combination with fed-batch cultivation in bioreactor scale yielded a final concentration of 9.1 g L^{-1} within 82 h [Marc et al., 2017]. Tamakawa et al. integrated homologous and *Clostridia* isopropanol pathway genes into the genome of the yeast *Candida utilis*, simultaneously overexpressing two genes responsible for precusor acetyl-CoA and acetoacetyl-CoA supply. Thus, a final isopropanol concentration of 9.5 g L^{-1} could be reached within 52 h of batch cultivation, whereas fed-batch cultivation led to a concentration of 27.2 g L^{-1} isopropanol after 196 h [Tamakawa et al., 2013]. In an attempt to utilize light and CO_2 for isopropanol production, the phototrophic cyanobacterium *Synechococcus elongatus* was engineered and bestowed with the isopropanol pathway genes. Although production of trace amounts of isopropanol could be achieved by anaerobic and light conditions (1 mg L^{-1} in 360 h), the highest concentration of 26.5 mg L^{-1} after 216 h was only reached by cultivation of *S. elongatus* under dark and anaerobic conditions by utilization of acetate from stored glycogen as carbon source and phosphate and nitrogen limitation [Kusakabe et al., 2013]. By separation of growth and production phase via switching from light and aerobic (carbon fixation by photosynthesis and conversion to glycogen) to dark and anaerobic conditions (conversion of glycogen to acetate and isopropanol) and subsequently back to light/aerobic conditions (conversion of acetate to isopropanol), the final isopropanol concentration could be increased 6fold to 146 mg L^{-1} [Hirokawa et al., 2015]. The isopropanol pathway was likewise introduced into another cyanobacterium *Synechocystis sp.* PCC6803 and yielded 227 mg L^{-1} isopropanol within 20 days in a light-driven reaction [Zhou et al., 2016].

2.3.3 Enzymes of the Isopropanol Pathway

The metabolic pathway which enables solvent generation by *Clostridium* bacteria was described in 2.3.1 and pictured in Figure 2-5, page 23. Analogously, the biosynthetic pathway for selective isopropanol production from the central metabolite acetyl-CoA comprises four catalytic steps: a) condensation of acetyl-CoA, b) coenzyme A (CoA) removal, c) decarboxylation and d) hydrogenation. Thus, re-construction of the isopropanol route in other hosts requires application of four enzymes, which are described here in more detail.

First step in the conversion of acetyl-CoA to isopropanol is the thermodynamically unfavorable formation of a carbon-carbon bond by Claisen condensation of two molecules of acetyl-CoA yielding acetoacetyl-CoA (Figure 2-6). This reaction is catalyzed by the acetyl-CoA acetyltransferase (Act, EC 2.3.1.9), also known as acetoacetyl-CoA thiolase or β-ketothiolase due to the reverse reaction being a thiolytic cleavage.

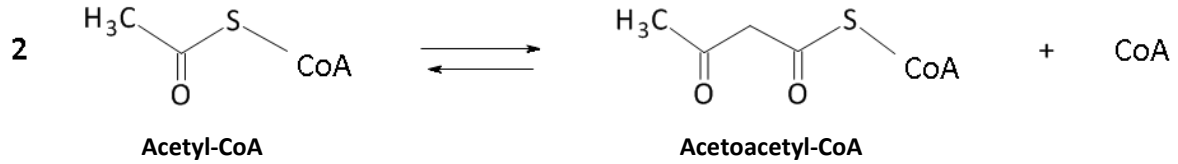

Acetyl-CoA **Acetoacetyl-CoA**

Figure 2-6: Enzymatic reaction catalyzed by the acetyl-CoA acetyltransferase (Act) – EC 2.3.1.9.
Source: BRENDA – The Comprehensive Enzyme Information System.

Act belongs to the enzyme family of thiolases, which catalyzes the reversible thiolytic cleavage of 3-ketoacyl-CoA into acyl-CoA and acetyl-CoA, involving a covalent intermediate formed with a catalytic cysteine [Haapalainen et al., 2006]. Thiolases are key enzymes in the synthesis of fatty acids and the storage compound PHB in bacteria as well as in the formation of a wide range of natural products (secondary metabolites) in eukaryotes, among which are polyketides and isoprenoids (e.g. terpenes, steroid hormones [Holstein and Hohl, 2004]). In its reverse action, thiolases are part of the β-oxidation (fatty acid degradation). Thus, two major types of thiolases can be discriminated which favorably act either in anabolic (EC 2.3.1.9) or catabolic (EC 2.3.1.16) processes under physiological conditions. The Act utilized in isopropanol biosynthesis of *Clostridia* belongs to the anabolic/synthetic thiolases (a.k.a. thiolase II) and is suggested to be the rate-limiting step in the respective pathways [Fox et al., 2014]. Act displays a tetrameric subunit structure, which is stabilized by interactions between an extended loop protruding out of each of the four subunits [Haapalainen et al., 2006]. Cofactors or metal ions are not involved in the reaction [Haapalainen et al., 2006]. The enzyme is competitively inhibited by its product, reduced CoA (CoASH), by oxidation of the catalytic Cys88 [Ithayaraja et al., 2016]. Other inhibitors for Act are ATP and butyryl-CoA [Wiesenborn et al., 1988].

The second step in the conversion of acetyl-CoA to isopropanol is the reversible removal of the CoA moiety from acetoacetyl-CoA to generate acetoacetate (Figure 2-7). Simultaneously, acetyl-CoA is regenerated by transfer of CoA to a carboxylic acid (in this case: acetate), forming a thioester bond. This reaction is catalyzed by the acetate CoA-transferase (Acct, EC 2.8.3.8), also known as acetoacetate:acetate/butyrate CoA-transferase or acetoacetyl-CoA:acetate/butyrate:CoA transferase.

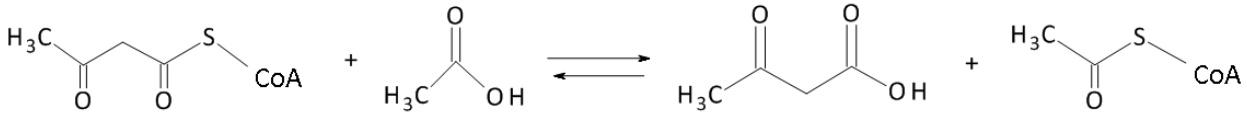

Figure 2-7: Enzymatic reaction catalyzed by the acetate CoA-transferase (Acct) - EC 2.8.3.8.
Source: BRENDA – The Comprehensive Enzyme Information System.

Acct belongs to the enzyme family of transferases, specifically CoA-transferases, which catalyze reversible transfer reactions of CoA from CoA-thioesters to free acids for activation of various carbon compounds. The enzyme name changes according to the organic acid to which the CoA moiety is transferred [Heider, 2001]. In *Clostridia*, Acct is responsible for the conversion of acetoacetyl-CoA to acetoacetate using either acetate or butyrate as CoA acceptor. By this, produced acids are re-utilized during solventogenesis to produce acetone/isopropanol and butanol, as described in 2.3.1 [Wiesenborn et al., 1989]. Acct is a heterodimer of two subunits, forming a tetramer of two subunit pairs (A_2B_2) [Sramek et al., 1977a]. Cooperation of metal ions is not described for the reaction. CoA and other acyl-CoA substrates are competitive inhibitors to acetoacetyl-CoA in a concentration-dependent manner in the acetoacetate-generating direction [Sramek and Frerman, 1975a; Sramek et al., 1977b]. Acetate and butyrate are competitive inhibitors for each others conversion, with acetate being the preferred reactant. For the *Clostridium* Acct, inhibition by physiological levels of acetone and butanol was observed [Wiesenborn et al., 1989].

Third step in the conversion of acetyl-CoA to isopropanol is the decarboxylation of acetoacetate to acetone, which is an irreversible process due to the emanation of CO_2 (Figure 2-8). The reaction is crucial for the production of solvents, because it channels the carbon flux towards acetone and isopropanol generation.

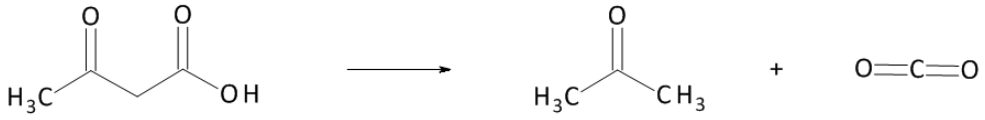

Figure 2-8: Enzymatic reaction catalyzed by the acetoacetate decarboxylase (Adc) - EC 4.1.1.4.
Source: BRENDA – The Comprehensive Enzyme Information System.

The acetoacetate conversion reaction is catalyzed by the acetoacetate decarboxylase (Adc, EC 4.1.1.4), one of the best studied enzymes in the field of microbial solvent production [Davies, 1943]. Adc belongs to the family of decarboxylases, which catalyzes the addition or removal of carboxyl groups to or from a compound. In *Clostridia*, Adc catalyzes the final step in acetone formation. In mammals, Adc is involved in the ketone body production/degradation pathway [Kalapos, 2003; Lopez-Soriano et al., 1985; Lopez-Soriano and Argiles, 1986]. *Clostridium* Adc is a homododecamer of 365 kDa with a subunit size of 27.5 kDa [Gerischer and Durre, 1990]. Neither metal ions nor coenzymes are required for decarboxylation [Rozzell and Benner, 1984]. The reaction mechanism involves a Schiff base formation with the substrate at Lys115 [Tagaki and Westheimer, 1968]. There are various known inhibitors of the Adc, e.g. acetopyruvic acid as competitive inhibitor, heavy metals like Ag and Hg or potassium cyanide as general inhibitors [Davies, 1943; Tagaki et al., 1968]. Several monovalent anions (e.g. borohydride) bind

covalently to the catalytic site of the enzyme, depending on their size and on the nature of the solvent [Fridovich, 1963].

Final step in the conversion of acetyl-CoA to isopropanol is the reduction and hydrogenation of acetone to isopropanol (Figure 2-9). The reaction is catalyzed by the NADPH-dependent enzyme isopropanol dehydrogenase (Idh, EC 1.1.1.80), named according to the reverse reaction. Further names of the enzyme are secondary alcohol dehydrogenase, because of its ability to produce secondary alcohols from aldehydes and 2-ketones, or propan-2-ol:$NADP^+$ oxidoreductase (systematic name according to BRENDA).

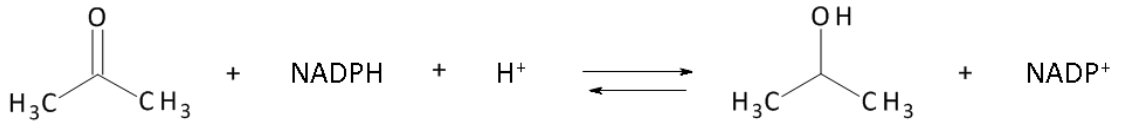

Acetone **Isopropanol**

Figure 2-9: Enzymatic reaction catalyzed by the isopropanol dehydrogenase (Idh) - EC 1.1.1.80.
Source: BRENDA – The Comprehensive Enzyme Information System.

Idh belongs to the ubiquitous family of alcohol dehydrogenases (ADHs), which catalyzes reactions involving primary/secondary alcohols and hemiacetals. Due to its characteristics, Idh can be assigned to the class of zinc- and NAD(P)H-dependent, medium-chain (~350 aa) ADHs [Reid and Fewson, 1994]. In contrast to the primary ADHs, which mainly act on primary alcohols like ethanol and n-butanol (1-butanol) or the corresponding aldehydes (acetaldehyde/butyraldehyde), the secondary ADHs prefer secondary alcohols like isopropanol and 2-butanol or the respective ketones acetone and butanone (methyl ethyl ketone) as substrate. In *Clostridia*, it was assumed that the reductive reaction of solvent formation (alcohol as the terminal electron acceptor) and NAD(P)H oxidation was essential for maintenance of oxidative power for energy-yielding processes in anaerobic bacteria. The reverse reaction might be responsible for introduction of alcohols as carbon source in the central metabolism [Reid and Fewson, 1994]. A homotetrameric assembly of the clostridial enzyme was confirmed by Korkhin et al. [Korkhin et al., 1998]. The single subunit is organized in a Rossmann fold cofactor-binding (residues 154-294, *C. beijerinckii* numbering) and a catalytic domain (1-153 and 295-351), both separated by a cleft, which harbors the zinc ion within the catalytic site at the bottom of the cleft. Known competitive inhibitors of Idh (investigated for the *T. brockii* isoenzyme) are pyrazole and hydroxylamine [McMahon and Mulcahy, 2002], as well as dimethyl sulfoxide (DMSO), a structural analogue of acetone [Kleifeld et al., 2000]. Forward reaction substrates acetone and NADPH are competitive inhibitors of the reverse reaction substrates isopropanol and $NADP^+$ and vice versa [Pereira et al., 1994].

2.4 Lignocellulose Hydrolysates as Feedstock for Microorganisms

Economic viability of a bio-based production process is strongly dependent on the price of the chosen substrate, i.e. the raw material/feedstock that is converted to the valuable and sellable product. In an industrial bio-solvent production process, the substrate accounts for about 40-60% of the overall costs, thus constituting a major factor to influence the competitiveness of a biorefinery with conventional petrochemical platforms [Jones and Woods, 1986; Lenz and Moreira, 1980; Qureshi and Blaschek, 2001]. In earlier microbial ABE fermentation or ethanol production, sugar from molasses or starch derived from corn was utilized as primary carbohydrate source. Rising prices of these so-called first generation

feedstocks played a vital part in the switch to fossil-based processes in the late 1950s [Lin and Blaschek, 1983]. In order to regain economic attractiveness, lignocellulose is now considered an interesting source of nutrients for second generation bio-bulk chemical production. Lignocellulosic plant biomass is the most abundant renewable resource on earth [Drissen et al., 2009; la Grange et al., 2010]. It can be taken from a variety of sources, e.g. hard- and softwood forests, grasses, agricultural residues like wheat straw or corn stover or waste products of the food-processing, woodworking or paper industry. Therefore, lignocellulose is cheap, available in sufficient quantities, sustainable and renewable because regrowable and recyclable, and generating very low net GHG emissions due to the carbon-fixation capacity of plants. Additionally, it is non-food and thus does not contribute to the "food versus fuel dilemma", which often arises with first generation feedstocks. Using industrial or municipal waste products has the advantage of exploiting materials as cheap feedstock that are otherwise discarded or even burned [Zondervan et al., 2011]. The three main constituents of lignocellulosic material (~90% of plant dry mass) are the polysaccharides cellulose and hemicellulose (jointly termed holocellulose) and lignin, which form the plant cell walls together with certain amounts of pectin and other compounds [Timell, 1967]. Their ratio varies depending on the biomass origin [Sun and Cheng, 2002]. For example, hardwood (woody angiosperms) generally contains a higher amount of cellulose (up to 55%), whereas softwood (gymnosperms) and annual plants (herbaceous angiosperms) usually have a higher content of hemicellulose and lignin [Mathews et al., 2015; Taherzadeh and Karimi, 2008]. The ratios also differ within a single plant species depending on its age and the environmental conditions [Timell, 1967]. In addition, woody material contains resins, phenols, quinones and tannins which often exert protective anti-microbial activities [Klinke et al., 2004].

By far the most abundant component in lignocellulose is cellulose. It is a linear polymer of the repeat unit cellobiose, a disaccharide of D-glucose monomers linked by β-1,4-glycosidic bonds. The long cellobiose chains are packed together by hydrogen bonds and van der Waals forces to form compact microfibrils [Delmer and Amor, 1995]. Around one third of the fibrillar cellulose is structurally unorganized (amorphous), whereas two thirds are present in crystalline form [Taherzadeh and Karimi, 2008]. The cellulose microfibrils are entwined by strands of pectin and hydrogen bonded by hemicelluloses, as well as covered by lignin [Delmer and Amor, 1995], as pictured in Figure 2-10.

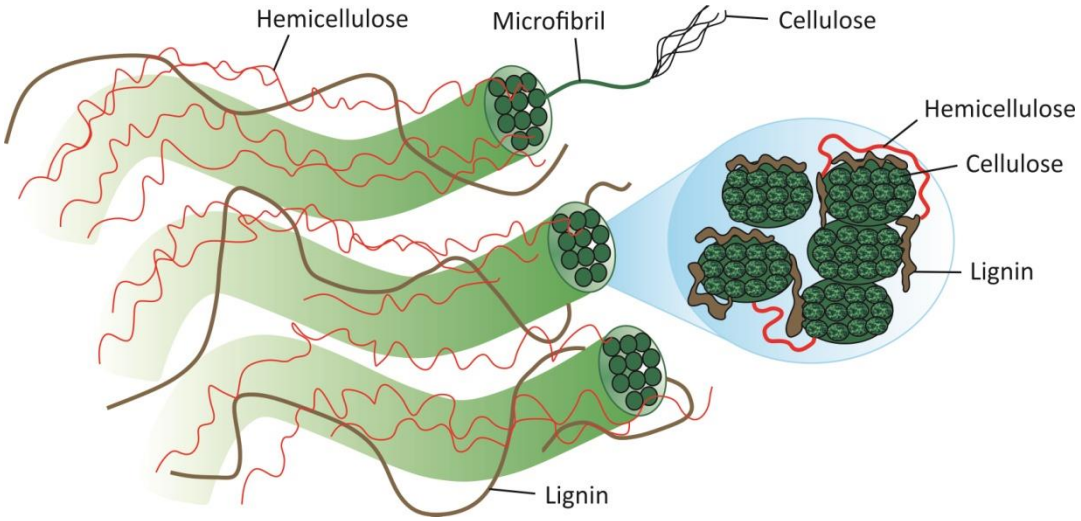

Figure 2-10: Schematic presentation of plant cell wall structure and microfibril cross-section.
Adapted from [Lee et al., 2014].

Hemicellulose, the second major component of plant cell walls, is a random, amorphous and branched heteropolymer comprised of pentoses (D-xylose, L-arabinose) and hexoses (D-mannose, D-glucose, D-galactose, D-rhamnose), linked by mostly β-1,4-glycosidic bonds or sometimes β-1,3-glycosidic bonds, and of uronic acids (e.g. D-glucuronic acid, D-galacturonic acid) [Kumar et al., 2009]. The structure and composition of hemicellulose monomers varies strongly between different plant species: D-mannose is e.g. more dominant in softwood, while hardwood hemicellulose contains more D-xylose and is often highly acetylated [Grethlein, 1985]. The third main lignocellulose constituent lignin is a complex and large aromatic polymer, which is amorphous, water-insoluble and consists of phenylpropane subunits in a three-dimensional structure. The monomers of the lignin network are coniferyl alcohol, coumaryl alcohol and sinapyl alcohol, which are cross-linked by alkyl-aryl, alkyl-alkyl and aryl-aryl ether bonds [Kumar et al., 2009]. In plant cell walls, lignin imparts structural support, impermeability and resistance against microbial invasion [Crawford and Crawford, 1976]. In general, softwood contains more lignin than hardwood, and the amount of each alcohol monomer varies strongly between different plant species [Mathews et al., 2015].

Only few organisms are actively able to digest woody biomass. For example, several brown-, white- and soft-rot fungi are capable of producing and excreting enzymes that catalyze the depolymerization of the main plant cell wall components cellulose, hemicellulose and lignin [Sun and Cheng, 2002]. Also some bacteria, e.g. the anaerobic *Clostridium thermocellum*, *C. cellulolyticum* and *C. stercorarium*, exhibit saccharolytic properties towards crystalline cellulose and xylan (a hemicellulose heteropolymer of mainly D-xylose units) [Gefen et al., 2012; Mingardon et al., 2011; Mitchell et al., 1995; Zverlov and Schwarz, 2008]. Most extensively studied in this context is the aerobic soft-rot fungus *Trichoderma reesei*, which secretes various cellulases and hemicellulases for plant decay [Montenecourt, 1983; Oksanen et al., 2000]. Unfortunately, the fungus is not suitable for biotechnological solvent production, and enzyme conversion rates and concentrations obtained are generally quite low (e.g. main cellobiohydrolase I: ~50 mg L^{-1} [Nykanen et al., 1997]). Thus, a plethora of expensive enzymes would be required for complete lignocellulose degradation (e.g. β-1,4-endoglucanase, β-1,4-exoglucanase/cellobiohydrolase and β-glucosidase for cellulose [la Grange et al., 2010]), which renders their isolated application uneconomic. In contrast to cellulolytic fungi, most microbes prefer the monomeric sugars, in most cases D-glucose, as carbon source. Therefore, the lignocellulosic feedstock must be broken up to release the individual constituents. In the past, numerous different pretreatment methods have been developed for liberation of usable sugars from the complex and recalcitrant material [Carvalheiro et al., 2008; Kumar et al., 2009; Lee et al., 2014; Sun and Cheng, 2002]. They usually aim at separation of the sugar fractions (cellulose and hemicellulose) from the protective lignin part ("delignification"), at the reduction of cellulose crystallinity and at increasing the porosity to facilitate accessibility for further hydrolysis without destroying the polysaccharides [Taherzadeh and Karimi, 2008].

The choice of pretreatment method is dependent on the type of lignocellulosic material and on the overall goal to be achieved. Some processes like milling or irradiation will only physically operate on the biomass, increasing the accessibility and decreasing the crystallinity without separating lignin from the polysaccharides. In contrast, most of the chemical treatments effectuate the partial or even complete delignification, although the harsh conditions applied can cause a certain loss of hemicellulosic sugars. Table 2-5 lists the most investigated pretreatment methods for lignocellulosic biomass, including their impact on the material and their general advantages and disadvantages.

Table 2-5: Summary of various pretreatment methods for lignocellulosic biomass.
Source: [Taherzadeh and Karimi, 2008].

Pretreatment	Active agent	Effect on biomass	Remarks
Physical			
Milling	Ball, hammer, colloid	Accessible surface area ↑ Cellulose crystallinity ↓ Degree of polymerization ↓	Energy demanding No removal of lignin Limited up-scaling potential No chemicals required
Irradiation	Gamma ray, electron beam, microwave		
Pyrolysis			
Hydrothermal			
(Physico-) Chemical			
Explosion	Steam, ammonia fiber, CO_2, SO_2	Accessible surface area ↑ Cellulose crystallinity ↓ Degree of polymerization ↓ Partial/complete delignification Partial/complete hydrolysis of hemicellulose	Effective Rapid conversion Scale-up possible Harsh conditions Formation of inhibitors Chemicals required
Alkali	Sodium/calcium hydroxide, ammonia, ammonium sulfite		
Acid	Sulfuric, hydrochloric, phosphoric acid		
Gas	Chlorine, nitrogen, sulfur dioxide		
Oxidizing agents	Hydrogen peroxide, wet oxidation, ozone		
Solvent extraction (“Organosolv”)	Ethanol-water, benzene-water, ethylene glycol, swelling agents		
Biological	Fungi Fungal enzymes	Delignification Degree of polymerization ↓ Partial hydrolysis of hemicellulose	Pretreatment required Low energy requirement No chemicals required Mild conditions Slow conversion Limited up-scaling potential

Of particular interest in the context of this work is the so-called “Organosolv” process, in which the biomass is submerged in a solvent-water mixture, heated and pressurized to extract and fractionate the main lignocellulose constituents. “Organosolv” is often combined with subsequent enzymatic hydrolysis to ensure the complete depolymerization of cellulose fibers. An advantage of this method is the quite distinct separation of (solid) cellulose fibers from (solubilized) hemicelluloses and lignin, in combination with minimized degradation of sugars. No previous milling of the feedstock is necessary and the organic solvent can be recycled and reused afterwards. Disadvantages are the high energy consumption and the high initial cost of solvent [Lee et al., 2014]. The lignocellulose hydrolysates resulting from this pretreatment process are either rich in D-glucose (cellulose/glucose fraction) or in C_5 sugars (hemicellulose fraction) and can serve as carbon and nutrient sources for subsequent microbial product generation. Due to its high purity, the remaining lignin fraction can be utilized for the production of phenolic resins, epoxies, adhesives, polyolefins and other valuable materials [Stewart, 2008].

A major limiting factor in the application of several pretreatment methods for biomass hydrolysis is the formation of lignocellulose-derived inhibitory compounds (hereafter denoted as inhibitors). Especially,

the most effective physicochemical processes lead to uncontrollable degradation reactions that promote inhibitor generation from decomposition of the main cell wall constituents. The term "inhibitors" is derived from the damaging effect on microorganisms, leading to inhibition of cell growth and disturbances in metabolic and enzymatic activities [Nicolaou et al., 2010]. The synergistic toxicity of inhibitors can eventually result in reduction of yield and production rate of the desired product and thus, severely impedes utilization of lignocellulose hydrolysates as cheap carbon sources in bio-based processes. Table 2-6 presents a selection from the bouquet of inhibitors emerging from lignocellulose pretreatment.

Table 2-6: Lignocellulose-derived inhibitors, their origin and general inhibitory cellular mechanisms.
Source: [a] [Nicolaou et al., 2010], [b] [Almeida et al., 2007], [c] [Palmqvist and Hahn-Hagerdal, 2000b], [d] [Sears et al., 1971], [e] [Ando et al., 1986], [f] [Dunlop, 1948], [g] [Ulbricht et al., 1984].

Inhibitory compound[b, c]	Origin	Inhibitory mechanism[a]
Weak aliphatic acids		Intracellular anion accumulation Drop of intracellular pH Uncoupling of membrane proton-motive force ATP depletion by active export Breakdown of membrane potential for energy generation
Acetic acid	Hemicellulose[c]	
Formic acid	HMF[g]	
Levulinic acid	HMF[g]	
Furan derivatives		Inhibition of energy metabolism Inhibition of enzymatic activity Depletion of NAD(P)H due to detoxification reactions Inactivation of cell replication
5-(Hydroxymethyl)furfural (HMF)	Hexoses[g]	
Furfural	Pentoses[f]	
Phenolic compounds	Lignin[d, e]	Damage of membrane integrity Generation of reactive O_2 species → Diversity of phenolics complicates proposition of a general mechanism
4-Hydroxybenzaldehyde		
Vanillin		
Syringaldehyde		
4-Hydroxybenzoic acid		
Vanillic acid		
Syringic acid		
Phenol		

Optimization of pretreatment processes often aims at minimization of inhibitor formation, balancing delignification, polysaccharide solubilization and degradation by variation of temperature, pH, time and applied chemicals. Also, several detoxification methods have been developed to purify lignocellulose hydrolysates from the inhibitory compounds or to mitigate their destructive effects. For example, "overliming", i.e. the addition of calcium hydroxide is known to effectively detoxify hydrolysates and increase the yield of the desired microbial product, but it can also lead to loss of monosaccharides [Larsson et al., 1999]. Strain adaptation or a careful feeding strategy can further improve utilization of lignocellulosic feedstock to ultimately contribute to the development of an economic bio-based refinery platform.

3 Aims and Objectives

The overall aim of this work was optimization of biotechnological isopropanol production by engineered *Escherichia coli*. To achieve this goal, the thesis concentrates on improvement of the cultivation conditions, the feedstock, the production process and the bacterial strain itself.

The research objectives focus on:

a) Construction and comparison of recombinant isopropanol-producing *E. coli* strains

b) Identification of suitable cultivation conditions for isopropanol production

c) Evaluation of a lignocellulose hydrolysate as carbon source for isopropanol production

d) Demonstration of process scale-up from 100 mL shake flask to a 10 L bioreactor

e) Assessment of an integrated method for product separation and recovery

f) Identification and elimination of a competing metabolic pathway

This work aims to offer insight into critical metabolic and enzymatic limitations of the process. It is targeted at improving the microbial isopropanol production in terms of concentration, yield and productivity using a beech wood hydrolysate as an alternative carbon source. The results will be used to provide recommendations for further strain optimization, enzyme selection and process design.

4 Material and Methods

4.1 Material

4.1.1 Chemicals

Table 4-1: List of chemicals.
Chemicals are listed in alphabetical order. Numbers and single letters are omitted in the order.

Chemical	Manufacturer/Supplier	Catalog no. / Lot
Acetic acid, ROTIPURAN®, 100%	Carl Roth GmbH & Co. KG, Karlsruhe, Germany	3738.1 / 075224934
Acetone, ROTISOLV® HPLC, ≥99.9%	Carl Roth GmbH & Co. KG	7328.2 / 989171
Acrylamide/bisacrylamide solution, Rotiphorese® 30% (29:1)	Carl Roth GmbH & Co. KG	A124.2 / 06725
Agar-agar, Kobe I (powder)	Carl Roth GmbH & Co. KG	5210.2 / 226243001
Agarose, peqGOLD Universal	VWR Chemicals, Darmstadt, Germany	35-1020 / H45140019
Ammonium chloride (NH_4Cl), ≥99.5%	Carl Roth GmbH & Co. KG	K298.1 / 131166479
Ammonium persulfate (APS), ≥98%	Carl Roth GmbH & Co. KG	9592.3 / 324212912
Ammonium sulfate ($(NH_4)_2SO_4$), ≥99.5%	Carl Roth GmbH & Co. KG	3746.1 / 425232553
Ampicillin sodium salt, ≥97%	Carl Roth GmbH & Co. KG	K029.2 / 296232377
L(+)-Arabinose, ≥99%	Carl Roth GmbH & Co. KG	5118.3 / 486225067
Bovine serum albumin (BSA), fraction V, ≥98%	Carl Roth GmbH & Co. KG	8076.2 / 067254757
Bromophenol blue sodium salt	Carl Roth GmbH & Co. KG	A512.1 / 293200287
Calcium chloride ($CaCl_2$), ≥94%	Carl Roth GmbH & Co. KG	A119.1 / 29678497
Chloramphenicol, ≥98.5%	Carl Roth GmbH & Co. KG	3886.1 / 373203159
Cobalt(II) chloride hexahydrate ($CoCl_2 \times 6\ H_2O$)	Carl Roth GmbH & Co. KG	T889.1 / 26897580
Coomassie brilliant blue G 250	Carl Roth GmbH & Co. KG	9598.2 / 03462798
Copper(II) sulfate pentahydrate ($CuSO_4 \times 5\ H_2O$)	Merck KGaA, Darmstadt, Germany	1.02790.0250 / A354690223
Di-Ammonium hydrogen citrate ($(NH_4)_2$-H citrate), ≥98%	Carl Roth GmbH & Co. KG	P735.2 / 455236238
Di-Potassium hydrogen phosphate (K_2HPO_4), ≥99%	Carl Roth GmbH & Co. KG	P749.3 / 244215281
Di-Sodium hydrogen phosphate dihydrate ($Na_2HPO_4 \times 2\ H_2O$), ≥99.5%	Carl Roth GmbH & Co. KG	4984.1 / 116240120
Ethylenediamine tetraacetic acid disodium salt dihydrate (Na_2-EDTA $\times 2\ H_2O$), ≥99%	Carl Roth GmbH & Co. KG	8043.1 / 275229139
Ethanol, denatured, ≥99.8%	Carl Roth GmbH & Co. KG	K928.2 / 197258238
Ethanol absolute	VWR Chemicals	20821.321 / 16C150506
Ethidium bromide solution, 1% (w/v)	Carl Roth GmbH & Co. KG	2218.1 / 24254590
D(+)-Glucose monohydrate ($C_6H_{12}O_6 \times H_2O$)	Carl Roth GmbH & Co. KG	6887.5 / 216244060
Glycerol, ROTIPURAN®, 99.5%	Carl Roth GmbH & Co. KG	3783.5 / 426250757
Glycine, ≥98.5%	Carl Roth GmbH & Co. KG	T873.2 / 514223093

Chemical	Manufacturer/Supplier	Catalog no. / Lot
Hydrochloric acid (HCl), fuming, ROTIPURAN®, 37%	Carl Roth GmbH & Co. KG	4625.2 / 234214371
Isopropanol (2-Propanol), ROTISOLV® HPLC, ≥99.9%	Carl Roth GmbH & Co. KG	7343.1 / 1096151
Isopropyl β-D-1-thiogalactopyranoside (IPTG), ≥99%	Carl Roth GmbH & Co. KG	2316.4 / 466251439
Iron(III) chloride ($FeCl_3$), ≥98.5%	Carl Roth GmbH & Co. KG	5192.1 / 205228662
Kanamycin sulfate, ≥750 I.U./mg	Carl Roth GmbH & Co. KG	T832.3 / 464222339
Magnesium chloride hexahydrate ($MgCl_2 \times 6\ H_2O$), ≥99%	Carl Roth GmbH & Co. KG	2189.2 / 136239269
Magnesium sulfate heptahydrate ($MgSO_4 \times 7\ H_2O$), ≥99%	Carl Roth GmbH & Co. KG	P027.1 / 484220520
Manganese(II) sulfate monohydrate ($MnSO_4 \times H_2O$), ≥98%	Carl Roth GmbH & Co. KG	4487.1 / 16359021
2-Mercaptoethanol, pure	SERVA Electrophoresis GmbH, Heidelberg, Germany	28625
Methanol, ROTISOLV® HPLC, ≥99.9%	Carl Roth GmbH & Co. KG	7342.1 / 10023001
Phosphoric acid (ortho-), 85%	Carl Roth GmbH & Co. KG	2608.2 / 124201055
L-Proline, Calbiochem	Sigma-Aldrich Chemie GmbH, Munich, Germany	5370 / D00125228
SDS, Roti®-Stock 20%	Carl Roth GmbH & Co. KG	1057.1 / 294216717
SIGMAFAST™ BCIP®/NBT tablets	Sigma-Aldrich Chemie GmbH	B5655-25TAB / SLBN0689V
Sodium azide (NaN_3), pure	AppliChem GmbH, Darmstadt, Germany	A1430,0100 / 8M005993
Sodium chloride (NaCl), ≥99.5%	Carl Roth GmbH & Co. KG	3957.1 / 473205342
Sodium hydroxide (NaOH), 99%	Carl Roth GmbH & Co. KG	6771.1 / 365233198
Sodium sulfate (Na_2SO_4), ≥99%	Carl Roth GmbH & Co. KG	8560.1 / 234211654
Struktol J673	Schill+Seilacher, Hamburg, Germany	5121607
Tetramethylethylenediamine (TEMED), 98.5%	Carl Roth GmbH & Co. KG	2367.3 / 196239027
Thiamine hydrochloride, ≥98.5%	Carl Roth GmbH & Co. KG	T911.1 / 503207747
TRIS, PUFFERAN®, ≥99.9%	Carl Roth GmbH & Co. KG	4855.3 / 366244777
Triton X® 100, pure	Carl Roth GmbH & Co. KG	3051.4 / 195227705
Tryptone/peptone ex casein	Carl Roth GmbH & Co. KG	8952.4 / 196244119
Tween® 20	Carl Roth GmbH & Co. KG	9127.1 / 13357019
D(+)-Xylose, ≥98.5%	Carl Roth GmbH & Co. KG	5537.2 / 465225068
Yeast extract (powder)	Carl Roth GmbH & Co. KG	2363.2 / 067252733
Zinc sulfate heptahydate ($ZnSO_4 \times 7\ H_2O$), ≥99.5%	Carl Roth GmbH & Co. KG	K301.1 / 49150037

4.1.2 Buffers and Solutions

Table 4-2: List of buffers and solutions.
Individual chemicals are listed in Table 4-1. Enzymes are listed in Table 4-11.

Buffer/solution	Ingredients	Concentration [g L^{-1}]^a	Preparation
APS solution	APS	Saturated	APS powder was added to 1 mL dH_2O in a 1.5 mL Eppendorf tube and vortexed until a satured solution was achieved.
L-arabinose solution, 10% (w/v)	L(+)-arabinose	100	Ingredient was solubilized in ddH_2O, sterile-filtered and stored in aliquots at -20 °C.
Blocking solution	BSA	30	Ingredient was solubilized in TBS buffer and stored at 4 °C.
	TBS buffer		
Destaining solution	Isopropanol	20% (v/v)	Ingredients were filled up to 100 mL with dH_2O.
	Acetic acid	10% (v/v)	
Electrophoresis buffer, 10×	TRIS	30.28	Ingredients were filled up to 1 L with dH_2O, stirred and heated until all components were solubilized.
	Glycine	144	
	SDS	10	
	NaN_3 solution, 10%	0.1% (v/v)	
Ethidium bromide solution, 0.1% (w/v)	Ethidium bromide	1	Ethidium bromide solution (1%) was diluted 1:10 with dH_2O.
Glucose solution, 50% (w/v)	$C_6H_{12}O_6 \times H_2O$	550	Ingredient was solubilized in dH_2O and autoclaved (15 min, 121 °C).
Lysis buffer	Tris buffer, 50 mM, pH 8.0		Ingredients were filled up to 5 mL with Tris buffer and solubilized. Lysis buffer was always freshly prepared.
	$MgCl_2 \times 6\ H_2O$	0.4066	
	Lysozyme	1	
	Benzonase	10 U mL^{-1}	
Resolving gel buffer	TRIS	181.8	Ingredients were solubilized in dH_2O, pH was adjusted to 8.8 with HCl and filled up to 1 L with dH_2O.
	SDS	4	
	NaN_3 solution, 10%	0.1% (v/v)	
SDS-PAGE sample buffer	TRIS	27.2	Ingredients were solubilized in dH_2O, pH was adjusted to 6.8 with HCl and filled up to 1 L with dH_2O. 2-Mercaptoethanol was added (10 µL mL^{-1}) shortly before sample preparation.
	SDS	50	
	Bromophenol blue	0.5	
	Glycerol	500	
NaN_3 solution, 10% (w/v)	Sodium azide	100	Ingredient was solubilized in dH_2O and filled up to 1 L with dH_2O.
Stacking gel buffer	TRIS	60.6	Ingredients were solubilized in dH_2O, pH was adjusted to 6.8 with HCl and filled up to 1 L with dH_2O.
	SDS	4	
	NaN_3 solution, 10%	0.1% (v/v)	
Staining solution	Coomassie G 250	1 tablet	Ingredients were solubilized in 150 mL dH_2O and filtered.
	Isopropanol	66.7% (v/v)	
	Acetic acid	33.3% (v/v)	
Substrate solution	SIGMAFAST™ BCIP/NBT	1 tablet	Ingredient was solubilized in 10 mL dH_2O.

Buffer/solution	Ingredients	Concentration [g L^{-1}][a]	Preparation
TAE buffer, 50×	TRIS	242	Ingredients were solubilized in dH_2O, pH was adjusted to 8.5 with HCl and filled up to 1 L with dH_2O.
	Acetic acid	5.71% (v/v)	
	Na_2-EDTA × 2 H_2O	18.6	
TBS buffer	TRIS	1.2114	Ingredients were solubilized in dH_2O, pH was adjusted to 7.5 with HCl and filled up to 1 L with dH_2O.
	NaCl	8.766	
TBS-TT buffer	TRIS	2.4228	Ingredients were solubilized in dH_2O, pH was adjusted to 7.5 with HCl and filled up to 1 L with dH_2O.
	NaCl	29.22	
	Tween® 20	0.05% (v/v)	
	Triton X® 100	0.2% (v/v)	
Transfer buffer	Methanol	20% (v/v)	Ingredients were solubilized in 1 L dH_2O.
	TRIS	3.0285	
	Glycine	14.4128	
	SDS	1	
Tris buffer, 50 mM, pH 8.0	TRIS	6.057	Ingredient was solubilized in dH_2O, pH was adjusted to 8.0 with HCl and filled up to 1 L with dH_2O.

[a] If not denoted differently.

4.1.3 Lignocellulose Hydrolysate

The lignocellulose hydrolysate used in this work was provided by Fraunhofer Center for Chemical-Biotechnological Processes (CBP; Leuna, Germany) and was prepared from beech wood. The hydrolyzation process is termed “Organosolv pulping” and involves an ethanol-water fractionation of the beech wood with glucose, lignin and xylose as the main products. In detail, industrially debarked beech wood (*Fagus sylvatica*) chips were pulped with a mixture of ethanol and water at high temperature and pressure (190 °C, 28 bar, 2 h) yielding the so-called mother liquor and the fiber fraction. Lignin was derived from the mother liquor via water dilution or thermal precipitation (“Organosolv lignin”). A fraction of C_5 sugars (mainly xylose) was obtained after ethanol recovery of the liquor. Glucose was generated by enzymatic hydrolysis of the fiber fraction (50 °C, pH 5, 48 h), after fiber washing and dewatering. The glucose fraction of the beech wood hydrolysate was used during the experiments of this work and is further denoted as BWH.

BWH was sterile-filtered (syringe filter ReliaPrep™, 0.2 µm mesh) before utilization as a carbon source in bacterial cultivations in shake flask scale. Sterile filtration was not performed for use of BWH in 10 L bioreactor scale. BWH was stored at 4 °C. Table 4-3 shows an HPLC analysis of substances contained in BWH.

Table 4-3: Content analysis of BWH – glucose fraction - batch no. K020/21.
Content analysis was performed via HPLC at CBP (Leuna, Germany). Measurements were performed with an Agilent system (Agilent Technologies, Inc., Santa Clara, CA, USA), with a Bio-Rad-Aminex HPX-87H column, refractive index detector and 0.005 M sulfuric acid as mobile phase. All standards were calibrated in a range of 0.1-10.0 g L^{-1} in ddH_2O.

Substance	Concentration [g L^{-1}]
Glucose	381.3
Xylose	94.6
Acetate	7.9
Cellobiose	5.5
Hydroxymethylfurfural	n.m.
Furfural	n.m.
Formate	n.m.
Levulinic acid	n.m.
Mannan	n.m.
Galactan	n.m.
Rhamnan	n.m.
Arabinan	n.m.

Residual ethanol was <0.2% (w/v). Detection limits were 0.02 g L^{-1} for hydroxymethylfurfural, 0.015 g L^{-1} for furfural and 0.03 g L^{-1} for formate and levulinic acid. n.m.… not measurable

4.1.4 Bacterial Strains

Table 4-4: List of bacterial strains.
DSMZ… *Deutsche Sammlung von Mikroorganismen und Zellkulturen* (Braunschweig, Germany).

***E. coli* strains**	**Genotype**	**Source**
DH5α	F^- Φ80lacZΔM15 Δ(lacZYA-argF)U169 recA1 endA1 hsdR17 (r_k^-, m_k^+) phoA supE44 thi-1 gyrA96 relA1 λ^-	Thermo Fisher Scientific - Life Technologies GmbH, Darmstadt, Germany
JM109[a]	recA1 endA1 gyrA96 thi hsdR17 supE44 relA1 λ^- Δ(lac-proAB) (F' traD36 proAB $laqI^qZ\Delta M15$)	DSMZ (DSM3423)

[a] Defective for synthesis of cell walls; strain forms mucoid colonies in minimal medium.

4.1.5 Bacterial Growth Media, Antibiotics and Supplements

Table 4-5: List of bacterial (complex) growth media.
Individual ingredients are listed in Table 4-1. Minimal medium recipe is listed in Table 4-19.

Medium	Ingredients[a]	Concentration [g L^{-1}]	Preparation
LB	Tryptone/peptone	10	Ingredients were solubilized in dH_2O, pH was adjusted to 7.0 with 5 N NaOH, filled up to 1 L with dH_2O and autoclaved.
	NaCl	10	
	Yeast extract	5	

[a] For preparation of agar plates, 15.0 g L^{-1} agar was added.

Table 4-6: List of antibiotics.
Antibiotics were solubilized in dH_2O, sterile-filtered (syringe filter ReliaPrep™, 0.2 µm mesh) and added to the cooled down (~55 °C) medium after autoclaving. For long-term storage antibiotics were aliquoted and stored at -20 °C. Substances are listed in Table 4-1.

Antibiotic	Stock concentration [mg mL^{-1}]	Final concentration in medium [µg mL^{-1}]
Kanamycin	50	50 (15 for Red®/ET® recombination)
Chloramphenicol	15	15
Ampicillin	50	50

Table 4-7: List of supplements.
Supplements were solubilized in dH_2O, sterile-filtered (syringe filter ReliaPrep™, 0.2 µm mesh) and added to the cultivation medium. For long-term storage, supplements were aliquoted and stored at -20 °C. Substance is listed in Table 4-1.

Supplement	Stock concentration [M]	Final concentration in medium [mM]
IPTG	1.0	0.1

4.1.6 Plasmid DNA

Table 4-8: List of acquired plasmid DNA.
Schematic plasmid maps and DNA sequences (if available) can be found in the denoted appendix section.

Plasmid	Features	Manufacturer/Supplier	Appendix
708-FLPe-Cm^R	FLPe recombinase gene, chloramphenicol resistance	Gene Bridges GmbH, Heidelberg, Germany	
pFRT[a]	FRT-PGK-gb2-neo-FRT template DNA for generating an FRT-flanked PGK-gb2-neo cassette; kanamycin resistance	Gene Bridges GmbH	
pRedET-Amp^R [a]	RecA recombinase gene, arabinose-inducible pBAD, ampicillin resistance, temperature-sensitive	Gene Bridges GmbH	
pHSG299	Kanamycin resistance, pMB1 ori, lac promoter	Takara Korea Biomedical Inc., Seoul, South Korea	Table A-1, page 176 Figure A-1, page 177

[a] Part of the Quick & Easy *E. coli* Gene Deletion kit (Gene Bridges GmbH, Heidelberg, Germany; Table 4-14).

Table 4-9: List of constructed plasmid DNA (this work).
Schematic plasmid maps and DNA sequences can be found in the denoted appendix section.

Plasmid	Features	Size [bp]	Appendix
pRK_ISO_1E2e3c4c	atoB (coding for Act-StrepII (1E), *E. coli*), atoDA (coding for Acct-His_{10} (2e), *E. coli*), adc (coding for Adc-FLAG (3c), *C. acetobutylicum*), adh (coding for Idh-c-Myc (4c), *C. beijerinckii*), kanamycin resistance, pMB1 ori, CER sequence	2788	Table A-2, page 178 Figure A-2, page 181
pRK_ISO_1C2e3c4c	thlA (coding for Act-StrepII (1C), *C. acetobutylicum*) atoDA (coding for Acct-His_{10} (2e), *E. coli*) adc (coding for Adc-FLAG (3c), *C. acetobutylicum*), adh (coding for Idh-c-Myc (4c), *C. beijerinckii*), kanamycin resistance, pMB1 ori, CER sequence	2782	Table A-3, page 182 Figure A-3, page 185

4.1.7 Primer Oligonucleotides

Table 4-10: List of primer oligonucleotides.
All primers were ordered from Eurofins Genomics (Ebersberg, Germany). Freeze-dried primers were solubilized in ddH_2O to a working concentration of 100 pmol μL^{-1}.

Primer name	Function	Sequence (5'-3')	T_M [°C]
ISO_insert	Sequencing primer for isopropanol pathway plasmid	TATGGACCTGGTAACCGGCAG	61.8
FRT_FW	Forward primer for generating an FRT-flanked PGK-gb2-neo cassette	CCAAAGCTAAAGTAAACAATGTTGATCCGGCGAAGCT GCAAGAATCCAGCAATTAACCCTCACTAAAGGGCG	58.4[a]
FRT_RV	Reverse primer for generating an FRT-flanked PGK-gb2-neo cassette	TCAGCGTTGATGTAGTTAGCAACGTATTCCTGAACTTT CTCGATACGTTCTAATACGACTCACTATAGGGCTC	58.9[a]
Genome_Pta_FW	Forward primer for verification of Red®/ET® recombination mutants	TAACAAACTGAACGCACCGGT	57.9
Genome_Pta_RV	Reverse primer for verification of Red®/ET® recombination mutants	CAGTCAGCTGATAACGGAACG	59.8

Underlined parts indicate regions serving as PCR primers for amplification of the linear functional homology cassette in Red®/ET® recombination (4.2.2.8, page 54). T_M… melting temperature according to manufacturer, [a] T_M was calculated by OligoAnalyzer 3.1 according to the annealing region (underlined).

4.1.8 Enzymes and Molecular Biology Reagents

Table 4-11: List of enzymes and molecular biology reagents.
Enzymes and molecular biology reagents were stored at -20 °C.

Enzyme/reagent	Manufacturer/Supplier	Catalog no.	Stock conc.
Benzonase® endonuclease[a]	Merck KGaA, Darmstadt, Germany	1.01695.0001	250 U μL^{-1}
dATP	Thermo Fisher Scientific - Life Technologies GmbH, Darmstadt, Germany	#R0141	100 mM
dCTP	Thermo Fisher Scientific	#R0151	100 mM
dGTP	Thermo Fisher Scientific	#R0161	100 mM
dTTP	Thermo Fisher Scientific	#R0171	100 mM
dNTP mix[b]	(Solution of dATP, dCTP, dGTP, dTTP)		2 mM
Phusion HF reaction buffer	Thermo Fisher Scientific	[d]	5×
Lysozyme, from chicken egg white, ~95% protein[c]	Sigma-Aldrich Chemie GmbH, Munich, Germany	L7651	1 mg mL^{-1}, 50400 U mg^{-1} solid
Phusion High-Fidelity DNA polymerase	Thermo Fisher Scientific	#F530L	2 U μL^{-1}
Pfu DNA polymerase	Thermo Fisher Scientific	#EP0502	2.5 U μL^{-1}
Pfu reaction buffer (with 25 mM $MgSO_4$)	Thermo Fisher Scientific	[d]	10×

[a] Degradation of DNA and RNA, [b] provision of deoxynucleoside triphosphates for PCR, [c] lysis of bacterial cell walls (glycoside hydrolase), [d] buffers were provided with the respective enzyme

4.1.9 Antibodies

Table 4-12: List of antibodies.

Antibody	Working concentration (dilution)	Incubation time [h]	Manufacturer/Supplier	Catalog no.	Lot no.
Anti-c-Myc 9E10[a]	(1:50)	2	Udo Conrad, IPK[c] Gatersleben, Germany (kindly provided)		
Anti-FLAG® M2, monoclonal, produced in mouse[a]	1 µg mL^{-1} (1:250)	1	Sigma-Aldrich Chemie GmbH, Munich, Germany	F3165	080M6034 087K6002V SLBJ7864V
Anti-polyHistidine, HIS-1, produced in mouse[a]	2.6 µg mL^{-1} (1:1000)	2	Sigma-Aldrich Chemie GmbH	H1029	013M4866 062M4809
Anti-StrepII®, monoclonal, produced in mouse[a]	0.07 µg mL^{-1} (1:3030)	1	Qiagen GmbH, Hilden, Germany	1025129	145036825 145049975
Anti-Mouse IgG-Alkaline phosphatase conjugated, polyclonal, produced in goat[b]	0.26 µg mL^{-1} (1:10000)	1	Sigma-Aldrich Chemie GmbH	A3562	SLBL8992V

[a] Stored at -20 °C. [b] Stored at 4 °C. [c] *Leibniz-Institut für Pflanzengenetik und Kulturpflanzenforschung*

4.1.10 Markers

Table 4-13: List of markers and loading dyes.

Marker / Loading dye	Manufacturer/Supplier	Catalog no.
MassRuler DNA ladder mix, ready-to-use[a]	Thermo Fisher Scientific – Life Technologies GmbH, Darmstadt, Germany	#SM0403
Loading dye (6×)[a]	Thermo Fisher Scientific	#R0611
PageRuler Prestained Protein Ladder[b]	Thermo Fisher Scientific	#26616

[a] Stored at 4 °C. [b] Stored according to manufacturer recommendations.

4.1.11 Kits

Table 4-14: List of kits.

Kits	Manufacturer/Supplier	Catalog no.
Acetic acid test kit[a]	R-Biopharm AG, Darmstadt, Germany	10148261035
ENZYTEC™ D/L-Lactic acid test kit[a]	R-Biopharm AG	E1255
GeneJET Plasmid Miniprep Kit[b]	Thermo Fisher Scientific – Life Technologies GmbH, Darmstadt, Germany	K0502
MSB® Spin PCRapace Purification Kit[b]	STRATEC Biomedical AG, Birkenfeld, Germany	1020220200
Quick & Easy *E. coli* Gene Deletion kit[b]	Gene Bridges GmbH, Heidelberg, Germany	K006

[a] Stored at 4 °C. [b] Stored according to manufacturer recommendations.

4.1.12 Instruments, Devices, Laboratory Equipment and Consumables

Table 4-15: List of instruments and devices.

Instrument/device	Manufacturer/Supplier
AGE HE 33 Mini Submarine unit	GE Healthcare Europe GmbH, Freiburg, Germany
Autoclave Varioklav®	H+P Labortechnik GmbH, Oberschleißheim, Germany
BIOSTAT® C bioreactor	Satorius Stedim Biotech GmbH, Göttingen, Germany
Centrifuge 5810 R	Eppendorf AG, Hamburg, Germany
Centrifuge 5415 R	Eppendorf AG
Centrifuge Avanti™ J-30I	Beckman Coulter GmbH, Krefeld, Germany
Electroporator 2510	Eppendorf AG
Electrophoresis Power Supply EPS 301	Thermo Fisher Scientific – Life Technologies GmbH, Darmstadt, Germany
Gas sensor “BAC2S” Junction Box for 24V-Sensors, model 2.02, No.: 03097[a] O_2 sensor No.: 13131, CO_2 sensor No.: 13130	BlueSens gas sensor GmbH, Herten, Germany
Gas chromatograph Agilent 7890A	Agilent Technologies Deutschland GmbH, Waldbronn, Germany
GeneGenius Gel Imaging system	Syngene Europe, Cambridge, United Kingdom
Hoefer™ Dual Gel Caster	Thermo Fisher Scientific
Incubator	BINDER GmbH, Tuttlingen, Germany
Infors Multitron Standard incubation shaker	Infors GmbH, Braunschweig, Germany
Laminar flow cabinet NuAire Biological Savety Cabinet Class II, Model NU-480-400E	Ibs tecnomara GmbH, Fernwald, Germany
PCR Biometra® Tpersonal	Biometra GmbH, Göttingen, Germany
Semi-dry blotter unit, 10 x 10 cm	Biostep GmbH, Burkhardtsdorf, Germany
Spectrophotometer Spectronic GENESYS 6	Thermo Fisher Scientific
Thermomixer comfort	Eppendorf AG
Vortexer RS-VA10	PHOENIX Instrument, Garbsen, Germany
YSI biochemistry analyzer 2700 select	YSI Inc., Yellow Springs, OH, USA

[a] for 1-point calibration at ambient air (20.97 Vol.% O_2, 0.04 Vol.% CO_2)

Table 4-16: List of laboratory equipment.

Laboratory equipment	Manufacturer/Supplier
Centrifuge bottles, 800 mL	Beckman Coulter GmbH, Krefeld, Germany
Cuvette Hellma® Quartz SUPRASIL®, 10 mm	Hellma GmbH & Co. KG, Müllheim, Germany
Erlenmeyer baffled cultivation flasks (100 mL, 300 mL, 500 mL, 2000 mL)	Glasgerätebau Ochs Laborfachhandel e.K., Bovenden, Germany
Freezer GSN24A23 (-20 °C)	Robert Bosch GmbH, Stuttgart, Germany
Freezer HERAfreeze™ HFU T (-80 °C)	Thermo Fisher Scientific – Life Technologies GmbH, Darmstadt, Germany
Graduated glass pipettes Fortuna™ (1, 2, 5, 10 mL)	Thermo Fisher Scientific
Microwave	CINEX electronic GmbH
Pipettes Research® plus	Eppendorf AG, Hamburg, Germany
Refrigerators (4 °C)	C. Bomann GmbH, Kempen, Germany, Bauknecht Hausgeräte GmbH, Stuttgart, Germany
Scanner CanoScan LiDE 210	Canon, Krefeld, Germany
SCHOTT Duran® bottles (various sizes)	SCHOTT AG, Mainz, Germany
Waterbath Thermo Haake® DC10	Sigma-Aldrich Chemie GmbH, Munich, Germany

Table 4-17: List of consumables.

Consumables	Manufacturer/Supplier	Catalog no.
CELLSTAR® tubes (15 mL, 50 mL), sterile	Greiner Bio-One GmbH, Frickenhausen, Germany	188261, 227261
Cryopreservation vials, sterile, 2 mL	Carl Roth GmbH & Co. KG, Karlsruhe, Germany	E292.1
Cuvettes (UV), semi-micro, 1.5-3.0 mL	Carl Roth GmbH & Co. KG	Y199.1
Cuvettes (VIS), semi-micro, 1.5-3.0 mL	Carl Roth GmbH & Co. KG	Y195.1
Drigalski spatula Delta™, sterile	Carl Roth GmbH & Co. KG	PC59.1
Electroporation cuvettes (1 mm)	Thermo Fisher Scientific – Life Technologies GmbH, Darmstadt, Germany	P41050
Eppendorf tubes (1.5 mL, 2.0 mL)	Eppendorf AG, Hamburg, Germany	0030120086, 0030120094
GC autosampler microsyringe, 10 µL	Agilent Technologies Deutschland GmbH, Waldbronn, Germany	#5181-3354
GC Ultra Inert Inlet Liner, wool	Agilent Technologies Deutschland GmbH	#5190-3164
GC vial caps, 9 mm, black screw	Agilent Technologies Deutschland GmbH	#5185-5838
GC vial glass inserts, 400 µL, 5.6 × 31 mm	Agilent Technologies Deutschland GmbH	#5183-2087
GC vials, 2 mL	Agilent Technologies Deutschland GmbH	#5182-0714
Inoculation loops, sterile	Greiner Bio-One GmbH	731171
Nitrocellulose Blotting membrane "Amersham™ Protran™ 0.2 µm NC"	GE Healthcare Europe GmbH, Freiburg, Germany	10600006
Parafilm®, 38 m × 10 cm	A. Hartenstein GmbH, Würzburg, Germany	#PF10
PCR tubes, 0.2 mL	A. Hartenstein GmbH	#RK08
Petri dishes, 94 mm × 16 mm, vented	Greiner Bio-One GmbH	633180
Pipette tips (10 µL, 200 µL, 1000 µL)	Eppendorf AG	0030010019, 0030010035, 0030010051
Syringe filters ReliaPrep™, sterile single-use, 0.2 µm mesh	Ahlstrom-Munksjö, Stockholm, Sweden	
Syringe filters Rotilabo® Mini-Tip, non-sterile 0.2 µm mesh, nylon membrane	Carl Roth GmbH & Co. KG	PP43.1
Syringes, Ecoject® plus, 10 mL, Luer Lock	Dispomed Witt oHG, Gelnhausen, Germany	21010
Syringes, Injekt®-F single-use, 1 mL	Carl Roth GmbH & Co. KG	T987.1
Whatman paper, 3 mm	Carl Roth GmbH & Co. KG	A126.1

4.1.13 Computer Programs and Online Tools

Table 4-18: List of computer programs and online tools.

Program/tool	Purpose	Manufacturer/Source
Accelrys Draw 4.0	Drawing of chemical formulas	Accelrys Inc., San Diego, CA, USA
BLASTp	Protein identification	NCBI, U.S. National Library of Medicine, Bethesda, MD, USA
Clustal Omega	Local sequence alignment	European Bioinformatics Institute [EMBL-EBI], Hinxton, UK
CorelDRAW Graphics Suite 11	Image-editing programs	Corel Corp., Ottawa, ON, Canada
DDBST Vapor pressure	Calculation of vapor pressure according to Antoine equation	[DDBST]
DNA/RNA GC Calculator	Calculation of GC content	[EndMemo]
EndNote X5	Reference manager	Clarivate Analytics LLC, Philadelphia, PA, USA
OpenLAB CDS ChemStation	Controlling, recording and integration of GC measurements	Agilent Technologies Deutschland GmbH, Waldbronn, Germany
SnapGene® Viewer 4.0.7	Creation of plasmid maps	GSL Biotech LLC, Chicago, IL, USA
GeneSnap 6.03	Recording of DNA gel pictures	SynGene (Synoptics Ltd.), Cambridge, UK
MFCS 2007	Controlling, regulating and recording of bioreactor variables	Sartorius Stedim Biotech GmbH, Göttingen, Germany
Microsoft Office Excel 2007	Calculation of arithmetic mean and standard deviation, linear regression	Microsoft Corporation, Redmond, WA, USA
Microsoft Office Word 2007	Thesis writing program	Microsoft Corporation
OligoAnalyzer 3.1	Primer properties calculation	Integrated DNA Technologies Inc., Coralville, IA, USA [IDT]
OriginPro 2016	Creation of graphs	OriginLab Corp., Northampton, MA, USA
Primer3web 4.0.0	Primer design	[Rozen]
ProtParam	Calculation of theoretical molecular protein mass and other protein parameters	SIB Swiss Institute of Bioinformatics, Lausanne, Switzerland [SIB]
PyMOL 1.3	Creation of protein 3D structures	Schrödinger LLC, New York, NY, USA
RNAfold	Calculation of minimum free energy optimal mRNA secondary structure	[TBI] [Gruber et al., 2008]

4.2 Methods

4.2.1 Microbiological Methods

4.2.1.1 Cultivation of Bacterial Cells in Shake Flask Scale

For an experimental cultivation of *E. coli* cells in shake flask scale, bacterial suspension from a long-term glycerol stock (4.2.1.4, page 52) was streaked onto an LB agar plate and incubated for ~16 h at 37 °C. A single colony was picked from the plate, transferred into 15 mL LB medium (Table 4-5; 100 mL Erlenmeyer flask with baffles) and incubated for ~16 h at 37 °C and 110 rpm (Infors incubation shaker). A second preculture of 100 mL LB medium (500 mL flask) was inoculated with bacterial suspension from

the first preculture to an OD_{600} = 0.2 and incubated at 37 °C and 100 rpm until an OD_{600} of 1.0 was reached (exponential phase). From this, main cultures were inoculated for shake flask experiments.

For plasmid amplification and isolation (4.2.2.5, page 53) or preparation of competent cells (4.2.2.3, page 52), only the first preculture was prepared in a 15 mL sterile CELLSTAR® tube with 5 mL LB medium.

Some experiments required the use of minimal medium (Table 4-19) instead of LB medium plus a carbon source (e.g. glucose). For recombinant bacteria, exclusion of non-desired microorganisms was accomplished by addition of appropriate concentrations of antibiotics to the cultivation medium (Table 4-6). Maintenance of aseptic working conditions was achieved by sterilization of equipment, solutions and consumables via autoclavation or filter-sterilization, working in a laminar flow cabinet and careful handling.

4.2.1.2 Cultivation of Bacterial Cells in Bioreactor Scale

For preparation of an experimental cultivation in bioreactor scale, *E. coli* cells were reactivated from a glycerol stock (4.2.1.4, page 52) and grown in two subsequent precultures, as described in 4.2.1.1. The second preculture was grown for ~10 h at 37 °C and 100 rpm and used to inoculate a third preculture with 500 mL LB medium (4 × 2000 mL Erlenmeyer flasks) to an OD_{600} = 0.05. Incubation at 30-37 °C and 80 rpm for ~12 h promoted growth to mid-exponential phase. After determination of cell concentration (4.2.3.1, page 59), the cells were harvested by centrifugation at 6000 rpm (centrifuge Avanti™ J-30I) and 4 °C for 10 min in sterile centrifuge bottles. Inoculum was prepared by resolubilization of cell pellets in 250 mL LB medium and transfer into a sterile inoculum bottle, which was connected to the reactor via sealed coupling. The laboratory scale bioreactor BIOSTAT® C (Satorius Stedim Biotech GmbH, Göttingen, Germany) with a height-to-volume ratio of 2:1 (vessel height: 700 mm, vessel diameter: 350 mm) and a working volume of 10 L was employed. The bioreactor was equipped with an agitator with three Rushton turbines (radial flow impellers with a diameter of 0.4 × vessel diameter) and four baffles (in 90° angle to the vessel wall) to optimize mixing and maintenance of a homogenous solution. Aerobic cultivation was conducted by gassing of the vessel with filtered air via a ring sparger. LB medium (Table 4-5) was prepared for a total volume of 10 L, taking into account addition of inoculum, initial (batch) glucose, antibiotics, as well as loss of volume due to *in situ* sterilization. 10% (w/v) sodium hydroxide and 20% (v/v) phosphoric acid were used for pH regulation and 20% (w/v) Struktol J673 as an antifoam emulsion. Antibiotics and IPTG were prepared in appropriate concentrations for 10 L (Table 4-6, Table 4-7). Batch glucose (= 2% (w/v)) and 50% (w/v) feed glucose solution were prepared and autoclaved. The bioreactor was assembled (including the steam-sterilized sampling valve), filled with medium and *in situ* sterilized (121 °C, 30 min). Calibration of pH electrode was performed prior to sterilization, while calibration of pO_2 electrode took place before the start of cultivation. Acid/base/antifoam solutions were connected via sterile couplings to the reactor, as well as the batch and feed glucose and other additional supplements and devices. Condensate loss due to sterilization was compensated by addition of sterile dH_2O. Prior to start of cultivation, glucose and antibiotics were pumped into the reactor and the pH was automatically adjusted to 7.0. Control variables were set to 37 °C, pH 7.0, 0.4 bar, 5 L pressurized air min^{-1} (= 0.5 vvm, i.e. the volume of gas flow per bioreactor volume per minute), 400 rpm (stirrer in cascade with airflow regulation for $pO_2 > 25\%$) via MFCS 2007 (Sartorius Stedim Biotech GmbH). Cultivation began with the addition of inoculum and start of recording by MFCS 2007. Samples were drawn via the sterilized sampling valve. Inductor and feed was added via ethanol-disinfected sealed tube couplings. After termination of cultivation, cell suspension was harvested via the effluent vent and the bioreactor was sterilized *in situ* after addition of dH_2O to the vessel. Cultivation variables were exported via MFCS 2007.

4.2.1.3 Adaptation of Escherichia coli *to Minimal Medium*

Adaptation of an *E. coli* strain from complex to minimal medium (MM) was performed by streaking an LB agar plate with the respective cells from a long-term storage glycerol stock (4.2.1.4, page 52). The plate was incubated for ~16 h at 37 °C. 15 mL LB medium (Table 4-5, 100 mL Erlenmeyer flask) were inoculated with a single colony from the plate and cultivated for ~16 h at 37 °C and 110 rpm. 100 mL fresh LB medium (500 mL flask) were inoculated with this preculture to an OD_{600} of 0.2, incubated at 37 °C and 100 rpm, while the OD_{600} was recorded. A 500 mL flask with 100 mL MM containing 2% (w/v) glucose was subsequently inoculated with bacterial suspension from the LB culture and incubated at 37 °C and 100 rpm. The OD_{600} was again recorded for comparison of growth rates in LB and MM. Repeated passages into fresh MM should obtain a growth rate μ (Equation 4-14, page 67) in MM which is similar to the one in LB medium. Glycerol stocks were prepared from the final adaptation culture at an OD_{600} ~2 and stored at -80 °C (4.2.1.4.). The basic recipe for MM is listed in Table 4-19. The medium was supplemented with 3 mL L^{-1} trace element solution (Table 4-20) and, depending on the *E. coli* strain (Table 4-4, page 41), with additives like thiamine or proline (Table 4-21).

Table 4-19: Mimimal medium according to [Wilms et al., 2001].
The ingredients were solubilized in 800 mL dH_2O, autoclaved for 15 min at 121 °C and filled up to 1 L with sterile-filtered dH_2O. 1 L MM was supplemented with 3 mL trace element solution (TES) (Table 4-20) and optionally with additives (Table 4-21). All chemicals are listed in Table 4-1.

Ingredient	Concentration [g L^{-1}]
Na_2SO_4	2.0
$(NH_4)_2SO_4$	2.68
NH_4Cl	0.5
K_2HPO_4	14.6
$Na_2HPO_4 \times 2\ H_2O$	4.0
$(NH_4)_2$-H citrate	1.0
$MgSO_4 \times 7\ H_2O$	0.5

Table 4-20: Trace element solution (TES) for minimal medium according to [Wilms et al., 2001].
The ingredients were solubilized in 1 L dH_2O and autoclaved for 15 min at 121 °C. All chemicals are listed in Table 4-1.

Ingredient	Concentration [g L^{-1}]
$CaCl_2$	0.5
$ZnSO_4 \times 7\ H_2O$	0.18
$MnSO_4 \times H_2O$	0.1
Na_2-EDTA $\times 2\ H_2O$	10.05
$FeCl_3$	8.35
$CuSO_4 \times 5\ H_2O$	0.16
$CoCl_2 \times 6\ H_2O$	0.18

Table 4-21: Additives for minimal medium according to [Wilms et al., 2001].
Each ingredient was solubilized separately in dH_2O and sterile-filtered. Solutions were stored at 4 °C. All chemicals are listed in Table 4-1.

Additive	Final concentration in MM [g L^{-1}]
Thiamine	0.01
L-Proline	0.01

4.2.1.4 Long-term Storage of Bacteria (Preparation of Glycerol Stocks)

Glycerol stocks were prepared to avoid cell lysis and enable storage of bacteria for a period of several years [Heckly, 1978]. To prepare a 20% glycerol stock, cell material from an agar plate was transferred to 5 mL LB medium (Table 4-5) in a 15 mL CELLSTAR® tube, optionally supplemented with antibiotics in appropriate concentrations (Table 4-6). The preculture was incubated for ~16 h at 37 °C and 180 rpm. 5 mL LB medium were inoculated with 500 µL of preculture and incubated for 2-3 hours at 37 °C and 180 rpm to ensure exponential growth. 800 µL of bacterial suspension was mixed with 200 µL sterile glycerol (autoclaved) in a cryopreservation vial. After vortexing and short submersion in liquid nitrogen, the glycerol stock was stored at -80 °C. Bacterial suspension from glycerol stocks was used to prepare precultures for cultivation experiments or to amplify and isolate plasmid DNA.

4.2.2 Molecular Biology Techniques

4.2.2.1 Agarose Gel Electrophoresis (AGE)

For a 1% gel according to [Mülhardt, 2013], 0.35 g agarose (peqGOLD Universal) was solubilized in 35 mL 1× TAE buffer (Table 4-2) by repeated heating in a microwave and shaking. After assembly of the gel apparatus (AGE HE 33 Mini Submarine unit), 20 µL of a 0.1% (w/v) ethidium bromide solution (Table 4-2) were added to the lukewarm agar solution. The solution was poured into the gel chamber and left for ~20 min to promote gellation. The comb was removed creating gel pockets and the gel was submerged in 1× TAE buffer. Samples were prepared by mixing 5 µL with 1 µL of 6× loading dye (Table 4-13). For estimation of DNA sizes, 5 µL MassRuler DNA ladder mix (Table 4-13) was used as marker. The electric field was applied for 60 min at 80 V and 400 mA (Electrophoresis Power Supply EPS 301) to separate DNA molecules by size. The DNA was analyzed under UV light via GeneGenius Gel Imaging system.

4.2.2.2 Purification of PCR Products

PCR products were purified via MSB® Spin PCRapace Purification Kit (Table 4-14) according to the manufacturer's manual by mixing with 250 µL binding buffer and pipetting into a spin filter in a 2 mL receiver tube. After centrifugation for 3 min at 12000 rpm (centrifuge 5415 R), elution was performed by addition of 15 µL warm (~50 °C) ddH_2O and incubation for 1 min with subsequent centrifugation for 1 min at 10000 rpm.

4.2.2.3 Preparation of Chemically Competent Cells

Preparation of chemically competent cells was performed according to [Mülhardt, 2013] by inoculation of a preculture with *E. coli* cell material and incubation for ~16 h at 37 °C and 180 rpm. The main culture containing 50 mL LB medium (300 mL flask) was inoculated with 1% (v/v) bacterial suspension from the

preculture and incubated at 37 °C and 110 rpm until an OD_{600} = 0.4-0.5 was reached. The suspension was split into two 50 mL sterile prechilled CELLSTAR® tubes and centrifuged for 10 min at 4 °C and 4000 rpm (centrifuge 5810 R). The supernatant was discarded and each pellet was resuspended by shaking in 25 mL ice-cold and freshly prepared 0.1 mM $CaCl_2$ solution. After incubation on ice for 30 min, the cells were centrifuged again for 10 min at 4 °C and 4000 rpm and the pellets were resuspended in 5 mL ice-cold 0.1 mM $CaCl_2$ solution. 750 µL sterile, ice-cold glycerol were added to each suspension, resulting in a 15% glycerol mixture that was divided into 100 µL aliquots (1.5 mL sterile, prechilled Eppendorf tubes). The tubes were submerged in liquid nitrogen and stored at -80 °C for further use.

4.2.2.4 Transformation by Chemical Reagents

100 µL aliquots of chemically competent *E. coli* cells (4.2.2.3) were thawed on ice for 5 min with intermittent slight shaking. After addition of 1-100 ng plasmid DNA, the cells were incubated on ice for 30 min. Heat shock treatment was performed in a water bath at 42 °C for 45 s [Hanahan, 1983]. After incubation on ice for 3 min, 400 µL LB medium were added and the bacterial growth was promoted for 1 h at 37 °C and 850 rpm (Thermomixer comfort). Concentration of cells was performed by short centrifugation at 8000 rpm (centrifuge 5415 R) and resuspension of the pellet in 100 µL LB medium. The bacterial suspension was plated on sterile antibiotic-containing (Table 4-6) LB agar plates and incubated for ~16 h at 37 °C. Formed bacterial colonies should contain the desired plasmid DNA.

4.2.2.5 Plasmid Amplification and Isolation

Amplification of plasmid DNA was performed inside the respective *E. coli* strain by preparation of a preculture (see 4.2.1.1, page 49) and harvest of the propagated cells by centrifugation at 4000 rpm for 10 min (centrifuge 5810 R). The supernatant was discarded and the pellet was resuspended in 250 µL "Resuspension Solution" (contains RNase A) of the GeneJET Plasmid Miniprep Kit (Table 4-14) and transferred to a 1.5 mL Eppendorf tube. 250 µL "Lysis Solution" (contains SDS and NaOH) were added to the resuspended pellet. The viscous solution was inverted 4-6 times and 350 µL "Neutralization Solution" (contains potassium acetate) was added, followed by 4-6 times invertation of the tube. After centrifugation at 15600 rpm (centrifuge 5415 R) for 5 min, the supernatant was transferred to a silica-based GeneJET spin column and centrifuged for 1 min at 15600 rpm. The column was washed 2 times with 500 µL "Wash Solution" (contains ethanol) by centrifugation at 15600 rpm for 1 min. The column was dried by centrifugation at 15600 rpm for 1 min and transferred to a new 1.5 mL Eppendorf tube. The adsorbed plasmid DNA was eluted by incubation with 50 µL ddH_2O for 2 min and centrifugation at 11000 rpm. The plasmid DNA was stored at -20 °C.

4.2.2.6 Determination of DNA Concentration

Purified DNA can be quantified by measuring its absorbance at a wavelength of 260 nm (A_{260}) with a spectrophotometer [Mülhardt, 2013]. Using the Lambert-Beer law (Equation 4-11, page 66), the amount of absorbed light can be related to the concentration of DNA molecules in the solution. The average attenuation coefficient for double-stranded (ds) DNA is 0.02 mL μg^{-1} cm^{-1} and an absorbance A_{260} = 1 equals 50 µg mL^{-1} pure dsDNA. Samples of isolated plasmid DNA (4.2.2.5) or purified PCR product (4.2.2.2) were diluted 1:40 with dH_2O in a total volume of 80 µL and inserted into a UV quartz cuvette. The sample was measured at 260 and 280 nm (Spectronic GENESYS 6) and the DNA concentration was calculated from the average of three DNA samples.

4.2.2.7 Sequencing of Plasmid DNA

Sequencing was performed to verify the presence of the desired plasmid in a recombinant host. 15 µL of plasmid DNA and 5 µL of corresponding sequencing primer (Table 4-10) were sent for sequencing to Eurofins Genomics (Ebersberg, Germany). Primers were designed using Primer3web 4.0.0 (Table 4-18). Alignment of the sequencing result with the respective DNA sequence was performed by Clustal Omega (Table 4-18).

4.2.2.8 Metabolic Engineering by Red®/ET® Recombination

Red®/ET® recombination according to [Zhang et al., 1998] is a technique used for targeted disruption (knockout) or alterations of genes in the *E. coli* genome, e.g. to block a competing metabolic pathway. The method relies on *in vivo* homologous recombination, i.e. the specific exchange of genetic material between two DNA molecules via corresponding homology regions in the DNA. The name stems from two Rac prophage coded proteins (RecE and RecT) and their respective functional counterparts in lambda phage (Red α and Red β), which are able to mediate recombination between a linear DNA molecule and circular DNA. Recombination, as depicted in Figure 4-1 (page 55), occurs when RecE (or Red α; 5'-3'-exonuclease) and RecT (or Red β; DNA annealing) are expressed in *E. coli*, initiating a double-stranded break repair (DSBR). In DSBR, a double-strand break is performed by the 5'-3'-exonuclease, creating a 3'-single-stranded DNA overhang. The DNA annealing protein binds the overhang and the complex is able to anneal to homologous DNA. The 3'-end becomes a primer for DNA replication, which subsequently repairs the double-stranded break. The recombination is further aided by lambda Gam protein, which inhibits the RecBCD DSBR mechanism of *E. coli* [Murphy, 2007].

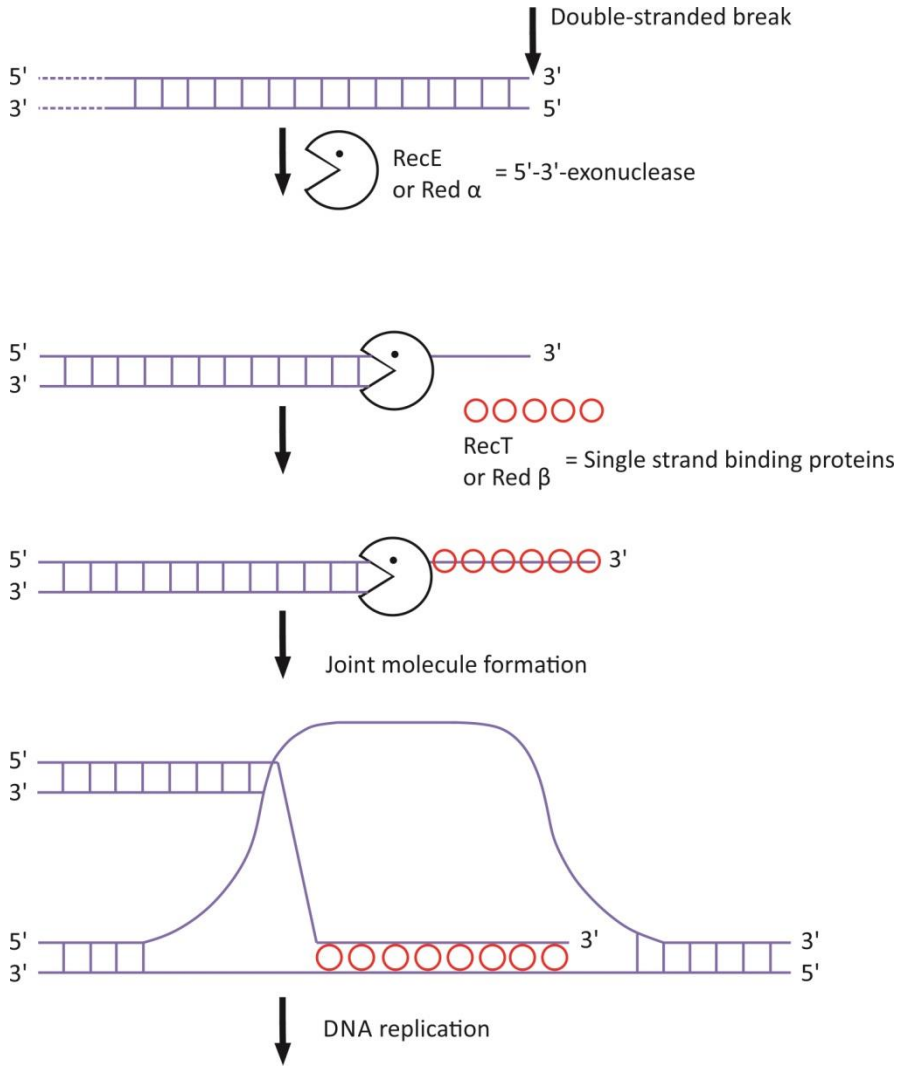

Figure 4-1: Mechanism of Red®/ET® recombination.
Source: Quick & Easy *E. coli* Gene Deletion kit manual (Gene Bridges GmbH, Heidelberg, Germany).

pRedET-Amp^R (Table 4-8, page 42), part of the Quick & Easy *E. coli* Gene Deletion kit by Gene Bridges GmbH (Table 4-14), carries the lambda phage red γβα operon under control of the arabinose-inducible pBAD promotor [Guzman et al., 1995] and confers ampicillin resistance. RecA is included in the polycistronic operon and plays a central role in homologous recombination, binding the homologous DNA molecules and catalyzing unidirectional branch migration to complete recombination. pRedET-Amp^R is a derivative of the thermo-sensitive pSC101 (low copy, oriR101), which encodes the RepA protein responsible for plasmid DNA replication [Miller et al., 1995]. RepA is temperature-sensitive, so that cells must be incubated at 30 °C to maintain the pRedET-Amp^R, while plasmid loss occurs at 37 to 43 °C.

First step in the experimental Red®/ET® recombination procedure comprises generation of a linear functional homology cassette, which is flanked by homology regions for targeted recombination in the *E. coli* genome (Figure 4-2, 1. step).

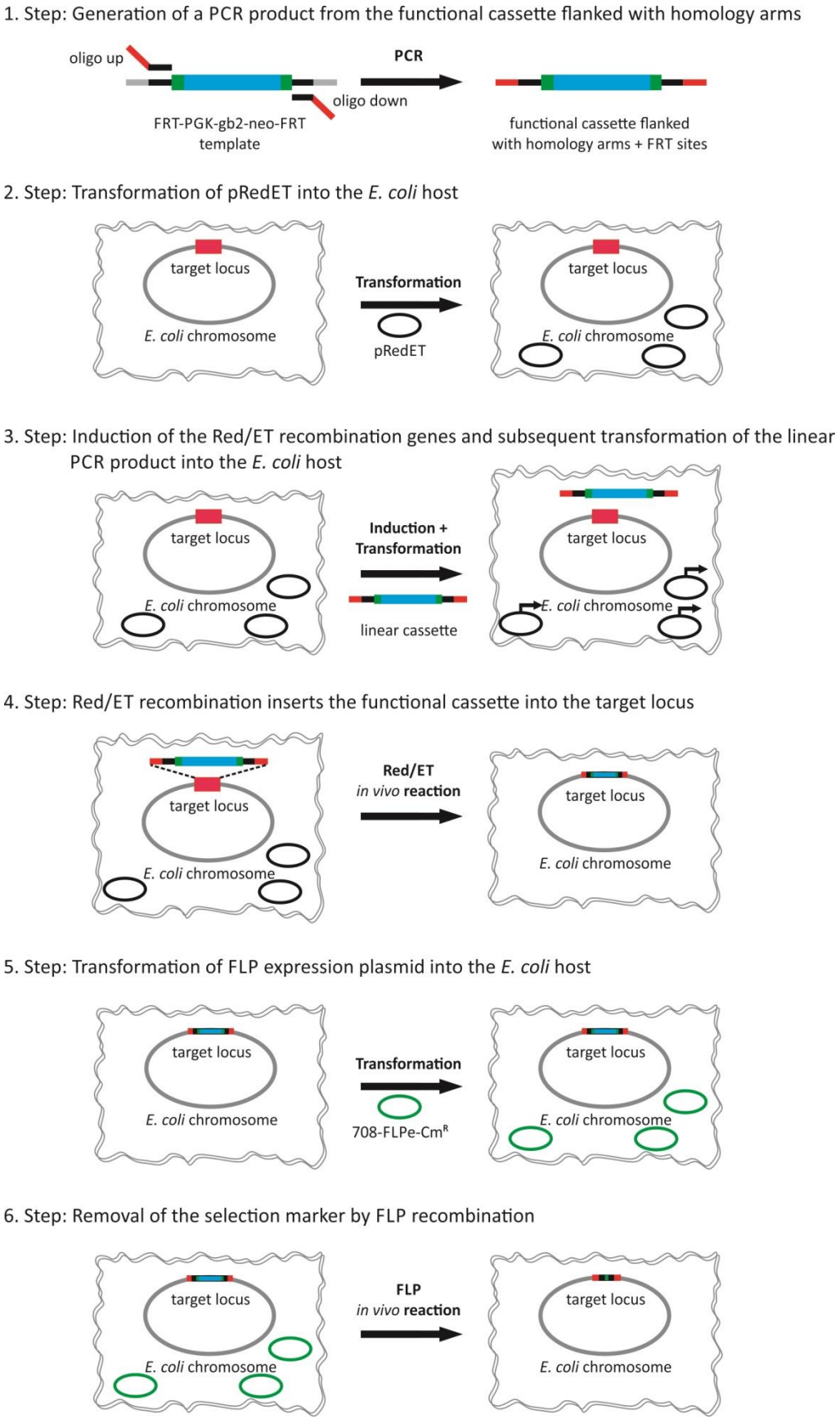

Figure 4-2: Experimental scheme for targeted disruption of genes in the *E. coli* genome by Red®/ET® recombination.

Source: Quick & Easy *E. coli* Gene Deletion kit manual (Gene Bridges GmbH, Heidelberg, Germany).

Two oligonucleotides were designed, which add the 50 bp homology regions by polymerase chain reaction (PCR) to the provided FRT-PGK-gb2-neo-FRT cassette (contained on pFRT, Table 4-8, page 42; see Appendix Figure A-4, page 187, for schematic presentation of the cassette). Forward oligonucleotide (FRT_FW, Table 4-10, page 43) incorporates 50 nucleotides adjacent upstream (5') to the intended recombination site plus the PCR primer sequence for amplification of the FRT-PGK-gb2-neo-FRT cassette at the 3'-end. The reverse oligonucleotide (FRT_RV) carries 50 nucleotides adjacent downstream (3') to the intended recombination site (in reversed complement orientation to the site) plus the PCR primer sequence for amplification of the FRT-PGK-gb2-neo-FRT cassette at the 3'-end. For amplification of the linear functional homology cassette, a PCR mastermix was prepared according to Table 4-22.

Table 4-22: PCR mastermix (1×) for amplification of the linear functional homology cassette for Red®/ET® recombination.
The components were pipetted into PCR tubes and placed into the PCR machine (PCR Biometra® Tpersonal).

Components	Volume [µL]
Phusion HF reaction buffer (5×)	10
pFRT (FRT-PGK-gb2-neo-FRT cassette = template DNA)	1
Forward primer FRT_FW (100 pmol μL^{-1})	1
Reverse primer FRT_RV (100 pmol μL^{-1})	1
dNTP mix (2 mM)	5
Phusion High-Fidelity DNA polymerase (2 U μL^{-1})	1
ddH_2O	ad 50

PCR was performed according to the temperature program in Table 4-23.

Table 4-23: PCR program for amplification of the linear functional homology cassette for Red®/ET® recombination.

Steps	Temperature [°C]	Time [min]
1. Denaturation of dsDNA (without polymerase)	98	5
2. Denaturation of dsDNA (with polymerase)	98	0.5
3. Annealing of primers	55	0.5
4. Elongation	72	2
5. Final elongation	72	10
6. Pause	4	∞

Step 2 to 4 were repeated 35 times.

Annealing temperature was set 2-5 °C below the melting temperature T_M of the utilized primer oligonucleotides. Elongation time was chosen according to processivity of the polymerase and the size of the DNA molecule to be amplified (template DNA). The resulting PCR product was purified with MSB® Spin PCRapace Purification Kit (Table 4-14, 4.2.2.2, page 52) and 5 µL sample were analyzed by AGE (4.2.2.1, page 52). DNA concentration was measured (4.2.2.6, page 53) and adjusted to 400 µg mL^{-1} prior to utilization of the cassette in recombination.

In step 2 (Figure 4-2), *E. coli* DH5α (Table 4-4) was transformed with the recombination plasmid pRedET-Amp^R (Table 4-8, page 42). *E. coli* DH5α cells were inoculated in 1 mL LB medium (Table 4-5) in a 1.5 mL Eppendorf tube with punctured lid for aeration. The cells were incubated for ~16 h at 37 °C and 1000 rpm (Thermomixer comfort). A 2 mL punctured Eppendorf tube containing 1.4 mL fresh LB medium

was inoculated with 30 µL preculture and cultivated for 3 h at 37 °C and 1000 rpm. The cells were prepared for a quick electroporation procedure by centrifugation for 30 s at 2 °C and 11000 rpm (centrifuge 5415 R) and placing the pellet on ice. The pellet was resuspended in 1 mL pre-cooled ddH_2O, and centrifugation and resuspension were repeated. After a final centrifugation for 30 s at 2 °C and 11000 rpm, the supernatant was discarded and the pellet was resuspended in the remaining ~20 µL medium. The cell suspension was kept on ice, while 1 µL of pRedET-Amp^R was added and mixed with the bacteria. Electroporation was performed in a 1 mm chilled electroporation cuvette with an electric pulse at 1350 V (Electroporator 2510). The electroporated cells were resuspended in 1 mL LB medium and incubated at 30 °C for 70 min and 1000 rpm. 100 µL cell suspension were plated on an LB agar plate containing ampicillin (50 µg mL^{-1}, Table 4-6) and incubated for ~16 h at 30 °C.

Step 3 (Figure 4-2) involves expression of the genes mediating Red®/ET® recombination by induction with L-arabinose, as well as transformation of the cells with the linear functional homology cassette by electroporation. A single colony of *E. coli* DH5α_pRedET-Amp^R was inoculated in 1 mL LB medium containing ampicillin (50 µg mL^{-1}, Table 4-6) in a lid-punctured Eppendorf tube and incubated for ~16 h at 30 °C and 1000 rpm. Two lid-punctured Eppendorf tubes with fresh 1.4 mL LB medium and ampicillin (50 µg mL^{-1}) were inoculated with 30 µL preculture and incubated for 2 h at 1100 rpm to OD_{600} = 0.3. 50 µL of 10% (w/v) L-arabinose solution (Table 4-2) were added for induction of recombination gene expression to one of the tubes (second tube was left as negative control). Both tubes were incubated for 1 h at 37 °C and 1100 rpm. Induced and non-induced cells were prepared for the quick electroporation procedure as described in step 2 and transformed with 2 µL linear functional homology cassette (see step 1) by electroporation. The cells were resuspended in 1 mL LB medium and incubated at 37 °C for 3 h and 1100 rpm to allow recombination and insertion of the functional cassette into the target locus (step 4, Figure 4-2). Both cultures were centrifuged for 30 s and 11000 rpm and resuspended in 100 µL LB medium. The cells were plated on an LB agar plate containing kanamycin (15 µg mL^{-1}, Table 4-6) and incubated for ~16 h at 37 °C to eliminate pRedET-Amp^R. Only colonies carrying the inserted modification were able to survive kanamycin selection.

For verification of mutants, obtained colonies were analyzed by PCR and AGE. A PCR mastermix containing primers directed against the genomic recombination site (Table 4-10, page 43) was prepared according to Table 4-24. Template DNA was prepared from a single colony, resuspended in 30 µL ddH_2O and boiled at 98 °C for 5 min.

Table 4-24: PCR mastermix (1×) for verification of Red®/ET® recombination mutants.
The components were pipetted into PCR tubes and placed into the PCR machine (PCR Biometra® Tpersonal).

Components	Volume [µL]
Pfu reaction buffer (with 25 mM $MgSO_4$)	5
Template DNA (= single colony)	2
Forward primer Genome_Pta_FW (100 pmol µL^{-1})	1
Reverse primer Genome_Pta_RV (100 pmol µL^{-1})	1
dNTP mix (2 mM)	5
Pfu DNA polymerase (2.5 U µL^{-1})	1
ddH_2O	ad 50

PCR was performed according to the temperature program in Table 4-25.

Table 4-25: PCR program for verification of Red®/ET® recombination mutants.

Steps	Temperature [°C]	Time [min]
1. Denaturation of dsDNA (without polymerase)	95	5
2. Denaturation of dsDNA (with polymerase)	95	1
3. Annealing of primers	57	1
4. Elongation	72	5
5. Final elongation	72	6
6. Pause	4	∞

Step 2 to 4 were repeated 25 times.

5 µL of the resulting PCR product were analyzed by AGE (4.2.2.1, page 52), checking insertion of the linear functional homology cassette into the *E. coli* genome.

Step 5 and 6 of the Red®/ET® recombination procedure (Figure 4-2) involve removal of the genomic kanamycin selection marker by transformation of the mutant cells with the FLP expression plasmid 708-FLPe-Cm^R (Table 4-8, page 42). The FLPe (flippase) recombinase encoded on the plasmid enables FLP-mediated site-directed recombination in *E. coli* by a temperature shift from 30 to 37 °C (λR promoter under control of the heat-labile cI857 repressor). Like pRedET-Amp^R, the FLP expression plasmid has a thermo-sensitive origin of replication, getting lost after prolonged incubation at 37 °C. After removal of the selection marker by FLPe recombinase, a single FRT site is left behind as a footprint [Schweizer, 2003]. A verified mutant was inoculated in 1 mL LB medium containing kanamycin (50 µg mL^{-1}, Table 4-6) in a lid-punctured Eppendorf tube and incubated for ~16 h at 37 °C and 1000 rpm. A second punctured Eppendorf tube with fresh 1.4 mL LB medium and kanamycin (50 µg mL^{-1}) was inoculated with 30 µL preculture and incubated for 2 h at 37 °C and 1000 rpm. The cells were prepared for the quick electroporation procedure as described in step 2 and transformed with 1 µL 708-FLPe-Cm^R by electroporation. The cells were resuspended in 1 mL LB medium (without antibiotics) and incubated at 30 °C for 70 min and 1000 rpm. The cells were plated on an LB agar plate containing kanamycin (15 µg mL^{-1}) and chloramphenicol (15 µg mL^{-1}, Table 4-6) and incubated for ~16 h at 30 °C. A single colony was inoculated in 1 mL LB medium (without antibiotics) and grown at 30 °C and 1000 rpm for 2 h. Temperature was changed to 37 °C and the cells were incubated for ~16 h at 1000 rpm. The temperature shift triggered expression of the FLPe recombinase and recombination of the FRT sites, removing the selection marker from the genome. The cells were then plated on an LB agar plate (without antibiotics) and grown for ~16 h at 37 °C. For verification of marker removal, the cells were plated in parallel (numbered streaks) on two LB agar plates, one containing kanamycin (15 µg mL^{-1}) and one without antibiotics, which were incubated ~16 h at 37 °C. Cells that grew on the plate without antibiotics, but not on the one with kanamycin, successfully removed the selection marker.

4.2.3 Analytical Methods

4.2.3.1 Determination of Cell Concentration

Bacterial growth was monitored by spectrophotometrical determination of cell concentration at different times throughout the cultivation. This was achieved by measurement of the optical density of a sample at the wavelength 600 nm (OD_{600}). A linear relationship between the number of cells and the absorbance is usually given between OD_{600} = 0.1-0.4 or 0.5, depending on the optical configuration of the device. The absorbance is also a function of cellular size and shape. Here, a bacterial cultivation sample was appropriately diluted with medium, vortexed and measured in a spectrophotometer (Spectronic

GENESYS 6) at 600 nm. The OD_{600} of a blank (medium) was subtracted from the sample OD_{600}, which was then multiplied with the dilution factor.

4.2.3.2 Soluble-Insoluble Partitioning of Proteins

1/OD samples were prepared as described in 4.2.3.3 and the pellets were resuspended in 130 µL lysis buffer (Table 4-2, page 39). Cell lysis was performed by incubation at 37 °C for 1 h, followed by centrifugation at 15600 rpm (centrifuge 5415 R) and 4 °C for 5 min. The soluble protein fraction was processed by transfer of 110 µL supernatant to prechilled 1.5 mL Eppendorf tubes. Proteins were precipitated by incubation with 440 µL ice-cold acetone (1:5) for 5 min and centrifugation at 15600 rpm and 4 °C for 10 min. Pellets were resolubilized in 85 µL SDS-PAGE sample buffer (Table 4-2) and heated at 99 °C for 3 min. The insoluble protein fraction was treated by resolubilization of pellets in 1 mL Tris buffer (50 mM, pH 8.0, Table 4-2) and centrifugation at 15600 rpm and 4 °C for 5 min. Resolubilization and centrifugation was repeated and the resulting pellets were solubilized in 100 µL SDS-PAGE sample buffer and heated at 99 °C for 3 min. Soluble and insoluble protein fractions were either directly subjected to SDS-PAGE (4.2.3.3) and/or Western Blot analysis (4.2.3.4) or stored at -20 °C.

4.2.3.3 Sodium Dodecyl Sulfate Polyacrylamide Gel Electrophoresis (SDS-PAGE)

Sodium dodecyl sulfate polyacrylamide gel electrophoresis (SDS-PAGE) was used to separate protein molecules by molecular mass via an electric field. For a 12.5% resolving gel according to [Laemmli, 1970], 1.25 mL resolving gel buffer, 2.1 mL acrylamide/bisacrylamide, 1.65 mL dH_2O, 5 µL tetramethylethylenediamine (TEMED) and 10 µL ammonium persulfate (APS) solution (see Table 4-1, page 37 & Table 4-2, page 39 for ingredients) were mixed and poured into the gel preparation device. To avoid bubbles and to facilitate polymerization, a layer of isopropanol was pipetted onto the gel. After ~20 min the layer was removed and a 4.5% stacking gel was prepared by mixing 0.625 mL stacking gel buffer, 0.375 mL acrylamide/bisacrylamide, 1.5 mL dH_2O, 5 µL TEMED and 4 µL APS solution and poured on top of the resolving gel. A comb was inserted to form gel pockets for sample application. After polymerization, the polyacrylamide (PA) gel was fixed into the gel electrophoresis device (Hoefer™ Dual Gel Caster) and 250 mL 1× electrophoresis buffer (Table 4-2) was applied. Sample preparation for SDS-PAGE was performed by taking of 1/OD samples from a bacterial culture and centrifugation for 1.5 min at 4 °C and 15600 rpm (centrifuge 5415 R). 1/OD samples contain an equal number of cells due to the determination of cell concentration in a bacterial culture (4.2.3.1) and sampling of a volume [mL] that is defined by the reciprocal of OD_{600}. 100 µL SDS-PAGE sample buffer (Table 4-2, plus 10 µL mL^{-1} fresh 2-mercaptoethanol) was added to the samples, which were subsequently heated at 99 °C for 3 min and applied to the gel pockets (10 µL for SDS-PAGE or 15 µL for Western Blot analysis, 5 µL PageRuler Prestained Protein Ladder as marker). For evaluation of protein solubility, 1/OD samples were subjected to soluble-insoluble fractionation (4.2.3.2) prior to treatment with SDS-PAGE sample buffer. Separation of proteins by gel electrophoresis was performed at 250 V and 40 mA for 6 min, followed by 250 V and 30 mA for 40 min. Afterwards, the PA gel was either soaked in staining solution (contains Coomassie brilliant blue G 250; Table 4-2) for ~16 h or subjected to electrophoretic protein transfer by Western Blot (4.2.3.4). The stained gel was placed in destaining solution (Table 4-2) for 0.5 h and again for 2-3 h into fresh destaining solution until the PA gel became colorless. The visualized proteins on the gel were scanned using CanoScan LiDE 210.

4.2.3.4 Western Blot Analysis

Western Blot (WB) analysis was used for immunochemical visualization of specific proteins of interest [Rehm, 2016]. 1/OD samples were prepared as described in 4.2.3.3, optionally subjected to soluble-insoluble partitioning (4.2.3.2), and separated by SDS-PAGE (4.2.3.3). A nitrocellulose membrane (NCM) and six Whatman papers were soaked in transfer buffer (Table 4-2, page 39) for 15 min before assembly of the transfer chamber (semi-dry blotter unit, Table 4-15, page 46). The NCM and the PA gel were placed between the Whatman papers inside the chamber, soaked in transfer buffer and air bubbles were removed. The electrophoretic transfer was performed at 20 V and 250 mA for 1 h. The NCM was incubated in 10 mL blocking solution (Table 4-2) for ~16 h and then washed twice for 10 min in 10 mL TBS-TT buffer (Table 4-2) and once for 10 min in 10 mL TBS buffer (Table 4-2). The NCM was incubated in 10 mL blocking solution containing the primary antibody (see Table 4-12, page 45, for working concentration and incubation time). If more than one primary antibody was used (e.g. a combination of anti-His_{10}, anti-FLAG and anti-c-Myc), the antibodies were applied successively using fresh blocking solution for each one and two washing steps with 10 mL TBS-TT buffer for 5 min and one washing step with 10 mL TBS buffer for 5 min in between. After incubation with the primary antibody/antibodies, the NCM was washed twice for 10 min in 10 mL TBS-TT buffer and once for 10 min in 10 mL TBS buffer. Then, the NCM was incubated in 10 mL blocking solution containing the secondary antibody (Table 4-12) with subsequent washing in 10 mL TBS-TT buffer four times for 10 min. Staining was performed by incubation of the NCM in substrate solution (BCIP/NBT, Table 4-2) for ~5 min. The visualized protein(s) of interest was/were scanned using CanoScan LiDE 210.

4.2.3.5 Quantification of Glucose by YSI

Bacterial glucose consumption was measured by YSI biochemistry analyzer 2700 select, which operates utilizing the immobilized enzyme glucose oxidase (GOx). Glucose is oxidized as it enters the measuring cell, producing hydrogen peroxide and D-glucono-1,5-lactone (Reaction 4-1). Hydrogen peroxide is then oxidized by the platinum electrode (Pt) resulting in a current that is proportional to the glucose concentration (Reaction 4-2).

Reaction 4-1 $\text{D-glucose} + O_2 \xrightarrow[GOx]{} \text{D-glucono-1,5-lactone} + H_2O_2$

Reaction 4-2 $H_2O_2 \xrightarrow[Pt]{} 2\,H^+ + O_2 + 2\,e^-$

Sample preparation for glucose measurement was performed according to the manufacturer's manual by removal of 1 mL bacterial suspension and centrifugation for 1.5 min at 4 °C and 15600 rpm (centrifuge 5415 R). The supernatant was diluted 1:5 with dH_2O and subjected to the YSI measurement.

4.2.3.6 Quantification of Acetate and Lactate by Enzymatic Test Kits

Acetate and lactate concentrations were determined using the Acetic acid test kit and the ENZYTEC™ D/L-Lactic acid test kit from R-Biopharm AG (Table 4-14, page 46). Samples for both tests were prepared by removing 1 mL of bacterial suspension and centrifugation for 1.5 min at 4 °C and 15600 rpm (centrifuge 5415 R). The supernatants were diluted 1:10 with dH_2O prior to the measurements.

Determination of acetate concentration relies on the stoichiometric formation of NADH by three coupled enzymatic reactions via acetyl-CoA synthetase (Acs), citrate synthase (CS) and L-malate dehydrogenase (L-MDH) (see manufacturer's manual for details). According to the manual, 500 µL solution 1 (L-malate, $MgCl_2 \times 6\ H_2O$), 100 µL solution 2 (ATP, CoA, NAD^+), 50 µL diluted sample (or dH_2O as blank) and 950 µL

dH_2O were pipetted into a UV cuvette and mixed. A_0 was measured at 340 nm (spectrophotometer Spectronic GENESYS 6). 5 µL of solution 3 (L-MDH, CS) were added, mixed and incubated for 3 min. Afterwards A_1 was measured at 340 nm. Reactions were started by the addition of 10 µL solution 4 (Acs) and mixing. After 15 min, A_2 was recorded at 340 nm. $\Delta A_{acetate}$ was calculated by Equation 4-1:

Equation 4-1
$$\Delta \boldsymbol{A_{acetate}} = \left[(\boldsymbol{A_2} - \boldsymbol{A_0})_{\boldsymbol{sample}} - \frac{(\boldsymbol{A_1}-\boldsymbol{A_0})^2_{\boldsymbol{sample}}}{(\boldsymbol{A_2}-\boldsymbol{A_0})_{\boldsymbol{sample}}}\right] - \left[(\boldsymbol{A_2} - \boldsymbol{A_0})_{\boldsymbol{blank}} - \frac{(\boldsymbol{A_1}-\boldsymbol{A_0})^2_{\boldsymbol{blank}}}{(\boldsymbol{A_2}-\boldsymbol{A_0})_{\boldsymbol{blank}}}\right].$$

With $\Delta A_{acetate}$, the concentration of acetate in the samples was calculated by Equation 4-2:

Equation 4-2
$$\boldsymbol{c_{acetate}} = \frac{\boldsymbol{V \cdot MW}}{\boldsymbol{\varepsilon \cdot d \cdot v \cdot 1000}} \cdot \Delta \boldsymbol{A_{acetate}} \cdot \boldsymbol{F}$$

with $c_{acetate}$ = acetate concentration [g L^{-1}], V = final volume [mL], MW = molecular mass of acetate [g mol^{-1}], ε = extinction coefficient of NADH at 340 nm = 6.3 [L $mmol^{-1}$ cm^{-1}], d = light path [cm], v = sample volume [mL], F = dilution factor.

Determination of lactate concentration relies on the stoichiometric formation of NADH by two coupled enzymatic reactions via D- or L-lactate dehydrogenase (D-LDH or L-LDH) and glutamate-pyruvate transaminase (GPT) (see manufacturer's manual for details). According to the manual, 500 µL solution 1 (L-glutamate), 100 µL solution 2 (NAD^+), 10 µL solution 3 (GPT), 50 µL diluted sample (or dH_2O as blank) and 450 µL dH_2O were pipetted into a UV cuvette and mixed. After 5 min, A_1 was measured at 340 nm. 10 µL solution 4-D (D-LDH) were added, mixed and incubated for 30 min. Afterwards A_2 was measured at 340 nm. 10 µL solution 4-L (L-LDH) were added mixed and incubated for 30 min and A_3 was recorded at 340 nm. $\Delta A_{D\text{-}lactate}$ was calculated by Equation 4-3 and $\Delta A_{L\text{-}lactate}$ by Equation 4-4:

Equation 4-3
$$\Delta \boldsymbol{A_{D-lactate}} = (\boldsymbol{A_2} - \boldsymbol{A_1})_{\boldsymbol{sample}} - (\boldsymbol{A_2} - \boldsymbol{A_1})_{\boldsymbol{blank}},$$

Equation 4-4
$$\Delta \boldsymbol{A_{L-lactate}} = (\boldsymbol{A_3} - \boldsymbol{A_2})_{\boldsymbol{sample}} - (\boldsymbol{A_3} - \boldsymbol{A_2})_{\boldsymbol{blank}}.$$

The concentration of D- or L-lactate in the samples was calculated by Equation 4-5:

Equation 4-5
$$\boldsymbol{c_{D-/L-lactate}} = \frac{\boldsymbol{V \cdot MW}}{\boldsymbol{\varepsilon \cdot d \cdot v \cdot 1000}} \cdot \Delta \boldsymbol{A_{D-/L-lactate}} \cdot \boldsymbol{F}$$

with $c_{D-/L\text{-}lactate}$ = D- or L-lactate concentration [g L^{-1}], V = final volume before or after addition of solution 4-L [mL], MW = molecular mass of lactate [g mol^{-1}], ε = extinction coefficient of NADH at 340 nm = 6.3 [L $mmol^{-1}$ cm^{-1}], d = light path [cm], v = sample volume [mL], F = dilution factor.

4.2.3.7 Quantification of Isopropanol, Acetone and Ethanol by Gas Chromatography

Isopropanol, acetone and ethanol were quantified by gas chromatography (GC), a separation technique for volatile substances in gas phase, based on their physico-chemical properties. The analytes distribute between a mobile phase (inert carrier gas) and a stationary phase (liquid/polymer adsorbed onto a column surface) and are retarded by interaction with the stationary phase, causing the compounds to elute at different retention times. Separation is influenced by the vapor pressure of the compound, the difference in polarity between analyte and stationary phase, column temperature, carrier gas flow rate, and column length. Detection of analytes takes place at the flame ionization detector (FID), where hydrocarbon-containing compounds are burned, generating a measurable electric current. The increase in current is mass flow-dependent and appears as a chromatographic peak (y-axis) against the retention time (x-axis).

Sample preparation for GC analyses was performed by removal of 1 mL bacterial suspension, centrifugation for 1.5 min at 4 °C and 15600 rpm (centrifuge 5415 R) and filtration of the supernatant (syringe filter Rotilabo®, 0.2 µm mesh, nylon membrane). Supernatants were either stored at -20 °C or directly processed for GC analysis. GC vials with glass inserts were filled with 150 µL internal standard (0.5% (m/v) methanol solution) and 150 µL sample solution. GC measurements of one sample were performed in triplicates from one vial according to the method in Table 4-26.

Table 4-26: GC device, method and operation conditions.
FID... flame ionization detector.

Parameter		Comments
Gas chromatograph	Agilent 7890A	Agilent Technologies Deutschland GmbH, Waldbronn, Germany
Solvent	ddH_2O	
Internal standard	Methanol	0.5% (m/v) methanol in ddH_2O
Automatic injector	Agilent 7693	Liquid applications; Agilent Technologies Deutschland GmbH
Sample injection size	0.5 µL	
Inlet	Split mode (1:5), 250 °C, 7 psi	
Carrier gas	Hydrogen	Mobile phase
Liner	GC Ultra Inert Inlet Liner (wool, Agilent Technologies Deutschland GmbH, Cat. no. #5190-3164)	Glass wool retains matrix components and facilitates evaporation
GC column	CP-PoraBOND U fused silica PLOT (25 m length, 0.32 mm internal diameter, 7 µm film thickness, Agilent Technologies Deutschland GmbH, Cat. no. CP7381)	Capillary of polyimide coated fused-silica layered inside a with high polarity porous polymer, water-resistant, stable up to 300 °C
Oven temperature profile	100 °C (1 min) – gradient 10 °C/min until 200 °C – hold for 5 min at 200 °C	Temperature program allows early-eluting analytes to separate adequately, while shortening the time for late-eluting analytes to pass through the column
Detector	FID, 250 °C, detection limit 1 pg s^{-1}	Agilent Technologies Deutschland GmbH
Ignition gases	Hydrogen/air mixture	Ignition of FID flame
Make-up gas	Nitrogen	Mixed with ignition and carrier gases inside FID to generate detector gas flow

Identification of analytes was performed by comparison of sample retention times with retention times of pure substances (reference standards) analyzed under exactly the same conditions. Quantification of compounds is achieved by integrating the area under the respective peak curve (AUC), which is proportional to the amount of analyte present in the sample. The AUC is correlated to the analyte concentration by creation of a calibration curve (detector response to a series of known analyte concentrations) and by calculation of a relative response factor (ratio of analyte to constant amount of internal standard) in a relative response factor calibration (see 4.2.4.2, page 66). Here, a calibration curve was created according to the GC manufacturer's manual by preparation of a 5% (m/v) stock solution of each isopropanol, acetone and ethanol in ddH_2O. Dilution with ddH_2O yielded a series of solutions with known analyte concentrations. To mimic sample preparation, each solution was filtered (syringe filter Rotilabo®, 0.2 µm mesh, nylon membrane). Methanol was used as internal standard and a stock solution of 0.5% (m/v) methanol was prepared. GC vials with glass inserts were filled with 150 µL internal

standard and 150 µL analyte solution. GC measurements were performed in triplicates from one vial to evaluate the instrumental error. Figure 4-3 displays the calibration curves for isopropanol, acetone and ethanol, plotting the relative response factor (RRF) of the analytes against the known concentrations of the dilution series.

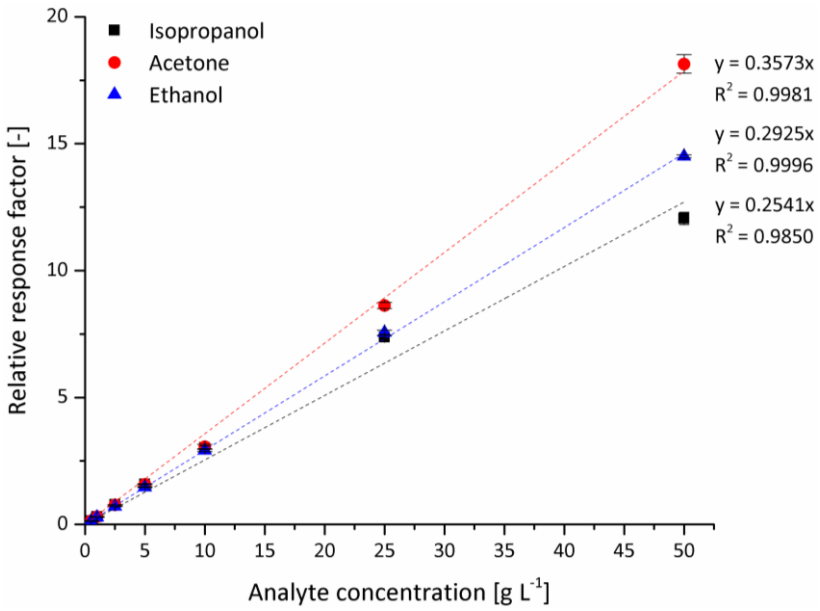

Figure 4-3: RRF calibration curves of isopropanol, acetone and ethanol.
A series of solutions with known isopropanol, acetone and ethanol concentrations was prepared and filtered (syringe filter Rotilabo®, 0.2 µm mesh, nylon membrane). Methanol was used as internal standard to calculate the RRF according to Equation 4-12, page 66. GC measurements were performed in triplicates from one vial. Arithmetic mean, standard deviation, slope and coefficient of determination were calculated using Excel 2007. Error bars display the standard deviation of n = 3 (technical replicates).

The coefficient of determination R^2 indicates a linear correspondence between the analyte RRF and the known analyte concentrations. In subsequent GC analyses, the unknown analyte concentration in a sample was calculated by Equation 4-13 (page 66) from the arithmetic mean of AUC triplicate measurements of analyte and internal standard from one GC vial and the slope of the RRF calibration curves (Figure 4-3).

4.2.3.8 Quantification of O_2 Consumption, CO_2 Generation and Respiratory Quotient

Bacterial O_2 consumption and CO_2 generation in 10 L bioreactor scale was determined by online measurement of O_2 and CO_2 in the reactor exhaust gas in [%] via BlueSens gas sensor "BAC2S". The carbon dioxide production rate (CPR) was calculated according to Equation 4-6:

Equation 4-6
$$\boldsymbol{CPR = \frac{FL \cdot P}{V_B \cdot R \cdot T} \cdot \left(X_{CO2_OUT} - X_{CO2_IN}\right)}$$

with CTR = carbon dioxide production rate [mol L^{-1} h^{-1}], FL = airflow [m^3 h^{-1}], P = normal pressure ≈ 101.3 [kPa], V_B = bioreactor volume [m^3], R = ideal gas constant [J K^{-1} mol^{-1}], T = temperature [K], X_{CO2_OUT} = amount of CO_2 in exhaust gas [-], X_{CO2_IN} = amount of CO_2 in air supply [-].

The bacterial CO_2 production (CO) in [mol] was calculated with regard to the CPR by Equation 4-7:

Equation 4-7
$$\boldsymbol{CO = \frac{CPR \cdot V_B \cdot (t_x - t_0)}{1000}}.$$

The oxygen transfer rate (OTR) into the medium was calculated according to Equation 4-8:

Equation 4-8 $$\boldsymbol{OTR = \frac{FL \cdot P}{V_B \cdot R \cdot T} \cdot \left(X_{O2_IN} - X_{O2_OUT}\right)}$$

with OTR = oxygen transfer rate [mol L^{-1} h^{-1}], FL = airflow [m^3 h^{-1}], P = normal pressure ≈ 101.3 [kPa], V_B = bioreactor volume [m^3], R = ideal gas constant [J K^{-1} mol^{-1}], T = temperature [K], X_{O2_IN} = amount of O_2 in air supply [-], X_{O2_OUT} = amount of O_2 in exhaust gas [-].

In steady-state, i.e. constant concentration of dissolved oxygen in the cultivation medium, it can be assumed that OTR = OUR (cellular oxygen uptake rate).

The bacterial O_2 consumption (OC) in [mol] was calculated with regard to the OUR by Equation 4-9:

Equation 4-9 $$\boldsymbol{OC = \frac{OUR \cdot V_B \cdot (t_x - t_0)}{1000}}.$$

The respiratory quotient (RQ), a value describing the cellular respiratory activity, was calculated from bacterial CO_2 production and O_2 consumption by Equation 4-10:

Equation 4-10 $$\boldsymbol{RQ = \frac{CO}{OC}}.$$

4.2.3.9 Peptide Mass Fingerprint Analysis by MALDI-TOF/TOF Mass Spectrometry

Protein degradation was analyzed by peptide mass fingerprint analysis (PMF), kindly performed by Angelika Schierhorn (Institute of Biochemistry and Biotechnology, Martin Luther University Halle-Wittenberg, Germany). Utilized chemicals and devices are property of the Institute of Biochemistry and Biotechnology. PMF is an analytical technique based on protein cleavage into smaller peptides, peptide ionization, detection and subsequent comparison with a database of known proteins. Whole proteins, but also degradation parts thereof, can thus be identified. The procedure involves taking 1/OD samples from bacterial cultivations, optionally division into soluble/insoluble protein fractions (4.2.3.2, page 60), and separation by SDS-PAGE (4.2.3.3, page 60). After gel staining, bands of interest (e.g. potential degradation products) were excised and subjected to in-gel trypsin digestion. For this, gel pieces were incubated with 10 mM dithiothreitol in 100 mM ammonium bicarbonate for 45 min at 50 °C. The solution was removed and further incubated with 55 mM iodoacetamide in 100 mM ammonium bicarbonate for 45 min in the dark to modifiy cysteine residues. The solution was removed and gel pieces were washed three times with dH_2O, twice with 100 mM ammonium bicarbonate and finally with 100 mM ammonium bicarbonate in 50% acetonitrile. Gel pieces were dried, re-swollen in 20 µL 50 mM ammonium bicarbonate (pH 8.0) and digested with trypsin for ~16 h at 37 °C. For analysis, 0.5 µL of sample solution were mixed with 0.5 µL 7% (w/v) 2,5-dihydroxybenzoic acid in methanol solution and deposited onto a stainless steel target. PMF spectra were recorded on an Ultraflex-II TOF/TOF (Time of Flight) mass spectrometer (Bruker Daltonic, Bremen, Germany) equipped with MALDI (Matrix-Assisted Laser Desorption/Ionization) source, nitrogen laser, LIFT cell for fragment ion postacceleration and gridless ion reflector. Flex Control 3.0, Flex Analysis 3.0 and Biotools 3.0 were used to operate the instrument and analyze the data. For external calibration, a peptide/protein calibration mixture (Bruker, Daltonics, Bremen, Germany) was applied.

4.2.4 Calculations and Equations

4.2.4.1 Lambert-Beer Law in Spectrophotometry

Lambert-Beer law describes the absorbance, i.e. the attenuation of light intensity by absorption, reflection, scattering etc. while travelling through an absorbing substance, depending on the concentration of the absorbing substance and the layer thickness. The absorbance is expressed by the ratio of incident to transmitted spectral radiant power (Equation 4-11):

Equation 4-11

$$\boldsymbol{A = log_{10}\left(\frac{I_0}{I_1}\right) = \varepsilon \cdot c \cdot d}$$

with A = absorbance [-], I_0 = incident radiant flux [W m^{-2}], I_1 = transmitted radiant flux [W m^{-2}], ε = extinction coefficient [L mol^{-1} cm^{-1}] or [mL μg^{-1} cm^{-1}], c = concentration of the absorbing substance [mol L^{-1}] or [µg mL^{-1}], d = layer thickness [cm].

The law is valid within the following limits: (a) homogenous distribution of the absorbing substance, (b) negligible multiple scattering, (c) negligible variation of extinction coefficient, (d) negligible intrinsic emission, (e) low concentrated solutions (<0.01 mol L^{-1}).

4.2.4.2 Gas Chromatography Calibration

Relative response factor (RRF) calibration in GC analysis involves utilization of an internal standard of constant amount that is similar in physical and chemical characteristics to the analyte and does not react with sample or solvent. RRF is the ratio of the detector response of an analyte (AUC_A) and the detector response of the internal standard (AUC_{IS}), whereas AUC_{IS} should be constant. RRF is calculated for each analyte from the arithmetic mean of AUC triplicate measurements from one GC vial (Equation 4-12):

Equation 4-12

$$\boldsymbol{RRF_A = \frac{\overline{AUC_A}}{\overline{AUC_{IS}}}.}$$

Plotting RRF_A against the known analyte concentrations c_A of a dilution series and curve fitting by simple linear regression yields a correlation between RRF_A and c_A, the slope S_A, and a coefficient of determination R^2. The unknown concentration of an analyte in a sample c_A is then calculated by (Equation 4-13):

Equation 4-13

$$\boldsymbol{c_A = \frac{RRF_A}{S_A}.}$$

4.2.4.3 Parameters for Evaluation of Bacterial Cultivations and Product Formation

Rating the performance of a bacterial cultivation can be achieved by calculation of parameters concerned with biomass growth, substrate consumption and product formation (Table 4-27).

Table 4-27: Parameters for evaluation of bacterial cultivations.

Category	Parameter	Code	Unit(s)
Biomass growth	Cell dry weight (maximum)	x_{max}	g biomass L^{-1}
	Growth rate (maximum)	μ_{max}	h^{-1}
	Doubling time	t_d	h
	Biomass yield	$Y_{X/S}$	g biomass g^{-1} substrate
			mol biomass mol^{-1} substrate
			mol% biomass/substrate
	Volumetric biomass productivity	P_X	g biomass L^{-1} h^{-1}
Substrate consumption	Substrate consumption (maximum)	s_{max}	g substrate L^{-1}
	Volumetric consumption rate	P_S	g substrate L^{-1} h^{-1}
	Specific consumption rate	Q_S	g substrate g^{-1} biomass h^{-1}
Product formation	Product concentration (maximum)	p_{max}	g product L^{-1}
	Product yield (from substrate)	$Y_{P/S}$	g product g^{-1} substrate
			mol product mol^{-1} substrate
			mol% product/substrate
	Product yield (biomass-related)	$Y_{P/X}$	g product g^{-1} biomass
			mol product mol^{-1} biomass
			mol% product/biomass
	Volumetric product productivity	P_P	g product L^{-1} h^{-1}
	Specific product productivity	Q_P	g product g^{-1} biomass h^{-1}

Cell/biomass concentration can e.g. be determined via optical density measurement with a spectrophotometer (4.2.3.1, page 59). As a rule of thumb, OD_{600} = 1 corresponds to a cell dry weight of 0.3 g L^{-1} [Soini et al., 2008]. Maximum cell dry weight x_{max} in a cultivation depends e.g. on available nutrients and oxygen supply. The bacterial growth rate μ states the velocity with which x_{max} is reached. Monod defined the bacterial growth rate in exponential phase as constant (μ = constant or μ_{max}) [Monod, 1949], because the cells divide at maximum velocity described by the following equation (Equation 4-14):

Equation 4-14
$$\mu_{max} = \frac{(ln\, x_t - ln\, x_0)}{(t_t - t_0)}$$

with μ_{max} = maximal growth rate [h^{-1}], x = cell dry weight [g L^{-1}], t = time of cultivation [h].

μ_{max} is an organism-specific parameter for growth on a defined substrate, e.g. glucose. The exponential growth phase should be differentiated from the lag (μ = 0) and acceleration phase (μ increasing) as well as the retardation (μ declines), stationary (μ = 0) and death phase (μ < 0). In a bacterial cultivation, the exponential phase can be determined by plotting ln x (at sampling time points) versus time. The y-axis intercept is then ln x_0 (= cell dry weight at t_0 [g L^{-1}]) and the linear section of the slope is μ_{max}. The period of time required by the cells to double their amount is named (maximal) cellular doubling time t_d and is described in Equation 4-15:

Equation 4-15
$$t_d = \frac{ln\, 2}{\mu_{max}}$$

with t_d = doubling time [h], μ_{max} = maximal growth rate [h^{-1}].

The ratio of produced biomass to the amount of consumed substrate is defined as the biomass yield $Y_{X/S}$ (Equation 4-16):

Equation 4-16 $$\boldsymbol{Y_{X/S} = \frac{(x_t - x_0)}{(s_t - s_0)}}$$

with $Y_{X/S}$ = biomass yield [g biomass g^{-1} substrate], x = cell dry weight [g L^{-1}], s = substrate concentration [g L^{-1}].

The biomass yield expresses the ability of an organism to grow on a certain substrate. Biomass yield can also be calculated in mol biomass per mol substrate. A simple approximation for the molar mass of biomass is $C_4H_7O_2N_1$ or 101 g mol^{-1}. A suitable expression for the yield can also be given in %mol biomass per substrate, ranging from zero to 100% conversion of substrate to biomass (Equation 4-17):

Equation 4-17 $$\boldsymbol{Y_{X/S}[\%mol] = Y_{X/S}[mol/mol] \cdot 100\ .}$$

Biomass yield can be calculated for the whole cultivation (overall yield) or for certain periods, e.g. exponential phase or stationary phase. This generally applies to all yield coefficients and productivities, depending on the emphasis of the experimental results (e.g. to point out the period of highest productivity or to focus on the overall process performance). Biomass yield is usually calculated for one defined substrate, considering it is the only carbon source in the medium. This is not true in case of complex media supplemented with glucose. Nevertheless, glucose is the preferred substrate of *E. coli*, and yields have been calculated on the assumption of glucose as sole carbon source. Important information about the substrate are the maximum amount of substrate consumed over the cultivation period and volume (s_{max}) and the velocity of substrate consumption, either given as a rate per volume P_S (Equation 4-18) or per cell dry weight Q_S (Equation 4-19):

Equation 4-18 $$\boldsymbol{P_S = \frac{(s_t - s_0)}{(t_t - t_0)}}$$

with P_S = volumetric substrate consumption rate [g substrate L^{-1} h^{-1}], s = substrate concentration [g L^{-1}], t = time of cultivation [h];

Equation 4-19 $$\boldsymbol{Q_S = \frac{(s_t - s_0)}{(x_t - x_0) \cdot (t_t - t_0)}}$$

with Q_S = specific substrate consumption rate [g substrate g^{-1} biomass h^{-1}], s = substrate concentration [g L^{-1}], x = cell dry weight [g L^{-1}], t = time of cultivation [h].

Analogous to Equation 4-18, the volumetric productivity for biomass can be calculated by Equation 4-20:

Equation 4-20 $$\boldsymbol{P_X = \frac{(x_t - x_0)}{(t_t - t_0)}}$$

with P_X = volumetric biomass productivity [g biomass L^{-1} h^{-1}], x = cell dry weight [g L^{-1}], t = time of cultivation [h].

Product formation can be assessed by stating the maximum amount of product formation over the cultivation period and volume (p_{max}). Analogous to the biomass yield (Equation 4-16), a product yield can be calculated by Equation 4-21:

Equation 4-21 $$\boldsymbol{Y_{P/S} = \frac{(p_t - p_0)}{(s_t - s_0)}}$$

with $Y_{P/S}$ = product yield [g product g^{-1} substrate], p = product concentration [g L^{-1}], s = substrate concentration [g L^{-1}].

The product yield coefficient $Y_{P/S}$ describes the amount of product generated by the biocatalyst by conversion of the substrate. It can also be expressed as mol product per mol substrate or %mol product per substrate (Equation 4-22):

Equation 4-22 $$\boldsymbol{Y_{P/S}[\%mol] = Y_{P/S}[mol/mol] \cdot 100\ .}$$

The biomass-related product yield $Y_{P/X}$ is the ratio of product present to the amount of biomass produced (Equation 4-23):

Equation 4-23 $$\boldsymbol{Y_{P/X} = \frac{(p_t - p_0)}{(x_t - x_0)}}$$

with $Y_{P/X}$ = biomass-related product yield [g product g^{-1} biomass], p = product concentration [g L^{-1}], x = cell dry weight [g L^{-1}].

The biomass-related product yield can also be expressed as mol product per mol biomass or mol% product per biomass.

Product productivity describes the rate with which a product is produced and can be used for comparison and valuation of different production processes. It can either be given as rate per volume of a cultivation P_P (Equation 4-24) or per cell dry weight Q_P (Equation 4-25).

Equation 4-24 $$\boldsymbol{P_P = \frac{(p_t - p_0)}{(t_t - t_0)}}$$

with P_P = volumetric product productivity [g product L^{-1} h^{-1}], p = product concentration [g L^{-1}], t = time of cultivation [h].

Equation 4-25 $$\boldsymbol{Q_P = \frac{(p_t - p_0)}{(x_t - x_0) \cdot (t_t - t_0)}}$$

with Q_P = specific productivity [g product g^{-1} biomass h^{-1}], p = product concentration [g L^{-1}], x = cell dry weight [g L^{-1}], t = time of cultivation [h].

5 Results

5.1 Construction of Isopropanol-Producing *E. coli* Strains

The central aim of this research project was optimization of microbial isopropanol production with regard to concentration, yield and productivity. To accomplish this purpose, first a microbial organism was chosen to act as biocatalyst. Thoughtful choice of the production host and pathway genes as well as rational design of the final expression construct greatly influences the production result. The development of an isopropanol-producing microorganism is described in the following.

5.1.1 The Production Host

In literature, natural and recombinant isopropanol-producing microorganisms are described (see 2.3.1, page 22 and 2.3.2, page 25) and a 4-step enzymatic cascade for isopropanol synthesis from acetyl-CoA is known (2.3.3, page 29). In this work, specifications for an isopropanol-producing organism were set as a) high carbon-throughput for fast growth and production, b) flexible oxygen requirements for easy handling and process scalability, c) capability to use a wide range of carbon sources for cultivation on a cheap substrate, d) availability of genetic tools and easily manipulable genome for fast and easy modification. These requirements preclude the use of *C. beijerinckii*, the natural isopropanol producer, as well as recombinant *C. acetobutylicum*, as they fail in three of the four categories: Although their broad acceptance of a variety of feedstock (see 2.3.1) might seem favorable, their strictly anaerobic metabolism and their tendency for endospore formation in adverse environmental conditions [Torres et al., 2011] pose major challenges for process scale-up. Cultivation of *Clostridia* involves tedious preculture propagation to maintain an oxygen-free environment and to avoid bacteriophage infection and *Lactobacilli* contamination [Lenz and Moreira, 1980]. Their relatively slow growth and the so-called “acid crash” further complicate their handling. “Acid crash” is a phenomenon, which may occur in pH-uncontrolled cultivations resulting in the premature cessation of solvent production [Maddox et al., 2000; Wang et al., 2011]. *Clostridia* usually generate a mixture of products in a strain-, substrate-, medium- and cultivation-dependent manner. Main metabolic product of solventogenesis is, in most cases, butanol, but also acetoin, 2,3-butanediol, ethanol [Collas et al., 2012] and sometimes 1,2-propanediol [Forsberg et al., 1987], in addition to several acids (acetate, butyrate, propionate) and acetone/isopropanol. The variety of obtained products impedes downstream processing and increases the price of purification. It also lowers the yield of the target product isopropanol and may cause problems for cell viability due to the cummulative toxicity of the products [Sikkema et al., 1995]. Attempts to decrease butanol synthesis in favor of isopropanol production by genetic modification in *Clostridia* have not been performed until now. But knockout experiments indicate that shifting the bacterial metabolism towards a certain product is difficult and afflicted with unpredictable effects [Huang et al., 2010]. As an alternative to *Clostridia*, *E. coli* was deemed a suitable production organism, because it meets all of the four named specifications and is one of the five organisms already successfully utilized for selective, recombinant isopropanol production (Table 2-4, page 27). In contrast to recombinant cyanobacteria, it can achieve reasonable isopropanol productivities and does not require time-consuming genomic integration of the genes of interest as *C. utilis*. Unlike *C. necator*, *E. coli* is able to proliferate in the absence of oxygen and utilizes a wide range of sugar carbon sources [Clomburg and

Gonzalez, 2010; Rumbold et al., 2009], while *C. necator* is restricted to fructose. *E. coli* allows relatively simple modification of its genome with commercially available tools, so that a selective channeling of the carbon flux to isopropanol formation is possible. Using a plasmid-based approach enables creation of an isopropanol producer in a short period of time and allows for high gene expression combined with maximum flexibility in terms of interchangeability of genes and/or regulatory elements.

5.1.2 The Expression Vector and Isopropanol Pathway Genes

Construction of the final expression vector necessitates several choices regarding a) the suitable plasmid, b) the selection marker, c) additional vector elements, d) the genes of interest, e) regulatory elements like promoters and operators, f) detection/purification aids. In this work, pHSG299 [Takeshita et al., 1987] (see Table 4-8, page 42 and Figure A-1, page 177 for features and plasmid map) was chosen as a base plasmid because of its relatively small size of 2673 bp in combination with a pMB1-derived origin of replication and a kanamycin resistance gene. The vector size was important due to the considerable size of the gene construct to be introduced, minding that plasmid size >10 kb can affect plasmid isolation and limit efficient gene expression in *E. coli* [Yang and Yang, 2012]. The medium to high copy number (30-200 copies per cell) of the vector and a CER sequence should ensure plasmid stability. The CER sequence is a recombination site involved in dimer/multimer segregation and equal partitioning of the vector to the daughter cells during cell division [Summers and Sherratt, 1988]. The antibiotic resistance marker was chosen to provide sufficient means for selection of plasmid-transformed cells and sustained selection pressure during bacterial cultivation. Kanamycin as a selection agent is often considered superior to ampicillin or chloramphenicol, because the first can be degraded in the culture medium by the β-lactamase, and elimination of the second antibiotic is costly to the cell due to acetyl-CoA consumption [Takeshita et al., 1987]. By default, pHSG299 carries a lac promoter/operator for binding of RNA polymerase and initiation/regulation of mRNA transcription. In the final expression vector, a 398 bp fragment containing the lac promoter/operator was removed by insertion of the isopropanol gene construct via *Xba*I and *Acl*I restriction sites (Figure A-1, page 177). In the construct, each gene of the isopropanol cascade (with one exception, see below) is expressed via its own promoter (monocistronic), in contrast to a polycistronic expression (all genes via one promoter). At the time of construct design, the gene organization of the isopropanol pathway in *C. beijerinckii* NRRL B593 (DSM 6423) was not known. But in *C. acetobutylicum* ATCC 824, each gene of the (acetone) pathway is under the control of its own promoter and located on the plasmid pSOL1 [Gerischer and Durre, 1990; Petersen et al., 1993]. An exception comprises the second and third gene, ctfA and ctfB, which are expressed as a polycistronic mRNA and constitute two subunits of one protein (acetate CoA-transferase, Acct; see 2.3.3, page 29). Therefore, monocistronic expression was chosen to stay as close as possible to the original biosynthetic isopropanol pathway. Instead of the excised lac promoter, the strong tac promoter was used for gene expression. The tac promoter is a hybrid of the -35 region of the trp and the -10 region of the lac UV5 promoter, which is 11 times more efficient than the parental lac and 3 times stronger than the trp promoter [Deboer et al., 1983]. Via its own lac operator, the tac promoter is still repressed by the lacI gene product in the absence of an inductor. The tac promoter/operator region includes a ribosome binding site (Shine-Dalgarno sequence) upstream of the start codon, responsible for recruitment of a ribosome during initiation of protein translation. An rrnB T1 terminator downstream the last pathway gene leads to termination of transcription [Orosz et al., 1991]. Four of five genes (excluding the second gene) were C-terminally fused to a peptide tag-coding DNA sequence, which facilitates detection and potential purification of the respective protein. The four different tags (StrepII, His_{10}, FLAG, c-Myc) were chosen due to their relatively short sequences of 8-11 amino acids, and thus minimal effect on tertiary

protein structure and enzyme activity [Terpe, 2003]. Insertion of several restriction sites throughout the expression construct allows exchange of genes, regulatory elements or tags.

Selection of the individual genes for the expression construct was based on the enzymatic isopropanol cascade in *Clostridia* (2.3.3, page 29) and performed according to the known catalytic properties of the enzymes. In literature, isoenzymes from *Clostridia*, *E. coli* and *T. brockii* are described to catalyze the four reaction steps from acetyl-CoA to isopropanol in recombinant *E. coli*. Although numerous more isoenzymes exist, at least for the first two reactions, it was decided to contemplate only those that have already been tested for expression in *E. coli*. Table 5-1, Table 5-2, Table 5-3 and Table 5-4 list the kinetic parameters of those enzymes.

Table 5-1: Kinetic parameters of selected Act isoenzymes.

Organism	**K_M [mM]**	**k_{cat}[a] [s^{-1}]**	**Specific activity [U mg^{-1}]**	**Reference**
C. acetobutylicum	0.27 (acetyl-CoA)[b] 0.032 (acetoacetyl-CoA)[c] 0.0048 (CoA)[c]	n.d.	216	[Wiesenborn et al., 1988]
E. coli	0.47 (acetyl-CoA)[d] 0.1386 (acetyl-CoA)[e] 0.017 (acetoacetyl-CoA)[e] 0.008 (CoA)[e]	n.d. 6.5	1078	[Duncombe and Frerman, 1976] [Ithayaraja et al., 2016]

[a] turnover number (V_{max}/K_M), [b] 30 °C and pH 7.4, [c] 30 °C and pH 8.0, [d] 25 °C and pH 8.1, [e] 30 °C and pH 7.8, U… enzyme units [U = µmol min^{-1}], n.d…. not determined

Both Act isoenzymes from *C. acetobutylicum* and *E. coli* exhibit a similar affinity (Michaelis constant K_M) in the range of K_M = 0.14-0.47 mM towards the substrate acetyl-CoA, but differ in specific activity, which is higher for the *E. coli* variant (1078 vs. 216 U mg^{-1}). The two isoenzymes are similar in number of amino acids and protein size (see Table A-6, page 187, and Table A-8, page 188). In *C. acetobutylicum* ATCC 824, Act is encoded by the gene thlA (GenBank® accession number (AS): NP_349476.1), while in *E. coli* K-12, Act is encoded by the gene atoB (AS: AAC75284.1). A sequence alignment of both Act nucleotide sequences shows a relatively high sequence identity (number of identical residues to total number of residues) of 56%. Homology (shared ancestry) of genes is assumed when two nucleic acid sequences display a ≥30% match [EMBL-EBI]. Alignment of amino acid sequences yields an identity of 62%, while a homology relation is already suggested at a matching of 10% (better: 30%). Based on the similarity of both isoenzymes and the kinetic parameters, a clear candidate could not be chosen. Act is suggested to have a crucial function in isopropanol synthesis as the pathway branching enzyme [Fox et al., 2014], and therefore, both isoenzymes were tested for application in isopropanol production in this work.

Table 5-2: Kinetic parameters of selected Acct isoenzymes.

Organism	K_M [mM]	k_{cat}[a] [s^{-1}]	Specific activity [U mg^{-1}]	Reference
C. acetobutylicum	1200 (acetate)[b] 0.021 (acetoacetyl-CoA)[b]	n.d.	29.1	[Wiesenborn et al., 1989]
E. coli	53.1 (acetate)[d] 0.021 (acetoacetyl-CoA)[d] 0.24 (acetyl-CoA)[d] 1.86 (acetoacetate)[d]	n.d.	160[c]	[Sramek and Frerman, 1975b] [Sramek and Frerman, 1977]

[a] turnover number, [b] 30 °C and pH 7.5, [c] 24 °C and pH 8.1, [d] 25 °C and pH 8.1, U… enzyme units [U = µmol min^{-1}], n.d…. not determined

The two Acct isoenzymes have the same affinity to acetoacetyl-CoA, but differ considerably in the Michaelis constant K_M of acetate (53 mM for the *E. coli* variant, 1200 mM for *C. acetobutylicum*) and specific activity (160 vs. 29 U mg^{-1}). The high K_M of the clostridial variant can be explained by its role in the shift from acidogenesis to solventogenesis. The enzyme is only supposed to be active in high acid concentrations when the produced acids are re-utilized [Hartmanis et al., 1984; Wiesenborn et al., 1989]. The *Clostridium* enzyme is encoded by two genes, ctfA (AS: NP_149326.1) and ctfB (AS: NP_149327.1), which are transcribed in one operon and translated into the two Acct subunits (ctfA = subunit A; ctfB = subunit B). In *E. coli*, the two genes atoD (AS: NP_416725.1) and atoA (AS: NP_416726.1) (atoD = subunit α; atoA = subunit β) are transcribed in the same manner. The resulting enzyme is suggested to be involved in the bacterial lipid metabolism [Pauli and Overath, 1972]. Sequence alignment of the nucleotide sequences reveals an identity of 53% between ctfA and atoD, or 55% between ctfB and atoA respectively. The matching amino acids between subunits A and α are 46% and between subunits B and β 53%. Thus, both enzymes can be considered homologs. Here, the *E. coli* variant was chosen for the isopropanol gene construct, due to its higher specific acitivty and affinity to acetate.

Table 5-3: Kinetic parameters of selected Adc isoenzymes.

Organism	K_M [mM]	k_{cat}[a] [s^{-1}]	Specific activity [U mg^{-1}]	Reference
C. acetobutylicum	4.1 (acetoacetate)[b] 8 (acetoacetate)[c]	165	n.d.	[Ho et al., 2009] [Davies, 1943]

[a] turnover number, [b] pH 5.95 and 25 °C, [c] pH 5.0 and 37.5 °C, U… enzyme units [U = µmol min^{-1}], n.d.... not determined

In *C. acetobutylicum*, Adc is encoded by the adc gene (AS: NP_149328.1), but the enzyme can also be found in other *Clostridium* species like e.g. *C. beijerinckii*, *C. pasteurianum* and *C. botulinum*. Adc from *C. acetobutylicum* is the only one with experimental evidence at protein level and resolved crystal structure [Ho et al., 2009], while the others are inferred from homology. To date, the *C. acetobutylicum* variant is the only Adc utilized in recombinant acetone/isopropanol production and was therefore chosen for the expression construct.

Table 5-4: Kinetic parameters of selected Idh isoenzymes.

Organism	K_M [mM]	k_{cat}[a] [s^{-1}]	Specific activity [U mg^{-1}]	Reference
C. beijerinckii NRRL B593	0.98 (acetone)[b] 0.022 (NADPH)[b] 9.8 (isopropanol)[b]	138.8	62.5	[Ismaiel et al., 1993]
	1.0 (acetone)[c] 0.018 (NADPH)[c]	55.2	n.d. 89	[Hiu et al., 1987]
T. brockii	3.9 (isopropanol)[d]	n.d.	20.6	[McMahon and Mulcahy, 2002]
	1.0 (isopropanol)[e]			
	0.22 (isopropanol)[f] 0.083 ($NADP^+$)[f]	3.6		[Kleifeld et al., 2003]
			59.0 (isopropanol)[g] 10.4 (acetone)[g]	[Lamed and Zeikus, 1981]

[a] turnover number, [b] 25 °C and pH 7.5, [c] 25 °C and pH 7.5 under argon atmosphere, [d] 23 °C and pH 7.8, [e] 37 °C and pH 7.8, [f] 40 °C and pH 9.0, [g] 40 °C and pH 7.8, U… enzyme units [U = µmol min^{-1}], n.d.... not determined

In *C. beijerinckii*, Idh is encoded by the gene adh (AS: AAA23199.2). But also the *T. brockii* variant (AS: X64841.1) has already been tested for recombinant isopropanol production [Hanai et al., 2007]. Alignment of the nucleotide and amino acid sequences shows a high degree of identity (72% and 76%). Both isoenzymes exhibit a similar number of amino acids, a homotetrameric quaternary structure and a zinc ion located within the catalytic site. Although both are able to accept several secondary alcohols and the corresponding 2-ketones, they show a distinct preference for isopropanol/acetone and an $NADP^+$/NADPH-dependence [Ismaiel et al., 1993; Lamed and Zeikus, 1981]. The Idh of *C. beijerinckii* displays a tenfold lower K_M for acetone in comparison to isopropanol, suggesting that reduction of acetone is the favored reaction direction. The kinetic parameters for the *T. brockii* variant are more ambiguous, displaying a relatively low K_M and a higher specific activity for isopropanol as a substrate. Therefore, Idh of *C. beijerinckii* was chosen for the isopropanol gene construct. Figure 5-1 shows a schematic presentation of the final expression construct comprising the isopropanol production cascade, replacing the excised 398 bp fragment in pHSG299. Amino acid sequences of the four tagged gene products and further enzyme parameters in comparison to the original (untagged) proteins can be found in Appendix A.2 (page 187).

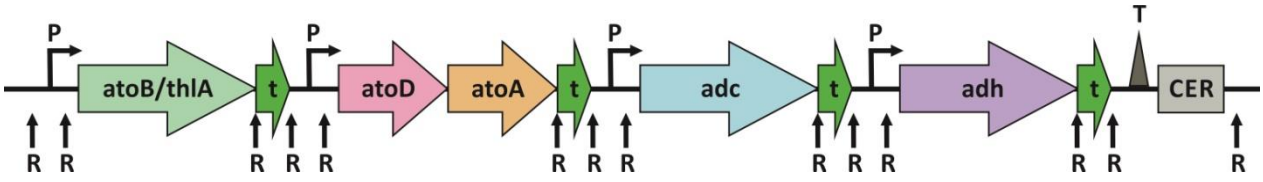

Figure 5-1: Schematic presentation of the expression construct for isopropanol production in *E. coli*.
The gene cassette was introduced into pHSG299 via *Xba*I and *Acl*I restriction sites.
P… promoter, R… restriction site, t… tag, T… terminator, CER… CER sequence.
atoB or thlA encodes Act, atoDA ecodes Acct, adc encodes Adc, adh encodes Idh.

The five genes of interest either originate from *E. coli* K-12 MG1655 (homolog) or from *C. acetobutylicum* ATCC 824 or *C. beijerinckii* NRRL B593 (heterolog). To optimize translation of the resulting mRNAs, all genes were optimized for codon usage and GC content of *E. coli*. Codon usage bias between organisms refers to differences in the utilization frequency of redundant codons and the composition of their tRNA

pools. *E. coli* prefers certain codons over others, which leads to reduced translation efficiencies if mRNA is translated from more rare codons [Welch et al., 2009]. Codon bias can further influence the secondary structure of mRNA and protein folding [Angov, 2011]. Codon usage optimization changed the GC content of the clostridial genes from 37-38% to 45-54% (calculated using DNA/RNA GC Content Calculator), causing a nucleotide change of 24-26% (calculated by Clustal Omega). Homolog genes from *E. coli* (atoB, atoDA) were also optimized by 21-24% nucleotide change to ensure utilization of the most abundant codons. Codon usage optimization, gene synthesis and subcloning of the expression construct into pHSG299 was performed by DNA2.0 (Menlo Park, CA, USA) and Thermo Fisher Scientific - Life Technologies GmbH (Darmstadt, Germany), resulting in two different isopropanol pathway expression vectors pRK_ISO_1E2e3c4c and pRK_ISO_1C2e3c4c (see Table A-2, page 178 & Figure A-2, page 181 and Table A-3, page 182 & Figure A-3, page 185 for DNA sequences and plasmid maps). Numbers denote the four gene products, 1 = Act, 2 = Acct, 3 = Adc and 4 = Idh, whereas letters indicate the origin of the genes, E/e = *E. coli* and C/c = *Clostridium*.

5.1.3 Engineered *E. coli* Strains for Isopropanol Production

The two isopropanol expression vectors were transformed into chemically-competent *E. coli* DH5α (see 4.2.2.3, 4.2.2.4 for methods), amplified, isolated (4.2.2.5) and checked by complete sequencing (4.2.2.7). Final transformation was performed into *E. coli* DH5α and JM109 (see Table 4-4, page 41 for genotypes). Clones were selected on kanamycin-containing LB agar plates and verified by sequencing with a primer oligonucleotide (Table 4-10, page 43) specific for the isopropanol pathway plasmid to confirm the successful transformation. Glycerol stocks were prepared (4.2.1.4) to conserve the positive clones for later experiments. Table 5-5 lists the four resulting strains.

Table 5-5: Engineered *E. coli* strains for isopropanol production.
Utilized peptide tags are a) StrepII for Act, b) His_{10} for subunit β of Acct, c) FLAG for Adc and d) c-Myc for Idh. DNA sequences and plasmid maps are displayed in Table A-2 & Figure A-2 and Table A-3 & Figure A-3.

E. coli strain	Expression vector	Recombinant genes	Final strain name
DH5α	pRK_ISO_1E2e3c4c	atoB, atoDA, adc, adh	*E. coli* DH5α_1E
	pRK_ISO_1C2e3c4c	thlA, atoDA, adc, adh	*E. coli* DH5α_1C
JM109	pRK_ISO_1E2e3c4c	atoB, atoDA, adc, adh	*E. coli* JM109_1E
	pRK_ISO_1C2e3c4c	thlA, atoDA, adc, adh	*E. coli* JM109_1C

5.2 Isopropanol Production from Glucose by Engineered *E. coli* in Shake Flask Scale

The engineered *E. coli* strains (Table 5-5) were subjected to an experimental series in 100 mL shake flask scale, evaluating and comparing the isopropanol production performance with regard to (a) the two different gene combinations, i.e. the two expression plasmids pRK_ISO_1E2e3c4c and pRK_ISO_1C2e3c4c differing in the origin of the first gene, (b) the *E. coli* host and (c) different induction temperatures. Aim of the experiments was to identify the recombinant strain, gene combination and temperature that result in the highest isopropanol concentration. The strains were cultivated as described in 4.2.1.1 (page 49), inoculating the main test cultures in LB medium to an OD_{600} of 0.1. Glucose was added to the medium as a carbon source. Kanamycin (50 µg mL^{-1}) was used to maintain the selection pressure. To promote fast growth, the cells were grown at 37 °C and 100 rpm to an OD_{600} = 0.5 – 0.6. Cultivation temperature was then either kept at 37 °C or lowered to 24 °C prior to induction of gene expression with 0.1 mM IPTG. Samples were taken at certain time intervals to monitor the bacterial growth (OD_{600} by spectrophotometry, 4.2.3.1), the isopropanol, acetone and ethanol production (by gas chromatography (GC), 4.2.3.7), the acetate and lactate formation (by enzymatic test kits, 4.2.3.6), the protein production (Western Blot (WB) analysis of 1/OD samples of whole cell extracts or soluble/insoluble protein fractions, 4.2.3.2, 4.2.3.3, 4.2.3.4) and glucose consumption (glucose measurement by YSI, 4.2.3.5).

For the sake of clarity, the cultivation results for the engineered strains harboring the two different isopropanol pathway plasmids are presented in separate subchapters.

5.2.1 The Isopropanol Pathway Plasmid pRK_ISO_1E2e3c4c in *E. coli* DH5α and JM109

Engineered *E. coli* strains containing the isopropanol pathway plasmid pRK_ISO_1E2e3c4c with the first gene of *E. coli* origin (see Table A-2, page 178 & Figure A-2, page 181 for DNA sequence and plasmid map) were tested for isopropanol production in 100 mL shake flask scale. The effect of induction temperature on growth and product synthesis by *E. coli* DH5α_1E and *E. coli* JM109_1E in glucose-supplemented LB medium is depicted in Figure 5-2. All recombinant *E. coli* strains grew with a maximal growth rate μ_{max} = 0.5-0.6 h^{-1} in exponential phase. Exponential growth continued for strains kept at 37 °C until stationary phase was reached (t = 6-7 h). While DH5α_1E achieved a maximal OD_{600} of 3.0 after 24 h at 37 °C, JM109_1E only grew to a maximal OD_{600} of 1.5. Growth was retarded for cells cultivated at 24 °C after induction, although they eventually reached stationary phase after 24 h with an OD_{600} of 2.4 for DH5α_1E and 2.8 for JM109_1E.

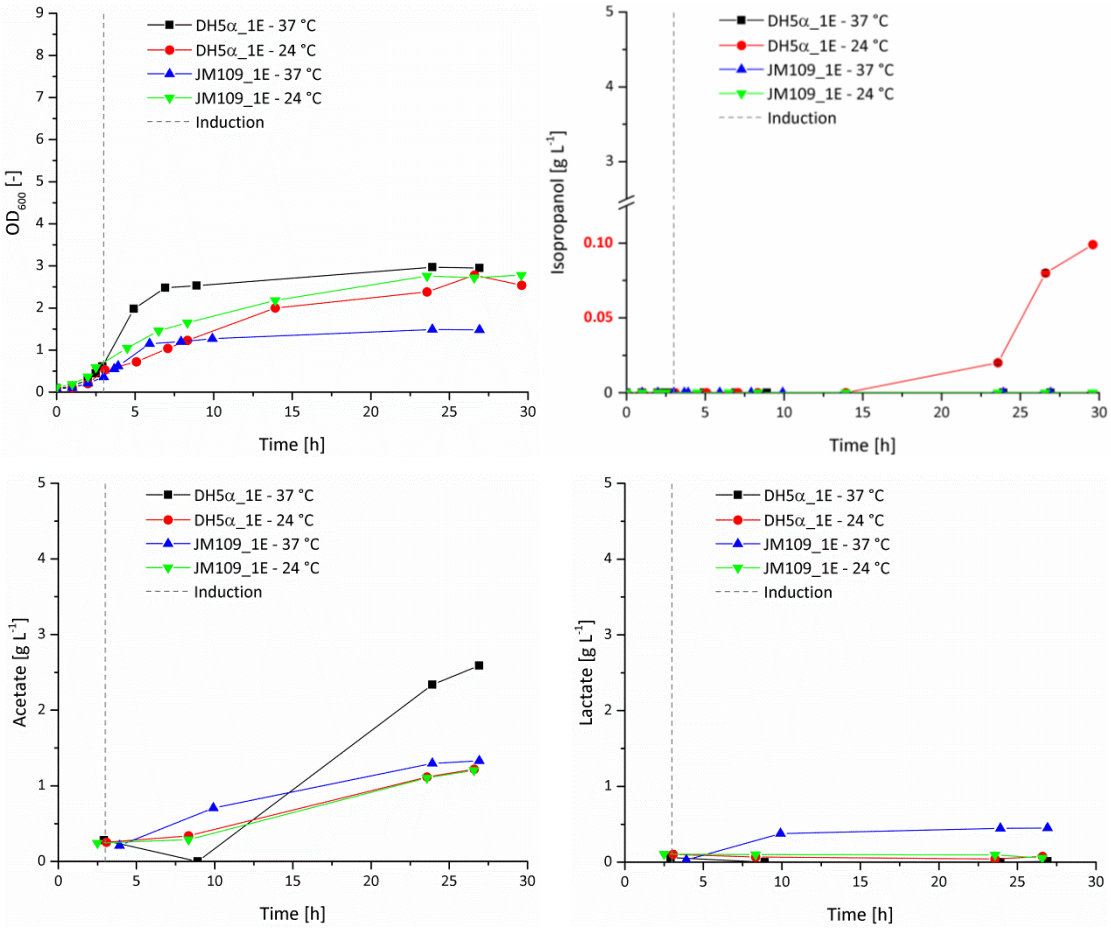

Figure 5-2: Influence of induction temperature on growth and isopropanol, acetate and lactate production of *E. coli* DH5α_1E and *E. coli* JM109_1E.

Recombinant *E. coli* DH5α and JM109 were inoculated to an OD_{600} = 0.1 in 100 mL LB medium containing 2% (w/v) glucose, which was replenished if necessary. Cultures were grown at 37 °C, 100 rpm until induction. Cultivation temperature was either kept at 37 °C or lowered to 24 °C before addition of 0.1 mM IPTG. Samples were taken at intervals for determination of cell concentration, glucose consumption, protein and product analysis. GC analysis: Error bars display the standard deviation of n = 3 (technical replicates).

Isopropanol production was only observed for *E. coli* DH5α_1E at 24 °C after induction, whereas neither of the strains grown at 37 °C, nor JM109_1E at 24 °C generated any isopropanol. For *E. coli* DH5α_1E at 24 °C, isopropanol was first detected at the onset of stationary phase (t = 24 h) and a final isopropanol concentration of 0.1 g L^{-1} was achieved after 30 h. Table 5-6 gives a summary on isopropanol

concentration, yield and productivity, i.e. the production parameters of the recombinant *E. coli* strains, after 24 h at the two different induction temperatures. In this work, for the sake of comparability, production parameters were calculated after 24 h of cultivation (if not otherwise stated).

Table 5-6: Influence of induction temperature on isopropanol production parameters of *E. coli* DH5α_1E and *E. coli* JM109_1E after 24 h.

Isopropanol yields were calculated according to 4.2.4.3 (page 66), Equation 4-23, Equation 4-21, Equation 4-22. Isopropanol productivities were calculated according to Equation 4-24, Equation 4-25.

p_{max}… product concentration, $Y_{P/X}$… product yield (biomass-related), $Y_{P/S}$… product yield (from substrate), P_P... volumetric productivity, Q_P… specific productivity (biomass-related)

E. coli strain	Temperature [°C]	p_{max} [g L^{-1}]	$Y_{P/X}$ [g g^{-1} biomass]	$Y_{P/S}$ [mol mol^{-1} glucose][a]	$Y_{P/S}$ [mol%][a]	P_P [g L^{-1} h^{-1}]	Q_P [g g^{-1} biomass h^{-1}]
DH5α	37	0.00	0.000	0.000	0.0	0.000	0.000
	24	**0.02**	**0.030**	**0.029**	**2.9**	**0.001**	**0.001**
JM109	37	0.00	0.000	0.000	0.0	0.000	0.000
	24	0.00	0.000	0.000	0.0	0.000	0.000

[a] For calculation purposes, glucose is considered the sole carbon source in the medium.

Neither acetone nor ethanol was detectable in the cultivation medium of all hosts. Acetate concentrations in the medium were rising similarly for strains grown at 24 °C, reaching a concentration of 1.1 g L^{-1} acetate after 24 h. At 37 °C, acetate generation differed between the two hosts. While JM109_1E steadily produced acetate up to 1.3 g L^{-1} after 24 h, the concentration in the medium of DH5α_1E decreased to zero (t = 9 h) and quickly rose again to yield the highest acetate concentration of all strains after 24 h (2.3 g L^{-1}). Lactate concentrations in the medium were either constant for JM109_1E at 24 °C or decreasing over the cultivation period for DH5α_1E at 24 and 37 °C. In contrast, JM109_1E at 37 °C already generated four times more lactate at t = 9 h compared to the other strains.

Analysis of protein production via soluble-insoluble fractionation of cell extracts and WB revealed that the first enzyme of the isopropanol pathway, the Act of *E. coli* origin with C-terminal StrepII-tag, denoted as Act-StrepII (1E), could not be detected at the expected (calculated theoretical) molecular mass of 41.6 kDa in the soluble fraction of samples taken from the 37 °C cultivations (Figure 5-3 A & C, odd numbered lanes). For DH5α_1E at 37 °C, the enzyme was only visible at ~41 kDa in its insoluble form (Figure 5-3 A, even numbered lanes), while it could not be seen at all in samples of JM109_1E at 37 °C (Figure 5-3 C). Additional bands were visible at ~23 kDa, ~35 kDa and ~38 kDa in the insoluble fractions of DH5α_1E at 37 °C (A, even numbered lanes), DH5α_1E at 24 °C (B) and JM109_1E at 24 °C (D), while samples of JM109_1E at 37 °C displayed only bands at ~35 kDa and ~38 kDa (C). In samples of JM109_1E at 24 °C (D), barely visible signals at ~41 kDa indicate a very weak production of Act-StrepII (1E). But soluble Act-StrepII (1E) could only be clearly detected at ~41 kDa for *E. coli* DH5α_1E at 24 °C (B, odd numbered lanes). Regardless of the solubility, the enzyme was already detected before induction for DH5α_1E cultivated at both temperatures (A, lane 2 and B, lane 1 & 2).

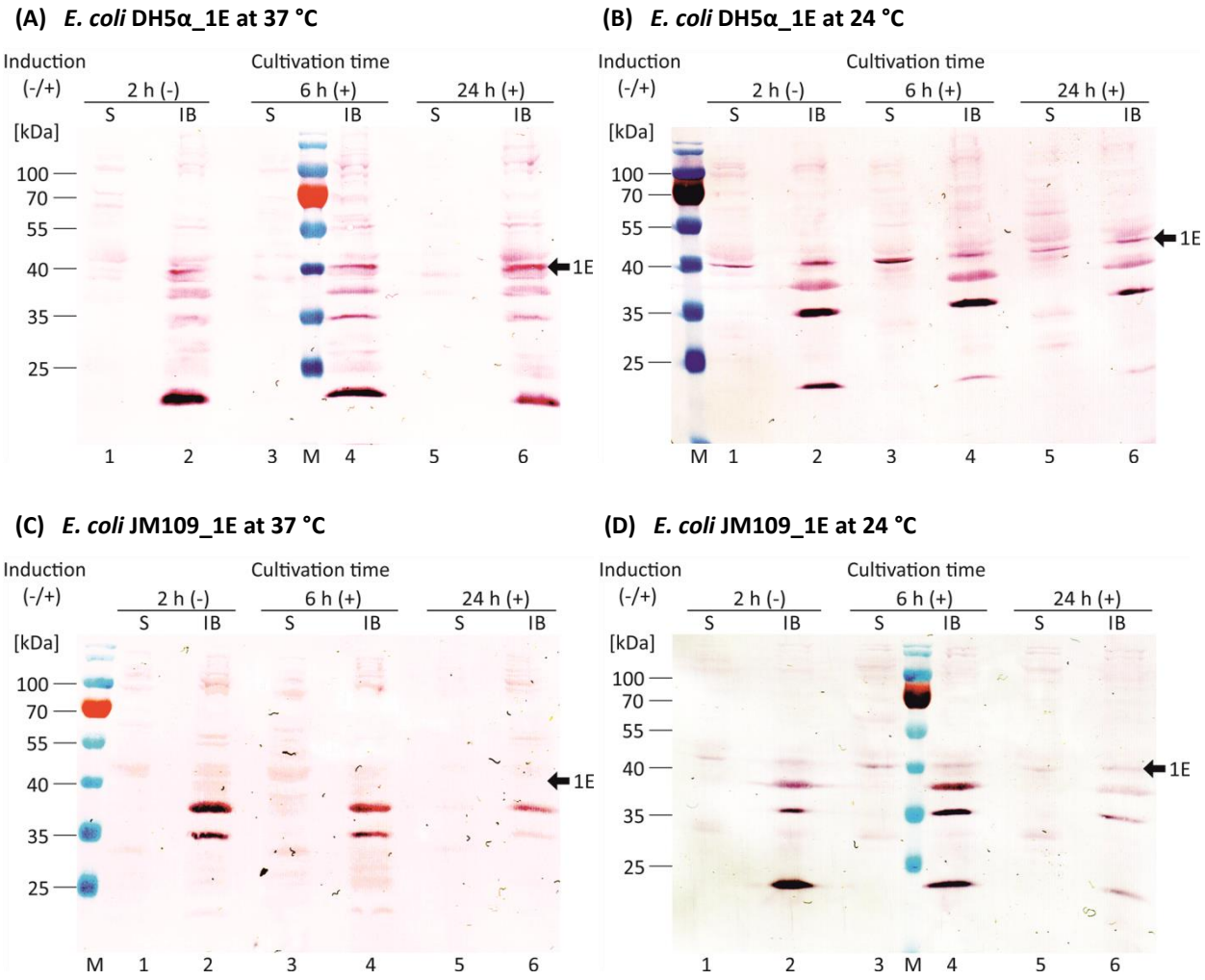

Figure 5-3: Influence of induction temperature on production of Act-StrepII (1E) in *E. coli* DH5α_1E (A, B) and *E. coli* JM109_1E (C, D).

Recombinant *E. coli* DH5α and JM109 were grown in 100 mL LB medium, 2% (w/v) glucose at 37 °C, 100 rpm. Cultivation temperature was either kept at 37 °C (A, C) or lowered to 24 °C (B, D) before addition of 0.1 mM IPTG. 1/OD samples were taken at intervals, lysed and divided into soluble and insoluble cell extract fraction (4.2.3.2). Extracts were separated by SDS-PAGE and Act-StrepII (1E) was visualized by WB with anti-StrepII® and anti-Mouse IgG-conjugated alkaline phosphatase antibodies (dye: BCIP/NBT) (see Table 4-12 for antibodies).

Lanes with odd numbers display the soluble fraction (S), whereas lanes with even numbers display the insoluble fraction (IB) samples. Arrows indicate the detected proteins. Theoretical molecular protein masses were calculated using ProtParam: MW of Act-StrepII (1E) = 41.6 kDa.

Act… acetyl-CoA acetyltransferase

Analysis of the other isopropanol pathway gene products showed presence of all three proteins in all strains cultivated at 37 and 24 °C, predominantly in the insoluble fractions (Figure 5-4, even numbered lanes). The Acct subunit β with C-terminal His_{10}-tag, denoted as Acct-His_{10} (2e), could be detected in all samples at the expected molecular mass of 24.7 kDa. At 37 °C, it was detectable in the soluble fraction of both strains even before induction (A & C, lane 1), but seemed to vanish from this fraction after induction (A & C, lane 3 & 5). At 24 °C, its soluble presence was more pronounced in DH5α_1E throughout the cultivation (B, odd numbered lanes), while it was only weakly detected in JM109_1E (D, odd numbered lanes). At ~29 kDa, the Adc with C-terminal FLAG-tag, denoted as Adc-FLAG (3c), was visible to approximately equal shares in soluble and insoluble samples of DH5α_1E at 37 and 24 °C (A & B), also before induction. In JM109_1E, its soluble presence was favored in samples cultivated at 24 °C

(compare C & D, odd numbered lanes). The Idh with C-terminal c-Myc-tag, denoted as Idh-c-Myc (4c), was strongly produced in both hosts at both induction temperatures at ~39 kDa, though the enzyme seemed to reside mainly in the insoluble fraction (even numbered lanes). At 24 °C, solubility of Idh-c-Myc (4c) was enhanced for both recombinant *E. coli* strains (B & D, odd numbered lanes) compared to the cultivations at 37 °C (A & C, odd numbered lanes).

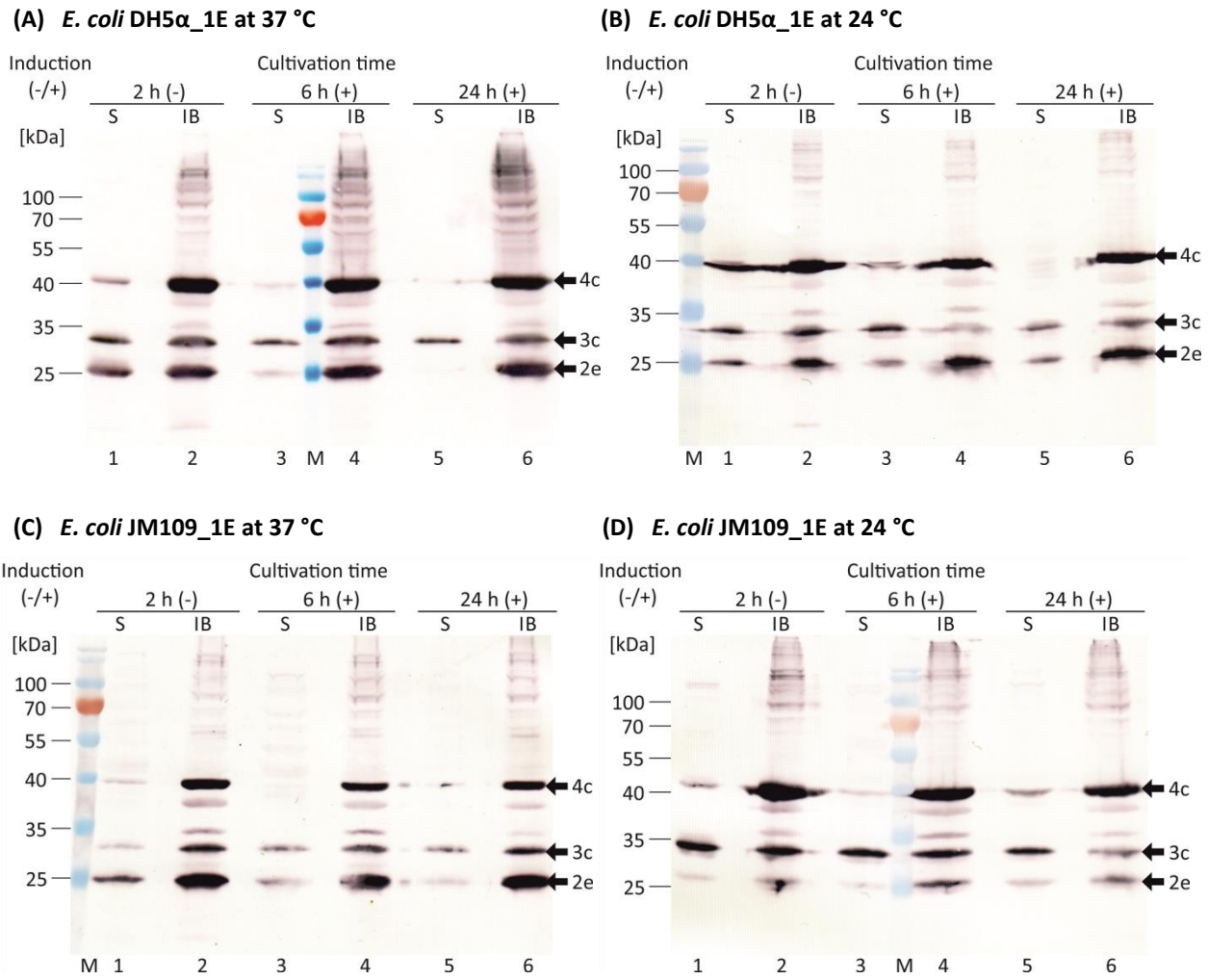

Figure 5-4: Influence of induction temperature on production of Acct-His$_{10}$ (2e), Adc-FLAG (3c) & Idh-c-Myc (4c) in *E. coli* DH5α_1E (A, B) and *E. coli* JM109_1E (C, D).

Recombinant *E. coli* DH5α and JM109 were grown in 100 mL LB medium, 2% (w/v) glucose at 37 °C, 100 rpm. Cultivation temperature was either kept at 37 °C (A, C) or lowered to 24 °C (B, D) before addition of 0.1 mM IPTG. 1/OD samples were taken at intervals, lysed and divided into soluble and insoluble cell extract fraction (4.2.3.2). Extracts were separated by SDS-PAGE and Acct-His$_{10}$ (2e) was visualized by WB with anti-polyHistidine, Adc-FLAG (3c) with anti-FLAG® and Idh-c-Myc (4c) with anti-c-Myc and anti-Mouse IgG-conjugated alkaline phosphatase antibodies (dye: BCIP/NBT) (see Table 4-12 for antibodies).
Lanes with odd numbers display the soluble fraction (S), whereas lanes with even numbers display the insoluble fraction (IB) samples. Arrows indicate the detected proteins. Theoretical molecular protein masses were calculated using ProtParam: MW of Acct-His$_{10}$ (2e) = 24.7 kDa, MW of Adc-FLAG (3c) = 28.9 kDa, MW of Idh-c-Myc (4c) = 39.0 kDa.
Acct… acetate CoA-transferase, Adc… acetoacetate decarboxylase, Idh… isopropanol dehydrogenase

Overall, soluble production of the isopropanol pathway enzymes was supported by a decreased induction temperature of 24 °C. Isopropanol production could only be observed for *E. coli* DH5α_1E (although only in low amounts) when cultivation temperature was decreased from 37 to 24 °C at the point of induction.

5.2.2 The Isopropanol Pathway Plasmid pRK_ISO_1C2e3c4c in *E. coli* DH5α and JM109

Isopropanol production in shake flask scale was further tested with recombinant *E. coli* strains harboring the isopropanol pathway plasmid pRK_ISO_1C2e3c4c with the first gene from *C. acetobutylicum* origin (see Table A-3, page 182 & Figure A-3, page 185 for DNA sequence and plasmid map). Additionally, cultures of non-transformed *E. coli* DH5α and JM109 were carried along as negative controls at 24 °C. Figure 5-5 displays the effect of induction temperature on growth of and isopropanol synthesis by *E. coli* DH5α_1E and *E. coli* JM109_1E. Non-transformed *E. coli* and JM109_1C grew with a μ_{max} of 0.7-0.8 h^{-1} in exponential phase, whereas DH5α_1C achieved a μ_{max} of 0.6 h^{-1}. Stationary phase was reached for non-transformed strains and JM109_1C at 37 °C after 10.5 h, while DH5α_1C at 24 and 37 °C and JM109_1C at 24 °C continued to grow until t = 24 h. *E. coli* DH5α_1C at 24 °C even displayed linear growth until the end of cultivation. Maximal cell density in stationary phase was highest for DH5α_1C at 37 °C with an OD_{600} = 8.6, followed closely by DH5α_1C at 24 °C with an OD_{600} = 7.1. The non-transformed strains displayed the lowest biomass accumulation, reaching only a final OD_{600} of 2.6 (DH5α) and 1.9 (JM109).

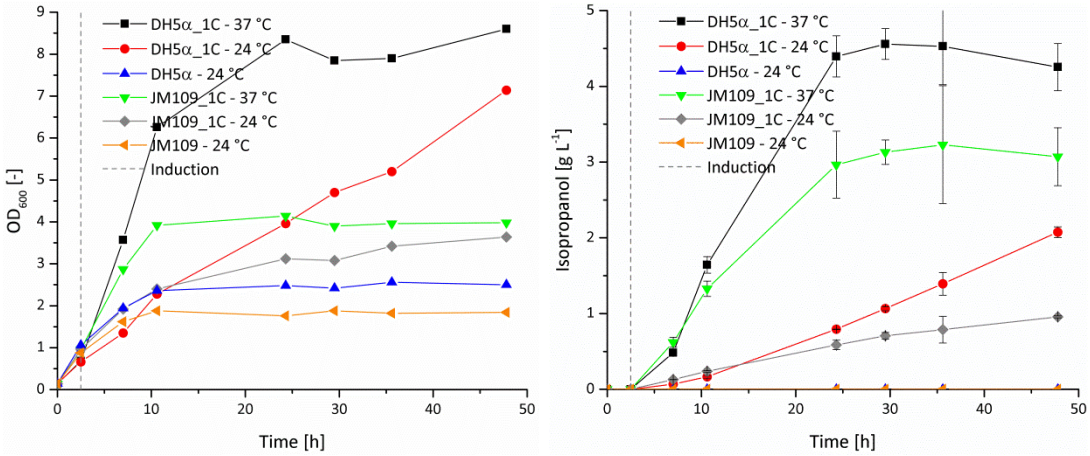

Figure 5-5: Influence of induction temperature on growth and isopropanol production of *E. coli* DH5α_1C and *E. coli* JM109_1C.
Recombinant *E. coli* DH5α and JM109 were inoculated to an OD_{600} = 0.1 in 100 mL LB medium containing 2% (w/v) glucose, which was replenished if necessary. Cultures were grown at 37 °C, 100 rpm until induction. Cultivation temperature was either kept at 37 °C or lowered to 24 °C before addition of 0.1 mM IPTG. Non-transformed *E. coli* DH5α and JM109 served as a negative control (with addition of 0.1 mM IPTG). Samples were taken at intervals for determination of cell concentration, glucose consumption, protein and product analysis. GC analysis: Error bars display the standard deviation of n = 3 (technical replicates).

Isopropanol was not produced by the non-transformed *E. coli* (negative control). All recombinant strains showed isopropanol formation in varying amounts (Figure 5-5). Highest isopropanol concentration of 4.4 g L^{-1} was achieved by DH5α_1C at 37 °C after 24 h, while JM109_1C at 37 °C ranked second highest with 3.0 g L^{-1}. At 24 °C, the recombinant strains reached isopropanol concentrations of 0.6-0.8 g L^{-1} after 24 h. Beyond 24 h, isopropanol generation was more or less stagnant for recombinant hosts kept at 37 °C and JM109_1C at 24 °C, while DH5α_1C at 24 °C continued production until the end of cultivation (t = 48 h) with a final concentration of 2.1 g L^{-1}. Table 5-7 summarizes the influence of different induction temperatures on isopropanol production parameters after 24 and 48 h for the recombinant strains with pRK_ISO_1C2e3c4c.

Table 5-7: Influence of induction temperature on isopropanol production parameters of *E. coli* DH5α_1C and *E. coli* JM109_1C after 24 and 48 h.

Isopropanol yields were calculated according to 4.2.4.3 (page 66), Equation 4-23, Equation 4-21, Equation 4-22. Isopropanol productivities were calculated according to Equation 4-24, Equation 4-25.

p_{max}… product concentration, $Y_{P/X}$… product yield (biomass-related), $Y_{P/S}$… product yield (from substrate), P_P... volumetric productivity, Q_P… specific productivity (biomass-related)

E. coli strain	Temperature [°C]	Time [h]	p_{max} [g L^{-1}]	$Y_{P/X}$ [g g^{-1} biomass]	$Y_{P/S}$ [mol mol^{-1} glucose][a]	$Y_{P/S}$ [mol%][a]	P_P [g L^{-1} h^{-1}]	Q_P [g g^{-1} biomass h^{-1}]
DH5α_1C	24	24	0.79	0.703	0.320	32.0	0.033	0.027
		48	2.07	1.003	0.348	34.8	0.043	0.020
	37	24	**4.39**	1.794	**0.587**	**58.7**	**0.181**	0.072
		48	4.25	1.698	0.422	42.2	0.089	0.034
JM109_1C	24	24	0.59	0.665	0.232	23.2	0.024	0.026
		48	0.96	0.937	0.269	26.9	0.020	0.018
	37	24	2.97	2.498	0.547	54.7	0.122	**0.098**
		48	3.07	**2.742**	0.457	45.7	0.064	0.054

[a] For calculation purposes, glucose is considered the sole carbon source in the medium.

All in all, cultivation of *E. coli* DH5α_1C at 37 °C displayed the highest isopropanol concentration $p_{max,}$ isopropanol yield from glucose $Y_{P/S}$ and volumetric productivity P_P after 24 h. JM109_1C at 37 °C scored best for biomass-related isopropanol yield $Y_{P/X}$ and specific productivity Q_P, although an overall lower isopropanol concentration was achieved compared to DH5α_1C at 37 °C. Isopropanol precursor acetone could also be detected in the cultivation medium of most recombinant strains, except for JM109_1C at 24 °C. Figure 5-6 depicts the production of acetone, ethanol, acetate and lactate by *E. coli* DH5α_1C and JM109_1C at the different induction temperatures. Acetone production was highest in DH5α_1C at 37 °C, followed by JM109_1C at 37 °C and DH5α_1C at 24 °C.

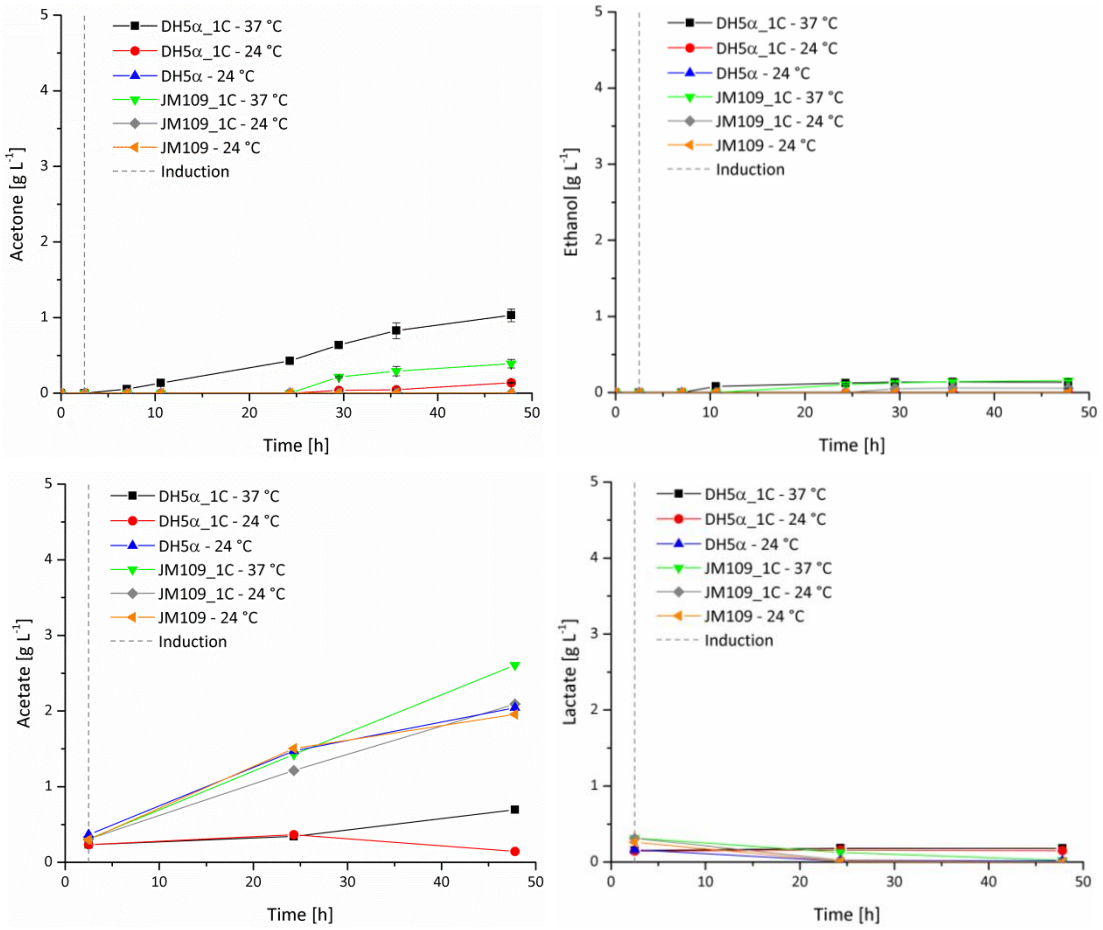

Figure 5-6: Influence of induction temperature on acetone, ethanol, acetate and lactate production of *E. coli* DH5α_1C and *E. coli* JM109_1C.

Recombinant *E. coli* DH5α and JM109 were inoculated to an OD_{600} = 0.1 in 100 mL LB medium containing 2% (w/v) glucose, which was replenished if necessary. Cultures were grown at 37 °C, 100 rpm until induction. Cultivation temperature was either kept at 37 °C or lowered to 24 °C before addition of 0.1 mM IPTG. Non-transformed *E. coli* DH5α and JM109 served as a negative control (with addition of 0.1 mM IPTG). Samples were taken at intervals for determination of cell concentration, glucose consumption, protein and product analysis. GC analysis: Error bars display the standard deviation of n = 3 (technical replicates).

Ethanol could not be detected in the cultivation medium of non-transformed *E. coli* or DH5α_1C at 24 °C, but low concentrations of 0.05-0.06 g L^{-1} were found in medium samples of JM109_1C at 24 °C. Recombinant strains kept at 37 °C displayed slightly higher ethanol concentrations of 0.13-0.16 g L^{-1} towards the end of cultivation. Acetate was produced in considerable amounts in non-transformed strains and JM109_1C at 24 and 37 °C, ranging between 2.0 and 2.6 g L^{-1} at t = 48 h. For DH5α_1C, acetate generation was lower, reaching only a final concentration of 0.1 g L^{-1} and 0.7 g L^{-1} at 24 °C and 37 °C respectively. Lactate concentrations for DH5α_1C at 24 and 37 °C remained in a range of 0.15-0.18 g L^{-1} throughout the cultivation period, while initially present lactate in the medium of non-transformed strains and JM109_1C decreased below 0.02 g L^{-1} after 48 h.

Protein analysis of whole cell extracts by WB (total protein in 1/OD samples) displayed a strong production of Act-StrepII (1C) at the expected molecular mass of ~43 kDa for both recombinant strains at 37 and 24 °C even before induction (Figure 5-7 A & B, lanes 2 & 3). A corresponding band could not be seen in samples of the non-transformed strains (A & B, lanes 1, 4, 7). As observed before in the WB for Act-StrepII (1E) (Figure 5-3, page 79), faint bands were visible at ~35 and ~38 kDa, which also appeared for non- transformed cells, indicating a non-recombinant gene product. Additional signals were detected

at ~40, ~32 and ~28 kDa exclusively in samples of DH5α_1C and JM109_1C (Figure 5-7 A & B, lanes 2, 3, 5, 6, 8, 9). In non-transformed JM109, a 30 kDa protein could be seen (B, lanes 1, 4, 7), which was not visible in samples of non-transformed DH5α. Generally, detection of Act-StrepII (1C) at the correct molecular mass was more pronounced in cells cultivated at 37 °C, at least after induction (A & B, lanes 5 & 8 vs. lanes 6 & 9).

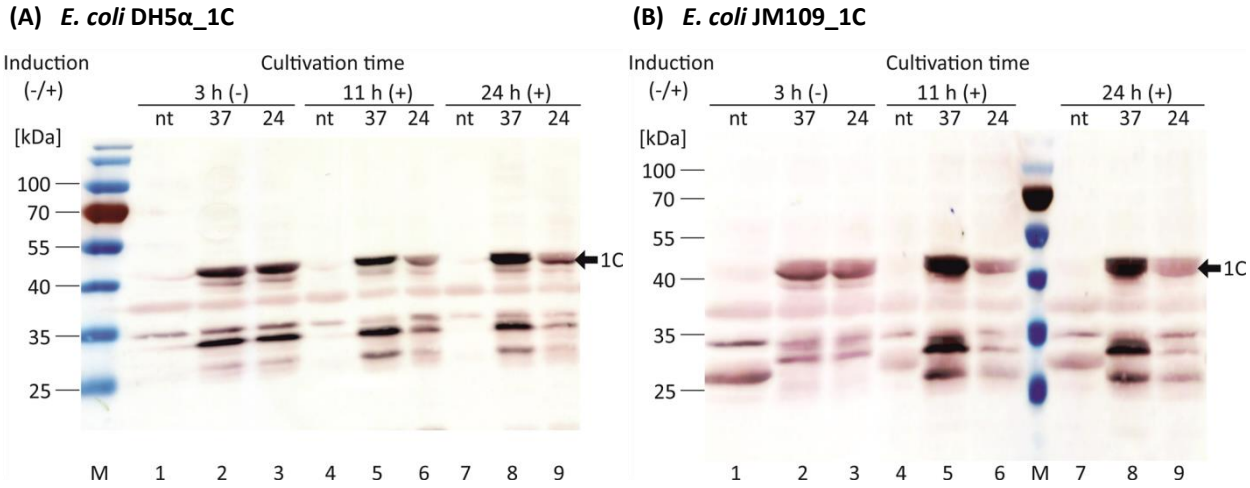

Figure 5-7: Influence of induction temperature on production of Act-StrepII (1C) in *E. coli* DH5α_1C (A) and *E. coli* JM109_1C (B).

Recombinant *E. coli* DH5α and JM109 were grown in 100 mL LB medium, 2% (w/v) glucose at 37 °C, 100 rpm. Cultivation temperature was either kept at 37 °C or lowered to 24 °C before addition of 0.1 mM IPTG. Non-transformed (nt) *E. coli* DH5α and JM109 served as a negative control (with addition of 0.1 mM IPTG). 1/OD samples were taken at intervals and lysed. Extracts (TOTAL PROTEIN) were separated by SDS-PAGE and Act-StrepII (1C) was visualized by WB with anti-StrepII® and anti-Mouse IgG-conjugated alkaline phosphatase antibodies (dye: BCIP/NBT) (see Table 4-12 for antibodies).
Arrows indicate the detected proteins. Theoretical molecular protein masses were calculated using ProtParam: MW of Act-StrepII (1C) = 42.5 kDa.
Act… acetyl-CoA acetyltransferase

Acct-His_{10} (2e) could be detected in samples of all recombinant strains at the expected molecular mass of ~25 kDa (Figure 5-8 A & B left, lanes 2, 3, 5, 6, 8, 9) in similar amounts at 24 and 37 °C. A band at ~35 kDa, which was also present in non-transformed cells, indicated an *E. coli* host protein. Adc-FLAG (3c) and Idh-c-Myc (4c) were both visible at the expected molecular masses of ~29 and ~39 kDa in samples of DH5α_1C and JM109_1C. Their production appeared to be favored at 37 °C after induction (A & B right, lanes 5 & 8 vs. lanes 6 & 9).

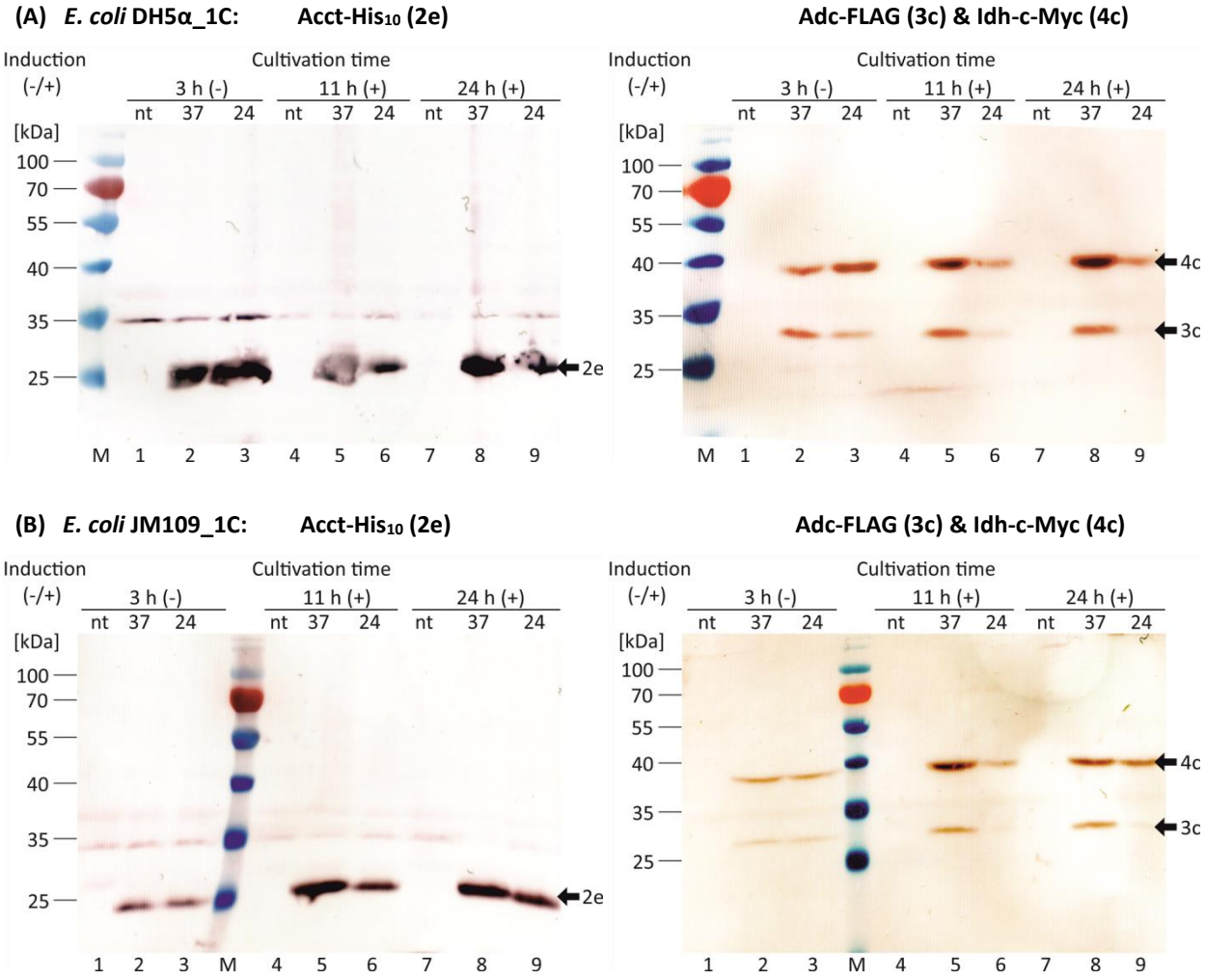

Figure 5-8: Influence of induction temperature on production of Acct-His$_{10}$ (2e), Adc-FLAG (3c) & Idh-c-Myc (4c) in *E. coli* DH5α_1C (A) and *E. coli* JM109_1C (B).

Recombinant *E. coli* DH5α and JM109 were grown in 100 mL LB medium, 2% (w/v) glucose at 37 °C, 100 rpm. Cultivation temperature was either kept at 37 °C or lowered to 24 °C before addition of 0.1 mM IPTG. Non-transformed (nt) *E. coli* DH5α and JM109 served as a negative control (with addition of 0.1 mM IPTG). 1/OD samples were taken at intervals and lysed. Extracts (TOTAL PROTEIN) were separated by SDS-PAGE and Acct-His$_{10}$ (2e) was visualized by WB with anti-polyHistidine, Adc-FLAG (3c) with anti-FLAG® and Idh-c-Myc (4c) with anti-c-Myc and anti-Mouse IgG-conjugated alkaline phosphatase antibodies (dye: BCIP/NBT) (see Table 4-12 for antibodies).

Arrows indicate the detected proteins. Theoretical molecular protein masses were calculated using ProtParam: MW of Acct-His$_{10}$ (2e) = 24.7 kDa, MW of Adc-FLAG (3c) = 28.9 kDa, MW of Idh-c-Myc (4c) = 39.0 kDa.

Acct… acetate CoA-transferase, Adc… acetoacetate decarboxylase, Idh… isopropanol dehydrogenase

Protein solubility was not investigated in this case. Repetition of the experiment with *E. coli* DH5α_1C at 37 °C (in the scope of a master thesis by Benjamin Schrank "*Untersuchungen zur Produktion von Aceton und Isopropanol mit* Escherichia coli", 2015), including soluble-insoluble fractionation of cell extracts and WB, displayed that all four enzymes were indeed produced in their soluble form after 24 h (see Appendix Figure A-5, page 192).

In conclusion, cultivation of *E. coli* DH5α_1C and JM109_1C at 37 °C seemed more beneficial for recombinant protein and isopropanol production, than lowering the temperature to 24 °C post-induction. After 24 h, DH5α_1C already generated 1.5 times more isopropanol than JM109_1C, marking DH5α_1C as the best isopropanol producer in 100 mL shake flask scale. In general, engineered strains

with pRK_ISO_1C2e3c4c showed superior isopropanol production performance in comparison to the strains harboring pRK_ISO_1E2e3c4c with the first gene of *E. coli* origin (see 5.2.1).

Detection of acetone in the cultivation medium of the isopropanol-producing strains (Figure 5-6, page 83) suggested an insufficient activity of Idh-c-Myc (4c), possibly due to insolubility at 37 °C (as shown for *E. coli* DH5α_1E and JM109_1E in Figure 5-4, page 80). To increase its solubility, Idh-c-Myc (4c) was N-terminally fused with the SUMO tag, a small ubiquitin-like modifier peptide, which is known to enhance stability and solubility of recombinant proteins in prokaryotic and eukaryotic expression systems [Panavas et al., 2009]. SUMOylation cloning and evaluation of its effect on isopropanol formation was performed in the scope of a project work by Benjamin Schrank ("Cloning of a SUMOylated isopropanol dehydrogenase and investigations on its solubility and isopropanol production", 2015). Unfortunately, SUMOylation of Idh-c-Myc (4c) resulted in a decreased isopropanol concentration of 1.4 g L^{-1} after 24 h, compared to utilization of the non-SUMOylated enzyme with 4.4 g L^{-1}. With SUMO-Idh-c-Myc (4c), acetone concentration in the medium increased to 0.7 g L^{-1} after 24 h, compared to 0.4 g L^{-1} with the unmodified Idh-c-Myc (4c), indicating an impaired enzyme activity caused by the SUMO fusion. Therefore, subsequent experiments in this work were performed with cells harboring the original Idh-c-Myc (4c).

5.3 Isopropanol Production from Beech Wood Hydrolysate by Engineered *E. coli* in Shake Flask Scale

Lignocellulose hydrolysates have the potential to be used as feedstock for microorganisms instead of glucose, as described in 2.4 (page 31). But the required treatment for biomass hydrolysis often induces formation of inhibitors, which can have detrimental effects on growth and production of the desired product (see Table 2-6, page 35). The following experiments were performed to evaluate the use of the glucose fraction of a beech wood hydrolysate (BWH; see 4.1.3, page 40) as substrate for isopropanol synthesis by recombinant *E. coli*. *E. coli* DH5α_1C was cultivated at 37 °C in 100 mL shake flask scale and samples were analyzed analogous to 5.2 (page 76). To eliminate influences of other nutrient sources in the medium, *E. coli* DH5α_1C was first adapted to and then tested in minimal medium (MM; 4.2.1.3, page 51) instead of (complex) LB medium, using either BWH or pure glucose as carbon source. Figure 5-9 compares growth and glucose consumption of the recombinant cells over a period of 54 h in MM supplemented with BWH or glucose.

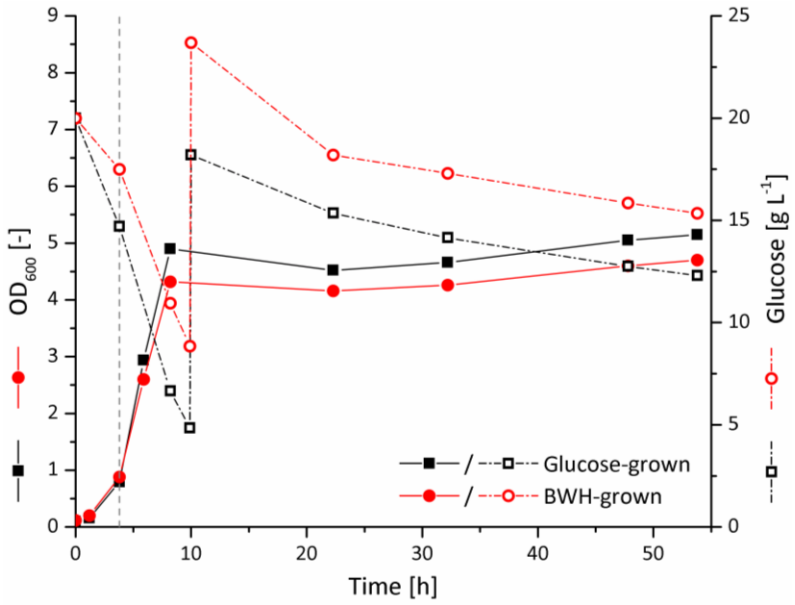

Figure 5-9: Comparison of BWH and glucose as carbon source for *E. coli* DH5α_1C in MM.
Recombinant *E. coli* DH5α were inoculated to an OD_{600} = 0.1 in 100 mL MM containing 2% (w/v) glucose or BWH with an equivalent amount of glucose. Cultures were grown at 37 °C, 100 rpm. Induction was performed by addition of 0.1 mM IPTG at OD_{600} = 0.5 - 0.6. Samples were taken at intervals for determination of cell concentration, glucose consumption and product analysis.
MM… minimal medium

Growth behavior of *E. coli* DH5α_1C was not notably influenced by utilization of BWH as a carbon source. Maximal growth rate in exponential phase on BWH was similar to μ_{max} on glucose (0.53 vs. 0.57 h^{-1}). Only a slightly lower maximal OD_{600} in stationary phase could be observed for BWH-grown cells (glucose-grown: 5.1, BWH-grown: 4.7 after 54 h). The glucose-grown cells consumed a total of 1.01 g glucose and the BWH-grown cells 0.94 g within 54 h. Isopropanol (or acetone) could not be detected at any time during the cultivation with either BWH or glucose. Plasmid isolation (4.2.2.5, page 53) and sequencing (4.2.2.7, page 54) confirmed the presence of the expression vector pRK_ISO_1C2e3c4c inside the cells on MM, but WB analysis was unable to detect the isopropanol pathway gene products (results not shown). Therefore, subsequent experiments were performed in LB medium. Figure 5-10 displays the growth behavior, glucose consumption and acetone production of *E. coli* DH5α_1C over a period of 99 h in LB medium using BWH as carbon source.

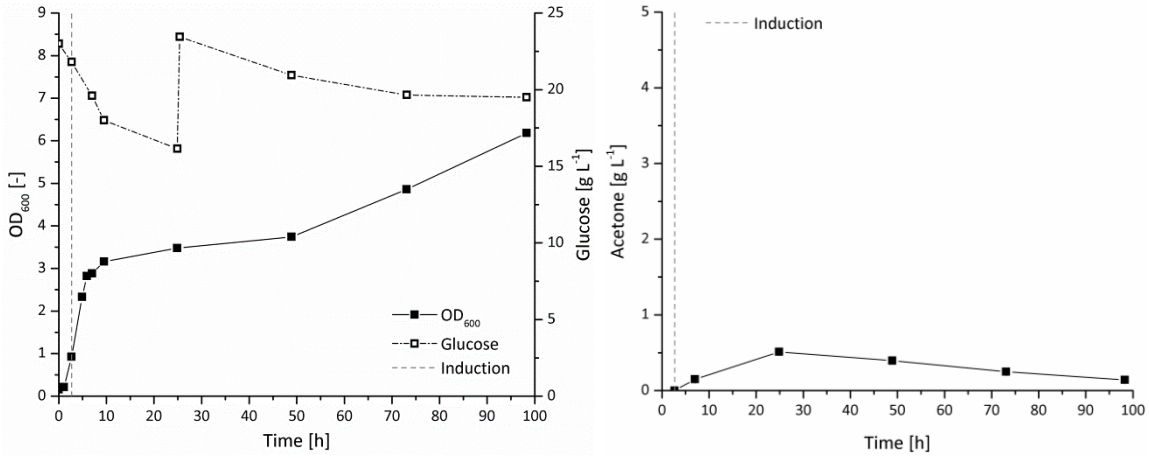

Figure 5-10: Growth, glucose consumption and acetone production using BWH as a carbon source for *E. coli* DH5α_1C in LB.

Recombinant *E. coli* DH5α were inoculated to an OD_{600} = 0.1 in 100 mL LB containing BWH with 2% (w/v) glucose, which was replenished if necessary. Cultures were grown at 37 °C, 100 rpm. Induction was performed by addition of 0.1 mM IPTG at OD_{600} = 0.5 - 0.6. Samples were taken at intervals for determination of cell concentration, glucose consumption and product analysis. GC analysis: Error bars display the standard deviation of n = 3 (technical replicates).

E. coli DH5α_1C achieved a μ_{max} of 0.7 h^{-1} in exponential phase and reached stationary phase with an OD_{600} = 3.2 at t = 10 h. After a period of constant cell concentration, the strain resumed growth (t = 50 h) and achieved an OD_{600} of 6.2 after 99 h. Isopropanol was not produced, but 0.5 g L^{-1} acetone were generated after 24 h. Hereafter, acetone concentration diminished again to 0.1 g L^{-1} after 99 h. Acetone yield was 0.541 g g^{-1} biomass or 23.2 mol% from substrate after 24 h. At the point of induction, acetate concentration in the medium was already 0.7 g L^{-1}. In comparison, *E. coli* DH5α_1C in LB and pure glucose achieved an isopropanol concentration of 4.4 g L^{-1} and a yield of 1.794 g g^{-1} biomass or 58.7 mol% from substrate in the same time (Table 5-7, page 82).

It can be concluded that application of BWH as carbon source exerts a negative effect on isopropanol production. To investigate this effect, BWH was mixed with pure glucose in different concentrations and utilized as carbon source for isopropanol production in LB medium. Figure 5-11 depicts a growth comparison of *E. coli* DH5α_1C in LB supplemented with 2% (w/v) glucose, either from 0% (pure glucose), 50%, 75% or 100% BWH.

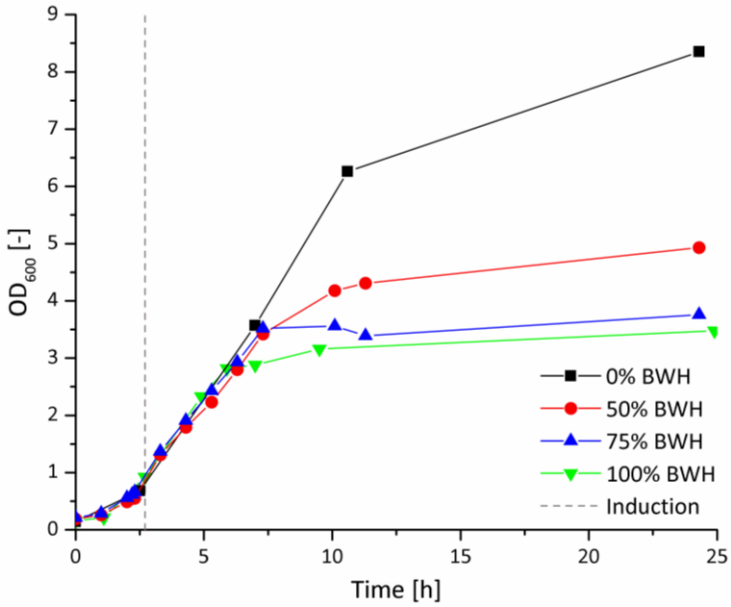

Figure 5-11: Influence of different BWH concentrations on growth of *E. coli* DH5α_1C.
Recombinant *E. coli* DH5α were inoculated to an OD_{600} = 0.1 in 100 mL LB containing 2% (w/v) glucose from 0% (pure glucose), 50%, 75%, 100% BWH, which was replenished if necessary. Cultures were grown at 37 °C, 100 rpm. Induction was performed by addition of 0.1 mM IPTG at OD_{600} = 0.5 - 0.6. Samples were taken at intervals for determination of cell concentration, glucose consumption and product analysis.

Growth rate during exponential phase was similar for all cultivations (μ_{max} = 0.6-0.7 h^{-1}), irrespective of the BWH concentration used. But a difference could be observed for the onset of stationary phase and for the final OD_{600}. The higher the concentration of BWH used, the earlier was the entry into stationary phase and the lower was the maximum OD_{600} after 24 h. The highest isopropanol concentration in the medium was achieved with 0% BWH. Figure 5-12 shows the influence of different BWH concentrations on isopropanol and acetone production, ranging from no isopropanol after 24 h with 100% BWH, 0.5 g L^{-1} with 75% and 1.8 g L^{-1} with 50% to 4.4 g L^{-1} isopropanol with 0% BWH (pure glucose).

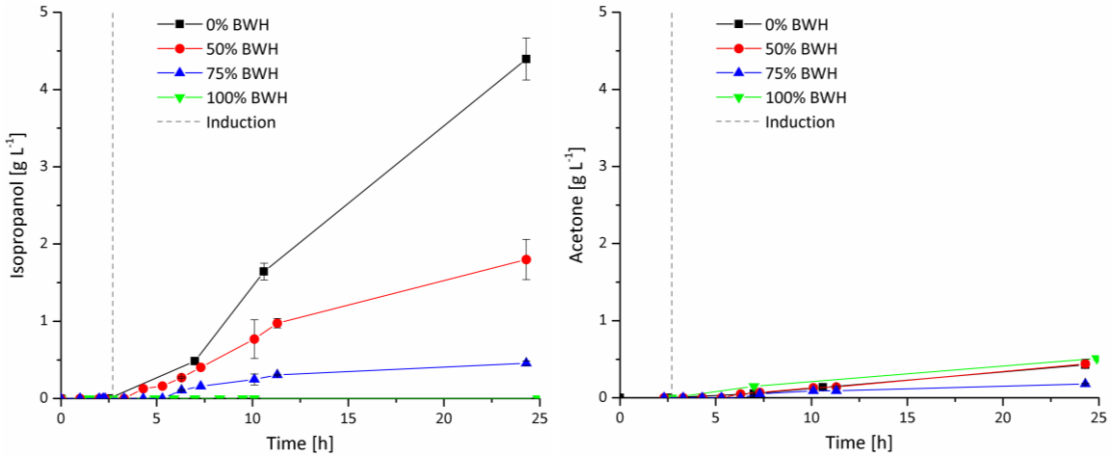

Figure 5-12: Influence of different BWH concentrations on isopropanol and acetone production of *E. coli* DH5α_1C.
Recombinant *E. coli* DH5α were inoculated to an OD_{600} = 0.1 in 100 mL LB containing 2% (w/v) glucose from 0% (pure glucose), 50%, 75%, 100% BWH, which was replenished if necessary. Cultures were grown at 37 °C, 100 rpm. Induction was performed by addition of 0.1 mM IPTG at OD_{600} = 0.5 - 0.6. Samples were taken at intervals for determination of cell concentration, glucose consumption and product analysis. GC analysis: Error bars display the standard deviation of n = 3 (technical replicates).

Acetone concentrations after 24 h were similar for all cultivations (0.2-0.5 g L^{-1}), irrespective of the BWH concentration used. Table 5-8 summarizes the influence of different BWH concentrations on the isopropanol production parameters of *E. coli* DH5α_1C and illustrates the downward trend of those parameters: The higher the BWH concentration in the medium, the lower the biomass- or substrate-related isopropanol yield and the volumetric or biomass-related productivity.

Table 5-8: Influence of different BWH concentrations on isopropanol production parameters of *E. coli* DH5α_1C after 24 h.

Isopropanol yields were calculated according to 4.2.4.3 (page 66), Equation 4-23, Equation 4-21, Equation 4-22. Isopropanol productivities were calculated according to Equation 4-24, Equation 4-25.

p_{max}… product concentration, $Y_{P/X}$… product yield (biomass-related), $Y_{P/S}$… product yield (from substrate), P_P... volumetric productivity, Q_P… specific productivity (biomass-related)

BWH [%]	p_{max} [g L^{-1}]	$Y_{P/X}$ [g g^{-1} biomass]	$Y_{P/S}$ [mol mol^{-1} glucose][a]	$Y_{P/S}$ [mol%][a]	P_P [g L^{-1} h^{-1}]	Q_P [g g^{-1} biomass h^{-1}]
0	4.39	1.794	0.587	58.7	0.181	0.072
50	1.80	1.349	0.376	37.6	0.074	0.050
75	0.46	0.474	0.129	12.9	0.019	0.017
100	0.00	0.000	0.000	0.0	0.000	0.000

[a] For calculation purposes, glucose is considered the sole carbon source in the medium.

To elucidate a possible source of inhibition, acetate and lactate concentrations in the cultivation medium were determined (see 4.2.3.6, page 61). Figure 5-13 displays the total acetate concentration in the medium as well as the (calculated) amount of acetate that was solely produced by *E. coli* and not associated with BWH addition.

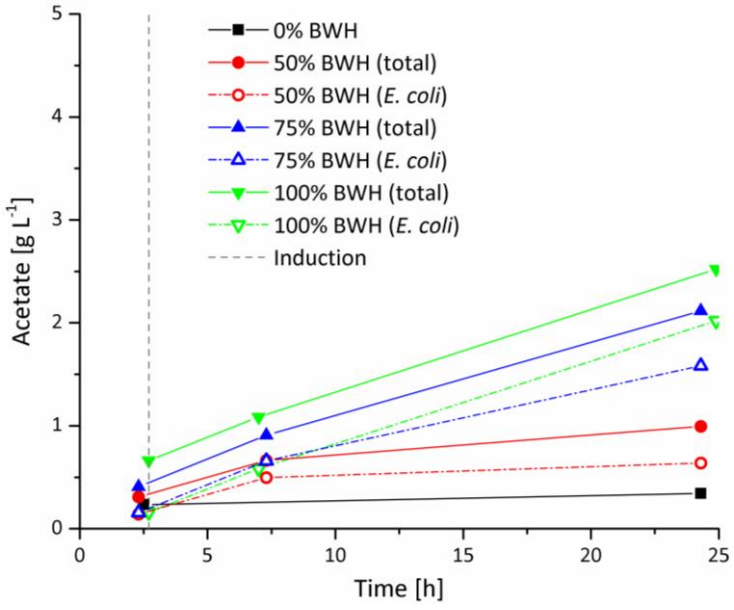

Figure 5-13: Acetate concentration in the cultivation medium of *E. coli* DH5α_1C grown with different BWH concentrations.

Recombinant *E. coli* DH5α were inoculated to an OD_{600} = 0.1 in 100 mL LB containing 2% (w/v) glucose from 0% (pure glucose), 50%, 75%, 100% BWH, which was replenished if necessary. Cultures were grown at 37 °C, 100 rpm. Induction was performed by addition of 0.1 mM IPTG at OD_{600} = 0.5 - 0.6. Samples were taken at intervals for determination of acetate concentration.

BWH itself contains acetate in a concentration of 7.9 g L^{-1} (Table 4-3, page 41). Use of BWH instead of pure glucose resulted in a higher starting acetate concentration in the medium, depending on the

amount of BWH added. The total acetate concentration in the medium after 24 h with 100% and 75% BWH was considerably higher than the acetate concentration for 50% or 0% BWH cultivations, in which acetate concentrations rose only slowly (50% BWH) or almost stayed constant (pure glucose) during 24 h. Also, the acetate produced by *E. coli* DH5α_1C was highest for 100% BWH (2.0 g L^{-1}) after 24 h, followed by 75% BWH (1.6 g L^{-1}) and 50% BWH (0.6 g L^{-1}). Table 5-9 lists the *E. coli*-originating acetate production parameters after 24 h for *E. coli* DH5α_1C in LB supplemented with different BWH concentrations.

Table 5-9: Influence of different BWH concentrations on acetate production parameters of *E. coli* DH5α_1C after 24 h.

Acetate yields were calculated according to 4.2.4.3 (page 66), Equation 4-23, Equation 4-21, Equation 4-22. Acetate productivities were calculated according to Equation 4-24, Equation 4-25.

p_{max}… product concentration, $Y_{P/X}$… product yield (biomass-related), $Y_{P/S}$… product yield (from substrate), P_P... volumetric productivity, Q_P… specific productivity (biomass-related)

BWH [%]	p_{max} [g L^{-1}]	$Y_{P/X}$ [g g^{-1} biomass]	$Y_{P/S}$ [mol mol^{-1} glucose][a]	$Y_{P/S}$ [mol%][a]	P_P [g L^{-1} h^{-1}]	Q_P [g g^{-1} biomass h^{-1}]
0	0.34	0.139	0.046	4.6	0.014	0.006
50	0.64	0.581	0.162	16.2	0.026	0.018
75	1.58	1.995	0.545	54.5	0.065	0.058
100	2.03	2.132	0.885	88.5	0.081	0.078

[a] For calculation purposes, glucose is considered the sole carbon source in the medium.

It can be seen that an increased concentration of BWH in the medium resulted in a higher biomass- and substrate-related acetate yield, as well as in a higher volumetric and biomass-related acetate productivity. The trend is in opposition to the results for isopropanol production with different BWH concentrations (Table 5-8). Lactate was only produced in low amounts by *E. coli* DH5α_1C. After 24 h, lactate concentration in the medium with pure glucose was 0.18 g L^{-1}, with 50% and 75% BWH 0.02 and 0.01 g L^{-1}, and with 100% BWH 0.03 g L^{-1}.

In conclusion, BWH as carbon source for *E. coli* DH5α_1C exerted an inhibitory effect on isopropanol production in shake flask scale. The acetate already contained in BWH might be a possible source of inhibition for the production process. *E. coli* DH5α_1C produced more acetate and less isopropanol when more BWH was present in the medium. To further elucidate the inhibitory effect, BWH was purified in six different ways, ranging from the use of an acid cation and a weak anion exchanger for demineralization and decolorization, to activated coal for removal of color, flavor and aromatic substances and combinations of these methods. In addition, ethanol precipitation and evaporation was applied, as well as recrystallization to remove the acetate. Purification of BWH was performed in the scope of a project work by Holger Becker ("*Katalytische Hydrierung von Glukoselösung als Basisprozess für einen Batchreaktor*", 2016) at the Fraunhofer CBP (Leuna, Germany). 10 mL of each purified BWH were provided for shake flask experiments in LB, analogous to the experiments described in this chapter. Unfortunately, isopropanol was not produced by *E. coli* DH5α_1C from either of the purified BWHs (results not shown). Again, only acetone was generated, although acetone concentrations could be slightly increased with the purified BWHs in comparison to use of the original BWH.

5.4 Isopropanol Production by Engineered *E. coli* in Bioreactor Scale

Engineered *E. coli* DH5α were subjected to cultivation in 10 L bioreactor scale with the aim to demonstrate scale-up of the 100 mL shake flask isopropanol production process. Precultures, inoculum

and medium were prepared as described in 4.2.1.2 (page 50). Mode of operation was fed-batch, i.e. the cells were first grown in LB medium with 2% (w/v) pure glucose, and then fed with pulses of carbon source. A feeding model for growth and isopropanol production in bioreactor scale was not available. Therefore, manual feeding was applied when glucose concentration in the medium was below 10 g L^{-1}, according to [Jojima et al., 2008]. Cultivation variables were set to 37 °C, pH 7.0, 0.4 bar, 400 rpm, 5 L air min^{-1} (pO_2 > 25%). Kanamycin (50 µg mL^{-1}) was used to maintain the selection pressure. Induction was achieved by addition of 0.1 mM IPTG in the mid-exponential growth phase (= OD_{600} ~6.0). Samples were taken at certain time intervals to monitor bacterial growth (OD_{600} by spectrophotometry, 4.2.3.1), the isopropanol, acetone and ethanol production (by GC, 4.2.3.7), the acetate and lactate formation (by enzymatic test kits, 4.2.3.6) and glucose consumption (glucose measurement by YSI, 4.2.3.5). After induction, sampling included preparation of 1/OD samples to monitor protein production (WB analysis of whole cell extracts or soluble/insoluble protein fractions, 4.2.3.2, 4.2.3.3, 4.2.3.4).

5.4.1 Glucose as Carbon Source for Isopropanol Production in Bioreactor Scale

Scale-up of isopropanol production by *E. coli* DH5α_1C was performed using pure glucose as carbon source. Figure 5-14 displays the growth behavior, glucose consumption and product formation of *E. coli* DH5α_1C in 10 L bioreactor scale.

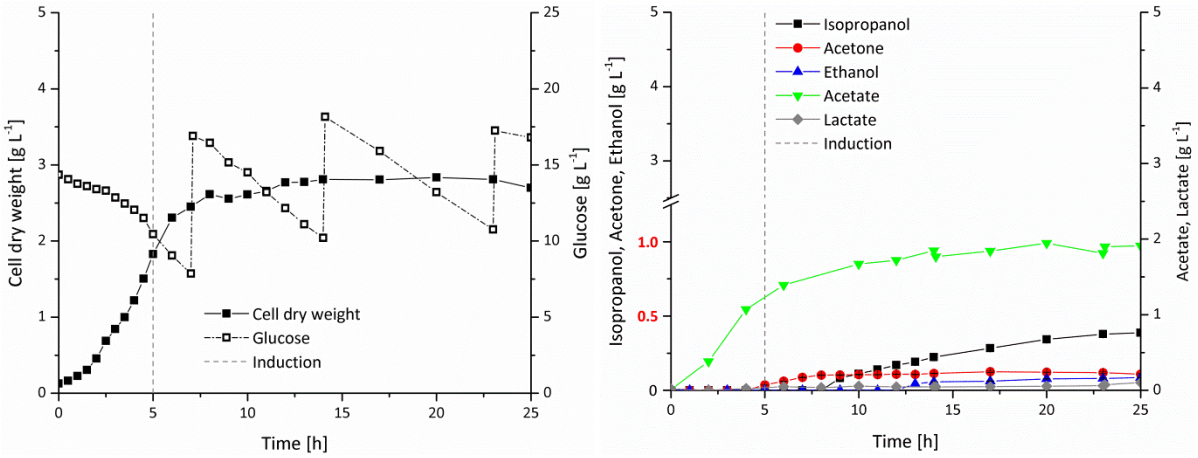

Figure 5-14: Growth, glucose consumption and product formation of *E. coli* DH5α_1C in LB plus glucose feed in 10 L bioreactor scale.

Recombinant *E. coli* DH5α were cultivated in 10 L LB medium containing 2% (w/v) glucose. Pulsed feeding of a 50% (w/v) glucose solution was applied when glucose concentration was below 10 g L^{-1}. Control variables were set to 37 °C, pH 7.0, 0.4 bar, 5 L air min^{-1}, 400 rpm (pO_2 > 25%). Induction was performed at OD_{600} ~6.0 with 0.1 mM IPTG. Samples were taken at intervals for determination of cell concentration, glucose consumption, protein and product analysis. Cell dry weight was calculated from OD_{600} according to 4.2.4.3. GC analysis: Error bars display the standard deviation of n = 3 (technical replicates).

E. coli DH5α_1C grew with a μ_{max} of 0.5 h^{-1} and a doubling time of 1.3 h in exponential phase and reached stationary phase at t = 8 h with a maximal cell dry weight x_{max} of 2.8 g L^{-1}. The overall volumetric glucose consumption rate P_S was 0.842 g L^{-1} h^{-1} during 24 h. Isopropanol production first occurred at t = 9 h, whereas acetone production already began at the point of induction (t = 5 h). Acetone concentration reached a plateau at the onset of isopropanol formation with a maximal acetone concentration of 0.1 g L^{-1}. After 24 h, isopropanol concentration was 0.4 g L^{-1}. Acetate formation correlated with cell growth, rising in exponential phase and stagnating in stationary phase with a maximal concentration of 1.9 g L^{-1}. Lactate was mainly produced at the end of cultivation, whereas ethanol generation already started at t = 13 h.

Figure 5-15 shows the time course of the control variables pH, rotational speed, pO_2, airflow, pressure and temperature, as well as base addition during the cultivation.

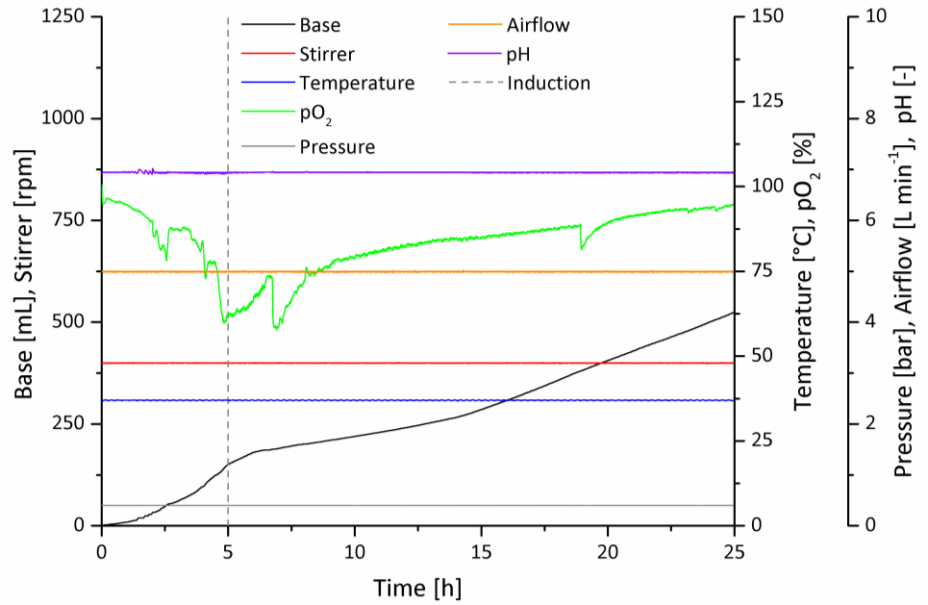

Figure 5-15: Time course of control variables and base addition for *E. coli* DH5α_1C in LB plus glucose feed in 10 L bioreactor scale.
Recombinant *E. coli* DH5α were cultivated in 10 L LB medium containing 2% (w/v) glucose. Pulsed feeding of a 50% (w/v) glucose solution was applied when glucose concentration was below 10 g L^{-1}. Control variables were set to 37 °C, pH 7.0, 0.4 bar, 5 L air min^{-1}, 400 rpm (pO_2 > 25%). Induction was performed at OD_{600} ~6.0 with 0.1 mM IPTG.

Period of strongest pH regulation by base addition was between 0 and 5 h, which correlated with exponential cell growth. Decrease of pO_2 corresponded to increased oxygen requirement in exponential phase, while oxygen requirement in stationary phase decreased.

Table 5-10 summarizes the product formation parameters of *E. coli* DH5α_1C in LB plus glucose feed in 10 L bioreactor scale after 24 h.

Table 5-10: Product formation parameters of *E. coli* DH5α_1C after 24 h in LB plus glucose feed in 10 L bioreactor scale.
Product yields were calculated according to 4.2.4.3 (page 66), Equation 4-23, Equation 4-21, Equation 4-22. Product productivities were calculated according to Equation 4-24, Equation 4-25.
p_{max}… product concentration, $Y_{P/X}$… product yield (biomass-related), $Y_{P/S}$… product yield (from substrate), P_P... volumetric productivity, Q_P… specific productivity (biomass-related)

Product	p_{max} [g L^{-1}]	$Y_{P/X}$ [g g^{-1} biomass]	$Y_{P/S}$ [mol mol^{-1} glucose][a]	$Y_{P/S}$ [mol%][a]	P_P [g L^{-1} h^{-1}]	Q_P [g g^{-1} biomass h^{-1}]
Isopropanol	0.39	0.150	0.055	5.5	0.015	0.006
Acetone	0.11	0.042	0.016	1.6	0.004	0.002
Ethanol	0.09	0.033	0.016	1.6	0.003	0.001
Acetate	1.91	0.736	0.271	27.1	0.076	0.028
Lactate	0.10	0.033	0.008	0.8	0.003	0.001
Biomass	2.70		0.219	21.9	0.103	

[a] For calculation purposes, glucose is considered the sole carbon source in the medium.

In 10 L bioreactor scale, *E. coli* DH5α_1C mostly produced acetate instead of isopropanol. Isopropanol yield from glucose $Y_{P/S}$ was only 5.5 mol%, which is one tenth of the yield achieved in 100 mL shake flask scale (58.7 mol%, Table 5-7, page 82). Acetone, ethanol and lactate yields from glucose were similar in both scales, but acetate yield was 6 times higher in bioreactor scale (27.1 vs. 4.6 mol%). In shake flask, *E. coli* DH5α_1C produced 4.4 g L^{-1} isopropanol after 24 h, whereas only 0.4 g L^{-1} was produced in 10 L. The biomass-related isopropanol yield $Y_{P/X}$ was much lower for the bioreactor cultivation (0.150 vs. 1.794 g g^{-1}). Biomass yield from glucose was comparable in both scales with 21.9 mol% (P_P: 0.103 g L^{-1} h^{-1}) in 10 L and 19.5 mol% (0.101 g L^{-1} h^{-1}) in shake flask.

Protein analysis displayed soluble production of Act-StrepII (1C) at the expected molecular mass of ~43 kDa (Figure 5-16 A, odd numbered lanes), even before induction (lane 1). Faint bands are visible at ~28, ~32, ~35 and ~38 kDa, especially in the insoluble fraction (even numbered lanes). The bands indicate possible degradation of the target protein, which was investigated by mass spectrometry in chapter 5.4.2 (page 98).

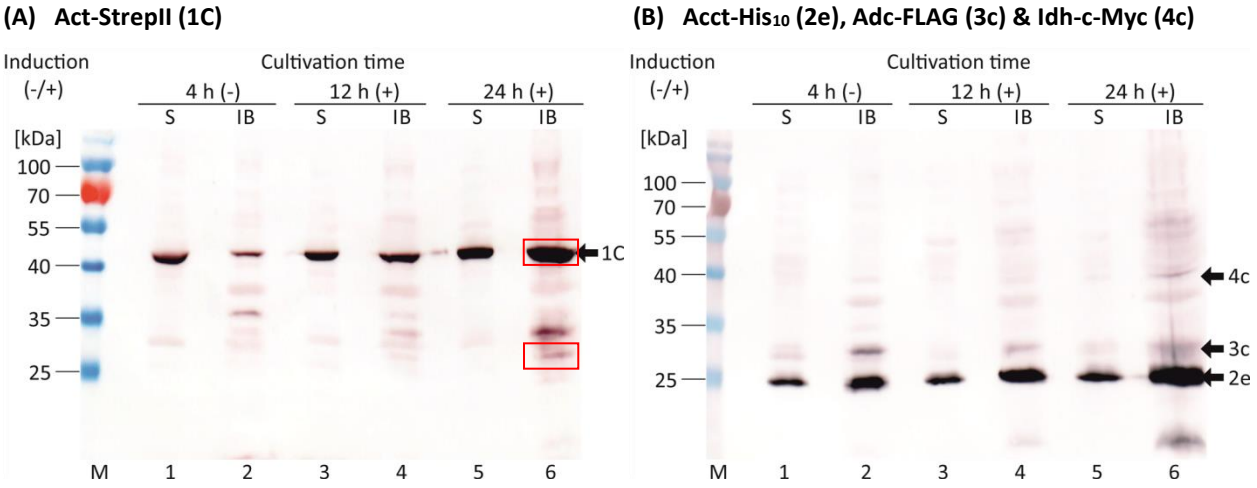

Figure 5-16: Production of Act-StrepII (1C) (A), Acct-His_{10} (2e), Adc-FLAG (3c) & Idh-c-Myc (4c) (B) in *E. coli* DH5α_1C in LB plus glucose feed in 10 L bioreactor scale.

Recombinant *E. coli* DH5α were cultivated in 10 L LB medium containing 2% (w/v) glucose. Pulsed feeding of a 50% (w/v) glucose solution was applied when glucose concentration was below 10 g L^{-1}. Control variables were set to 37 °C, pH 7.0, 0.4 bar, 5 L air min^{-1}, 400 rpm (pO_2 > 25%). Induction was performed at OD_{600} ~6.0 with 0.1 mM IPTG. 1/OD samples were taken at intervals, lysed and divided into soluble and insoluble cell extract fraction (4.2.3.2). Extracts were separated by SDS-PAGE and Act-StrepII (1C) was visualized by WB with anti-StrepII®, Acct-His_{10} (2e) with anti-polyHistidine, Adc-FLAG (3c) with anti-FLAG® and Idh-c-Myc (4c) with anti-c-Myc and anti-Mouse IgG-conjugated alkaline phosphatase antibodies (dye: BCIP/NBT) (see Table 4-12 for antibodies).
Lanes with odd numbers display the soluble fraction (S), whereas lanes with even numbers display the insoluble fraction (IB) samples. Arrows indicate the detected proteins. Red rectangle marks bands that were excised from a corresponding PA gel and analyzed by MALDI-TOF/TOF MS (4.2.3.9). Theoretical molecular protein masses were calculated using ProtParam: MW of Act-StrepII (1C) = 42.5 kDa, MW of Acct-His_{10} (2e) = 24.7 kDa, MW of Adc-FLAG (3c) = 28.9 kDa, MW of Idh-c-Myc (4c) = 39.0 kDa.
Act… acetyl-CoA acetyltransferase, Acct… acetate CoA-transferase, Adc… acetoacetate decarboxylase, Idh… isopropanol dehydrogenase

Acct-His_{10} (2e) was strongly produced in the soluble form at the expected molecular mass of ~25 kDa (Figure 5-16 B, odd numbered lanes). The third enzyme, Adc-FLAG (3c) (~29 kDa) was only detected in low amounts and more dominantly in the insoluble fraction (B, even numbered lanes), especially in later stages of cultivation. Idh-c-Myc (4c) can barely be seen at the expected molecular mass of ~39 kDa in soluble and insoluble fraction.

In conclusion, scale-up of isopropanol production by *E. coli* DH5α_1C from 100 mL shake flask to 10 L bioreactor scale could be considered problematic due to low isopropanol and high acetate formation.

E. coli DH5α_1E, with the first cascade gene of *E. coli* origin, was also tested for isopropanol production in bioreactor scale under the same conditions as *E. coli* DH5α_1C. In shake flask scale, this strain produced only minor amounts of isopropanol at 24 °C (0.02 g L^{-1} in 24 h, Table 5-6, page 78) and no isopropanol at 37 °C. Additionally, gasstripping was evaluated as a means of isopropanol separation and recovery. At t = 25 h, gasstripping was initiated, i.e. the gaseous efflux was directed to two cooled and stirred bottles with ddH_2O, which were connected in series with a volume of 600 mL and 300 mL respectively (see Figure 5-25, page 104 for device). Figure 5-17 shows the growth behavior, glucose consumption and product formation of *E. coli* DH5α_1E in 10 L bioreactor scale.

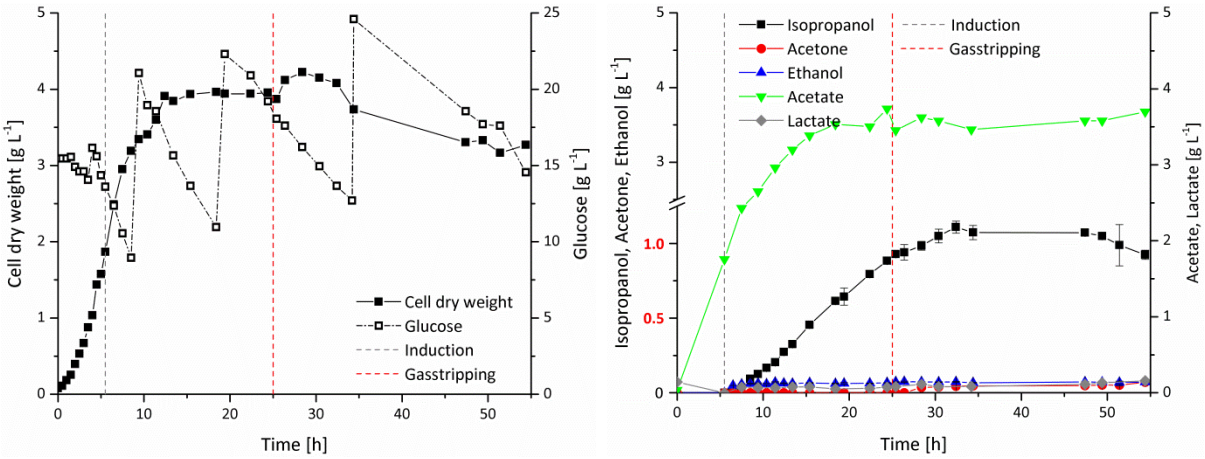

Figure 5-17: Growth, glucose consumption and product formation of *E. coli* DH5α_1E in LB plus glucose feed in 10 L bioreactor scale.

Recombinant *E. coli* DH5α were cultivated in 10 L LB medium containing 2% (w/v) glucose. Pulsed feeding of a 50% (w/v) glucose solution was applied when glucose concentration was below 10 g L^{-1}. Control variables were set to 37 °C, pH 7.0, 0.4 bar, 5 L air min^{-1}, 400 rpm (pO_2 > 25%). Induction was performed at OD_{600} ~6.0 with 0.1 mM IPTG. At t = 25 h, gasstripping was turned on (see Figure 5-25, page 104 for device). Samples were taken at intervals for determination of cell concentration, glucose consumption, protein and product analysis. Cell dry weight was calculated from OD_{600} according to 4.2.4.3. GC analysis: Error bars display the standard deviation of n = 3 (technical replicates).

The cells grew with a μ_{max} of 0.6 h^{-1} and a doubling time of 1.2 h in exponential phase. Stationary phase was reached at t = 12 h with a x_{max} of 4.2 g L^{-1}. Biomass decline occured at t = 32 h. The overall volumetric glucose consumption rate P_S was 0.808 g L^{-1} h^{-1} in 24 h. Isopropanol was first detected at t = 8 h and reached a maximum concentration of 1.1 g L^{-1} at t = 32 h, which decreased to 0.9 g L^{-1} at the end of cultivation. Acetone was first detected in the medium after 28 h and the concentration stayed as low as 0.07 g L^{-1} during 54 h. Ethanol and lactate concentrations remained low during the whole process (<0.1 and <0.2 g L^{-1}), but acetate concentration rose quickly in accordance with cell growth to a plateau of 3.7 g L^{-1}.

Results of the gasstripping experiment are displayed in a separate chapter in 5.5.1 (Figure 5-27, page 106). Figure 5-18 shows the sudden decrease in pO_2 at t = 25 h, which correlates with the onset of stripping.

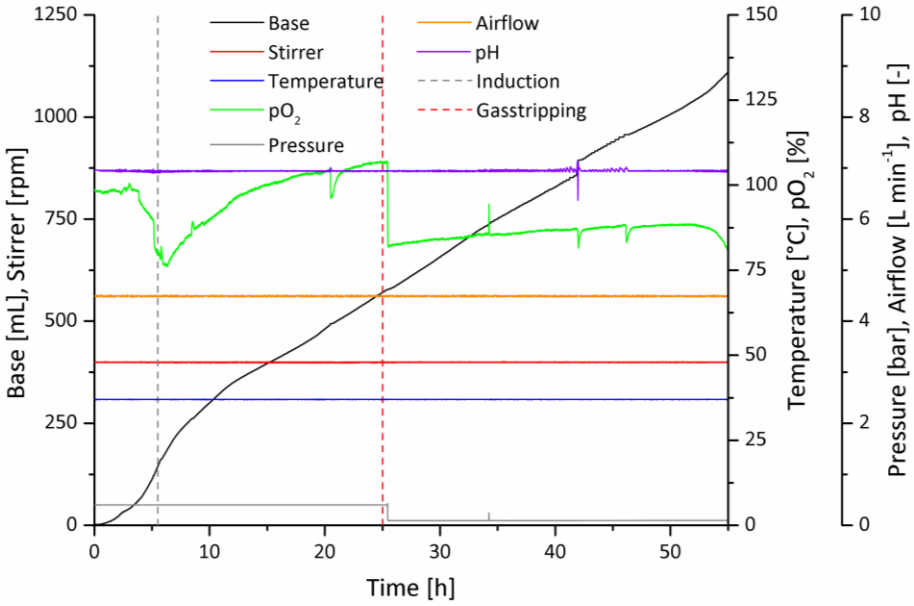

Figure 5-18: Time course of control variables and base addition for *E. coli* DH5α_1E in LB plus glucose feed in 10 L bioreactor scale.

Recombinant *E. coli* DH5α were cultivated in 10 L LB medium containing 2% (w/v) glucose. Pulsed feeding of a 50% (w/v) glucose solution was applied when glucose concentration was below 10 g L^{-1}. Control variables were set to 37 °C, pH 7.0, 0.4 bar, 5 L air min^{-1}, 400 rpm (pO_2 > 25%). Induction was performed at OD_{600} ~6.0 with 0.1 mM IPTG. At t = 25 h, gas efflux was directed into the gasstripping device (see Figure 5-25, page 104 for device).

Base supply heavily occurred in exponential phase and continued in a linear manner till the end of cultivation. Minor changes in pO_2 levels happened due to manual addition of antifoam emulsion. Airflow, stirrer, pressure, temperature and pH were kept or stayed constant.

Table 5-11 summarizes the product formation parameters of *E. coli* DH5α_1E in LB plus glucose feed in 10 L bioreactor scale after 24 h cultivation.

Table 5-11: Product formation parameters of *E. coli* DH5α_1E after 24 h in LB plus glucose feed in 10 L bioreactor scale.

Product yields were calculated according to 4.2.4.3 (page 66), Equation 4-23, Equation 4-21, Equation 4-22. Product productivities were calculated according to Equation 4-24, Equation 4-25.

p_{max}… product concentration, $Y_{P/X}$… product yield (biomass-related), $Y_{P/S}$… product yield (from substrate), P_P... volumetric productivity, Q_P… specific productivity (biomass-related)

Product	p_{max} [g L^{-1}]	$Y_{P/X}$ [g g^{-1} biomass]	$Y_{P/S}$ [mol mol^{-1} glucose][a]	$Y_{P/S}$ [mol%][a]	P_P [g L^{-1} h^{-1}]	Q_P [g g^{-1} biomass h^{-1}]
Isopropanol	0.88	0.227	0.134	13.4	0.036	0.009
Acetone	0.00	0.000	0.000	0.0	0.000	0.000
Ethanol	0.07	0.017	0.013	1.3	0.003	0.001
Acetate	3.74	0.955	0.565	56.5	0.152	0.038
Lactate	0.07	0.000	0.000	0.0	0.000	0.000
Biomass	3.95		0.352	35.2	0.159	

[a] For calculation purposes, glucose is considered the sole carbon source in the medium.

In comparison to the previous 10 L cultivation with *E. coli* DH5α_1C (Table 5-10, page 93), isopropanol concentration after 24 h was more than doubled to 0.9 g L^{-1}. Substrate-related isopropanol yield $Y_{P/S}$ went up to 13.4 mol%, which is more than 4fold the yield obtained by this strain in shake flask at 24 °C

(Table 5-6, page 78). Acetate was still the main product with a concentration of 3.7 g L^{-1}, a volumetric productivity P_P of 0.152 g L^{-1} h^{-1} and a substrate-related yield $Y_{P/S}$ of 56.5 mol%. Sum of all substrate-related yields is >100%, which indicates that DH5α_1E also consumed other carbon sources present in the medium.

Protein analysis reveals the presence of Act-StrepII (1E) at ~41 kDa almost exclusively in the insoluble fraction (Figure 5-19 A, even numbered lanes). Additional bands are visible at 25, 28, 35 and 38 kDa plus a rather thick band at ~23 kDa. The bands indicate possible degradation of the target protein, which was investigated by mass spectrometry in chapter 5.4.2 (page 98). Idh-c-Myc (4c) was mainly produced in its insoluble form at ~39 kDa, although small amounts could be detected in two of the soluble fractions (Figure 5-19 B, lane 5 & 7).

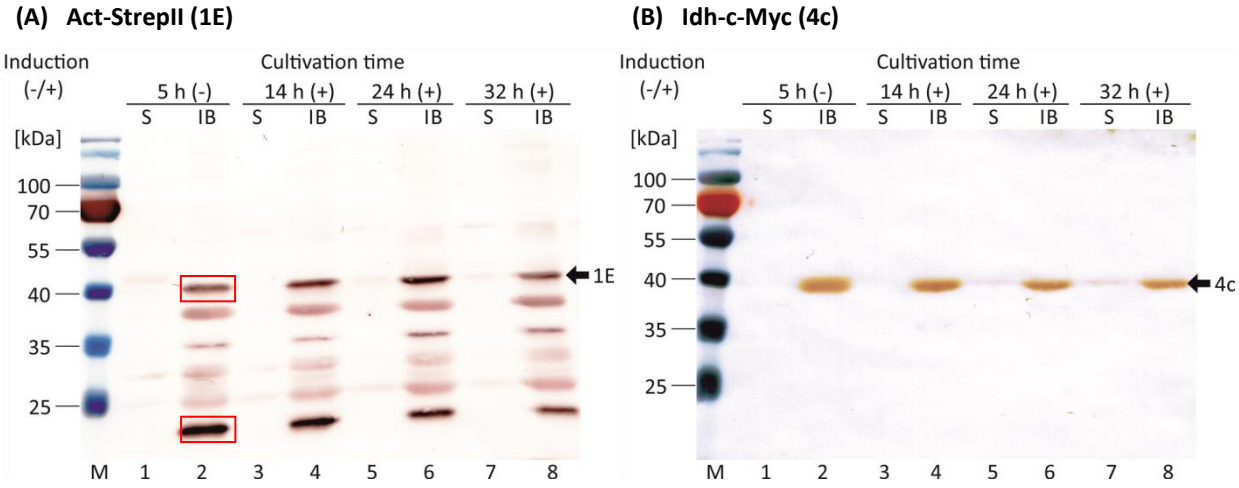

Figure 5-19: Production of Act-StrepII (1E) (A) and Idh-c-Myc (4c) (B) in *E. coli* DH5α_1E in LB plus glucose feed in 10 L bioreactor scale.

Recombinant *E. coli* DH5α were cultivated in 10 L LB medium containing 2% (w/v) glucose. Pulsed feeding of a 50% (w/v) glucose solution was applied when glucose concentration was below 10 g L^{-1}. Control variables were set to 37 °C, pH 7.0, 0.4 bar, 5 L air min^{-1}, 400 rpm (pO_2 > 25%). Induction was performed at OD_{600} ~6.0 with 0.1 mM IPTG. 1/OD samples were taken at intervals, lysed and divided into soluble and insoluble cell extract fraction (4.2.3.2). Extracts were separated by SDS-PAGE and Act-StrepII (1E) was visualized by WB with anti-StrepII®, Idh-c-Myc (4c) was detected with anti-c-Myc and anti-Mouse IgG-conjugated alkaline phosphatase antibodies (dye: BCIP/NBT) (see Table 4-12 for antibodies).
Lanes with odd numbers display the soluble fraction (S), whereas lanes with even numbers display the insoluble fraction (IB) samples. Arrows indicate the detected proteins. Red rectangle marks bands that were excised from a corresponding PA gel and analyzed by MALDI-TOF/TOF MS (4.2.3.9). Theoretical molecular protein masses were calculated using ProtParam: MW of Act-StrepII (1E) = 41.6 kDa, MW of Idh-c-Myc (4c) = 39.0 kDa.
Act… acetyl-CoA acetyltransferase, Idh… isopropanol dehydrogenase

In summary, scale-up of isopropanol production from 100 mL shake flask to 10 L bioreactor was demonstrated with glucose as carbon source. Surprisingly, the best performing strain in shake flask experiments, *E. coli* DH5α_1C, was inferior to *E. coli* DH5α_1E with regard to isopropanol concentration, yield from glucose and productivity in bioreactor scale. Possible reasons are discussed in chapter 6.3 (page 132), but were not further investigated. Subsequent experiments in this scale were performed with *E. coli* DH5α_1E.

5.4.2 Detection of Act Degradation by Mass Spectrometry

Aim of the following experiment was to analyze potential degradation of the first cascade enzyme Act-StrepII (1C/E) during isopropanol production by mass spectrometry (MS). For this, 1/OD samples were taken from the 10 L bioreactor cultivations of *E. coli* DH5α_1C and *E. coli* DH5α_1E in LB plus glucose feed (5.4.1, page 92). The samples were lysed, divided into soluble/insoluble fractions and separated by SDS-PAGE (4.2.3.3). In parallel, a WB was prepared (4.2.3.4) with the same samples. Gel portions were excised from the PA gel, corresponding to the prominent WB bands and considered to constitute either the intact enzyme or possible degradation products of Act-StrepII (1C/E). For *E. coli* DH5α_1C, gel bands at ~28 kDa and ~43 kDa were cut out (corresponding to Figure 5-16 A, lane 6, red rectangles, page 94). For *E. coli* DH5α_1E, gel bands at ~23 kDa and ~41 kDa were excised (corresponding to Figure 5-19 A, lane 2, red rectangles, page 97). Excised bands were subjected to in-gel trypsin digestion and analyzed by peptide mass fingerprint analysis (PMF) via MALDI-TOF/TOF MS (4.2.3.9, page 65). Obtained peptides were compared to the amino acid sequence of Act-StrepII (1C) or Act-StrepII (1E). Figure 5-20 lists the individual peptides detected in the samples of a) *E. coli* DH5α_1C and b) *E. coli* DH5α_1E and depicts the spatial congruency of the two amino acid sequences and the detected peptides.

Sample a) *E. coli* DH5α_1C

Size 28 kDa: 0 peptides detected

Size 43 kDa: 15 peptides detected – 45.8% coverage

MKEVVIASAVRTAIGSYGKSLKDVPAVDLGATAIKEAVKKAGIKPEDVNEVILGNVLQAGLGQNPARQASFKAGLPVE
IPAMTINKVCGSGLRTVSLAAQIIKAGDADVIIAGGMENMSRAPYLANNARWGYRMGNAKFVDEMITDGLWDAFNDYH
MGITAENIAERWNISREEQDEFALASQKKAEEAIKSGQFKDEIVPVVIKGRKGETVVDTDEHPRFGSTIEGLAKLKPA
FKKDGTVTAGNASGLNDCAAVLVIMSAEKAKELGVKPLAKIVSYGSAGVDPAIMGYGPFYATKAAIEKAGWTVDELDL
IESNEAFAAQSLAVAKDLKFDMNKVNVNGGAIALGHPIGASGARILVTLVHAMQKRDAKKGLATLCIGGGQGTAILLE
KCPRWSHPQFEK

Sample b) *E. coli* DH5α_1E

Size 23 kDa: 9 peptides detected – 43.8% coverage

MKNCVIVSAVRTAIGSFNGSLASTSAIDLGATVIKAAIERAKIDSQHVDEVIMGNVLQAGLGQNPARQALLKSGLAET
VCGFTVNKVCGSGLKSVALAAQAIQAGQAQSIVAGGMENMSLAPYLLDAKARSGYRLGDGQVYDVILRDGLMCATHGY
HMGITAENVAKEYGITREMQDELALHSQRKAAAAIESGAFTAEIVPVNVVTRKKTFVFSQDEFPKANSTAEALGALRP
AFDKAGTVTAGNASGINDGAAALVIMEESAALAAGLTPLARIKSYASGGVPPALMGMGPVPATQKALQLAGLQLADID
LIEANEAFAAQFLAVGKNLGFDSEKVNVNGGAIALGHPIGASGARILVTLLHAMQARDKTLGLATLCIGGGQGIAMVI
ERLNPRWSHPQFEK

Size 41 kDa: 4 peptides detected – 26.2% coverage

MKNCVIVSAVRTAIGSFNGSLASTSAIDLGATVIKAAIERAKIDSQHVDEVIMGNVLQAGLGQNPARQALLKSGLAET
VCGFTVNKVCGSGLKSVALAAQAIQAGQAQSIVAGGMENMSLAPYLLDAKARSGYRLGDGQVYDVILRDGLMCATHGY
HMGITAENVAKEYGITREMQDELALHSQRKAAAAIESGAFTAEIVPVNVVTRKKTFVFSQDEFPKANSTAEALGALRP
AFDKAGTVTAGNASGINDGAAALVIMEESAALAAGLTPLARIKSYASGGVPPALMGMGPVPATQKALQLAGLQLADID
LIEANEAFAAQFLAVGKNLGFDSEKVNVNGGAIALGHPIGASGARILVTLLHAMQARDKTLGLATLCIGGGQGIAMVI
ERLNPRWSHPQFEK

Figure 5-20: Spatial congruencies of detected peptides and amino acid sequences of Act-StrepII (1C) or Act-StrepII (1E).
PMF analysis was performed according to 4.2.3.9. Size indicates approximate cut-out region on the PA gel. Sequence-matching peptides are marked as blue rectangles. Additional amino acids (restriction site) and StrepII tag are underlined.

15 peptides in the 43 kDa cut-out could be assigned to Act-StrepII (1C), yielding a sequence coverage of 45.8%. Four peptides in the 41 kDa cut-out were assigned to the Act-StrepII (1E), resulting in a sequence coverage of 26.2%. Detected peptides for the two sequences (43 and 41 kDa) seemed to be equally distributed over the whole amino acid sequences, indicating the presence of the full-length proteins. No

peptides mapping the Act-StrepII (1C) sequence could be found in the 28 kDa cut-out, while nine peptides were detected in the 23 kDa cut-out, matching the sequence of Act-StrepII (1E) with a sequence coverage of 43.8%. The nine peptides are all located at the C-terminal part of the sequence, indicating a true degradation product of Act-StrepII (1E).

5.4.3 Beech Wood Hydrolysate as Carbon Source for Isopropanol Production in Bioreactor Scale

As in shake flask scale, BWH was investigated as an alternative carbon source to pure glucose for isopropanol production in 10 L bioreactor scale. To minimize the growth- and product-inhibiting effect of BWH, that manifested in shake flask experiments (5.3, page 86), *E. coli* DH5α_1E was first grown in LB medium containing 2% (w/v) pure glucose (batch phase). BWH was used in the feed, either in a 50% BWH/50% glucose mixture (first setup) or as 100% BWH (second setup). The cultivation conditions were analogous to the previous 10 L bioreactor experiments. Growth behavior, glucose consumption and product formation of the first setup with a 50% BWH/50% glucose feed are shown in Figure 5-21.

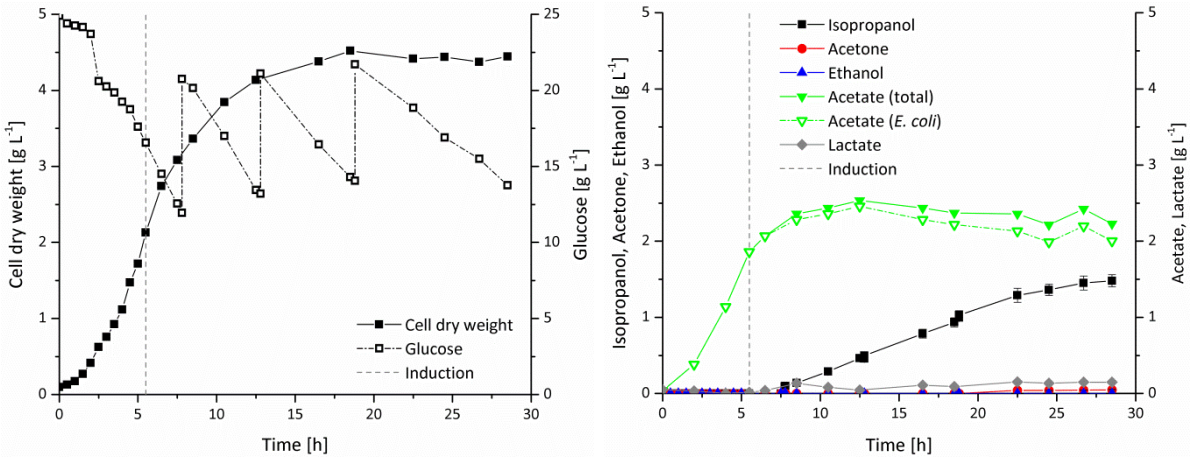

Figure 5-21: Growth, glucose consumption and product formation of *E. coli* DH5α_1E in LB plus 50% BWH/50% glucose feed in 10 L bioreactor scale.
Recombinant *E. coli* DH5α were cultivated in 10 L LB medium containing 2% (w/v) glucose. Pulsed feeding of a mixture consisting of 50% BWH and 50% pure glucose was applied when glucose concentration was below 10 g L^{-1}. Control variables were set to 37 °C, pH 7.0, 0.4 bar, 5 L air min^{-1}, 400 rpm (pO_2 > 25%). Induction was performed at OD_{600} ~6.0 with 0.1 mM IPTG. Samples were taken at intervals for determination of cell concentration, glucose consumption, protein and product analysis. Cell dry weight was calculated from OD_{600} according to 4.2.4.3. GC analysis: Error bars display the standard deviation of n = 3 (technical replicates).

E. coli DH5α_1E achieved a μ_{max} of 0.6 h^{-1} and a doubling time of 1.1 h in exponential phase. In stationary phase (t = 16 h), the cells reached a x_{max} of 4.5 g L^{-1} and displayed an overall volumetric glucose consumption rate P_S of 1.320 g L^{-1} h^{-1} during 24 h of cultivation. Isopropanol formation was first detected after 8 h, showed a linear increase till 22 h and a maximum concentration of 1.5 g L^{-1} at the end of cultivation. Acetone was first detected after 22 h and concentration stayed low (0.05 g L^{-1}) during the whole cultivation. Ethanol was not produced at all and lactate only reached a maximum concentration of 0.15 g L^{-1} at t = 22 h. Acetate generation by *E. coli* DH5α_1E correlated with cell growth and reached a maximum at t = 12 h with 2.5 g L^{-1}, slowly decreasing afterwards. The total acetate concentration in the medium was slightly higher than the *E. coli*-associated (calculated) acetate concentration, due to the acetate added by BWH feed (Table 4-3, page 41). Time course of the control variables pH, rotational speed, pO_2, airflow, pressure and temperature, as well as of base addition during the cultivation was similar to the previous setup on glucose (see Appendix Figure A-6, page 193). Table 5-12 lists the product

formation parameters of *E. coli* DH5α_1E fed with the 50% BWH/50% glucose mixture after 24 h cultivation.

Table 5-12: Product formation parameters of *E. coli* DH5α_1E after 24 h in LB plus 50% BWH/50% glucose feed in 10 L bioreactor scale.

Product yields were calculated according to 4.2.4.3 (page 66), Equation 4-23, Equation 4-21, Equation 4-22. Product productivities were calculated according to Equation 4-24, Equation 4-25.

p_{max}… product concentration, $Y_{P/X}$… product yield (biomass-related), $Y_{P/S}$… product yield (from substrate), P_P... volumetric productivity, Q_P… specific productivity (biomass-related)

Product	p_{max} [g L^{-1}]	$Y_{P/X}$ [g g^{-1} biomass]	$Y_{P/S}$ [mol mol^{-1} glucose][a]	$Y_{P/S}$ [mol%][a]	P_P [g L^{-1} h^{-1}]	Q_P [g g^{-1} biomass h^{-1}]
Isopropanol	1.36	0.313	0.126	12.6	0.056	0.013
Acetone	0.04	0.009	0.004	0.4	0.002	0.000
Ethanol	0.00	0.000	0.000	0.0	0.000	0.000
Acetate[b]	1.99	0.450	0.182	18.2	0.080	0.018
Lactate	0.13	0.021	0.006	0.6	0.004	0.001
Biomass	4.44		0.240	24.0	0.177	

[a] For calculation purposes, glucose is considered the sole carbon source in the medium, [b] *E. coli*-associated acetate.

Although substrate-related isopropanol yield $Y_{P/S}$ was similar to the previous 10 L cultivation on pure glucose (12.6 vs. 13.4 mol%; Table 5-11, page 96), isopropanol concentration after 24 h was higher (1.4 vs. 0.9 g L^{-1}) and the biomass-related yield $Y_{P/X}$ increased by a third (0.313 vs. 0.227 g g^{-1}). *E. coli*-associated acetate concentration, yields and productivities were considerably lower, and slightly more biomass was produced than on pure glucose (4.4 vs. 4.0 g L^{-1}).

Protein analysis of the setup with pure glucose indicated an impaired activity of Idh-c-Myc (4c), due to insolubility (Figure 5-19 B, page 97). Here, a large portion of the Idh-c-Myc (4c) could be detected in the soluble fraction at the expected molecular mass of ~39 kDa (see Figure 5-22, odd numbered lanes).

Similar results were obtained for Acct-His_{10} (2e), visible at ~25 kDa, and to a lower (soluble) extent also for Adc-FLAG (3c) at ~29 kDa. Production of Act-StrepII (1E) was confirmed by WB analysis of whole cells extracts at ~41 kDa, including a rather intense band at ~23 kDa (see Appendix Figure A-7, page 193).

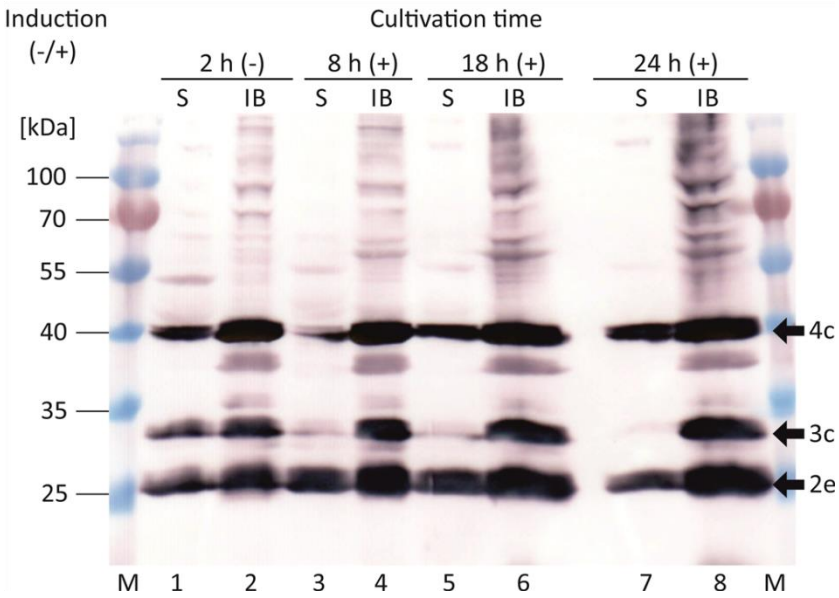

Figure 5-22: Production of Acct-His$_{10}$ (2e), Adc-FLAG (3c) & Idh-c-Myc (4c) in *E. coli* DH5α_1E in LB plus 50% BWH/50% glucose feed in 10 L bioreactor scale.

Recombinant *E. coli* DH5α were cultivated in 10 L LB medium containing 2% (w/v) glucose. Pulsed feeding of a mixture consisting of 50% BWH and 50% pure glucose was applied when glucose concentration was below 10 g L^{-1}. Control variables were set to 37 °C, pH 7.0, 0.4 bar, 5 L air min^{-1}, 400 rpm (pO_2 > 25%). Induction was performed at OD_{600} ~6.0 with 0.1 mM IPTG. 1/OD samples were taken at intervals, lysed and divided into soluble and insoluble cell extract fraction (4.2.3.2). Extracts were separated by SDS-PAGE and Acct-His$_{10}$ (2e) was visualized by WB with anti-polyHistidine, Adc-FLAG (3c) with anti-FLAG® and Idh-c-Myc (4c) with anti-c-Myc and anti-Mouse IgG-conjugated alkaline phosphatase antibodies (dye: BCIP/NBT) (see Table 4-12 for antibodies).

Lanes with odd numbers display the soluble fraction (S), whereas lanes with even numbers display the insoluble fraction (IB) samples. Arrows indicate the detected proteins. Theoretical molecular protein masses were calculated using ProtParam: MW of Acct-His$_{10}$ (2e) = 24.7 kDa, MW of Adc-FLAG (3c) = 28.9 kDa, MW of Idh-c-Myc (4c) = 39.0 kDa.

Acct… acetate CoA-transferase, Adc… acetoacetate decarboxylase, Idh… isopropanol dehydrogenase

In the second setup, *E. coli* DH5α_1E was grown in LB medium containing 2% (w/v) pure glucose and fed with 100% BWH solution. Figure 5-23 shows the growth behavior, glucose consumption and product formation of *E. coli* DH5α_1E with 100% BWH feed in 10 L bioreactor scale.

E. coli DH5α_1E displayed a μ_{max} of 0.7 h^{-1} and a doubling time of 1.0 h in exponential phase. Stationary phase was reached at t = 15 h, although a slight increase in growth could be seen towards the end of cultivation. The cells achieved a x_{max} of 4.4 g L^{-1} and an overall volumetric glucose consumption rate P_S of 1.378 g L^{-1} h^{-1} during 24 h. Due to the lower glucose content of 38% (w/v) in BWH (Table 4-3, page 41) compared to the 50% (w/v) glucose solution, pulsed feeding had to be applied more frequently than in the setup with pure glucose or 50% BWH/50% glucose feed. Isopropanol was first detected at t = 7 h and showed an almost linear increase, apart from two short-term decreases of isopropanol concentration in the medium at t = 21 and 27 h, until a concentration of 1.8 g L^{-1} was reached after 30 h. Acetone first occurred after 18 h and ethanol after 29 h. Lactate concentration continuously increased to 0.4 g L^{-1} after 30 h. Acetate formation by *E. coli* DH5α_1E correlated with growth, but BWH feeding increased the total acetate concentration in the medium to 4.7 g L^{-1} after 30 h. For comparison, total acetate concentration at that time was 2.2 g L^{-1} for feed with 50% BWH/50% glucose (Figure 5-21, page 99) and 3.6 g L^{-1} for feed with pure glucose (Figure 5-17, page 95).

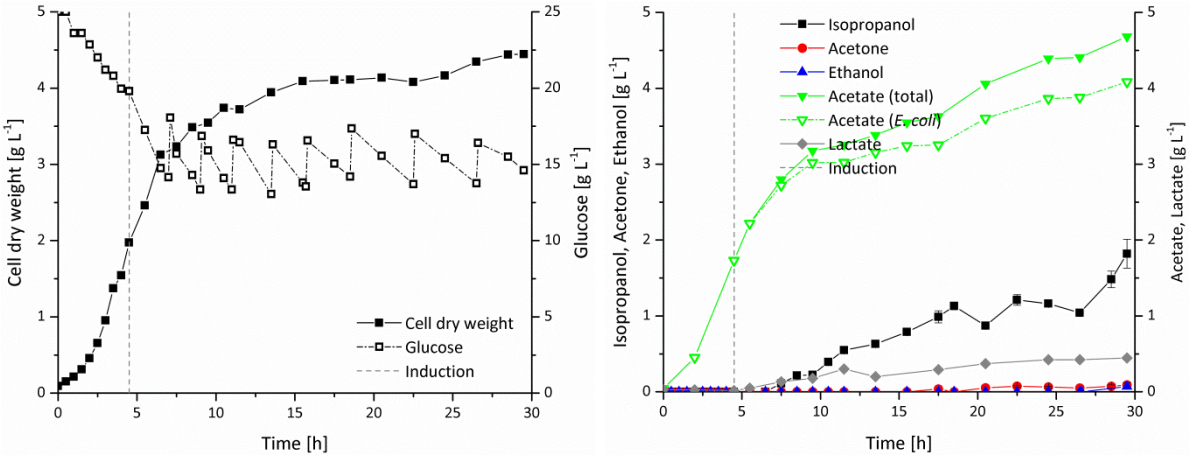

Figure 5-23: Growth, glucose consumption and product formation of *E. coli* DH5α_1E in LB plus 100% BWH feed in 10 L bioreactor scale.

Recombinant *E. coli* DH5α were cultivated in 10 L LB medium containing 2% (w/v) glucose. Pulsed feeding of 100% BWH was applied when glucose concentration was below 10 g L^{-1}. Control variables were set to 37 °C, pH 7.0, 0.4 bar, 5 L air min^{-1}, 400 rpm (pO_2 > 25%). Induction was performed at OD_{600} ~6.0 with 0.1 mM IPTG. Samples were taken at intervals for determination of cell concentration, glucose consumption, protein and product analysis. Cell dry weight was calculated from OD_{600} according to 4.2.4.3. GC analysis: Error bars display the standard deviation of n = 3 (technical replicates).

Time course of the control variables pH, rotational speed, pO_2, airflow, pressure and temperature, as well as of base addition with 100% BWH feed was similar to the previous setup on pure glucose or with 50% BWH/50% glucose feed (see Appendix Figure A-8, page 194). Table 5-13 summarizes the product formation parameters of *E. coli* DH5α_1E after 24 h with 100% BWH feed.

Table 5-13: Product formation parameters of *E. coli* DH5α_1E after 24 h in LB plus 100% BWH feed in 10 L bioreactor scale.

Product yields were calculated according to 4.2.4.3 (page 66), Equation 4-23, Equation 4-21, Equation 4-22. Product productivities were calculated according to Equation 4-24, Equation 4-25.

p_{max}… product concentration, $Y_{P/X}$… product yield (biomass-related), $Y_{P/S}$… product yield (from substrate), P_P... volumetric productivity, Q_P… specific productivity (biomass-related)

Product	p_{max} [g L^{-1}]	$Y_{P/X}$ [g g^{-1} biomass]	$Y_{P/S}$ [mol mol^{-1} glucose][a]	$Y_{P/S}$ [mol%][a]	P_P [g L^{-1} h^{-1}]	Q_P [g g^{-1} biomass h^{-1}]
Isopropanol	1.16	0.285	0.103	10.3	0.047	0.011
Acetone	0.06	0.016	0.006	0.6	0.003	0.001
Ethanol	0.00	0.000	0.000	0.0	0.000	0.000
Acetate[b]	3.86	0.938	0.340	34.0	0.156	0.037
Lactate	0.42	0.097	0.023	2.3	0.016	0.004
Biomass	4.16		0.216	21.6	0.166	

[a] For calculation purposes, glucose is considered the sole carbon source in the medium, [b] *E. coli*-associated acetate.

Biomass- and substrate-related acetate yield increased considerably in comparison to the cultivation with 50% BWH/50% glucose (0.938 g g^{-1} and 34.0 mol% vs. 0.450 g g^{-1} and 18.2 mol%; compare Table 5-12, page 100). Isopropanol concentration, yields and productivities were slightly lower with 100% BWH, but lactate levels were considerably higher than for the 50% BWH/50% glucose feed setup (0.4 vs. 0.1 g L^{-1}).

Protein analysis detected the Act-StrepII (1E) mostly in its insoluble form at ~41 kDa (Figure 5-24 A, even numbered lanes), but a small part was also present in the soluble fraction (odd numbered lanes). Faint

bands were visible at 25, 28, 35 and 38 kDa in addition to a thicker band at ~23 kDa. Acct-His_{10} (2e), Adc-FLAG (3c) and Idh-c-Myc (4c) were almost equally produced in soluble and insoluble form at ~25, ~29 and ~39 kDa (Figure 5-24 B).

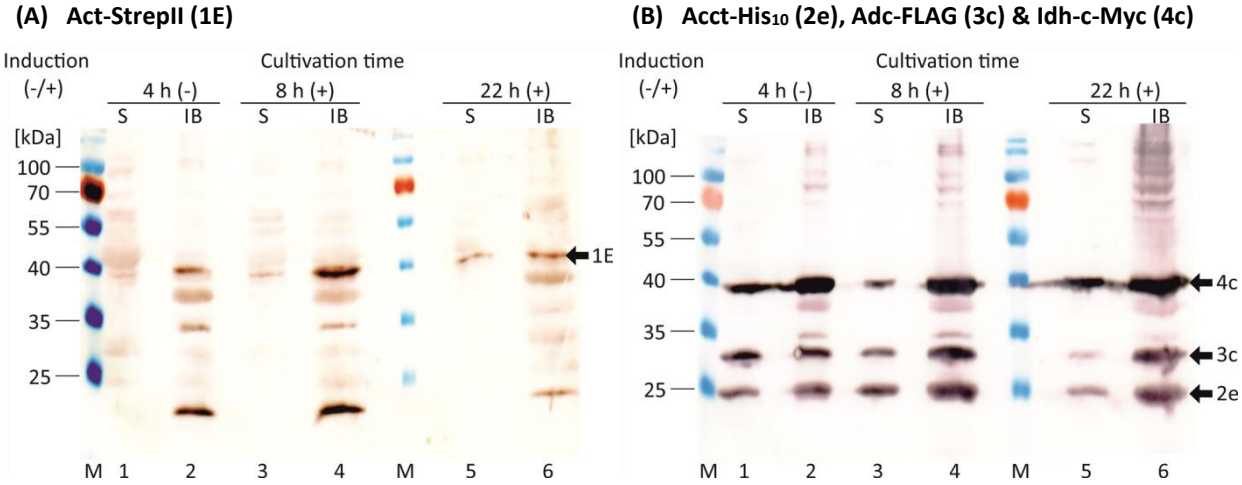

Figure 5-24: Production of Act-StrepII (1E) (A), Acct-His_{10} (2e), Adc-FLAG (3c) & Idh-c-Myc (4c) (B) in *E. coli* DH5α_1E in LB plus 100% BWH feed in 10 L bioreactor scale.

Recombinant *E. coli* DH5α were cultivated in 10 L LB medium containing 2% (w/v) glucose. Pulsed feeding of 100% BWH was applied when glucose concentration was below 10 g L^{-1}. Control variables were set to 37 °C, pH 7.0, 0.4 bar, 5 L air min^{-1}, 400 rpm (pO_2 > 25%). Induction was performed at OD_{600} ~6.0 with 0.1 mM IPTG. 1/OD samples were taken at intervals, lysed and divided into soluble and insoluble cell extract fraction (4.2.3.2). Extracts were separated by SDS-PAGE and Act-StrepII (1E) was visualized by WB with anti-StrepII®, Acct-His_{10} (2e) with anti-polyHistidine, Adc-FLAG (3c) with anti-FLAG® and Idh-c-Myc (4c) with anti-c-Myc and anti-Mouse IgG-conjugated alkaline phosphatase antibodies (dye: BCIP/NBT) (see Table 4-12 for antibodies).

Lanes with odd numbers display the soluble fraction (S), whereas lanes with even numbers display the insoluble fraction (IB) samples. Arrows indicate the detected proteins. Theoretical molecular protein masses were calculated using ProtParam: MW of Act-StrepII (1E) = 41.6 kDa, MW of Acct-His_{10} (2e) = 24.7 kDa, MW of Adc-FLAG (3c) = 28.9 kDa, MW of Idh-c-Myc (4c) = 39.0 kDa. Act… acetyl-CoA acetyltransferase, Acct… acetate CoA-transferase, Adc… acetoacetate decarboxylase, Idh… isopropanol dehydrogenase

Experiments in shake flask scale with BWH as carbon source resulted in an impediment of bacterial growth and isopropanol production, yielding acetone, not isopropanol as product (5.3, page 86). In contrast, application of BWH in 10 L bioreactor scale, either in the form of a 50% BWH/50% glucose feed or a 100% BWH feed, after initial growth on pure glucose, did not display a negative impact on isopropanol synthesis. In conclusion, BWH could be considered an alternative carbon source for isopropanol production by *E. coli* DH5α_1E in the measurable, controllable and adjustable environment of a 10 L bioreactor.

5.5 Isopropanol Separation and Recovery by Gasstripping

Isopropanol is typically used as a disinfectant for medical and healthcare purposes due to its bactericidal effect. In a microbial isopropanol production process, the alcohol accumulates in the cultivation medium and slowly poisons the bacterium. Here, gasstripping was assessed as a suitable means for *in situ* product separation and recovery in 10 L bioreactor scale to alleviate the toxic effect and to simultaneously allow isopropanol purification from the cultivation broth.

5.5.1 Gasstripping with Gas Washing Bottles

Aim of the following experiment was to evaluate the effectiveness of a gasstripping setup in 10 L bioreactor scale with a (cell-free) model solution of 3 g L^{-1} isopropanol in 10 L LB medium plus 2% (w/v) glucose. Setup of the gasstripping device is depicted in Figure 5-25.

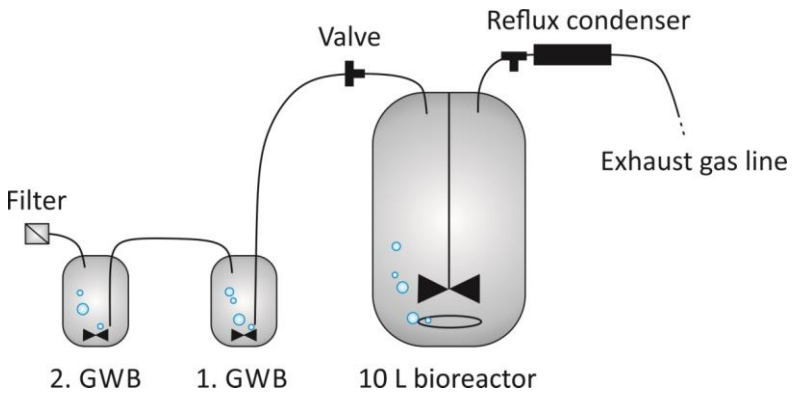

Figure 5-25: Setup of gasstripping device with 2 gas washing bottles in 10 L bioreactor scale.
BIOSTAT® C was filled with a model solution of 3 g L^{-1} isopropanol in 10 L LB medium plus 2% (w/v) glucose. Control variables were set to 37 °C, pH 7.0, 0.4 bar, 5 L air min^{-1}, 400 rpm. Exhaust gas was diverted to 2 cooled and stirred GWB (connected in series, 300 mL ddH_2O, -10 °C) by opening a valve and automated shut-off of exhaust gas line due to the pressure drop in the vessel (pressure control valve). Samples were taken at intervals from bioreactor and 2 GWB for determination of product concentration (4.2.3.6, 4.2.3.7).
GWB… gas washing bottle(s)

The model solution was incubated at 37 °C, 0.4 bar, 400 rpm and gassed with 5 L air min^{-1}, analogous to the cell-containing 10 L bioreactor experiments (5.4, page 91). Gasstripping was started by opening a threeway valve and subsequent automated shut-off of the exhaust gas line by a pressure control valve due to the pressure drop in the vessel. Exhaust gas was instead directed to two cooled and stirred gas washing bottles (further denoted as GWB; connected in series by silicone tubing, filled with 300 mL ddH_2O, cooled to -10 °C with a sodium chloride-ice mixture). Samples were taken at intervals to measure the isopropanol concentration in the vessel and each GWB. Figure 5-26 displays the isopropanol concentration in the bioreactor and the two GWB over the course of a 4 h gasstripping period with the model solution, as well as the amount and percentage of isopropanol that was transferred from the bioreactor to the GWB.

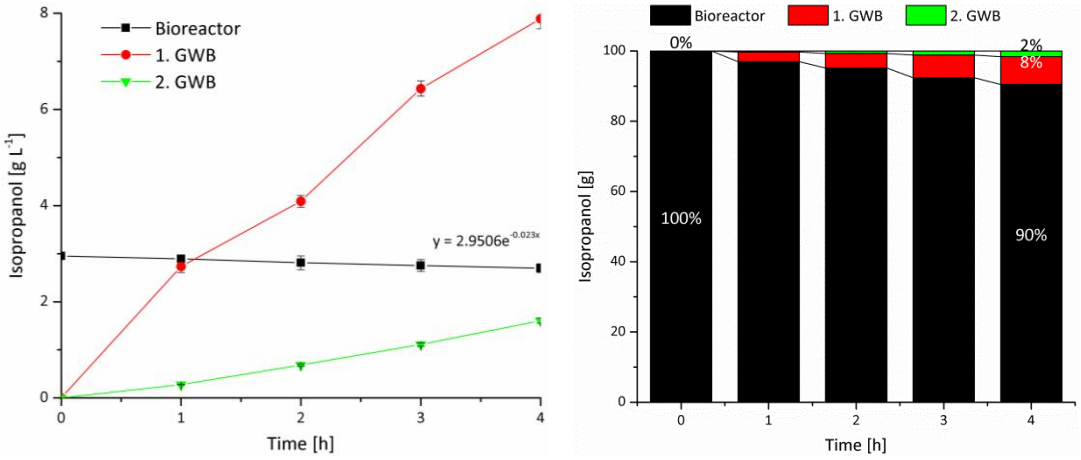

Figure 5-26: Gasstripping with model solution - Isopropanol concentration in 10 L bioreactor and 2 gas washing bottles - Isopropanol transfer from bioreactor to gas washing bottles.
BIOSTAT® C was filled with a model solution of 3 g L^{-1} isopropanol in 10 L LB medium plus 2% (w/v) glucose. Control variables were set to 37 °C, pH 7.0, 0.4 bar, 5 L air min^{-1}, 400 rpm. Exhaust gas was diverted to 2 cooled and stirred GWB (connected in series, 300 mL ddH_2O, -10 °C) by opening a valve and automated shut-off of exhaust gas line due to the pressure drop in the vessel (pressure control valve). Samples were taken at intervals from bioreactor and 2 GWB for determination of isopropanol concentration (4.2.3.7). GC analysis: Error bars display the standard deviation of n = 3 (technical replicates).
GWB… gas washing bottle(s)

Isopropanol concentration in the bioreactor decreased, while isopropanol concentration in the two GWB increased within 4 h, especially in the first GWB. An exponential trendline determines a mass transfer coefficient $k = 0.023\ h^{-1}$ for the isopropanol transfer from liquid to gas phase. The net outflow of isopropanol from the 10 L bioreactor was 2.85 g after 4 h or ~10%, indicating that this gasstripping setup could be successfully utilized for the removal of isopropanol from the medium.

Previous experiments with engineered *E. coli* displayed that, besides isopropanol, other metabolites like acetone, ethanol, acetate and lactate were produced and present in the cultivation medium. Therefore, gasstripping was performed on a cultivation with living cells in 10 L scale to evaluate the flux of generated, potentially volatile products from liquid to gas phase. The GWB gasstripping setup (Figure 5-25) was applied to the bioreactor cultivation of *E. coli* DH5α_1E in LB medium with 2% (w/v) glucose and pulsed glucose feeding (see 5.4.1, Figure 5-17, page 95). The only difference to the model solution setup was the use of 600 mL ddH_2O instead of 300 mL in the 1. GWB. Flux of volatiles was measured from t = 25-54 h. Figure 5-27 shows the accumulating amount of isopropanol, acetone and ethanol in the 10 L bioreactor and the 2 GWB over the cultivation time.

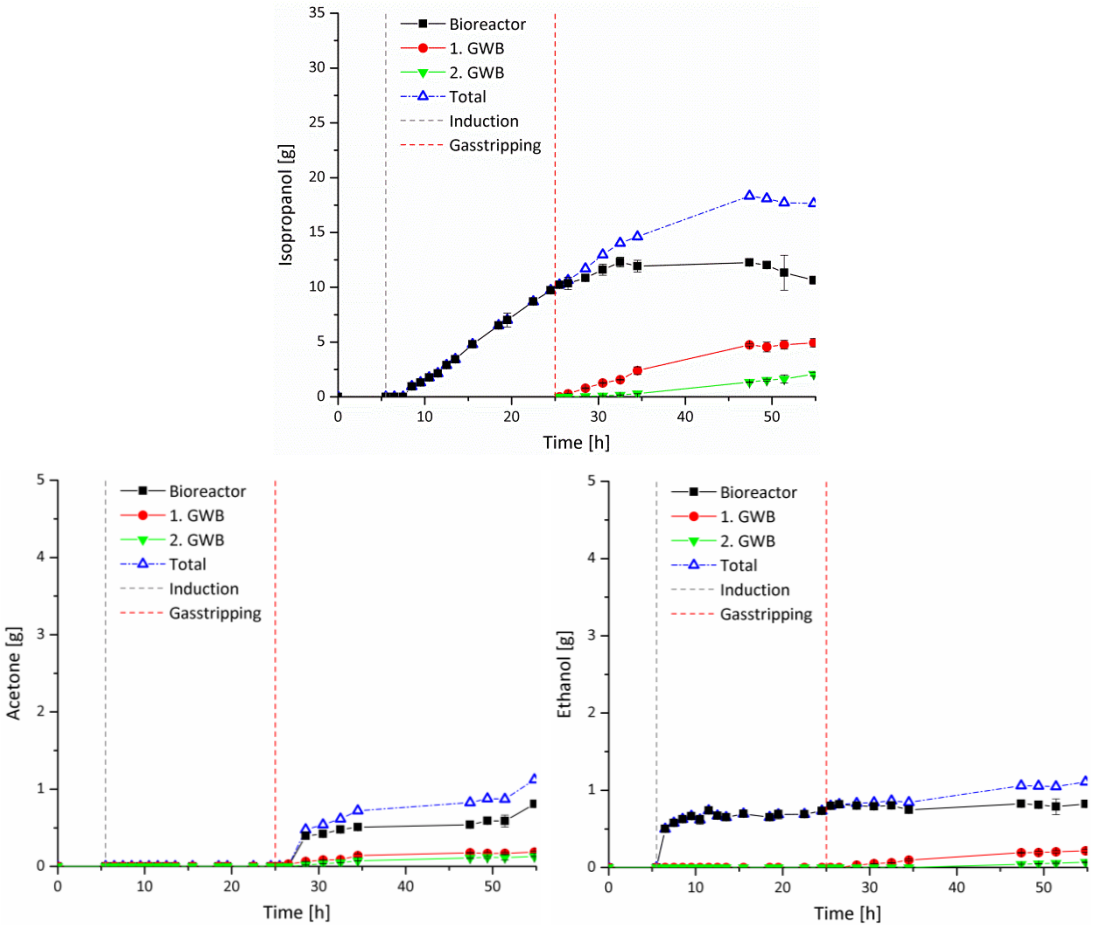

Figure 5-27: Amount of volatile metabolic products in 10 L bioreactor and 2 gas washing bottles during cultivation of *E. coli* DH5α_1E in LB plus glucose feed with gasstripping.
Recombinant *E. coli* DH5α were cultivated in 10 L LB medium containing 2% (w/v) glucose. Pulsed feeding of a 50% (w/v) glucose solution was applied when glucose concentration was below 10 g L^{-1}. Control variables were set to 37 °C, pH 7.0, 0.4 bar, 5 L air min^{-1}, 400 rpm (pO_2 > 25%). At t = 25 h, gasstripping was turned on (see Figure 5-25 for device). Exhaust gas was diverted to 2 cooled and stirred GWB (connected in series, 600 & 300 mL ddH_2O, -10 °C) by opening a valve and automated shut-off of exhaust gas line due to the pressure drop in the vessel (pressure control valve). Samples were taken at intervals from bioreactor and 2 GWB for determination of product concentration (4.2.3.6, 4.2.3.7). GC analysis: Error bars display the standard deviation of n = 3 (technical replicates).
GWB… gas washing bottle(s)

Flux of products to the 1. and 2. GWB could be observed for isopropanol, acetone and ethanol directly after onset of stripping at t = 25 h. Neither acetate nor lactate could be detected in both GWB. Without the gasstripping results, it could be assumed that isopropanol production by *E. coli* DH5α_1E reached a plateau and stopped after 32 h in the bioreactor. But isopropanol continued to accumulate in both GWB. Including gasstripping, the total amount of captured isopropanol was thus increased by ~66%, totaling to 17.65 g produced isopropanol after 54 h. Total amount of acetone increased by ~38% to 1.12 g and the total amount of ethanol increased by ~35% to 1.11 g. Acetone was already detected in the 1. GWB at t = 26 h (0.05 g L^{-1}, 0.03 g), 2 h before it was first observed in the bioreactor at t = 28 h (0.04 g L^{-1}, 0.39 g). These findings demonstrate that acetone and ethanol were also readily stripped via exhaust gas re-routing with the GWB setup.

5.5.2 Gasstripping with Condensation Trap and Liquid Nitrogen

Constant aeration of the bioreactor in an aerobic production process causes evaporation, which is usually counteracted by implementation of a reflux condenser. Efficient stripping of volatiles by gas re-routing with GWB, as shown in 5.5.1, raises the question whether product "loss" also occurs during a standard bioreactor cultivation (without intended gasstripping) via aeration. Therefore, a second gasstripping setup was applied to determine the extent of volatile product evaporation in 10 L bioreactor scale. Here, gasstripping was performed by directing the condenser-cooled down exhaust gas to a condensation trap (further denoted as CT). The CT was filled with liquid nitrogen to condense and freeze the gas efflux of a 30 min period. The frozen efflux was thawed again in a 37 °C water bath, weighed and analyzed for isopropanol, acetone and ethanol concentration. The collection of exhaust gas via CT was repeated every 2 h. Figure 5-28 depicts a schematic setup of the gasstripping device with CT and liquid nitrogen in 10 L bioreactor scale.

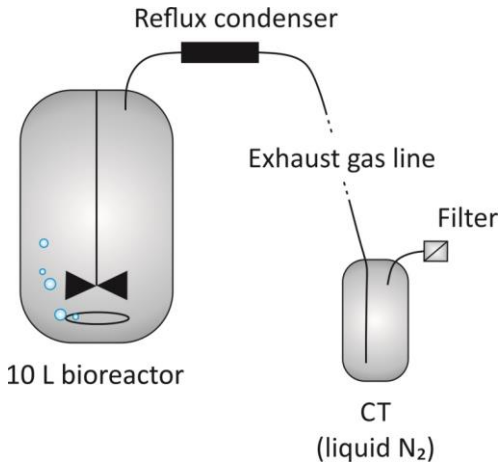

Figure 5-28: Setup of gasstripping device with a condensation trap and liquid nitrogen in 10 L bioreactor scale.
BIOSTAT® C control variables were set to 37 °C, pH 7.0, 0.4 bar, 5 L air min^{-1}, 400 rpm. Cooled down exhaust gas was diverted to a CT, cooled with liquid nitrogen. Efflux was frozen and collected for 30 min, thawed, weighed and analyzed for product concentration (4.2.3.6, 4.2.3.7). Collection of exhaust gas was repeated in a 2 h interval.
CT… condensation trap

Liquid nitrogen/CT gasstripping was applied during the whole cultivation period of *E. coli* DH5α_1E in LB medium with 2% (w/v) glucose and pulsed feeding of 100% BWH (see 5.4.3, Figure 5-23, page 102). Figure 5-29 shows the accumulating amount of isopropanol, acetone and ethanol in the 10 L bioreactor and CT over the cultivation time.

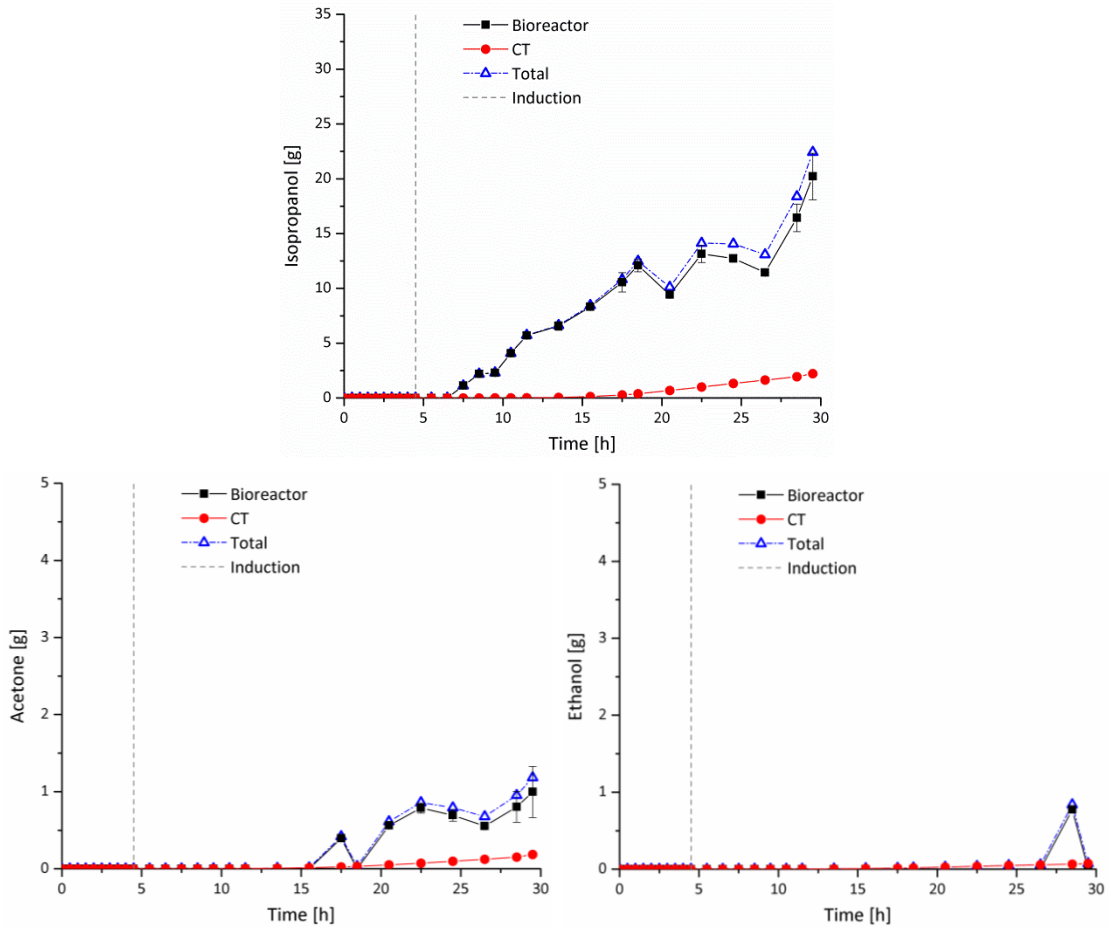

Figure 5-29: Amount of volatile metabolic products in 10 L bioreactor and condensation trap during cultivation of *E. coli* DH5α_1E in LB plus 100% BWH feed with gasstripping.
Recombinant *E. coli* DH5α were cultivated in 10 L LB medium containing 2% (w/v) glucose. Pulsed feeding of 100% BWH was applied when glucose concentration was below 10 g L^{-1}. Control variables were set to 37 °C, pH 7.0, 0.4 bar, 5 L air min^{-1}, 400 rpm (pO_2 > 25%). Gasstripping with liquid nitrogen (see Figure 5-28 for device) was applied throughout the whole cultivation. Cooled down exhaust gas was diverted to a CT, cooled with liquid nitrogen. Efflux was frozen and collected for 30 min, thawed, weighed and analyzed for product concentration (4.2.3.6, 4.2.3.7). Collection of exhaust gas was repeated in a 2 h interval. GC analysis: Error bars display the standard deviation of n = 3 (technical replicates).
CT… condensation trap

Gasstripping with liquid nitrogen allowed detection of isopropanol, acetone and ethanol in CT as early as t = 6 h in minimal amounts (isopropanol: 1.9 mg, acetone: 0.5 mg, ethanol: 0.6 mg), although acetone and ethanol were first measured at t = 17 h and t = 28 h in the bioreactor. Acetate and lactate could not be detected in the CT samples. These findings suggest that product “loss” by aeration already occurs in early stages of cultivation, despite the applied exhaust gas reflux condenser. Including stripping with CT, the total amount of captured isopropanol was increased by ~11%, totaling to 22.43 g produced isopropanol after 30 h. Total amount of acetone increased by ~18% to 1.18 g and the total amount of ethanol increased by 9% to 0.84 g. This means that volatile product “loss” has to be accounted for in every aerobic bioreactor cultivation.

5.6 Optimization of Isopropanol Production by Minimization of Acetate Production

A major objective of this work was improvement of microbial isopropanol production in terms of concentration, yield and productivity. Acetate, as a major metabolic product of *E. coli*, is not only known to inhibit cell growth and protein production [Aristidou et al., 1995; Kim and Cha, 2003], but its production also decreases the availability of the isopropanol precursor acetyl-CoA. Subsequent experiments concentrated on decreasing the acetate-generating capacity of the recombinant host to improve isopropanol production.

5.6.1 Knockout of Phosphotransacetylase in *E. coli* and Verification of Gene Disruption

Aim of the following set of experiments was disruption of the major acetate synthesis pathway Pta-Ack (phosphotransacetylase, further denoted as Pta; acetate kinase, further denoted as Ack) in *E. coli*. Red®/ET® recombination technique (4.2.2.8, page 54) was applied for targeted disruption of the pta gene in *E. coli* DH5α and to obtain Pta-deficient mutants. The knockout was performed in the scope of a master thesis by Joyshree Ganguly ("Knockout of the acetate-producing pathway enzyme phosphotransacetylase (Pta) in *E. coli* and evaluation of its effects on the bacterial metabolism", 2016). First step in the pta knockout procedure (4.2.2.8, Figure 4-2, page 56) was generation of a linear FRT-PGK-gb2-neo-FRT cassette flanked by homology arms, which target the desired recombination site in the *E. coli* genome. Oligonucleotide design was performed by choosing homology regions directly adjacent to either side of the intended insertion site in the pta gene (see Table A-4, page 186 for DNA sequence of pta gene). Figure 5-30 shows the amplified product, generated by PCR (see Table 4-22 and Table 4-23 for detailed procedure) with the chosen primers (Table 4-10) and analyzed by AGE (4.2.2.1).

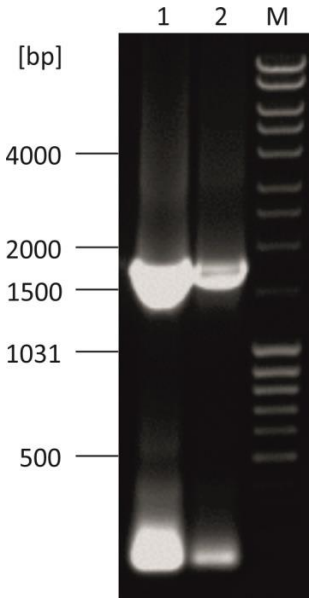

Figure 5-30: Generation of a linear functional homology cassette for targeted disruption of the pta gene in *E. coli*.
PCR was performed with primers (Table 4-10) targeting the pta gene insertion site (Table A-4), according to Table 4-22 (PCR mastermix) and Table 4-23 (PCR temperature program) with pFRT (plasmid containing FRT-PGK-gb2-neo-FRT cassette) as template DNA. DNA analysis was performed by AGE (4.2.2.1).
Lane 1 displays the amplified, pooled and purified (4.2.2.2) FRT-PGK-gb2-neo-FRT cassette with added homology arms at 1737 bp (DNA concentration: 1242 µg mL^{-1}).
Lane 2 depicts the PCR product adjusted to 400 µg mL^{-1}.
M… Marker (MassRuler DNA ladder mix, Thermo Fisher Scientific, Germany)
The original figure was kindly provided by J. Ganguly.

PCR amplification of the FRT-PGK-gb2-neo-FRT cassette (1637 bp) with additional 2× 50 bp homology regions resulted in a product with the size of 1737 bp, as confirmed by AGE. The PCR products of five reactions were subsequently pooled, purified (lane 1) and adjusted to a DNA concentration of 400 µg mL^{-1} (lane 2) prior to further utilization of the functional cassette. The linear functional homology cassette was introduced into *E. coli* DH5α, carrying pRedET-Amp^R enabling Red®/ET® recombination by induction with L-arabinose as described in 4.2.2.8 (Figure 4-2, page 56). Thus, the cassette was inserted into the target site, disrupting the pta gene in the genome of *E. coli* DH5α.

After Red®/ET® recombination in *E. coli* DH5α, the potential Pta-deficient mutants were verified by PCR (see Table 4-24 and Table 4-25 for detailed procedure) and AGE (4.2.2.1), as shown in Figure 5-31.

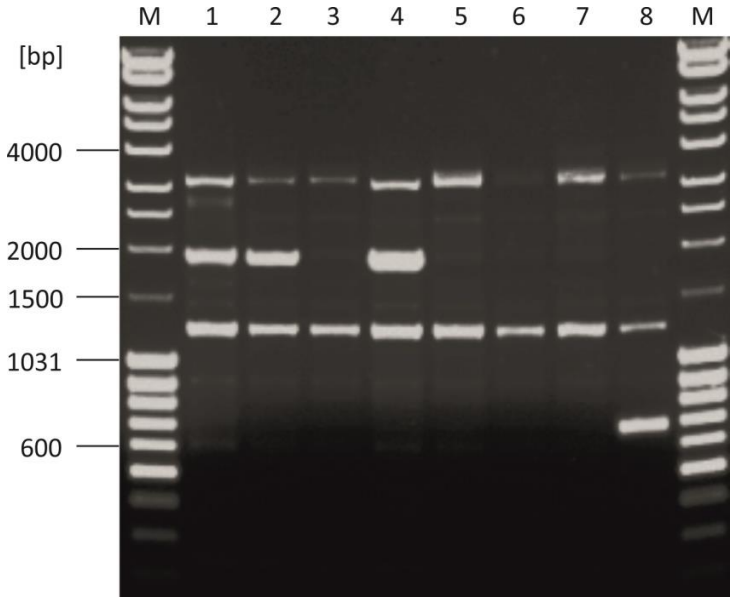

Figure 5-31: Verification of targeted pta gene disruption in *E. coli* DH5α on DNA level.
Red®/ET® recombination in *E. coli* DH5α was performed as described in 4.2.2.8 to disrupt the pta gene. PCR was performed with primers directed against the genomic recombination site (Table 4-10), according to Table 4-24 (PCR mastermix) and Table 4-25 (PCR temperature program) with potential Pta-deficient mutants as template DNA. DNA analysis was performed by AGE (4.2.2.1).
Lanes 1-7 display the DNA patterns of potential Pta-deficient mutants.
Lane 8 depicts the DNA pattern of non-mutated *E. coli* DH5α (negative control).
Disruption of the pta gene yields a band of 1888 bp size. Intact pta gene shows a band of 677 bp size.
M… Marker (MassRuler DNA ladder mix, Thermo Fisher Scientific, Germany)
The original figure was kindly provided by J. Ganguly.

Successful recombination yielded a band of 1888 bp size (linear functional homology cassette = 1637 bp plus 2× 50 bp homology regions plus regions framed by genomic primers = 74 + 77 bp) with primers directed against the genomic recombination site (Table 4-10). Thus, intended disruption of the pta gene could be confirmed for mutants shown in lane 1, 2 and 4 (band at 1888 bp). Non-integration of the functional cassette resulted in a band of 677 bp (intact pta gene; see Table A-4, page 186 for DNA sequence), visible in lane 8 (negative control = non-mutated *E. coli* DH5α genomic DNA).

Subsequently, removal of the kanamycin selection marker was performed on the positively tested mutants, as described in 4.2.2.8. Marker-free, mutant *E. coli* DH5α (further denoted as *E. coli* DH5αΔpta) were successfully obtained by comparison of bacterial growth on kanamycin-containing LB agar plates and LB agar plates without antibiotics (results not shown).

One of the confirmed mutants was selected for verification of the pta knockout on metabolic product level. The non-functionality of Pta should be demonstrated via diminished acetate production by *E. coli* DH5αΔpta. The cells were first adapted from LB to MM (4.2.1.3) to avoid falsification of acetate measurements by complex medium components. Main shake flask cultures of *E. coli* DH5αΔpta and of non-mutated *E. coli* DH5α were grown at 37 °C and 100 rpm in 100 mL MM containing 2% (w/v) glucose. An additional pulse of 1% (w/v) glucose was applied after 6 h cultivation. Samples were taken to monitor the bacterial growth (OD_{600} by spectrophotometry, 4.2.3.1) and acetate formation (by enzymatic test kit, 4.2.3.6). Figure 5-32 depicts the growth of *E. coli* DH5αΔpta and non-mutated *E. coli* DH5α, as well as the acetate production of both strains.

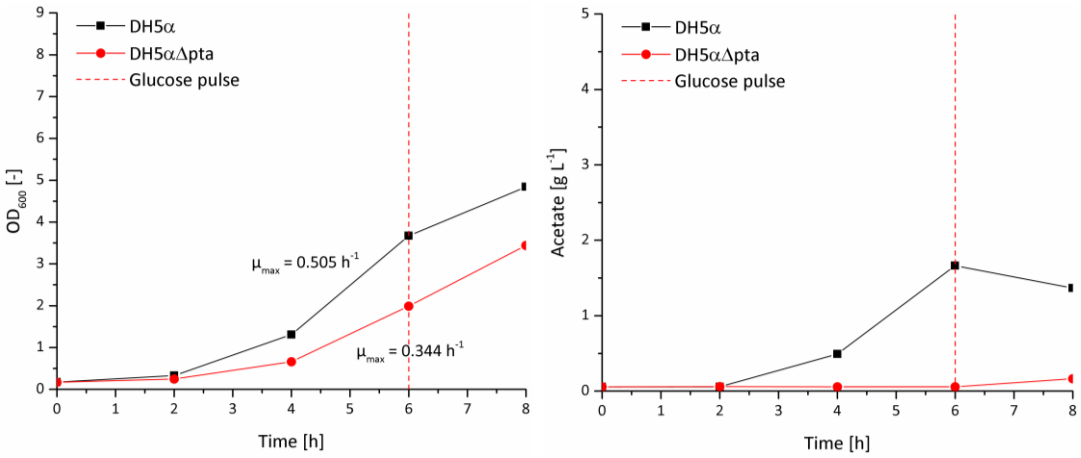

Figure 5-32: Verification of targeted pta gene disruption in *E. coli* DH5α on metabolic product level.
E. coli DH5α and *E. coli* DH5αΔpta were grown at 37 °C, 100 rpm in 100 mL MM containing 2% (w/v) glucose. An additional pulse of 1% (w/v) glucose was applied after 6 h cultivation. Samples were taken at intervals for determination of cell concentration and acetate production analysis (4.2.3.6).
MM… minimal medium

E. coli DH5α achieved a μ_{max} of 0.5 h^{-1} in exponential phase, whereas DH5αΔpta grew slower, with a μ_{max} = 0.3 h^{-1}, indicating an effect of the mutation on cellular metabolism. Acetate concentration in the medium of the mutant stayed constant at 0.06 g L^{-1}, only rising slightly after the glucose pulse (t = 6 h) to 0.16 g L^{-1} after 8 h. In contrast, the non-mutated strain displayed the already observed correlation between acetate production and growth, reaching a maximum acetate concentration of 1.66 g L^{-1} after 6 h. Table 5-14 summarizes the effect of targeted pta gene disruption on growth and acetate formation parameters in comparison to the non-mutated strain.

Table 5-14: Influence of targeted pta gene disruption in *E. coli* DH5α on growth rate and acetate formation parameters after 8 h.
Parameters were calculated according to section 4.2.4.3 (page 66).
μ_{max}… maximal growth rate, p_{max}… product concentration, $Y_{P/X}$… product yield (biomass-related), P_P... volumetric productivity, Q_P... specific productivity (biomass-related)

Strain	μ_{max} [h^{-1}]	p_{max} [g L^{-1}]	$Y_{P/X}$ [g g^{-1} biomass]	P_P [g L^{-1} h^{-1}]	Q_P [g g^{-1} biomass h^{-1}]
E. coli DH5α	0.5	1.366	0.935	0.164	0.113
E. coli DH5αΔpta	0.3	0.164	0.098	0.014	0.013

The biomass-related acetate yield $Y_{P/X}$ and productivity Q_P of the mutant strain decreased by ~90% compared to the original strain. In conclusion, knockout of the pta gene in *E. coli* DH5αΔpta was successfully verified on DNA and metabolic product level and the non-functionality of Pta was demonstrated via strongly diminished acetate production by *E. coli* DH5αΔpta.

5.6.2 Influence of Phosphotransacetylase Knockout on Isopropanol Production by Engineered *E. coli* in Bioreactor Scale

Aim of subsequent experiments was to investigate the effect of the pta knockout on isopropanol production. *E. coli* DH5αΔpta was chemically transformed with the isopropanol pathway plasmid pRK_ISO_1E2e3c4c or pRK_ISO_1C2e3c4c (4.2.2.3, 4.2.2.4) and positive clones were selected on kanamycin-containing LB agar plates. Glycerol stocks were prepared (4.2.1.4) and plasmids were isolated (4.2.2.5) and verified by sequencing (4.2.2.7) to confirm the successful transformation (see Table 4-10 for primer). *E. coli* DH5αΔpta_1E and *E. coli* DH5αΔpta_1C were subjected to cultivations in 10 L bioreactor scale on LB medium, using glucose as carbon source. Precultures, inoculum and medium were prepared according to 4.2.1.2. Induction, antibiotic selection, feed and sample preparation was performed as described in the equivalent bioreactor cultivations on glucose in 5.4 (page 91). Cultivation variables were likewise set to 37 °C, pH 7.0, 0.4 bar, 400 rpm, 5 L air min^{-1} (pO_2 > 25%). Figure 5-33 displays the growth behavior, glucose consumption and product formation of *E. coli* DH5αΔpta_1E in 10 L bioreactor scale.

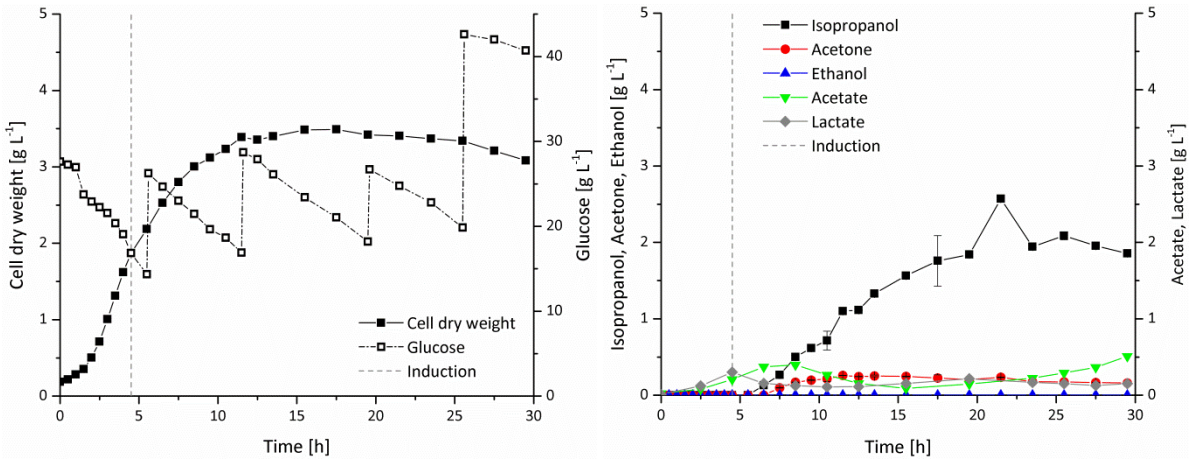

Figure 5-33: Growth, glucose consumption and product formation of *E. coli* DH5αΔpta_1E in LB plus glucose feed in 10 L bioreactor scale.
Recombinant *E. coli* DH5αΔpta were cultivated in 10 L LB medium containing 2% (w/v) glucose. Pulsed feeding of a 50% (w/v) glucose solution was applied when glucose concentration was below 10 g L^{-1}. Control variables were set to 37 °C, pH 7.0, 0.4 bar, 5 L air min^{-1}, 400 rpm (pO_2 > 25%). Induction was performed at OD_{600} ~6.0 with 0.1 mM IPTG. Samples were taken at intervals for determination of cell concentration, glucose consumption, protein and product analysis. Cell dry weight was calculated from OD_{600} according to 4.2.4.3. GC analysis: Error bars display the standard deviation of n = 3 (technical replicates).

E. coli DH5αΔpta_1E grew with a μ_{max} of 0.5 h^{-1} and a doubling time of 1.3 h in exponential phase, reaching a maximal cell dry weight x_{max} of 3.5 g L^{-1} in stationary phase after 12 h. The overall volumetric glucose consumption rate P_S was 1.574 g L^{-1} h^{-1} after 24 h. Isopropanol was first detected at t = 6 h and quickly rose to a final concentration of 1.9 g L^{-1} after 30 h. Acetone was detected at t = 7 h and reached a maximum concentration of 0.3 g L^{-1} after 11 h. Acetate production stayed below 0.4 g L^{-1} in exponential phase and reached a maximum of 0.5 g L^{-1} at the end of cultivation. Lactate concentration peaked at t = 5 h with 0.3 g L^{-1}, but decreased afterwards, while ethanol was not generated. Table 5-15 shows a summary of product formation parameters of *E. coli* DH5αΔpta_1E in 10 L bioreactor scale after 24 h.

Table 5-15: Product formation parameters of *E. coli* DH5αΔpta_1E after 24 h in LB plus glucose feed in 10 L bioreactor scale.

Product yields were calculated according to 4.2.4.3 (page 66), Equation 4-23, Equation 4-21, Equation 4-22. Product productivities were calculated according to Equation 4-24, Equation 4-25.

p_{max}… product concentration, $Y_{P/X}$… product yield (biomass-related), $Y_{P/S}$… product yield (from substrate), P_P... volumetric productivity, Q_P… specific productivity (biomass-related)

Product	p_{max} [g L^{-1}]	$Y_{P/X}$ [g g^{-1} biomass]	$Y_{P/S}$ [mol mol^{-1} glucose][a]	$Y_{P/S}$ [mol%][a]	P_P [g L^{-1} h^{-1}]	Q_P [g g^{-1} biomass h^{-1}]
Isopropanol	1.94	0.608	0.158	15.8	0.083	0.025
Acetone	0.18	0.055	0.015	1.5	0.008	0.002
Ethanol	0.00	0.000	0.000	0.0	0.000	0.000
Acetate	0.22	0.063	0.016	1.6	0.009	0.003
Lactate	0.02	0.049	0.009	0.9	0.007	0.002
Biomass	3.37		0.154	15.4	0.135	

[a] For calculation purposes, glucose is considered the sole carbon source in the medium.

Substrate-related acetate yield $Y_{P/S}$, as well as volumetric acetate productivity P_P, was drastically lower compared to the equivalent cultivation with *E. coli* DH5α_1E on glucose in this scale (1.6 vs. 56.5 mol%; 0.009 vs. 0.152 g L^{-1} h^{-1}; Table 5-11, page 96), indicating the successful suppression of acetate production via pta knockout. In contrast, substrate-related isopropanol yield $Y_{P/S}$ increased by 2.4 mol% to 15.8 mol%. Volumetric isopropanol productivity P_P more than doubled to 0.083 g L^{-1} h^{-1} in comparison to the non-Pta-deficient strain. Time course of control variables and base addition was comparable to the equivalent cultivation with *E. coli* DH5α_1E (see Appendix Figure A-9, page 194).

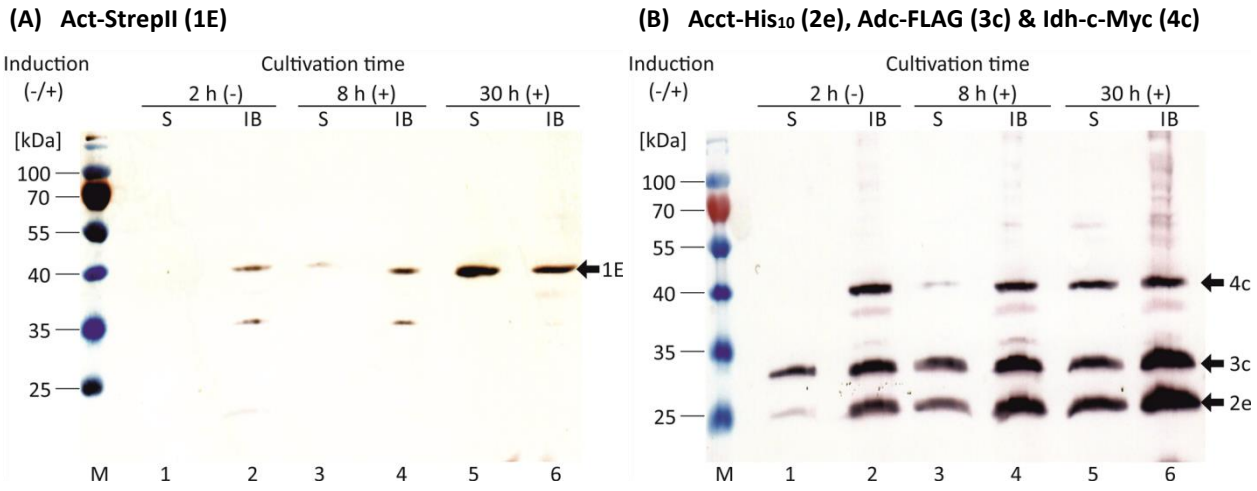

Figure 5-34: Influence of pta disruption on production of Act-StrepII (1E) (A), Acct-His_{10} (2e), Adc-FLAG (3c) & Idh-c-Myc (4c) (B) in *E. coli* DH5αΔpta_1E in LB plus glucose feed in 10 L bioreactor scale.

Recombinant *E. coli* DH5αΔpta were cultivated in 10 L LB medium containing 2% (w/v) glucose. Pulsed feeding of a 50% (w/v) glucose solution was applied when glucose concentration was below 10 g L^{-1}. Control variables were set to 37 °C, pH 7.0, 0.4 bar, 5 L air min^{-1}, 400 rpm (pO_2 > 25%). Induction was performed at OD_{600} ~6.0 with 0.1 mM IPTG. 1/OD samples were taken at intervals, lysed and divided into soluble and insoluble cell extract fraction (4.2.3.2). Extracts were separated by SDS-PAGE and Act-StrepII (1E) was visualized by WB with anti-StrepII®, Acct-His_{10} (2e) with anti-polyHistidine, Adc-FLAG (3c) with anti-FLAG® and Idh-c-Myc (4c) with anti-c-Myc and anti-Mouse IgG-conjugated alkaline phosphatase antibodies (dye: BCIP/NBT).

Lanes with odd numbers display the soluble fraction (S), whereas lanes with even numbers display the insoluble fraction (IB) samples. Arrows indicate the detected proteins. Theoretical molecular protein masses were calculated using ProtParam: MW of Act-StrepII (1E) = 41.6 kDa, MW of Acct-His_{10} (2e) = 24.7 kDa, MW of Adc-FLAG (3c) = 28.9 kDa, MW of Idh-c-Myc (4c) = 39.0 kDa. Act… acetyl-CoA acetyltransferase, Acct… acetate CoA-transferase, Adc… acetoacetate decarboxylase, Idh… isopropanol dehydrogenase

Protein analysis displayed a weak soluble production of the Act-StrepII (1E) at the expected molecular mass of ~41 kDa 4 h after induction (Figure 5-34 A, lane 3). But at the end of cultivation (t = 30 h), Act-StrepII (1E) was nearly equally produced in its soluble and insoluble form (lane 5 & 6).

The other three enzymes were strongly produced even before induction, but mostly detected in the insoluble fraction (Figure 5-34 B, lane 2), apart from the Adc-FLAG (3c) (~29 kDa) being visible in the soluble fraction (lane 1). At 4 h after induction (t = 8 h), Acct-His_{10} (2e) could be detected in the soluble fraction (lane 3) at 25 kDa. At the end of cultivation even Idh-c-Myc (4c) was strongly present in its soluble form at ~39 kDa (lane 5). In comparison to the strain with the intact pta gene (Figure 5-19, page 97), the first and last enzyme could now be produced in a more soluble form, at least towards the end of the cultivation.

Gasstripping with liquid nitrogen/CT (see 5.5.2, Figure 5-28, page 107 for device) was applied over the whole cultivation period. Figure 5-35 depicts the accumulating amount of volatile products in the 10 L bioreactor and the CT.

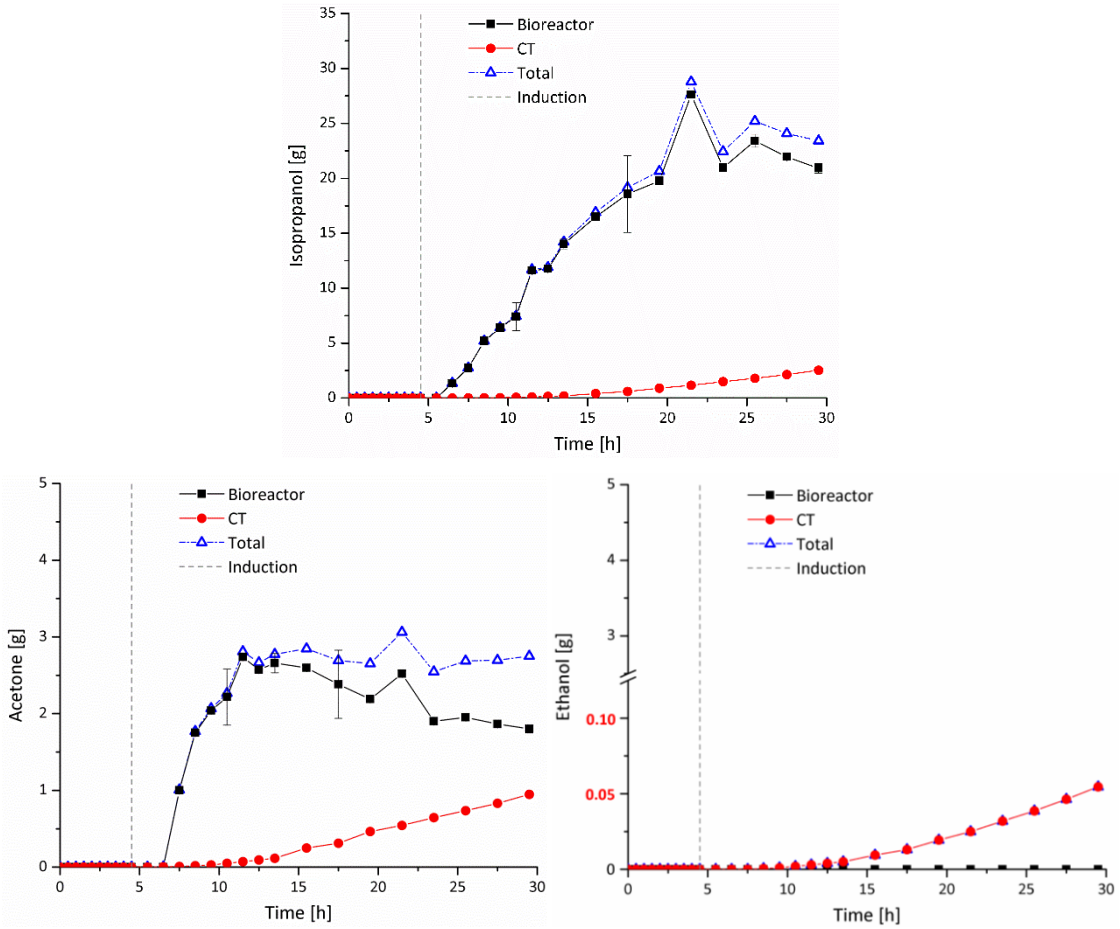

Figure 5-35: Amount of volatile metabolic products in 10 L bioreactor and condensation trap during cultivation of *E. coli* DH5αΔpta_1E in LB plus glucose feed with gasstripping.
Recombinant *E. coli* DH5αΔpta were cultivated in 10 L LB medium containing 2% (w/v) glucose. Pulsed feeding of a 50% (w/v) glucose solution was applied when glucose concentration was below 10 g L^{-1}. Control variables were set to 37 °C, pH 7.0, 0.4 bar, 5 L air min^{-1}, 400 rpm (pO_2 > 25%). Gasstripping with liquid nitrogen (see Figure 5-28 for device) was applied throughout the whole cultivation. Cooled down exhaust gas was diverted to a CT, cooled with liquid nitrogen. Efflux was frozen and collected for 30 min, thawed, weighed and analyzed for product concentration (4.2.3.7). Collection of exhaust gas was repeated in a 2 h interval. GC analysis: Error bars display the standard deviation of n = 3 (technical replicates).
CT… condensation trap

Ethanol could not be detected in the bioreactor itself, while it started to collect in the CT at t = 8 h, accumulating up to 0.05 g after 30 h. Stripping of isopropanol even began before induction (t = 4 h) and eventually increased the total amount of isopropanol by ~12% to 23.43 g. Acetone efflux commenced in concert with isopropanol, before detection in the bioreactor, and raised the total amount of generated acetone to 2.75 g at the end of cultivation. Assumed that all products were captured by the gasstripping device, this depicts an increase by ~53% compared to 1.80 g acetone in the bioreactor. This means that, while the actual "loss" of isopropanol by aeration was small, a relatively high percentage of the produced acetone was stripped from the bioreactor before it could be converted to isopropanol (compare discussion in 6.4, page 141).

Online measurement of O_2 and CO_2 in the reactor exhaust gas (see 4.2.3.8, page 64 for method and calculations) was performed in a 2 h interval for a 1.5 h period, while gasstripping was turned off. Carbon dioxide production rate (CPR), oxygen uptake rate (OUR) and the respiratory quotient (RQ) were calculated accordingly and displayed in Figure 5-36, along with the specific growth rate µ of *E. coli* DH5αΔpta_1E.

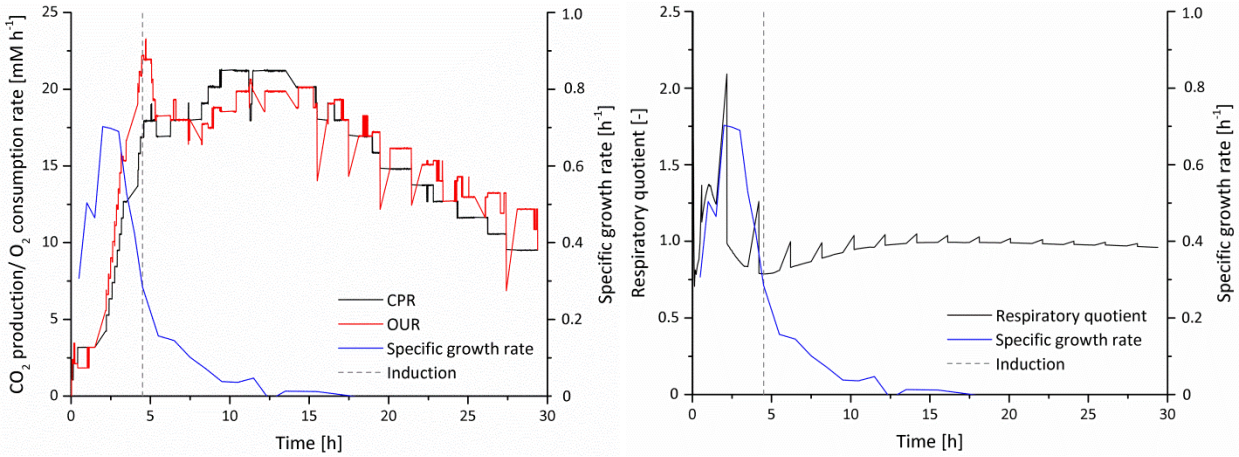

Figure 5-36: Carbon dioxide production rate, oxygen uptake rate and respiratory quotient of *E. coli* DH5αΔpta_1E in LB plus glucose feed in 10 L bioreactor scale.

Recombinant *E. coli* DH5αΔpta were cultivated in 10 L LB medium containing 2% (w/v) glucose. Pulsed feeding of a 50% (w/v) glucose solution was applied when glucose concentration was below 10 g L^{-1}. Control variables were set to 37 °C, pH 7.0, 0.4 bar, 5 L air min^{-1}, 400 rpm (pO_2 > 25%). Online measurement of O_2 and CO_2 in reactor exhaust gas (4.2.3.8) was performed in a 2 h interval for 1.5 h, while gasstripping was turned off. Production/consumption rates and respiratory quotients were calculated according to equations in 4.2.3.8.
CPR… carbon dioxide production rate, OUR… oxygen uptake rate, RQ… respiratory quotient

OUR and CPR rose steeply with increasing µ in exponential phase. Growth rate peaked shortly before the point of induction (t = 4.5 h) and steadily declined afterwards. OUR reached a peak of highest consumption of 23.2 mM O_2 h^{-1} at t = 4.7 h and continued on a fluctuating plateau for the next ~10 h and decreased towards the end of cultivation. CPR was highest between 9.5-13.5 h (21.2 mM CO_2 h^{-1}), and displayed a constant descent afterwards, when µ oscillated around zero. *E. coli* DH5αΔpta_1E consumed a total of 3.817 mol O_2 over a period of 24 h (0.254 g L^{-1} h^{-1}), and generated 3.738 mol CO_2 (0.685 g L^{-1} h^{-1}) in the same time, yielding an RQ of 0.979. RQ was highest in exponential phase with a peak at t = 2.2 h and an RQ = 2.092. Then, RQ dropped to its lowest value of 0.787 at the point of induction, but rose again and stayed around ~1 for the second half of cultivation.

The second Pta-deficient strain, *E. coli* DH5αΔpta_1C, was likewise tested for isopropanol production in 10 L bioreactor scale in LB with glucose feed. Figure 5-37 depicts the growth behavior, glucose consumption and product formation of *E. coli* DH5αΔpta_1C.

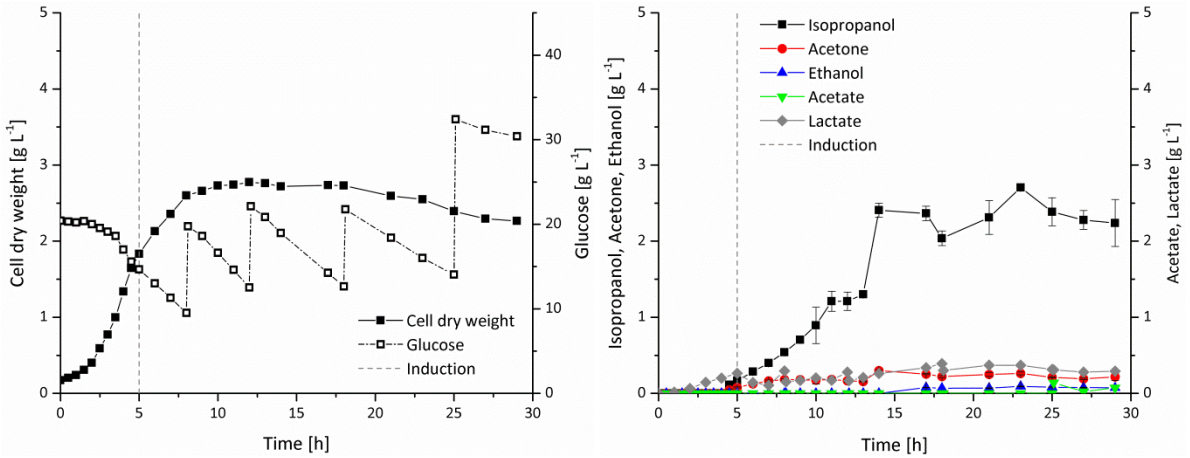

Figure 5-37: Growth, glucose consumption and product formation of *E. coli* DH5αΔpta_1C in LB plus glucose feed in 10 L bioreactor scale.

Recombinant *E. coli* DH5αΔpta were cultivated in 10 L LB medium containing 2% (w/v) glucose. Pulsed feeding of a 50% (w/v) glucose solution was applied when glucose concentration was below 10 g L^{-1}. Control variables were set to 37 °C, pH 7.0, 0.4 bar, 5 L air min^{-1}, 400 rpm (pO_2 > 25%). Induction was performed at OD_{600} ~6.0 with 0.1 mM IPTG. Samples were taken at intervals for determination of cell concentration, glucose consumption, protein and product analysis. Cell dry weight was calculated from OD_{600} according to 4.2.4.3. GC analysis: Error bars display the standard deviation of n = 3 (technical replicates).

E. coli DH5αΔpta_1C achieved a μ_{max} of 0.5 h^{-1} and a doubling time of 1.3 h in exponential phase, equal to the first Pta-deficient strain. But stationary phase was reached with a ~20% lower maximal cell dry weight x_{max} of 2.8 g L^{-1} after 12 h. The overall volumetric glucose consumption rate P_S was 1.412 g L^{-1} h^{-1} after 24 h. Isopropanol was detected even 0.5 h before induction (t = 4.5 h) and gradually increased to 2.7 g L^{-1} at t = 23 h, the highest isopropanol concentration achieved so far in 10 L bioreactor scale. Acetone was first detected at the time of induction and reached a concentration of 0.2 g L^{-1} after 29 h. Acetate production was first observed after 25 h and only reached a maximum of 0.1 g L^{-1} after 29 h. Lactate and ethanol concentrations stayed below 0.4 and 0.1 g L^{-1} throughout the cultivation. Time course of control variables and base addition was comparable to the equivalent cultivation of the non-Pta-deficient *E. coli* DH5α_1C (see Appendix Figure A-10, page 195). Table 5-16 summarizes the product formation parameters of *E. coli* DH5αΔpta_1C in 10 L bioreactor scale after 24 h.

Table 5-16: Product formation parameters of *E. coli* DH5αΔpta_1C after 24 h in LB plus glucose feed in 10 L bioreactor scale.

Product yields were calculated according to 4.2.4.3 (page 66), Equation 4-23, Equation 4-21, Equation 4-22. Product productivities were calculated according to Equation 4-24, Equation 4-25.

p_{max}… product concentration, $Y_{P/X}$… product yield (biomass-related), $Y_{P/S}$… product yield (from substrate), P_P... volumetric productivity, Q_P… specific productivity (biomass-related)

Product	p_{max} [g L^{-1}]	$Y_{P/X}$ [g g^{-1} biomass]	$Y_{P/S}$ [mol mol^{-1} glucose][a]	$Y_{P/S}$ [mol%][a]	P_P [g L^{-1} h^{-1}]	Q_P [g g^{-1} biomass h^{-1}]
Isopropanol	2.39	1.065	0.203	20.3	0.095	0.040
Acetone	0.21	0.094	0.018	1.8	0.008	0.004
Ethanol	0.08	0.036	0.009	0.9	0.003	0.001
Acetate	0.00	0.000	0.000	0.0	0.000	0.000
Lactate	0.31	0.139	0.018	1.8	0.012	0.005
Biomass	2.39		0.113	11.3	0.089	

[a] For calculation purposes, glucose is considered the sole carbon source in the medium.

Acetate production was completely abolished during the first 24 h of cultivation. In comparison to the equivalent 10 L cultivation with *E. coli* DH5α_1C (Table 5-10, page 93), substrate-related isopropanol yield $Y_{P/S}$ after 24 h increased by 14.8 mol% to 20.3 mol%. Volumetric isopropanol productivity P_P was increased by a factor of 6 to 0.095 g L^{-1} h^{-1} and biomass-related isopropanol productivity Q_P improved by a factor of 7 to 0.04 g g^{-1} h^{-1}.

Protein analysis displayed comparable results to the first Pta-deficient strain *E. coli* DH5αΔpta_1E for the soluble production of Acct-His_{10} (2e), Adc-FLAG (3c) and Idh-c-Myc (4c) after induction (compare Figure 5-38 B to Figure 5-34 B, page 113). But in contrast to the weak soluble production of Act-StrepII (1E) (Figure 5-34 A), Act-StrepII (1C) was visible at the expected molecular mass of ~43 kDa in its soluble form even before induction (Figure 5-38 A, lane 1) as well as over the whole cultivation period (lane 3 & 5).

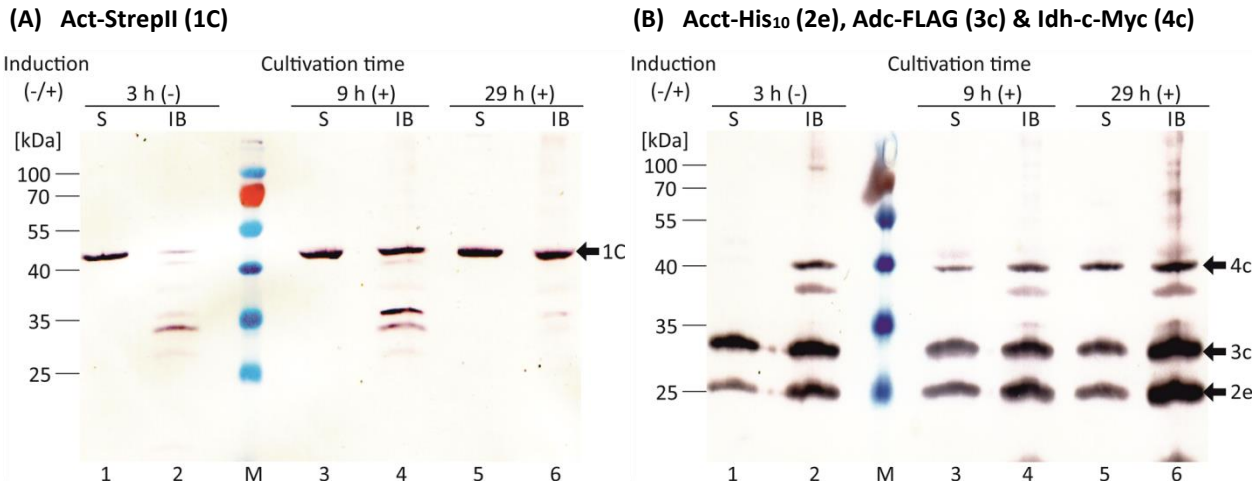

Figure 5-38: Influence of pta disruption on production of Act-StrepII (1C) (A), Acct-His$_{10}$ (2e), Adc-FLAG (3c) & Idh-c-Myc (4c) (B) in *E. coli* DH5αΔpta_1C in LB plus glucose feed in 10 L bioreactor scale.

Recombinant *E. coli* DH5αΔpta were cultivated in 10 L LB medium containing 2% (w/v) glucose. Pulsed feeding of a 50% (w/v) glucose solution was applied when glucose concentration was below 10 g L^{-1}. Control variables were set to 37 °C, pH 7.0, 0.4 bar, 5 L air min^{-1}, 400 rpm (pO_2 > 25%). Induction was performed at OD_{600} ~6.0 with 0.1 mM IPTG. 1/OD samples were taken at intervals, lysed and divided into soluble and insoluble cell extract fraction (4.2.3.2). Extracts were separated by SDS-PAGE and Act-StrepII (1C) was visualized by WB with anti-StrepII®, Acct-His$_{10}$ (2e) with anti-polyHistidine, Adc-FLAG (3c) with anti-FLAG® and Idh-c-Myc (4c) with anti-c-Myc and anti-Mouse IgG-conjugated alkaline phosphatase antibodies (dye: BCIP/NBT) (see Table 4-12 for antibodies).

Lanes with odd numbers display the soluble fraction (S), whereas lanes with even numbers display the insoluble fraction (IB) samples. Arrows indicate the detected proteins. Theoretical molecular protein masses were calculated using ProtParam: MW of Act-StrepII (1C) = 42.5 kDa, MW of Acct-His$_{10}$ (2e) = 24.7 kDa, MW of Adc-FLAG (3c) = 28.9 kDa, MW of Idh-c-Myc (4c) = 39.0 kDa.

Act… acetyl-CoA acetyltransferase, Acct… acetate CoA-transferase, Adc… acetoacetate decarboxylase, Idh… isopropanol dehydrogenase

In comparison to protein analysis of *E. coli* DH5α_1C in 10 L scale (Figure 5-16, page 94), production of the first enzyme seemed similar (compare Figure 5-38 A to Figure 5-16 A). But differences could be observed for Adc-FLAG (3c) (~29 kDa) and Idh-c-Myc (4c) (~39 kDa) (compare Figure 5-38 B to Figure 5-16 B). While Adc-FLAG (3c) was mostly insoluble and Idh-c-Myc (4c) was barely produced in the strain with the intact pta gene, both enzymes were detected in their soluble form in *E. coli* DH5αΔpta_1C after induction. Thus, it can be assumed that the pta knockout exerted a positive influence on gene expression and soluble production of the third and fourth isopropanol pathway enzyme.

In conclusion, disruption of the major acetate pathway Pta-Ack was successfully achieved with an almost complete suppression of acetate production in 10 L bioreactor scale. As a consequence, isopropanol concentration, yield and productivity of recombinant *E. coli* could be increased.

6 Discussion

Primary aim of this work was optimization of the selective isopropanol production by *Escherichia coli*. The research was part of a joint project in the Leading-Edge Cluster "BioEconomy", financed by the Federal Ministry of Education and Research (*Bundesministerium für Bildung und Forschung*, BMBF), to establish a biorefinery platform for the pilot scale production of bio-propene from lignocellulosic feedstock. For this purpose, sufficient quantities of bio-isopropanol as precursor for the conversion to propene should be provided. Focus of this work was set on construction and comparison of isopropanol-producing *E. coli* strains, identification of suitable cultivation conditions and evaluation of a lignocellulose hydrolysate as carbon source for isopropanol production in shake flask scale. Further research concentrated on process scale-up to 10 L bioreactor scale, assessment of an integrated product separation/recovery method and metabolic optimization of the production strain. In the following, realization and investigation of those aspects are discussed in detail and compared with already existing achievements in these fields.

6.1 Comparison of Isopropanol-Producing *E. coli* Strains in Shake Flask Scale

Results presented in chapter 5.1 (page 70) and 5.2 (page 76) are jointly discussed in this chapter to evaluate the combined effect of expression construct design, microbial host and cultivation conditions on isopropanol production by engineered *E. coli* in shake flask scale. In 5.1, the construction of *E. coli* strains with isopropanol-producing abilities was described, including choice of production host, expression vector and isopropanol pathway genes. In 5.2, the resulting strains were tested for their isopropanol production performance on glucose-containing LB medium. Objective was to construct an *E. coli* strain that is able to achieve high isopropanol concentrations. *E. coli* was chosen as host organism, because it meets the specifications of high carbon throughput, flexible oxygen requirements, broad substrate range and easy manipulable genome. The final expression construct (Figure 5-1, page 74) was designed by rational choice of isopropanol pathway genes, antibiotic marker, promoters, detection tags and other vector elements. The genes of interest were codon usage optimized and cloned into a suitably small plasmid. The two final expression vectors were introduced into two different *E. coli* strains, yielding four recombinant *E. coli* strains: DH5α_1E, DH5α_1C, JM109_1E and JM109_1C (Table 5-5, page 75).

In literature, direct comparison of different *E. coli* strains for isopropanol production is not described. But Bermejo et al. and May et al. tested several strains for plasmid-based acetone production and found out that the genetic background and carbon metabolism of the host was crucial for achieving high acetone concentrations [Bermejo et al., 1998; May et al., 2013]. Basically all laboratory and industrial *E. coli* strains are derived from the two so-called wildtypes, *E. coli* B and K-12. Those two strains and their derivatives display major differences in their central carbon metabolism [Phue and Shiloach, 2004] and acetate production [Shiloach et al., 1996]. In the K-12 derivatives, the glyoxylate shunt is inactive due to missing transcription of isocitrate lyase (Icl) and malate synthase (MalS). In addition, pyruvate oxidase (PoxB) transcription is high and acetyl-CoA synthetase (Acs) transcription is low in K-12, while the reverse is true for the B derivatives [Phue and Shiloach, 2004], leading to faster growth, higher cell densities and lower acetate synthesis for the B strains [Shiloach et al., 2010]. The successfully transformed strains DH5α and JM109 are both descendants of *E. coli* K-12. DH5α and JM109 are bacterial strains particularly

developed for cloning purposes. They carry chromosomal mutations of the recA and endA genes, which minimize recombination events of foreign DNA with host DNA, increase the stability of inserts and improve the quality of plasmid isolations. RecA is an *E. coli* protein essential for homologous recombination and DNA repair. The mutated recA1 leaves foreign vector DNA unaltered [Bryant, 1988]. Mutation of the DNA-specific endonuclease I endA (endA1) prevents non-specific DNA degradation, which is part of a bacterial protection mechanism [Bernardi and Cordonnier, 1965]. Additionally, the restriction system of unmethylated DNA is disabled in DH5α and JM109 (genotype: hsdR17 (r_k^-, m_k^+); see Table 4-4, page 41), aiding in incorporation and maintenance of foreign DNA [Palmer and Marinus, 1994].

The four resulting *E. coli* strains were evaluated for isopropanol production from glucose in 100 mL shake flask scale at two different induction temperatures to identify the most suitable host, gene combination and cultivation temperature. Highest isopropanol concentration of 4.4 g L^{-1} was achieved with *E. coli* DH5α_1C at 37 °C after 24 h. Choice of the isopropanol pathway genes, namely the first one, displayed the strongest effect on the production result. The two strains with pRK_ISO_1C2e3c4c and the first gene of clostridial origin were able to generate isopropanol at both induction temperatures, although in varying concentrations (Table 5-7, page 82). For the expression plasmid pRK_ISO_1E2e3c4c with the first gene of *E. coli* origin, only one strain DH5α_1E achieved isopropanol production at 24 °C (0.1 g L^{-1} in 30 h). DH5α_1E at 37 °C and JM109_1E at both temperatures were not able to produce the desired product (Table 5-6, page 78). Thus, the first pathway enzyme seems to be a deciding factor for successful isopropanol production. Results of the isopropanol pathway protein WB analyses can serve as a possible explanation here.

Soluble production of all isopropanol pathway enzymes with pRK_ISO_1E2e3c4c could only be achieved in the isopropanol-producing *E. coli* DH5α_1E at 24 °C and in JM109_1E at 24 °C, although the latter strain did not produce isopropanol. Weak production of the crucial first enzyme might be a reason for this. At 37 °C, solubility of the pathway enzymes decreased in comparison to 24 °C, especially for Act-StrepII (1E) and Idh-c-Myc (4c). Adc-FLAG (3c) seemed to be soluble in both strains and at both induction temperatures. Table 6-1 summarizes the protein detection results for *E. coli* DH5α_1E and JM109_1E at 24 °C and 37 °C (summary of Figure 5-3, page 79 and Figure 5-4, page 80). For the sake of simplicity, the insoluble protein fraction is termed inclusion bodies (in the following denoted as IB).

Table 6-1: Production of isopropanol pathway enzymes in *E. coli* DH5α_1E and JM109_1E at 24 °C and 37 °C in LB medium with 2% (w/v) glucose and 0.1 mM IPTG.
S… soluble production, (S)… weak soluble production, IB… inclusion bodies (only), D… potential degradation

E. coli strain	Temperature [°C]	Act-StrepII (1E)		Acct-His_{10} (2e)	Adc-FLAG (3c)	Idh-c-Myc (4c)
DH5α_1E	24	**S**	D	**S**	**S**	**S**/(S)[2]
	37	IB	D	**S**/(S)[2]	**S**	(S)/IB[2]
JM109_1E	24	(S)	D	(S)	**S**	**S**
	37	-[1]	-[1]	**S**/(S)[2]	**S**	(S)

[1] not detectable, [2] decreasing solubility after induction

For strains with pRK_ISO_1C2e3c4c, protein solubility was investigated only for *E. coli* DH5α_1C at 37 °C. In this case, all four recombinant proteins could be detected in their soluble form (Appendix Figure A-5, page 192). Isopropanol could be detected in all cultivations with pRK_ISO_1C2e3c4c, therefore solubility of the isopropanol pathway proteins can be assumed (at least partly).

Solubility of the isopropanol pathway proteins was investigated here for the first time. It was analyzed by soluble/insoluble fractionation of intracellular proteins, SDS-PAGE and WB (as described in 4.2.3.2., 4.2.3.3, 4.2.3.4) and serves as an indication for the proper folding and functional actitivity of enzymes [Baneyx and Mujacic, 2004]. The method itself has several restrictions with regard to its applicability. First, correct protein detection depends on complete lysis of the *E. coli* cells. Incomplete lysis due to inactivity of the lysis buffer component lysozyme might result in false negative detection results. Cell lysis can either be monitored by microscopy or by carrying along a soluble, peptide-tagged (host) protein as positive control. The latter could also be used confirm the operability of the WB, i.e. the proper protein transfer from PA gel to NCM and the application of suitable antibody concentrations. Protein detection is also dependent on the binding capacity of the NCM and the detection limit of the BCIP/NBT substrate solution. Keeping these restrictions in mind, qualitative and comparative analysis between different cultivation samples is possible.

Protein aggregation is often the result of heterologous gene overexpression by a strong promoter. An accelerated protein synthesis rate can lead to incorrect folding and stronger interaction of hydrophobic protein regions [Kiefhaber et al., 1991]. Lower cultivation temperatures may favor the kinetics of protein folding versus protein aggregation and reduce the concentration of unfolded protein intermediates in the cell [Donovan et al., 1996]. Interestingly, Act-StrepII (1E) was not produced at all in JM109_1E at 37 °C, and only weakly at 24 °C. Act-StrepII (1E) can be considered the most delicate of the enzymes due to its strong tendency for aggregation and degradation. Potential degradation of this enzyme could be observed as a ~23 kDa band in the WB of *E. coli* DH5α_1E at both temperatures and JM109_1E at 24 °C (Figure 5-3, A, B, D, page 79). Act from *E. coli* was already applied once in an enzymatic cascade for isopropanol production by *E. coli*. Although its solubility was not investigated, the enzyme could be considered active, because isopropanol was produced at 37 °C [Hanai et al., 2007]. The enzyme was also implemented into several other artificial metabolic pathways and, while Act seems to perform well at 37 °C in some examples, complex enzymatic cascades involving Act were also expressed at temperatures as low as 18 °C to ensure correct folding and interplay of the proteins [Zhu et al., 2014]. In the present work, besides using a different *E. coli* host and vector/promoter system, Act-StrepII (1E) was encoded by a codon usage optimized version of the gene atoB, which was additionally fused to a C-terminal StrepII tag. Further details about Act-StrepII (1E) degradation are discussed in 6.3 (page 132).

For strains with pRK_ISO_1C2e3c4c, an induction temperature of 37 °C promoted higher isopropanol production compared to cultivation at 24 °C (Table 5-7, page 82). WB analysis of whole cell extracts (Figure 5-7, page 84 and Figure 5-8, page 85) showed that protein production was increased at 37 °C (stronger WB signal). Assuming that the pathway enzymes were (at least partly) soluble, a temperature increase of 13 °C could be expected to accelerate the reaction velocity by a factor of 2-3 (van't Hoff equation). Isopropanol was not generated by the non-transformed strains *E. coli* DH5α and JM109 (Figure 5-5, page 81), illustrating the ability of the recombinant strains to produce the desired product by expression of the isopropanol pathway genes. Comparison of WB protein patterns of recombinant and non-transformed bacteria showed that the previously detected ~35 and ~38 kDa proteins (compare Figure 5-3, page 79, Figure 5-4, page 80, Figure 5-7, page 84, Figure 5-8, page 85) originate from *E. coli* host proteins, because they were also visible in samples of the non-transformed controls. The unique appearance of WB signals at ~40, ~32 and ~28 kDa (Figure 5-7, page 84) for Act-StrepII (1C) in samples of the recombinant cells points towards degradation of the first enzyme. Further details about Act-StrepII (1C) degradation are discussed in 6.3 (page 132).

Interestingly, a ~30 kDa protein was present in samples of non-transformed JM109 that could not be detected in non-transformed DH5α (compare Figure 5-7 A and B, page 84). This protein obviously comprises an anti-StrepII®-like binding epitope and was strongly produced in non-transformed JM109, illustrating a difference on protein level between the two utilized strains. A potential candidate for the protein was identified by protein blast (BLASTp, Table 4-18) as the gene product of yecE (AS: NP_416382.1, 31.5 kDa). The protein features an N-terminal amino acid array, WSHPKWVR, which is similar to the antibody binding region, WSHPQFEK. The gene yecE is mapped in the parental strain of JM109 and DH5α, *E. coli* K-12, and is known as a hot spot for bacteriophage integration and excision [Mellmann et al., 2008; Zhai et al., 2005]. Little details are known about the creation of JM109 and DH5α, but the latter strain might have acquired a disruption of yecE during the process. Unfortunately, a genome sequence of DH5α is not publicly available (Source: NCBI, U.S. National Library of Medicine, Bethesda, MD, USA). Direct comparison of the production performance of both strains displayed that engineered *E. coli* DH5α was generally able to achieve higher isopropanol concentrations than JM109. After 24 h, isopropanol concentration in the medium of DH5α_1C was 33-48% higher compared to JM109_1C (Table 5-7, page 82).

Isopropanol formation in *E. coli* DH5α_1C and JM109_1C was already detected in mid-exponential phase (t = 7 h; Figure 5-5, page 81). The production rate seemed to be coupled to growth, as could be expected from a primary metabolite due to its direct connection to the glycolytic flux. WB analysis revealed the presence of all four isopropanol pathway enzymes (Figure 5-7, page 84, Figure 5-8, page 85) even before induction by IPTG. The employed tac promoter, like all lac-derived promoters, is de-repressed by binding of IPTG to the lac repressor LacI, which is then released from the lac operator site, so that RNA polymerase can bind and initiate transcription [Reznikoff, 1992]. The phenomenon of a “leaky” promoter was often observed for lac-derived strong promoters in complex medium. This basal level of transcription arises from (a) the chemical equilibrium of bound/unbound repressor molecules LacI, and/or (b) from the presence of inducer-like substances in complex medium [Donovan et al., 1996]. LB medium contains yeast extract, which can comprise traces of lactose, which can function as an inducer of transcription [Nair et al., 2009]. Promoter leakiness can be problematic due to entailed growth reduction and/or plasmid instability. It could be alleviated by introduction of a modified lacI gene into the *E. coli* genome ($lacI^q$ phenotype, stronger-binding LacI) or into the expression vector [Glascock and Weickert, 1998].

Marked differences in growth could be observed between non-transformed and isopropanol-producing strains (Figure 5-5, page 81). *E. coli* DH5α_1C and JM109_1C displayed a 2-3fold higher maximal cell density after 48 h compared to their non-recombinant equivalents at the same temperature. This is surprising because recombinant cells usually exhibit a decreased growth due to the metabolic burden associated with plasmid replication and protein production [Bentley et al., 1990]. In addition, *E. coli* DH5α_1C achieved a ~2fold higher maximal cell density than JM109_1C at the same temperature. These growth differences might be associated with 4-6fold increased acetate production for JM109_1C and non-transformed strains in comparison to DH5α_1C (Figure 5-6, page 83). Growth retardation and entry into stationary phase is often the result of the presence of an inhibitory metabolic product [Luli and Strohl, 1990; Shimizu et al., 1988] and/or the depletion of an essential nutrient [Monod, 1949]. Organic acids are known to impair protein production, especially when present at the point of induction [Aristidou et al., 1995; Jensen and Carlsen, 1990; Kim and Cha, 2003; Kim et al., 2015b]. Acetate is a known inhibitor of cellular functions [Koh et al., 1992; Luli and Strohl, 1990] and, in this special case, also a competitor for the isopropanol precursor acetyl-CoA (Figure 2-5, page 23). For engineered acetone-

producing *E. coli* strains, Bermejo et al. and May et al. observed that higher acetone generation was in most cases linked to higher growth and lower acetate excretion [Bermejo et al., 1998; May et al., 2013]. Jojima et al. reported that isopropanol-producing *E. coli* generated less acetate and consumed more glucose in comparison to the control strain [Jojima et al., 2008]. It can be assumed that strains like DH5α_1C, which are able to divert the carbon flux towards acetone/isopropanol instead of acetate formation, are advantageous for establishment of an isopropanol production process.

Stagnation of isopropanol production was observed for *E. coli* JM109_1C and DH5α_1C at both induction temperatures after 24-30 h of cultivation, except for DH5α_1C at 24 °C (Figure 5-5, page 81). This phenomenon was already described for isopropanol-producing *E. coli* by other researchers [Inokuma et al., 2010; Jojima et al., 2008]. It was suggested that termination of production in stationary phase might be the result of nutrient limitation. Inokuma et al. tried to overcome this limitation by repeated addition of concentrated SD-8 medium and achieved a prolonged isopropanol production for up to 240 h [Inokuma et al., 2010]. In the present work, isopropanol production continued solely for DH5α_1C at 24 °C, which correlates with its sustained growth until the end of cultivation.

Accumulation of acetone in the cultivation medium of all recombinant strains (except for JM109_1C at 24 °C; Figure 5-6, page 83) indicates an insufficient catalytic activity of the fourth enzyme Idh-c-Myc (4c). Potential explanations could be insolubility of the enzyme (Figure 5-4, page 80) or depletion of cofactor NADPH required for the reaction. SUMOylation of Idh-c-Myc (4c) did not achieve the desired increase in solubility and activity of the enzyme, but rather displayed a detrimental effect on isopropanol synthesis. Application of fusion tags often improves folding, solubility and/or stability of difficult-to-produce proteins [Marblestone et al., 2006]. But suitability of a fusion tag can only be determined empirically. Alternative fusion motifs to SUMO could be e.g. glutathione S-transferase (GST), thioredoxin (TRX) or NusA. Solubility of enzymes could be supported by coexpression of chaperone or foldase genes [Carvalho and Meneghini, 2008; Ikura et al., 2002; Nishihara et al., 1998]. The cofactor NADPH is mainly generated via the oxidative pentose phosphate pathway enzymes glucose-6-phosphate dehydrogenase (G6PDH, EC 1.1.1.49) and 6-phosphogluconate dehydrogenase (6PGDH, EC 1.1.1.44), but also via the TCA cycle enzyme isocitrate dehydrogenase (IDH, EC 1.1.1.42) and several others (malic enzyme, pyridine nucleotide transhydrogenases) [Spaans et al., 2015]. During maintenance metabolism of non-growing cells in carbon-excess stationary phase, the glycolytic flux (i.e. glucose uptake rate) and NADPH production are observed to be quickly reduced and tend to be an order of magnitude lower than during exponential phase [Chubukov and Sauer, 2014]. Uncoupling of isopropanol synthesis from NADPH generation might thus be beneficial for a sustained production process. Korkhin et al. suggested an amino acid substitution of G198D, Y218F, S199G and R200G in Idh (*C. beijerinckii*) to shift cofactor preference from NADPH to NADH. Production of NADH was not found to be reduced as drastically as synthesis of NADPH in stationary phase [Dhamdhere and Zgurskaya, 2010]. Despite the slightly lower redox potential of NADH (E'_0 (NADH) = -0.320 V, E'_0 (NADPH) = -0.324 V), this might render NADH a more suitable cofactor for acetone conversion. Alternatively, co-overexpression of an NADPH-generating enzyme like G6PDH or PntAB (*E. coli* transhydrogenase) might aid in replenishing the cellular NADPH pool [Cui et al., 2014].

Utilization of different isoenzymes for problematic proteins of the isopropanol cascade might be an alternative to enzyme optimization. Table 6-2 lists a selection of isoenzymes, which have not, but could be applied for recombinant isopropanol production in *E. coli*.

Table 6-2: Alternative isoenzymes for recombinant isopropanol production in *E. coli*.

Enzyme	Gene	Organism	Features	Reference
Alternative to Act				
Act[a]	Acat1	*R. norvegicus*	1/44 K_M (acetyl-CoA) of Act (*C. acetobutylicum*)	[Huth et al., 1974]
Acc & NphT7[b]	acc & nphT7	*S. elongatus* *Streptomyces* sp.	ATP/CO_2-driven alternative reaction via malonyl-CoA	[Lan and Liao, 2012]
Alternative to Acct				
YbgC[c]	ybgC	*H. influenzae*	Acyl-CoA thioesterase (H_2O instead of acetate as 2nd substrate)	[May et al., 2013]
Alternative to Adc				
Adc[d]	adc	*C. violaceum*	2fold k_{cat}[f] of Adc (*C. acetobutylicum*)	[Ho et al., 2009]
Alternative to Idh				
Idh[e]	ADH1	*E. histolytica*	1/50 K_M (acetone) & 27fold k_{cat}/K_M[g] of Idh (*C. beijerinckii*)	[Kumar et al., 1992]

[a] UniProt accession number P17764, [b] UniProt accession number ACCA_SYNE7/ACCD_SYNE7 and D7URV0, [c] UniProt accession number P44679, [d] UniProt accession number A6M020, [e] UniProt accession number P35630, [f] turnover number, [g] catalytic efficiency

One interesting approach would be substitution of the thermodynamically unfavorable Act-mediated acetyl-CoA condensation with the ATP-driven malonyl-CoA synthesis, followed by the decarboxylative condensation with acetyl-CoA to acetoacetyl-CoA. Both reactions are irreversible due to hydrolysis of ATP in the first step and removal of CO_2 in the second step. By substituting Act (*E. coli* atoB gene) with an acetyl-CoA carboxylase Acc (*S. elongatus* PCC 7942) and acetoacetyl-CoA synthase NphT7 (*Streptomyces* sp. strain CL190), Lan et al. could successfully achieve a ~4fold increase in 1-butanol production by recombinant cyanobacteria [Lan and Liao, 2012]. A potential alternative for the *C. beijerinckii* Idh might be the isoenzyme from *E. histolytica* with its high affinity for acetone (0.02 vs. 0.98 mM for *C. beijerinckii* Idh) [Kumar et al., 1992]. Enzyme optimization or pathway variation, as described above, could be a suitable means to improve isopropanol production, although it was not in the focus and could not be realized within the scope of this work.

Design of an artificial multi-enzyme cascade for acetone/isopropanol production by *E. coli* has been attempted by several researchers. Table 6-3 lists the published expression constructs for isopropanol/acetone production by *E. coli* including production hosts, cultivation media, achieved isopropanol/acetone concentrations and cultivation times. The suitability of the different approaches in comparison to the ones implemented here will be discussed in the following.

Table 6-3: Comparison of expression construct designs for isopropanol (and acetone) production by *E. coli* in shake flask scale.
Origin of genes denoted by color code: *E. coli*, *C. acetobutylicum*, *C. beijerinckii*, *T. brockii*, *B. subtilis*, *H. influenzae*.
Red rectangle marks direct comparison of expression constructs. Blue rectangle marks isopropanol concentrations used for calculation of isopropanol production parameters in Table 6-4.
Glucose was used as carbon source in all experiments. If not otherwise denoted, induction temperature was 37 °C.

Genes	Promoter(s)	Vector(s)	Codon opt.	Strain	Medium	Isopropanol [g L^{-1}]	Time [h]	Reference
thlA-atoDA-adc adh [a]	2 × $P_L$lacO$_1$	pSA40, pZA31-luc	adh	B + lacI^{q} [n]	SD-8	1.1 [f g]	31	[Hanai et al., 2007]
thlA-ctfAB-adc adh [a]	2 × $P_L$lacO$_1$	pSA40, pZA31-luc	adh	B + lacI^{q} [n]	SD-8	2.3 [f g]	31	
atoB-ctfAB-adc adh [a]	2 × $P_L$lacO$_1$	pSA40, pZA31-luc	adh	B + lacI^{q} [n]	SD-8	2.3 [f g]	31	
atoB-atoDA-adc adh [a]	2 × $P_L$lacO$_1$	pSA40, pZA31-luc	adh	B + lacI^{q} [n]	SD-8	2.6 [f g]	31	
thlA-atoDA-adc adh [a]	2 × $P_L$lacO$_1$	pSA40, pZA31-luc	adh	B + lacI^{q} [n]	SD-8	2.8 [f g] - 4.9 [f]	31	
(see above)					SD-8 [k]	14.7	48	[Inokuma et al., 2010]
(see above)					SD-8 + pH [k]	40.1	60	
thlA-ctfAB-adc- adh	4 × tac	pCRC200	No	JM109	SD-8	13.6	35	[Jojima et al., 2008]
thlA-atoDA-adc-adh	$P_L$lacO$_1$	pSA40	adh	B + lacI^{q} [n]	SD-8 [k]	5.2	18	[Soma et al., 2012]
thlA-atoDA-adc-adh	P_{lux}lacO	pSA40	adh	BW25113	M9/cas. [k l]	3.9 [h]	42	[Soma and Hanai, 2015]
thlA- ctfAB- adc-adh	J23119 [d]	pRS426 [i]	All genes	BW25113	SD-8 + pH	5.6	48	[Liang et al., 2017]
(see above)		pBR322 [j]			SD-8 + pH	8.6	48	
(see above)		pACYC184 [e]			SD-8 + pH	11.6	48	
thlA-atoDA- adc-adh	J23119 [d]	pRS426 [i]	All genes	BW25113	SD-8 + pH	7.5	48	
(see above)		pBR322 [j]			SD-8 + pH	10.8	48	
(see above)		pACYC184 [e]			SD-8 + pH	13.5	48	
(see above)		Integration			SD-8 + pH	6.5 [g]	48	
atoB-atoDA-adc-adh	4 × tac	pHSG299	All genes	DH5α	LB	0.0	24	**This work**
(see above)				JM109	LB	0.0	24	
thlA-atoDA-adc-adh	4 × tac	pHSG299	All genes	DH5α	LB	4.4	24	
(see above)				JM109	LB	3.0	24	
thlA-ctfAB-adc	thl	pUC19	No	B	SD-8 + pH [m]	5.4 (acetone)	31	[Bermejo et al., 1998]
thlA-ctfAB-adc	lac	pUC19	No	HB101	LB	2.8 (acetone)	24	[May et al., 2013]
thlA-srfAD [b] -adc	lac	pUC19	No	HB101	LB	0.9 (acetone)	24	
thlA-ybgC [c] -adc	lac	pUC19	No	HB101	LB	2.6 (acetone)	24	

[a] adh was expressed from a second vector, [b] UniProt accession number Q08788, [c] UniProt accession number P44679, [d] strong constitutive promoter, [e] low copy number plasmid (p15A ori), [f] with glucose depletion, [g] estimates taken from figures, [h] 0.05 mM IPTG, [i] high copy number plasmid, [j] medium copy number plasmid, [k] 30 °C induction temperature, [l] addition of casamino acids, [m] addition of magnesium and trace elements, [n] modified lacI gene in *E. coli* genome (lacI^{q} phenotype, stronger-binding LacI)

Choosing the most suitable expression construct from the ones presented in Table 6-3 is a difficult task. Many variables like host choice, cultivation medium, addition of supplements and pH regulation can influence the production outcome and a side-by-side comparison of all factors under exactly the same conditions is not available. But wherever the gene combination was varied and compared directly (red rectangle in Table 6-3), while all other parameters were held constant (same promoter(s), vector(s), strain, medium), isopropanol concentrations were highest for the use of these five genes: thlA (*C. acetobutylicum*), atoDA (*E. coli*), adc (*C. acetobutylicum*) and adh (*C. beijerinckii*) [Hanai et al., 2007; Liang et al., 2017]. This gene combination also turned out to be the most suitable one for isopropanol production in shake flask in the present work. Implementation of atoB (*E. coli*) for the first gene, ctfAB (*C. acetobutylicum*) for the second/third gene and adh (*T. brockii*) for the fifth gene resulted in lower isopropanol concentrations within the same time. Interestingly and in contrast to the results obtained with pRK_ISO_1E2e3c4c, Hanai et al. achieved only slightly lower isopropanol concentrations for the use of atoB (*E. coli*) instead of thlA (*C. acetobutylicum*) (2.6 vs. 2.8 g L^{-1}). A reason for the different results cannot be deduced from the available information, since WB analysis for the isopropanol pathway enzymes was first performed in the present work. Fusion of peptide tags to the isopropanol pathway proteins offered the possibility to track enzyme production profiles and to detect potential protein degradation. May et al. evaluated a possible alternative for the second/third gene, although in the context of acetone production by *E. coli*. The gene products of srfAD (*B. subtilis*) and ybgC (*H. influenzae*) are thioesterases and assumed to hydrolyze acetoacetyl-CoA to acetoacetate [Zhuang et al., 2002]. Implementation of ybgC (*H. influenzae*) generated similar acetone concentrations compared to ctfAB (*C. acetobutylicum*) (2.6 vs. 2.8 g L^{-1}), while srfAD (*B. subtilis*) only achieved 0.9 g L^{-1} acetone [May et al., 2013].

Most expression constructs for isopropanol production were designed as polycistronic systems, i.e. gene expression of multiple open reading frames (ORFs) by a single promoter [Bermejo et al., 1998; Liang et al., 2017; May et al., 2013; Soma and Hanai, 2015; Soma et al., 2012]. In contrast, only Jojima et al. chose a monocistronic system with an individual tac promotor for each gene [Jojima et al., 2008]. A special case is the bicistronic system of Hanai et al., which harbors the acetone pathway genes in an operon on one plasmid, while adh was placed on a second plasmid under control of a second promoter [Hanai et al., 2007]. The polycistronic system yields an mRNA that encodes for two or more proteins and is characteristic for prokaryotic organisms. A polycistronic mRNA would result in equal mRNA stability for all transcription products. Monocistronic mRNA only codes for one protein and is usually found in eukaryotic organisms, but also in the original biosynthetic acetone pathway of *C. acetobutylicum* ATCC 824 [Gerischer and Durre, 1990; Petersen et al., 1993]. Recent findings (not available at the time of construct design) suggest that ctfAB and adc of *C. beijerinckii* DSM 6423 are under the control of the same promoter, while thlA and adh are expressed by different promoters [de Gerando et al., 2018]. Comparison of isopropanol production parameters of selected expression constructs in *E. coli*, as depicted in Table 6-4 (page 128), revealed that the monocistronic expression construct of Jojima et al. scored best in biomass-related isopropanol productivity Q_P and volumetric productivity P_P (without pH control). Therefore, the expression constructs of the present work were designed accordingly as monocistronic systems. Unfortunately, the resulting strains did not achieve the same volumetric productivity as Jojima et al., but this could also be attributed to other factors (strain, medium etc.). Genomic integration of the biosynthetic isopropanol pathway genes into *E. coli* via CRISPR/Cas9 was performed by Liang et al., but isopropanol concentrations were halved in comparison to the plasmid-based approach (see Table 6-3). The authors suggested a link between lower production and lower gene expression levels. Optimization of ribosome binding sites by CRISPR EnAbled Trackable genome

Engineering (CREATE) increased isopropanol concentrations by 82% (compared to the initial integration approach) [Liang et al., 2017].

IPTG-inducible promoters were mostly utilized for isopropanol gene expression, except in the constructs of Liang et al. that featured a synthetic constitutive promoter [Liang et al., 2017]. Constitutive promoters can be considered more economical in industrial scale production due to omission of a costly inducer, but can also negatively affect cell growth or plamid stability. Direct comparison of different low, medium and high copy number vectors was performed by Liang et al. and evinced that application of a low copy number plasmid was beneficial for isopropanol production [Liang et al., 2017]. Codon usage optimization of the pathway genes was mostly performed on adh (*C. beijerinckii*) only [Hanai et al., 2007; Soma and Hanai, 2015; Soma et al., 2012]. Liang et al. applied codon usage optimization for all genes, even for the *E. coli*-derived atoDA [Liang et al., 2017]. Unfortunately, no direct comparison between codon-usage optimized genes and their non-optimized equivalents for recombinant isopropanol production is available. Therefore, the benefit of gene optimization in this case cannot be discussed here. Further details about optimization of the atoB and thlA genes are illustrated in 6.3 (page 132).

Selection of production host, medium, addition of supplements, pH regulation and cultivation conditions can have major impacts on isopropanol production, as already described in this work for the use of two different *E. coli* strains and induction temperatures. In literature, cultivations were mostly performed at 37 °C. Three publications described cultivation at 30 °C, but they did not state a reason or show a comparison to other temperatures [Inokuma et al., 2010; Soma and Hanai, 2015; Soma et al., 2012], so that the benefit of temperature decrease cannot be assessed. SD-8 was mostly used as cultivation medium, in contrast to the LB medium utilized in this work. With SD-8, most publications report strikingly higher cell densities for their isopropanol-generating strains with OD_{600} values at ~15 [Liang et al., 2017], ~25 [Soma et al., 2012] and ~30 [Hanai et al., 2007]. On LB, *E. coli* DH5α_1C reached an OD_{600} of ~8, which is in accordance with the OD_{600} = 10 obtained by May et al. for acetone production on LB [May et al., 2013]. SD-8 is a yeast extract-fortified semi-defined medium that exerts a pH buffering effect by KH_2PO_4/Na_2HPO_4. It contains a defined amount of nitrogen in the form of NH_4Cl and double the amount of yeast extract (5 vs. 10 g L^{-1}) compared to LB medium. Inokuma et al. observed that additional control of pH drastically increased isopropanol concentrations and volumetric productivity (0.306 vs. 0.668 g L h^{-1}; Table 6-4, page 128) [Inokuma et al., 2010]. It can be concluded that an increased supply of nutrients and pH buffering by SD-8 medium as well as additional pH regulation exerts a beneficial effect on isopropanol production.

Besides product concentration p_{max} and volumetric productivity P_P, biomass-related yield $Y_{P/X}$ and productivity Q_P as well as product yield from glucose $Y_{P/S}$ are important parameters for evaluation of a biotechnological process. Concentration and volumetric productivity describe the final obtained product concentration and the rate of its production as a direct measure of the production capability. In contrast, biomass-related yield $Y_{P/X}$ and productivity Q_P provide information on the performance of the production organism by stating the amount of product achieved per amount of available biomass (per hour). Product yield from glucose $Y_{P/S}$ allows an estimation of process economy and selectivity. As can be deduced from the isopropanol production pathway (Figure 2-5, page 23), maximum theoretical yield $Y_{P/S}$ from 1 mol glucose is 1 mol isopropanol ($Y_{P/S}$ = 100 mol% or 0.33 g g^{-1}) under ideal conditions. In the best case, all production parameters would be as high as possible, but in a real process, substrate-related yield cannot be 100 mol%, because the production host also requires carbon source for biomass generation and maintenance. A balance between biomass production, glucose consumption and

isopropanol synthesis is crucial for a successful process, because a higher number of cells produce more of the desired product, but also consume more substrate.

Table 6-4: Isopropanol production parameters of selected expression constructs in engineered *E. coli* on glucose.
Marked (blue rectangle) isopropanol concentrations of Table 6-3 (page 125) were used for calculation of isopropanol production parameters. Isopropanol yields were calculated according to 4.2.4.3 (page 66), Equation 4-23, Equation 4-21, Equation 4-22. Isopropanol productivities were calculated according to Equation 4-24, Equation 4-25.
p_{max}… product concentration, P_P... volumetric productivity, $Y_{P/X}$… product yield (biomass-related), Q_P… specific productivity (biomass-related), $Y_{P/S}$… product yield (from substrate)

p_{max} [g L^{-1}]	P_P [g L^{-1} h^{-1}]	$Y_{P/X}$ [g g^{-1} biomass]	Q_P [g g^{-1} biomass h^{-1}]	$Y_{P/S}$ [mol%][a]	Reference
4.9[c]	0.161[b c]	0.935[b c]	0.031[b c]	36.8[c]	[Hanai et al., 2007]
14.7	0.306	**2.008[b]**	0.042[b]	23.3[b]	[Inokuma et al., 2010]
40.1[d]	**0.668**	1.114[b]	0.019[b]	**74.1[b]**	[Inokuma et al., 2010]
13.6	**0.389**	**2.386**	**0.066**	**50.3**	[Jojima et al., 2008]
5.2	0.248	0.642	0.031	34.6[b]	[Soma et al., 2012]
3.9	0.093	0.056[b]	0.001[b]	**59.0[b]**	[Soma and Hanai, 2015]
13.5[d]	0.281	**3.169**	**0.066**	**67.5**	[Liang et al., 2017]
4.4	0.181	**1.794**	**0.072**	**58.7**	**This work (DH5α_1C)**
3.0	0.122	**2.498**	**0.098**	**54.7**	**This work (JM109_1C)**

[a] For calculation purposes, glucose is considered the sole carbon source in the medium, [b] estimates taken from figures for calculation, [c] with glucose depletion, [d] pH control

Although *E. coli* DH5α_1C and JM109_1C at 37 °C did not achieve highest isopropanol concentrations and volumetric productivities compared to the literature (Table 6-4), they scored best in biomass-related productivity Q_P, showing their production potential. In addition, both strains were able to keep up with literature values for isopropanol yield from glucose $Y_{P/S}$ (without pH regulation), displaying a good selectivity for the desired product. It can be concluded that *E. coli* DH5α_1C is a suitable candidate for selective isopropanol production and that identified cultivation conditions can be employed in process scale-up.

6.2 Beech Wood Hydrolysate as Carbon Source for Isopropanol-Producing *E. coli* in Shake Flask Scale

Establishment of an economically viable microbial production process requires utilization of a cheap substrate for conversion to the desired product. As described in 2.4 (page 31), lignocellulose hydrolysates gained much attention as feedstock due to the abundance and diversity of the raw material, as well as its renewability and sustainability. As a drawback, lignocellulose has to be pretreated prior to its application as substrate. This pretreatment often causes the formation of inhibitors (Table 2-6, page 35), which are known to exert a detrimental effect on microbial metabolism and can reduce the yield and productivity of a production process [Joensson et al., 2013].

In the present work, a lignocellulose hydrolysate from beech wood was evaluated for the first time as carbon source for isopropanol production by engineered *E. coli*. Beech wood is a close-grained, wear-resistant, tough, bendable hardwood timber. In this case, it is derived from the deciduous European beech or common beech (*Fagus sylvatica*). Due to its properties, the wood is frequently used in furniture and carpentry industry as well as for the manufacturing of toys, tool handles and musical instruments. The European beech is widely available across Europe and its abundance and relatively cheap price, together with the massive amount of annual leftovers from the woodworking industry, make it a

favorable candidate to be utilized as renewable feedstock within the conceptual design of a biorefinery platform [Meier]. The glucose fraction of the beech wood hydrolysate (BWH) used in this work was obtained by "Organosolv pulping" (4.1.3, page 40), and mainly comprises D-glucose (381 g L^{-1}) and D-xylose (95 g L^{-1}), but also other constituents like acids (see Table 4-3, page 41) and minerals like Ca, Mg, K, Na, P, S (source: CBP, Leuna, Germany).

In 5.3 (page 86), BWH was tested as an alternative carbon source to glucose for the isopropanol-producing *E. coli* strain DH5α_1C in 100 mL shake flask scale. In minimal medium (MM), isopropanol (or acetone) production could not be detected for BWH- or glucose-grown cells. But growth and glucose consumption of DH5α_1C were comparable on both substrates (Figure 5-9, page 87). Protein analysis revealed that none of the isopropanol pathway proteins could be detected, although presence of the expression vector was confirmed by plasmid isolation and sequencing. Missing isopropanol synthesis in MM for glucose-grown *E. coli* DH5α_1C was surprising, due to the positive results in LB medium (5.2.2, page 81). MM was chosen due to its application in large scale processes as a cheaper and more reproducible option to complex medium. But it is also known that heterologous gene expression in MM is often only achieved by supplementation with either complex compounds like peptone or yeast extract or with various single amino acids [Donovan et al., 1996; Nancib et al., 1991; Ramirez and Bentley, 1993]. In literature, acetone/isopropanol production by engineered *E. coli* was only performed in complex medium [May et al., 2013], yeast extract-fortified semi-defined SD-8 [Bermejo et al., 1998; Hanai et al., 2007; Jojima et al., 2008; Liang et al., 2017; Soma et al., 2012] or M9 mineral medium with casamino acids [Soma and Hanai, 2015] (see Table 6-3, page 125). It can be concluded that isopropanol production by *E. coli* requires certain nutrients, which are not present in the MM used in this work. Optimization of MM by addition of individual nutrients rather than supplementation of a complex source might be able to identify the missing component(s).

In LB medium, isopropanol production was not observed for BWH-grown *E. coli* DH5α_1C, although 0.5 g L^{-1} acetone was produced within 24 h (Figure 5-10, page 88). When different BWH concentrations (mixed with pure glucose) were applied, it could be seen that less isopropanol was produced when more BWH was present in the medium (Figure 5-12, page 89). Also, acetate formation was higher (Figure 5-13, page 90 and Table 5-9, page 91), while acetone production was similar for different BWH concentrations (Figure 5-12). It can be assumed that application of BWH exerts an inhibitory effect on isopropanol production and that acetate formation was promoted instead. The observed acetone production indicates that at least some of the carbon flux was directed into the isopropanol pathway. Thus, absence of isopropanol production might be solely the result of an impaired activity of the fourth enzyme Idh-c-Myc (4c). This can be refuted by plotting the biomass-related acetone and isopropanol productivites Q_P against the applied BWH concentration. Figure 6-1 reveals that the specific acetone productivity only slightly increased, while isopropanol productivity drastically decreased with increasing BWH concentrations.

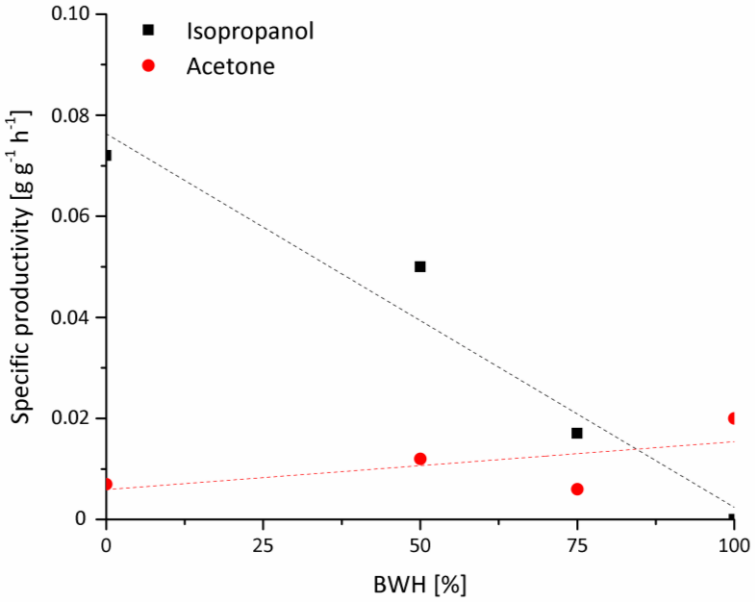

Figure 6-1: Influence of different BWH concentrations on specific isopropanol and acetone productivities of *E. coli* DH5α_1C.
Recombinant *E. coli* DH5α were inoculated to an OD_{600} = 0.1 in 100 mL LB containing 2% (w/v) glucose from 0% (pure glucose), 50%, 75%, 100% BWH, which was replenished if necessary. Cultures were grown at 37 °C, 100 rpm. Induction was performed by addition of 0.1 mM IPTG at OD_{600} = 0.5 - 0.6. Samples were taken at intervals for determination of cell concentration, glucose consumption and product analysis. Linear fit is depicted as dotted lines.

If the acetone pathway was not compromised, acetone productivity would increase more drastically with increasing BWH concentrations due to acetone accumulation and an impaired activity of Idh-c-Myc (4c). This finding indicates that BWH also negatively affects one or more of the acetone-producing reactions. In addition, increasing BWH concentrations caused a lower maximum OD_{600} for *E. coli* DH5α_1C and an earlier onset of stationary phase (Figure 5-11, page 89). Simultaneously, total glucose consumption decreased when more BWH was applied (compare pure glucose: 1.6 g, 50% BWH: 0.5 g, 75% BWH: 0.4 g, 100% BWH: 0.3 g glucose after 24 h). With higher BWH concentrations, the carbon flux seemed to be more readily directed to acetate generation than towards biomass or isopropanol production. This could be explained by inhibition of the TCA cycle and isopropanol pathway enzymes per se and/or by a higher cellular requirement for ATP during stress conditions [Nicolaou et al., 2010]. Acetate synthesis from acetyl-CoA generates one molecule ATP by the action of acetate kinase (Ack, EC 2.7.2.1) of the Pta-Ack pathway. As described in 2.4, lignocellulose hydrolysates can contain a bouquet of pretreatment-derived inbibitors (Table 2-6, page 35), that are able to trigger a plethora of different effects on cellular metabolism, membrane integrity, membrane transport, pH, enzyme activity and more. Thus, it is hard to localize the cellular site(s) of inhibitory action as well as to pinpoint the exact source of inhibition in BWH. Inhibition of the isopropanol pathway enzymes could be investigated by comparison of enzyme activities in the raw extract of BWH- and glucose-grown *E. coli* DH5α_1C. Supplementation of raw extract with the substrates of all four reactions, acetyl-CoA, acetoacetyl-CoA, acetoacetate and acetone, and analysis of the products might identify the most affected enzyme.

BWH was analyzed by HLPC at Fraunhofer CBP (Leuna, Germany) for the presence of selected known inhibitory substances. Interestingly, two of the most common inhibitors, hydroxymethylfurfural (HMF) and furfural, could not be detected in BWH (Table 4-3, page 41). Acetate was found in BWH in a concentration of 7.9 g L^{-1}, yielding a starting concentration of 0.6 g L^{-1} in 100 mL cultivation medium. Extracellular acetate is known to inhibit cell growth [Shimizu et al., 1988] and decreases the pH of the

medium, which might explain the differential growth behavior of *E. coli* DH5α_1C in MM and LB medium. Growth of BWH-grown cells was unaffected in MM (Figure 5-9, page 87), but negatively influenced for higher concentrations of BWH in LB (Figure 5-11, page 89). In contrast to LB, MM contains a buffer (Table 4-19, page 51), which keeps the pH constant over a longer period of cultivation, despite the presence of acids. Isopropanol-producing *E. coli* DH5α_1C in LB with pure glucose might achieve a higher cell density than non-isopropanol-producing *E. coli*, due to the detoxifying effect of acetate re-uptake from the medium for isopropanol production (Acct reaction; Figure 2-7, page 30), as already observed by Bermejo et al. and May et al. [Bermejo et al., 1998; May et al., 2013]. But a high BWH-associated acetate concentration at the beginning of the cultivation (Figure 5-13, page 90), together with a pH decrease, can impair protein production [Aristidou et al., 1995; Kim and Cha, 2003] and prevent isopropanol synthesis. Palmqvist and Hahn-Hagerdal assumed that the large concentration of undissociated weak acids in hydrolysates at low pH is one reason for inhibition of microbial growth and product generation [Palmqvist and Hahn-Hagerdal, 2000a]. Undissociated acids (e.g. pK_a of acetate = 4.75) are liposoluble and can readily diffuse across plasma membranes, subsequently disturbing intracellular pH, membrane proton-motive force and membrane potential [Nicolaou et al., 2010; Palmqvist and Hahn-Hagerdal, 2000b]. When acids cross the plasma membrane, dissociation occurs in the cytosol due to the neutral cellular pH, subsequently decreasing the intracellular pH [Pampulha and Loureiro-Dias, 1989]. As maintenance of a pH of 7.2-7.8 is crucial for enzyme activity and protein and nucleic acid stability of *E. coli* [Russell, 1992; Zilberstein et al., 1984], the cells rapidly adjust their pH by proton efflux, catalyzed by plasma membrane ATPase at the expense of ATP, until the ATP pool is depleted [Viegas and Sa-Correia, 1991; Wilks and Slonczewski, 2007]. Optimal pH for acetone conversion by Idh was reported to be in the range of 7.5-8.0 and rapidly decreasing below and above those values [Ismaiel et al., 1993]. Acidification of the cytosol by anion accumulation due to influx of hydrolysate-associated weak acids [Palmqvist and Hahn-Hagerdal, 2000b], thus might be a reason for the missing conversion. It was also observed that the cellular NADPH pool was diminished by the action of NADPH-dependent detoxification enzymes (oxidoreductases) [Gutierrez et al., 2002; Miller et al., 2009; Perez et al., 2008]. Therefore, cofactor competition might be another reason for potential Idh impairment in the presence of 100% BWH. pH adjustment of BWH prior to its addition to the medium might be able to alleviate the growth- and product-inhibiting effect of BWH.

In literature, hydrolysate-induced inhibition of growth and production for *E. coli* has been reported by several researchers [Mills et al., 2009; Palmqvist and Hahn-Hagerdal, 2000a; Rumbold et al., 2009; Saha and Cotta, 2012]. Liu et al. attributed the inhibitory effect to acetate generation during hydrolysate pretreatment [Liu et al., 2010]. Other researchers investigated the negative impact of different isolated lignocellulose-derived inhibitors on *E. coli*. Table 6-5 (page 132) displays a selection of inhibitors and their critical concentrations for growth of various *E. coli* strains.

Depending on the strain, acetate concentrations as low as 0.5 g L^{-1} can negatively influence cell growth. It has to be kept in mind that growth-inhibiting concentrations of lignocellulose-derived inhibitors, as stated in Table 6-5, do not reflect concentrations that are critical for production of a desired metabolite. In addition, Mussatto and Roberto stated that the individual inhibitors can exert a synergistic effect on *E. coli*, which could not be estimated from the inhibitory concentrations of the single substances [Mussatto and Roberto, 2004]. Purification of BWH did not enable isopropanol synthesis with *E. coli* DH5α_1C. Although e.g. recrystallisation yielded a hydrolysate that was devoid of acetate, it still contained substances that were detrimental for isopropanol production. It should also be considered

that purification in most cases leads to a certain loss of sugars and increases the overall production costs, lowering the economic value of BWH utilization as alternative feedstock.

Table 6-5: Lignocellulose-derived inhibitors and their critical concentrations for different *E. coli* strains.
Critical concentrations for 50% growth inhibition were determined by exposure to a single inhibitory compound.

Inhibitor	Critical concentration [g L^{-1}]	*E. coli* strain	Reference
Weak aliphatic acids			
Acetic acid	0.5	FRAG-1	[Roe et al., 1998]
	5.0	MG1655	[Rumbold et al., 2009]
	9.0	LY01[a]	[Zaldivar and Ingram, 1999]
Formic acid	2.5	LY01[a]	[Zaldivar and Ingram, 1999]
Levulinic acid	7.5	LY01[a]	[Zaldivar and Ingram, 1999]
Furan derivatives			
HMF	2.0	MG1655	[Rumbold et al., 2009]
	2.7	ATCC 1175	[Boopathy et al., 1993]
Furfural	0.5	BL21 (DE3)	[Lee et al., 2012b]
	1.0	MG1655	[Rumbold et al., 2009]
	2.4	LY01[a]	[Zaldivar et al., 1999]
	3.4	ATCC 1175	[Boopathy et al., 1993]
Phenolic compounds			
4-Hydroxybenzaldehyde	0.6	LY01[a]	[Zaldivar et al., 1999]
Vanillin	0.5	LY01[a]	[Zaldivar et al., 1999]
Syringaldehyde	0.6	LY01[a]	[Zaldivar et al., 1999]
4-Hydroxybenzoic acid	0.8	LY01[a]	[Zaldivar and Ingram, 1999]
Vanillic acid	0.5	BL21 (DE3)	[Lee et al., 2012b]
	1.1	LY01[a]	[Zaldivar and Ingram, 1999]
Syringic acid	1.6	LY01[a]	[Zaldivar and Ingram, 1999]

[a] Ethanologenic *E. coli* LY01 is highly tolerant to inhibitors.

6.3 Isopropanol Production from Glucose and Beech Wood Hydrolysate by Engineered *E. coli* in Bioreactor Scale

In this work, scale-up of an isopropanol production process with engineered *E. coli* was demonstrated for the first time (5.4, page 91). In 5.4.1 (page 92), glucose was utilized as carbon source for isopropanol production by *E. coli* DH5α_1C and DH5α_1E in 10 L bioreactor scale. In 5.4.2 (page 98), samples from both strains were analyzed for potential degradation of the first cascade enzyme Act-StrepII (1C/E) by mass spectrometry (MS). In 5.4.3 (page 99), BWH was tested as an alternative carbon source in the feed, after an initial batch phase on pure glucose. In the following, isopropanol production in 10 L bioreactor scale is discussed and compared to the experiments in 100 mL shake flask scale, as well as to published microbial isopropanol production processes in bioreactor scale.

Isopropanol production from glucose in 10 L bioreactor scale was achieved by both *E. coli* DH5α_1C and *E. coli* DH5α_1E, although the latter strain reproducibly reached a ~2fold higher isopropanol concentration after 24 h (0.9 vs. 0.4 g L^{-1}). *E. coli* DH5α_1E also achieved a higher μ_{max} in exponential phase, a prolonged growth phase of 4 h and a higher maximal cell dry weight x_{max} than DH5α_1C (Table 6-6). This is in stark contrast to the shake flask results, which evinced *E. coli* DH5α_1C as the best

isopropanol producer, while *E. coli* DH5α_1E did not synthesize the desired product, at least at 37 °C. Table 6-6 compares growth, glucose consumption and isopropanol formation parameters of *E. coli* DH5α_1C and *E. coli* DH5α_1E in shake flask and bioreactor scale.

Table 6-6: Growth, glucose consumption and isopropanol formation parameters of *E. coli* DH5α_1C and *E. coli* DH5α_1E after 24 h in LB plus feed with glucose in shake flask and bioreactor scale.
Parameters were calculated according to section 4.2.4.3 (page 66).
x_{max}… maximal cell dry weight, μ_{max}… maximal growth rate, P_S… volumetric substrate consumption rate, p_{max}… product concentration, $Y_{P/X}$… product yield (biomass-related), $Y_{P/S}$… product yield (from substrate), P_P... volumetric productivity

E. coli strain	Scale	x_{max} [g L^{-1}]	μ_{max} [h^{-1}]	P_S [g L^{-1} h^{-1}]	p_{max} [g L^{-1}]	$Y_{P/X}$ [g g^{-1} biomass]	$Y_{P/S}$ [mol%][a]	P_P [g L^{-1} h^{-1}]
1C	Flask	2.5	0.6	0.923	4.39	1.794	58.7	0.181
	Bioreactor	2.7	0.5	0.842	0.39	0.150	5.5	0.015
1E	Flask	0.9	0.6	0.226	0.00	0.000	0.0	0.000
	Bioreactor	4.0	0.6	0.808	0.88	0.227	13.4	0.036

[a] For calculation purposes, glucose is considered the sole carbon source in the medium.

In 10 L, *E. coli* DH5α_1E achieved a more than doubled isopropanol yield $Y_{P/S}$ from glucose in comparison to *E. coli* DH5α_1C, although volumetric glucose consumption P_S was in a similar range for both strains. Highest $Y_{P/S}$ in bioreactor scale was still 4.4fold lower than the highest $Y_{P/S}$ obtained in shake flask experiments (13.4 vs. 58.7 mol%), indicating that, in bioreactor scale, carbon flux was directed elsewhere. Higher maximum cell dry weight x_{max} in 10 L correlated with higher isopropanol concentration, as already observed for shake flask scale. In both scales, isopropanol synthesis began 2-3 h after induction in mid/late-exponential phase. It seemed to be connected to growth in a way that a high growth rate entailed a slightly time-delayed high isopropanol production rate. Interestingly, *E. coli* DH5α_1C first started to produce acetone at the point of induction rather than isopropanol in bioreactor scale. This finding could be correlated to weak (and insoluble) production of the Idh-c-Myc (4c) in exponential phase (Figure 5-16, page 94). Table 6-7 shows a comparison of isopropanol pathway enzyme production by *E. coli* DH5α_1C and DH5α_1E in 10 L bioreactor scale (summary of Figure 5-16, page 94 and Figure 5-19, page 97).

Table 6-7: Production of isopropanol pathway enzymes in *E. coli* DH5α_1C and *E. coli* DH5α_1E in LB with glucose as carbon source in 10 L bioreactor scale.
S… soluble production, (S)… weak soluble production, IB… inclusion bodies (only), (IB)… weak inclusion bodies (only), D… potential degradation, (D)… weak potential degradation

E. coli strain	Growth phase	Act-StrepII (1C or 1E)		Acct-His_{10} (2e)	Adc-FLAG (3c)	Idh-c-Myc (4c)
1C	Exponential	**S**	(D)	**S**	(S)	(IB)
	Stationary	**S**	D	**S**	(S)	(S)
1E	Exponential	IB	D	n.d.	n.d.	IB
	Stationary	(S)	D	n.d.	n.d.	(S)

n.d…. not determined

In both strains, Idh-c-Myc (4c) was first produced as IB, but production was strikingly stronger in *E. coli* DH5α_1E over the whole cultivation period, which might be a reason for the higher isopropanol production of this strain in bioreactor scale. For *E. coli* DH5α_1E, isopropanol production began in late exponential phase without detectable levels of acetone in the medium. In shake flask experiments, solubility of Idh-c-Myc (4c) in *E. coli* DH5α_1E was promoted by an induction temperature of 24 °C

(Figure 5-4, page 80). Therefore, a temperature decrease at the point of induction could be a possibility to alleviate enzyme insolubility in bioreactor scale. In contrast to the results in shake flask, soluble production of Adc-FLAG (3c) was hindered in larger scale. Soluble production of the first enzyme was detected for Act-StrepII (1C), while Act-StrepII (1E) in *E. coli* DH5α_1E was mostly detected in its insoluble form, which is in conformity with the WB results in shake flask scale at 37 °C (Figure 5-3, page 79). Potential degradation was observed for both enzymes in shake flask and bioreactor scale and investigated by MS (5.4.2, page 98). For the *E. coli* variant, protein degradation could be unequivocally verified by identification of nine peptides in the 23 kDa cut-out sample, covering the C-terminus of Act-StrepII (1E) (Figure 5-20, page 98). Degradation could not be verified for Act-StrepII (1C), as no peptides covering its amino acid sequence could be detected in the ~28 kDa gel piece sample. One reason might be that degradation did not strongly occur in the 10 L bioreactor cultivation of *E. coli* DH5α_1C, as only a faint band was visible in WB (Figure 5-16 A, page 94). Also, precise excision of the correct band was difficult due to the amount of *E. coli* host proteins in the corresponding PA gel (not shown). Presence of the full-length Act-StrepII (1C) was confirmed in the ~43 kDa sample, while only four peptides could be assigned to Act-StrepII (1E) in the ~41 kDa sample. But sequence coverage and size of those fragments suggest that the full-length enzyme was produced.

In this work, fusion to a C-terminal StrepII tag allowed tracing of Act and detection of degradation for the first time. The corresponding genes atoB and thlA were codon usage optimized to balance GC content and to avoid utilization of rare codons, which would recruit rare tRNAs. Codon usage also impacts gene expression by contributing to mRNA stability and regulation of translational velocity [Presnyak et al., 2015]. Nucleotide change by optimization was 23.5% for atoB and 23.9% for thlA, which might influence mRNA secondary structure. Secondary structure, especially at the 5'-end, plays a crucial role in mRNA stability and can affect accessibility of the ribosome binding site [Jana and Deb, 2005]. In codon usage optimization of the gene sequences, those parameters were considered, resulting in an enhanced mRNA stability of -83.1 kcal mol^{-1} for atoB and of -104.0 kcal mol^{-1} for thlA (minimum free energy optimal secondary structure calculation by RNAfold, Table 4-18; for nucleotide sequences see Table A-2, page 178 & Table A-3, page 182). As mRNA stability and ribosome binding site accessibility were ensured, detection of Act degradation by WB and MS rather points to a regulatory mechanism on protein level.

It is debatable if enzyme degradation, in this case, influences isopropanol production. Continuous enzyme synthesis by IPTG-induced gene expression might balance enzyme degradation. As both strains generate isopropanol in bioreactor scale, activity of the first cascade enzyme should be present. There is a chance that part of the activity also originated from one or more host enzymes. *E. coli* itself harbors two enzymes with acetyl-CoA acetyltransferase (or acetoacetyl-CoA thiolase) activity [Duncombe and Frerman, 1976; Feigenbaum and Schulz, 1975]. While the gene product of fadA (3-ketoacyl-CoA thiolase, Uniprot ID: P21151) has a broad substrate/product specificity including medium- and long-chain fatty acids [Kim et al., 2015a], the gene product of atoB mainly acts on acetoacetyl-CoA. The latter is involved in synthesis or degradation of fatty acids (β-oxidation) and was the model enzyme for Act-StrepII (1E). Native atoB is part of the so-called "acetoacetate degradation operon", which is transcriptionally regulated by an activator, the atoC gene product, in the presence of acetoacetate in the cultivation medium [Jenkins and Nunn, 1987; Mann and Lutke-Eversloh, 2013; Pauli and Overath, 1972]. In the artificial isopropanol production cascade, activation by atoC is substituted by induction via IPTG and thus, should not be a determining factor in gene expression. Nevertheless, it can be reasoned that a non-constitutive, regulated metabolic pathway is subject to de-activation and fast degradation mechanisms, either on mRNA or protein level. Observed degradation of Act-StrepII (1E) suggests the existence of such

a mechanism. Weaker degradation of Act-StrepII (1C) might be associated with its heterologous nature, thus escaping the regulatory machinery of the host organism. But the higher specific activity of the *E. coli* variant in comparison to the clostridial enzyme (1078 vs. 216 U mg^{-1}, Table 5-1, page 72) might compensate for stronger degradation (and higher insolubility) in bioreactor scale. In contrast to shake flask experiments, pH regulation, continuous gassing, pressurization and stirring allowed and facilitated maintenance of aerobiosis, waste gas CO_2 efflux, gas solubility and homogeneity of cells, nutrients, gasses and additives in the bioreactor. These factors might also be reasons for the deviating results of strain performance in both scales.

A typical problem associated with scale-up of a microbial production process using *E. coli* is the formation of acetate in the presence of glucose under aerobic conditions in exponential phase [Bernal et al., 2016; Shimizu et al., 1988]. Here, substrate-related acetate yield $Y_{P/S}$ of isopropanol-producing *E. coli* was observed to be 6 times higher in bioreactor than in shake flask scale (e.g. for *E. coli* DH5α_1C in shake flask: 4.6 mol%, in bioreactor: 27.1 mol%). In contrast, isopropanol yield from glucose rather decreased 5-10fold from small to larger scale. Ethanol and lactate constitute only 0-2 mol% of the substrate-related yields from glucose in both scales. Therefore, acetate must be considered the major product in bioreactor scale, although it has to be kept in mind that not all *E. coli* metabolites were measured (e.g. formate, succinate). Acetate is known to inhibit cell growth [Luli and Strohl, 1990; Shimizu et al., 1988] and to impair the production of recombinant proteins, especially when present at the point of induction [Aristidou et al., 1995; Jensen and Carlsen, 1990; Kim and Cha, 2003; Kim et al., 2015b]. At induction, acetate concentrations were already 1.3-1.7 g L^{-1} in the bioreactor, while in shake flask, they were as low as 0.2 g L^{-1} for isopropanol-producing *E. coli* DH5α_1C. As expected, acetate synthesis correlated with cell growth and generally ceased when the cells reached stationary phase. Therefore, acetate production seems to pose a major problem, although pH regulation in bioreactor scale might alleviate some of the detrimental effects of acid accumulation.

Maximum isopropanol production within 24 h can be estimated from the volumetric glucose uptake rate P_S. Assuming that all glucose is converted to isopropanol, which is 0.33 g g^{-1} in the ideal case, a volumetric isopropanol productivity P_P of 0.267-0.278 g L^{-1} h^{-1} can be expected from a P_S of 0.808-0.842 g L^{-1} h^{-1} in bioreactor scale (Table 6-6, page 133). Here, only 5.5-13.4% of the maximal theoretical value was reached, which equals an isopropanol productivity P_P of 0.015-0.036 g L^{-1} h^{-1} and a yield of 0.02-0.04 g g^{-1} from glucose. After 16 h of production (24 h cultivation period – 8 h before induction), an isopropanol concentration of 4.3-4.4 g L^{-1} should be potentially possible, if a constant P_S and isopropanol production rate after induction were assumed. It should be kept in mind that a yield of 0.33 g g^{-1} is almost impossible in a real biotechnological process, due to the energy and carbon demand of the host organism for biomass generation and maintenance. The generally accepted average biomass yield of *E. coli* grown on glucose is 0.5 g biomass g^{-1} glucose [Shiloach and Fass, 2005]. The ideal yield might be approachable by achieving prolonged isopropanol production in stationary phase and by minimization of by-product formation.

Literature on isopropanol production by non-clostridial organisms in bioreactor scale is scarce. Only one recent publication of Marc et al. deals with larger scale isopropanol synthesis from fructose by *Cupriavidus necator* in a 3 L bioreactor [Marc et al., 2017]. No literature is available for recombinant *E. coli*. Therefore, isopropanol formation parameters of 10 L bioreactor cultivations by *E. coli* DH5α_1C and *E. coli* DH5α_1E on glucose were additionally compared to those of selected recombinant and non-recombinant isopropanol-producing clostridial strains in larger scale (Table 6-8).

Table 6-8: Isopropanol production parameters of recombinant and natural isopropanol-producing organisms on pure carbon source in bioreactor scale.

Isopropanol yields were calculated according to 4.2.4.3 (page 66), Equation 4-23, Equation 4-21, Equation 4-22. Isopropanol productivities were calculated according to Equation 4-24, Equation 4-25.

p_{max}… product concentration, P_P... volumetric productivity, $Y_{P/X}$… product yield (biomass-related), Q_P… specific productivity (biomass-related), $Y_{P/S}$… product yield (from substrate)

E. coli… *Escherichia coli*, C*. necator*… *Cupriavidus necator*, *C. acetobutylicum*… *Clostridium acetobutylicum*, *C. beijerinckii*… *Clostridium beijerinckii*

Organism	Carbon source (scale)	p_{max} [g L^{-1}]	P_P [g L^{-1} h^{-1}]	$Y_{P/X}$ [g g^{-1} biomass]	Q_P [g g^{-1} biomass h^{-1}]	$Y_{P/S}$ [mol%]	Reference
(recombinant)							
E. coli DH5α_1C	Glucose (10 L)	0.4[d]	0.015 (24 h)	0.150	0.006 (24 h)	5.5[a]	**This work**
E. coli DH5α_1E	Glucose (10 L)	0.9[d]	0.036 (24 h)	0.227	0.009 (24 h)	13.4[a]	**This work**
C. necator[g]	Fructose (3 L)	8.5[d f]	0.121 (70 h)	0.639[b]	0.009 (70 h)	43.3[b]	[Marc et al., 2017]
C. necator[g] (GroESL)	Fructose (3 L)	9.1[d f]	0.111 (82 h)	0.537[b]	0.007 (82 h)	36.2[b]	
(recombinant clostridial)							
C. acetobutylicum	Glucose (1 L)	8.8[c]	0.196 (45 h)	n.d.	n.d.	37.7[a]	[Collas et al., 2012]
C. acetobutylicum	Glucose (2 L)	3.6[d]	0.046 (78 h)	n.d.[e]	n.d.[e]	11.0	[Jang et al., 2013]
C. acetobutylicum	Glucose (200 L)	3.5[d]	0.058 (60 h)	n.d.[e]	n.d.[e]	13.8	
(non-recombinant clostridial)							
C. beijerinckii[h]	Glucose (0.5 L)	2.2[d]	0.046 (48 h)	n.d.[e]	n.d.[e]	32.4[a b]	[Survase et al., 2011]
C. beijerinckii[h]	Glucose (1 L)	4.5[d]	0.100 (45 h)	n.d.	n.d.	35.0[a]	[Collas et al., 2012]

[a] For calculation purposes, glucose is considered the sole carbon source in the medium, [b] estimates taken from figures for calculation, [c] without pH regulation, [d] with pH regulation, [e] only OD_{600} stated in figures, [f] feed of phosphorus and trace elements, [g] PHB-deficient *C. necator* strain, [h] DSM 6423, n.d…. not determined

A direct comparison of the cultivations listed in Table 6-8 is difficult due to differences in scale, carbon source, cultivation time and process design. But isopropanol production parameters allow an estimation of the production capabilities of the respective organisms. Highest isopropanol concentration of 9.1 g L^{-1} was achieved by recombinant, PHB-deficient *C. necator* on fructose with co-production of the chaperones GroEL and GroES [Marc et al., 2017]. But it should be considered that additional feeding of nutrients allowed for a longer cultivation period of 82 h without cell deterioration. As already mentioned before in 6.1 (page 119), this strategy might also increase product concentrations and productivities, if applied for the engineered *E. coli* of this work. Nevertheless, volumetric productivity P_P and biomass- and substrate-related yields $Y_{P/X}$ and $Y_{P/S}$ were 2-4 times higher for *C. necator* than for *E. coli*. Interestingly, biomass-related productivity Q_P was in the same range for both organisms, as a result of the longer process duration for *C. necator*. Despite favorable results for concentration, yield and productivity, there are disadvantages associated with the *C. necator* process. The strict oxygen dependency of the organism complicates upscaling due to mass transfer deficiencies in larger bioreactors. Also, *C. necator* has to be

kept in nitrogen-limited conditions during production phase (bi-phasic cultivation) to divert the carbon flux to isopropanol production, which necessitates a complex process design and obstructs application of cheap substrates like hydrolysates. On the genetic level, *C. necator* harbors the L-arabiose-inducible ctfAB, adc and adh genes from clostridial origin on a plasmid as well as its own phbA, which encodes the acetyl-CoA acetyltransferase involved in PHB formation. Marc et al. stated that co-production of chaperones GroEL and GroES led to an increase in final isopropanol concentration and a higher cell viability and enzyme activity for Adc and Idh. But isopropanol production parameters were slightly lower for *C. necator* (GroESL), probably due to the extra metabolic burden of gene expression.

Isopropanol concentrations for isopropanol-producing *Clostridia* were generally higher than for engineered *E. coli* in bioreactor scale. But the large variety of production results for *Clostridia* suggests that the capacity for isopropanol synthesis is highly strain-dependent. Best isopropanol concentrations, productivities and yields were achieved in a 1 L bioreactor with recombinant *C. acetobutylicum* carrying the adh of *C. beijerinckii* in combination with overexpression of homologous thlA, ctfAB and adc genes [Collas et al., 2012]. In the strictly anaerobic cultivation, pH was intendedly not kept constant, which led to an improved acid re-assimilation in solventogenic phase (pH <5.0), probably due to an increased presence of protonated acids. Major challenges for scale-up of clostridial production processes were already discussed in 5.1.1 (page 70). A sole example for successful upscaling of isopropanol production was published by Jang et al., who achieved a transfer from 2 L to 200 L without a decrease in concentration, yield and productivity [Jang et al., 2013]. Interestingly, substrate-related yield $Y_{P/S}$ was comparable to the respective value for *E. coli* DH5α_1E in bioreactor scale.

Economic viability of a microbial production process can be approached by utilization of a cheap substrate to generate the desired product. In shake flask experiments, application of BWH as carbon source for *E. coli* DH5α_1C did not lead to isopropanol production, but resulted in the formation of acetate and acetone and in inhibition of bacterial growth (5.3, page 86). It was suspected that a pH decrease in the cultivation medium, caused by the acetate in BWH, was responsible for the impairment (6.2, page 128). In 10 L bioreactor scale, this assumption was tested by constant regulation of pH to 7.0. In contrast to shake flask scale, BWH was only used in the feed, after cell propagation and enzyme production was achieved by application of pure glucose in the initial batch phase. Feeding was performed by either using a 50% BWH/50% glucose mixture or 100% BWH. Direct comparison of feeding with pure glucose (Figure 5-17, page 95), 50% BWH (Figure 5-21, page 99) or 100% BWH (Figure 5-23, page 102), as depicted in Figure 6-2, revealed that isopropanol production and growth of *E. coli* DH5α_1E were not affected by BWH feeding in 10 L bioreactor scale.

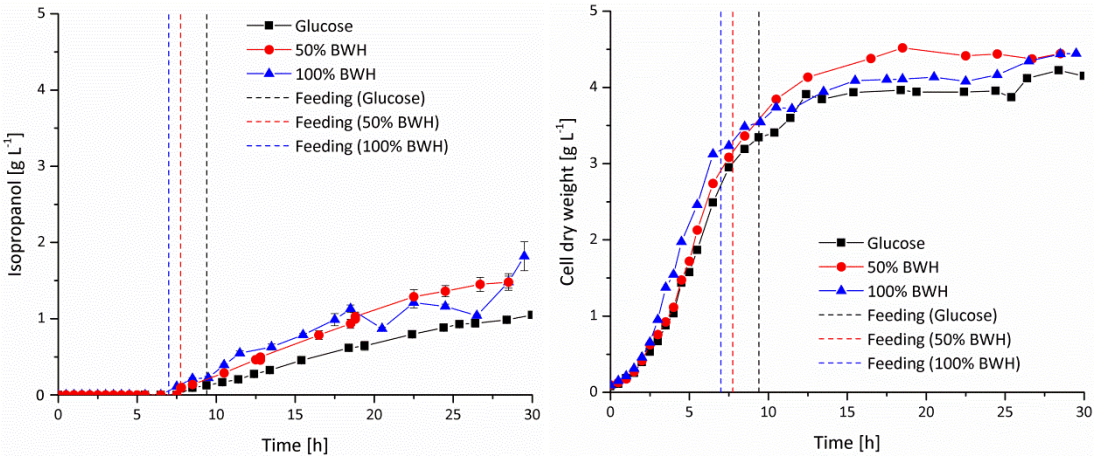

Figure 6-2: Comparison of isopropanol formation by and growth of *E. coli* DH5α_1E in LB plus feed with glucose or BWH in 10 L bioreactor scale.

Recombinant *E. coli* DH5α were cultivated in 10 L LB medium containing 2% (w/v) glucose. Pulsed feeding of either pure glucose, a 50% BWH/50% glucose mixture or 100% BWH was applied when glucose concentration was below 10 g L^{-1}. Control variables were set to 37 °C, pH 7.0, 0.4 bar, 5 L air min^{-1}, 400 rpm (pO_2 > 25%). Induction was performed at OD_{600} ~6.0 with 0.1 mM IPTG. Samples were taken at intervals for determination of cell concentration, glucose consumption, protein and product analysis. GC analysis: Error bars display the standard deviation of n = 3 (technical replicates).

Isopropanol production for all three setups started 2-3 h after induction (t = 4.5-5.5 h) and continued after entry into stationary phase. Interestingly, isopropanol concentration and cell dry weight displayed a steeper ascent and a higher maximum for the BWH-fed cultivations in comparison to the cultivation on pure glucose. The two short-term decreases in isopropanol concentration at t = 21 and 27 h for 100% BWH feed might be the result of insufficient mixing before sampling. By extrapolation of glucose consumption, it can be calculated that (batch) glucose was completely consumed after ~16-17 h (50% BWH) or ~14-15 h (100% BWH). Thus, it can be concluded that BWH served as a carbon source for *E. coli* DH5α_1E afterwards. Production of the isopropanol pathway enzymes was also not negatively affected by BWH supplementation. In contrast, increased isopropanol production might stem from the presence of soluble Act-StrepII (1E) and Idh-c-Myc (4c) already in late exponential phase, when feeding with 50% BWH/50% glucose or 100% BWH was initiated (compare WB results of Figure 5-22, page 101 and Figure 5-24, page 103 to Figure 5-19, page 97). Therefore, it can be concluded that BWH was accepted as a carbon source in the pH-regulated environment of a bioreactor without visible detrimental effects on growth and production. Table 6-9 compares growth, glucose consumption and isopropanol formation parameters of *E. coli* DH5α_1E after 24 h, either fed with 50% or 100% BWH or pure glucose.

Table 6-9: Growth, glucose consumption and isopropanol formation parameters of *E. coli* DH5α_1E after 24 h in LB plus feed with glucose or BWH in 10 L bioreactor scale.

Parameters were calculated according to section 4.2.4.3 (page 66).

x_{max}... maximal cell dry weight, μ_{max}... maximal growth rate, P_S... volumetric substrate consumption rate, p_{max}... product concentration, $Y_{P/X}$... product yield (biomass-related), $Y_{P/S}$... product yield (from substrate), P_P... volumetric productivity

E. coli strain	Feed	x_{max} [g L^{-1}]	μ_{max} [h^{-1}]	P_S [g L^{-1} h^{-1}]	p_{max} [g L^{-1}]	$Y_{P/X}$ [g g^{-1} biomass]	$Y_{P/S}$ [mol%][a]	P_P [g L^{-1} h^{-1}]
1E	Glucose	4.0	0.6	0.808	0.88	0.227	13.4	0.036
	50% BWH	4.4	0.6	1.320	1.36	0.313	12.6	0.056
	100% BWH	4.2	0.7	1.378	1.16	0.285	10.3	0.047

[a] For calculation purposes, glucose is considered the sole carbon source in the medium.

The slightly higher maximum cell dry weight x_{max} for 50% and 100% BWH-fed cells might be associated with the provision of additional nutrients like Ca, Mg, K, Na, P, S in BWH (source: CBP, Leuna, Germany). Pure glucose-fed *E. coli* DH5α_1E displayed a biomass decrease around t = 32 h, indicating that cell death outbalanced cell division (Figure 5-17, page 95). It would be worth investigating if continuation of BWH-feed beyond 30 h led to the same decline or if cell metabolism could be sustained. Isopropanol concentrations, volumetric productivities P_P and biomass-related yields $Y_{P/X}$ were higher for the BWH-fed cultivations. But glucose consumption rates P_S increased by a factor of 1.6-1.7, resulting in lower substrate-related yields $Y_{P/S}$. This indicates that carbon flux was generally increased, but directed elsewhere. Presence of inhibitors in BWH might have increased the cellular energy requirements due to detoxification efforts [Gutierrez et al., 2002; Miller et al., 2009; Perez et al., 2008], as described in 6.2 (page 128). Acetone and ethanol levels were not affected, but lactate concentrations were increased 2-6 times by feeding with 50% and 100% BWH. BWH feed generally increased the total acetate concentration in the medium (7.9 g acetate L^{-1} in BWH; Table 4-3, page 41). But the BWH-associated acetate did not display adverse effects on growth and isopropanol production when compared to the glucose-fed cultivation. Nevertheless, the majority of acetate is still generated by the bacterium itself. Thus, decreasing the acetate production capability of *E. coli* seems mandatory to increase the carbon flux towards isopropanol production. Restriction of acetate synthesis is often achieved by control of the substrate feeding rate to balance cell growth and glycolysis capacity (e.g. [Shimizu et al., 1988]). Development of a more sophisticated feeding strategy for BWH can also limit or prevent accumulation of potential inhibitors. Controlled dilution of BWH-associated acetate could allow re-uptake from the medium, as already observed for feeding with 50% BWH/50% glucose (Figure 5-21, page 99). BWH might also be applied in combination with MM instead of LB to evaluate the function of the hydrolysate as an additional source of nutrients for isopropanol production in bioreactor scale.

In solvent production, application of alternative carbon sources like molasses or corn instead of glucose has a long history. But the use of hydrolysates from lignocellulosic plant biomass is nowadays considered more favorable due to abundance and inexpensiveness of the feedstock, which can be taken from a variety of sources and does not compete with food supply. Table 6-10 (page 140) summarizes publications on microbial isopropanol production from lignocellulosic and other hydrolysates in bioreactor scale.

To date, no literature is available on isopropanol production by recombinant *E. coli* using a lignocellulosic (or other) hydrolysate. Only one publication exists that describes an engineered strain able to degrade and metabolize cellobiose (a cellulose degradation product) to isopropanol by employing a β-glucosidase anchored to the cell surface [Soma et al., 2012]. It was not included in Table 6-10, because pure, commercial cellobiose was employed, not a lignocellulose-derived substance yielding potential inhibitors, and because all experiments were carried out in 25 mL shake flask scale. Despite the frequent utilization of lignocellulose hydrolysates in ABE fermentation by *Clostridia* (e.g. [Ezeji and Blaschek, 2008; Lin et al., 2011; Qureshi et al., 2010a; Qureshi et al., 2010b]), few publications are available for their application in IBE, i.e. isopropanol-butanol-ethanol, production. Of those listed in Table 6-10, only Zhang et al. stated the actual size of the bioreactor working volume [Zhang et al., 2016]. Xin et al. only performed experiments with birchwood-derived xylan (a xylose polymer) in shake flask scale, but it was included in the list for the sake of completeness [Xin et al., 2017].

Table 6-10: Comparison of isopropanol production parameters of recombinant and natural isopropanol-producing organisms on lignocellulose and other hydrolysates in bioreactor scale.
Isopropanol yields were calculated according to section 4.2.4.3 (page 66), Equation 4-21, Equation 4-22. Isopropanol productivities were calculated according to Equation 4-24.
p_{max}… product concentration, P_P... volumetric productivity, $Y_{P/S}$… product yield (from substrate)

Organism	Hydrolysate (scale)	p_{max} [g L^{-1}]	P_P [g L^{-1} h^{-1}]	$Y_{P/S}$ [mol%]	p_{max} [g L^{-1}] on glucose	Reference
(recombinant)						
E. coli DH5α_1E	50% BWH[b] (10 L)	1.36[d]	0.056 (24 h)	12.6	0.88[d]	**This work**
E. coli DH5α_1E	100% BWH[b] (10 L)	1.16[d]	0.047 (24 h)	10.3	0.88[d]	**This work**
(recombinant clostridial)						
C. acetobutylicum	Spruce wood liquor[k] (n.s.)[l]	0.79	n.s.	n.s.	1.55	[Bankar et al., 2014]
(non-recombinant clostridial)						
C. beijerinckii[m]	Domestic organic waste[b, c] (n.s.)	3.00[a, e]	0.014[a] (210 h)	20.9[a]	2.50[a]	[Claassen et al., 2000]
C. beijerinckii[n]	Cassava bagasse[h] (2.5 L)[j]	6.69[d]	0.106 (63 h)	45.7	5.35[d]	[Zhang et al., 2016]
Clostridium sp.[f]	Birchwood xylan[g] (50 mL)[i]	0.54[a, e]	0.005[a] (120 h)	13.9[a]	0.55[e]	[Xin et al., 2017]

[a] Estimates taken from figures for calculation, [b] as feed with previous growth on glucose, [c] prepared by steam explosion (200 °C, 6 min) and enzymatic hydrolysis (50 °C, 72 h), [d] with pH regulation, [e] without pH regulation, [f] strain NJP7, [g] supplemented with commercial xylanases, [h] prepared by milling and hydrolysis with dilute sulfuric acid (120 °C, 120 min), [i] shake flask, [j] immobilized batch, [k] prepared by SO_2-ethanol-water pulping (150 °C, 10 min), evaporation, steam stripping and catalytic oxidation, [l] continous, immobilized cultivation (dilution rate of 0.25 h^{-1}), [m] strain LMD 84.48, [n] strain ATCC 6014, n.s.… not stated

Comparison of isopropanol synthesis parameters by the different microorganisms is difficult due to the variety of used hydrolysates, modes of cultivation (fed-batch, continous, immobilization of cells) and working volumes. Nevertheless, a common observation is that, except in one case [Bankar et al., 2014], utilization of lignocellulose hydrolysates achieved a similar or higher maximal isopropanol concentration p_{max} compared to the employment of pure glucose. Substrate-related product yields $Y_{P/S}$ obtained with *E. coli* DH5α_1E on BWH were comparable to those achieved with *Clostridium sp.* on birchwood xylan and only slightly lower compared to those achieved with a *C. beijerinckii* strain on hydrolysate of domestic organic waste [Claassen et al., 2000]. Zhang et al. stated an isopropanol production of 6.7 g L^{-1} from cassava bagasse hydrolysate (40.6 g L^{-1} glucose/xylose or 52 g L^{-1} total sugar), resulting in a high $Y_{P/S}$ of 45.7 mol% [Zhang et al., 2016]. Additionally, 12.3 g L^{-1} butanol, 1.8 g L^{-1} acetate and 0.8 g L^{-1} butyrate were produced, which would add up to a yield of 123.8 mol%, indicating the consumption of other carbon sources in the medium. Xylose consumption was not determined in the present work and evaluation of complete BWH sugar utilization should be a future task. Biomass-related isopropanol yield $Y_{P/X}$ and productivity Q_P cannot be compared because biomass concentrations were not given for the clostridial cultivations (except for OD_{600} values by Zhang et al.). Volumetric productivity P_P of *E. coli* DH5α_1E on BWH was in most cases higher than isopropanol productivities of *Clostridia*, probably due to

the simultaneous production of butanol, acetate and butyrate by the natural solvent producers and due to their comparably slow growth and metabolism.

6.4 *In Situ* Product Separation and Recovery by Gasstripping

Traditional solvent production, i.e. ethanol or ABE fermentation, relies on product separation and recovery/purification by distillation, downstream the microbial cultivation process. Disadvantages of separated production and recovery are a) accumulation of the desired product in the bioreactor in concentrations, which can be lethal to the host organism and terminate production, and b) high costs associated with energy-intensive distillation of dilute aqueous solutions. *In situ* (or integrated) product recovery can alleviate product toxicity and reduce the expenditures of downstream processing with regard to costs, time and workload [Groot et al., 1992]. In 5.5 (page 104), gasstripping was assessed for integrated isopropanol separation and recovery during aerobic cultivation of recombinant *E. coli*. Two different gasstripping techniques were applied in 10 L bioreactor scale. In 5.5.1 (page 104), gasstripping was demonstrated with two gas washing bottles (GWB), while in 5.5.2 (page 107), gasstripping was performed with a condensation trap (CT) using liquid nitrogen to freeze the gas efflux (see Figure 5-25, page 104 and Figure 5-28, page 107 for experimental setup of gasstripping devices). Direct comparison of both methods was neither intended, nor possible, because they were not applied over the same measuring period (GWB: 25-54 h, CT: 0-30 h) and in setups with different feed solution (GWB: pure glucose feed, CT: 100% BWH feed). Difference in feed solution densities can influence the volatile transfer from liquid to gas phase. Both techniques were rather investigated to answer different questions. Technically, the main difference between the two methods is the type of recovery for evaporated metabolites from gas phase. While stripping with GWB relies on re-solubilization of volatiles in cooled (-10 °C) liquid, the use of liquid nitrogen/CT depends on condensation/freezing of the cooled gas efflux.

In situ isopropanol separation and recovery was successfully established with a cell-free model solution (LB medium plus 2% (w/v) glucose) and a defined isopropanol concentration of 3 g L^{-1} in a 10 L bioreactor (Figure 5-26, page 105). The model solution isopropanol concentration was chosen based on those typically obtained in batch cultivations with *C. beijerinckii* (Table 6-8, page 136). With the GWB setup, ~10% of isopropanol were effectively stripped within 4 h from the cultivation medium into the two GWB. In literature, isopropanol concentrations between 15-18 g L^{-1} were shown to inhibit cell growth of *E. coli* up to 50% [Horinouchi et al., 2017; Ingram, 1976]. Although these concentrations were not reached in the present bioreactor cultivations, this gasstripping setup can potentially be used to alleviate product toxicity in the bioreactor to a certain extend. But complete separation of isopropanol from the medium will probably take a longer time (and thus more energy) than the production process itself, due to the exponential decline of the isopropanol efflux (see Figure 5-26, page 105). In addition, continued stripping could lead to isopropanol re-evaporation from the second GWB to the exhaust gas line. Product recovery could be optimized by increasing the GWB volumes and by installation of a terminal condenser or adsorber [Abdehagh et al., 2014] downstream the GWB.

Application of the GWB setup on a 10 L cultivation with *E. coli* DH5α_1E evinced that isopropanol was not the only metabolic product that could be stripped from the bioreactor. A simultaneous flux of isopropanol, acetone and ethanol was observed, while acetate and lactate were not detected in the GWB (Figure 5-27, page 106). By gasstripping with GWB, the total amount of captured products could be increased by 35-66%. The stripping process harnesses Henry's law, stating that the concentration of dissolved gas in a liquid is proportional to its partial pressure in gas phase. Vapor pressure of the volatile

products of recombinant *E. coli* are of $p_{Isopropanol}$ = 11.8 kPa, $p_{Acetone}$ = 50.1 kPa and $p_{Ethanol}$ = 15.2 kPa at 37 °C respectively (Pa = N m^{-2} or kg m^{-1} s^{-2}; calculated by DDBST; see Table 4-18, page 49). Accordingly, volatility can be expected to be in the following order: acetone > ethanol > isopropanol. This implies that gasstripping leads to a mixture of recovered products, which must be further purified to yield the desired product isopropanol. In addition, strong acetone evaporation causes depletion of the direct isopropanol precursor. Ethanol production might be eliminated by construction of a knockout strain, deficient in the ethanol synthesis pathway, i.e. acetaldehyde dehydrogenase (EC 1.2.1.10) and ethanol dehydrogenase (EC 1.1.1.1). A measure against the elusive nature of acetone might be implementation of a different acetone-converting enzyme, which would be able to catalyze isopropanol production at a faster pace (higher catalytic efficiency k_{cat}/K_M; see Table 6-2, page 124). Alternatively, the rate of aeration could be decreased to balance mass transfer and isopropanol synthesis. Inokuma et al. examined the effect of air flow rate variation on volatilization of isopropanol from a model solution by stripping with 2 GWB in 25 mL shake flask scale (30 °C). It was determined that an air flux of 1.0 vvm corresponds to the isopropanol production rate observed in a 60 h pH-controlled fed-batch process with recombinant *E. coli*. Subsequent experiments combining gasstripping with isopropanol-producing cells resulted in a constant removal of volatiles and yielded a final isopropanol concentration of 143 g L^{-1} after 240 h (cumulative sum of shake flask and recovery system) [Inokuma et al., 2010].

Requirement of constant aeration for isopropanol production by *E. coli* entails volatile and water evaporation in any case. In standard bioreactor cultivations, a reflux condenser is coupled to the exhaust gas line to decrease the loss. Utilization of the second gasstripping setup with liquid nitrogen/CT during cultivation of *E. coli* DH5α_1E at 37 °C displayed that the volatile metabolic products isopropanol, acetone and ethanol were evaporated already in early stages of cultivation by aeration, as a form of "unintended gasstripping" (Figure 5-29, page 108). Product "loss" by aeration amounted to 9-18% after 30 h of cultivation, indicating that concensation capacities of the applied exhaust gas reflux condenser were insufficient. Consequently, all isopropanol productivities and yields stated for 10 L bioreactor cultivations (without active gasstripping) in this work should be considered undervalued. As gasstripping itself cannot be omitted in aerobic isopropanol production, it must be considered an integral part of the process and designed accordingly to avoid loss of the valuable product. In anaerobic cultivation of e.g. *Clostridia*, this phenomenon is not as pronounced due to omitted aeration. But like all living organisms, clostridial metabolism also generates gases, i.e. CO_2 and H_2, which cause a stripping effect. Intentional gasstripping during ABE fermentation either uses those fermentation gases or nitrogen for expulsion of volatiles [Ezeji et al., 2004].

In literature, several alternative methods have been described for *in situ* separation and recovery of solvents from microbial cultivations. Table 6-11 lists their operating principles, advantages and disadvantages, and compares their costs and technical simplicity.

Table 6-11: Comparison of *in situ* product separation and recovery techniques for microbial solvent production.
Source: [a] [Groot et al., 1992], [b] [Durre, 1998], [c] [Mollah and Stuckey, 1993], [d] [Lee, 2016], [e] [Ezeji et al., 2010]

Separation technique	Principle[b]	Advantages	Disadvantages	Costs	Operational simplicity
Gasstripping	Gas perfusion of liquid, recovery by solubilization or condensation/freezing	Simple setup, no fouling[b], non-invasive	Low selectivity, more energy required than membrane processes, incomplete solvent removal[b, c]	Low[d]	High[a, b]
Liquid-liquid extraction	Contact of water-immiscible extractant with cultivation medium	High capacity, high selectivity, no fouling[b]	Further distillation required, risk of emulsion formation[b], extractant toxicity[d]	High[b, d]	Low[a]
Adsorption	Adherence to ion-exchange resins, desorption by heat	Energy-efficient[d]	Low selectivity, low capacity, fouling[b]	High[b]	Low[a]
Pervaporation	Selective diffusion across non-porous membrane, recovery of vapors by vacuum or sweep gas	High selectivity[b], non-invasive	Fouling, low membrane flux[b]	High[b]	High[a]
Membrane evaporation	Selective diffusion across porous membrane, recovery by vacuum and condensation	High membrane flux[b], non-invasive	Fouling, low selectivity[b]	High[b]	High[b]
Perstraction	Contact of extractant and medium via separation membrane	High selectivity[b], non-invasive	Further distillation required, large membrane area required, fouling[b]	High[e]	High[a, b]
Reverse osmosis	High-pressure separation by semipermeable membrane	Non-invasive	Further distillation required, fouling[b]	High[b]	High[b, e]

Striking advantage of gasstripping in comparison to other integrated separation techniques is the combination of relative operational simplicity with low material-associated costs, which make up for its higher energy-requirement [Abdehagh et al., 2014; van der Merwe et al., 2013] compared to membrane-based processes. Potential for industrial scale-up is rated high [Groot et al., 1992; Park and Geng, 1992; van der Merwe et al., 2013], also because gas perfusion is already part of the microbial cultivation. In addition, gasstripping is a non-invasive technique, which does not harm the bacteria or remove essential nutrients and acids from the medium [Ennis et al., 1987] and that can be applied in every mode of cultivation [Ezeji et al., 2004; Outram et al., 2017]. In conclusion, gasstripping can be considered a suitable, but improvable method for *in situ* product separation and recovery of a selective isopropanol production process in larger scale.

6.5 Optimization of Isopropanol Production by Minimization of Acetate Production via Phosphotransacetylase Knockout in *E. coli*

Aerobic acetate production by *E. coli* is caused by the so-called overflow mechanism (a.k.a. Crabtree effect; first discovered in yeast in aerobic ethanol production [Crabtree, 1929; De Deken, 1966]), as a result of the need to regenerate NAD^+ for glycolysis and to recycle CoA for conversion of pyruvate to acetyl-CoA. Presence of a highly assimilable carbon source like glucose triggers an increased carbon flux into the cell (glucose uptake rate) [Eiteman and Altman, 2006; Vemuri et al., 2006], which exceeds the metabolic (i.e. respiratory) capacity [Andersen and von Meyenburg, 1980; Holms, 1996]. In response to NADH accumulation and subsequent inhibition of citrate synthase (EC 2.3.3.1) [Molgat et al., 1992], the TCA cycle enzymes are inhibited, while pyruvate and/or acetyl-CoA accumulate [Chang et al., 1999; Wolfe, 2005]. As a consequence, the cellular energy status is compromised and acetate is excreted, while CoA and ATP are generated. It was found that *E. coli* growth rates above 0.14 h^{-1} could trigger acetate formation in an aerobic fed-batch cultivation [Korz et al., 1995].

Acetate production pathways in *E. coli* are redundant, indicating their multiple physiological roles in the bacterial metabolism. As a gut colonizer and facultative anaerobe, *E. coli* occupies a key function in the establishment and maintenance of the gut microbiome (together with *Enterococcus*) by decreasing the oxygen concentration and pH due to acetate and short-chain fatty acid production in newborns. Anaerobic acidophiles, e.g. *Bifidobacteria*, are then able to settle and grow in favorable conditions, slowly building up the required intestinal bacterial population. In adult guts, *E. coli* is responsible for creation of a stable reduced environment and supply of carbon sources for strict anaerobes [Wolfe, 2005]. In addition, acetate metabolites of *E. coli*, e.g. acetyl phosphate, are assumed to play a role in biofilm formation signaling pathways [Lynnes et al., 2013] and cell-cell communication [Marques et al., 2014; Shoaie et al., 2013]. Acetate is produced by *E. coli* via its precursor acetyl-CoA, which in turn is synthesized by oxidation of the glycolysis end product pyruvate, catalyzed by pyruvate dehydrogenase complex (Pdh) under aerobic conditions or by pyruvate formate lyase (Pfl) under anaerobic conditions respectively [De Graef et al., 1999; Knappe and Sawers, 1990]. Acetyl-CoA is a key metabolite in many biosynthetic pathways including the TCA cycle (energy production and biomass synthesis). During exponential growth, major acetate generation happens by phosphate group transfer to acetyl-CoA and subsequent dephosphorylation of acetyl phosphate via the two-step, constitutive Pta-Ack pathway (phosphotransacetylase, EC 2.3.1.8 and acetate kinase, EC 2.7.2.1), which is a reversible, high-capacity route (see Figure 6-3, page 145, circled numbers 3 & 4). The pathway is also able to re-use acetate when it is present in high concentrations in the medium (K_M = 7 mM for acetate) [Enjalbert et al., 2017; Fox and Roseman, 1986; Kakuda et al., 1994]. Acetate uptake can alternatively be realized by the irreversible action of the high-affinity (K_M = 0.2 mM for acetate), ATP-dependent acetyl-CoA synthetase (Acs, also acetate-CoA ligase, EC 6.2.1.1; Figure 6-3, circled number 8), resulting in the formation of acetyl-CoA [Wolfe, 2005]. In stationary phase (and under phosphate starvation), a second route for acetate synthesis, the PoxB pathway, is activated by RpoS sigma factor [Abdel-Hamid et al., 2001; Chang et al., 1994]. PoxB (pyruvate oxidase, EC 1.2.5.1; Figure 6-3, circled number 7) is a peripheral membrane flavoprotein that catalyzes the direct oxidative decarboxylation of pyruvate to acetate, releasing CO_2 and reducing FAD. The enzyme is assumed to decrease oxidative stress and maintain metabolic efficiency under microaerobic conditions [Bernal et al., 2016].

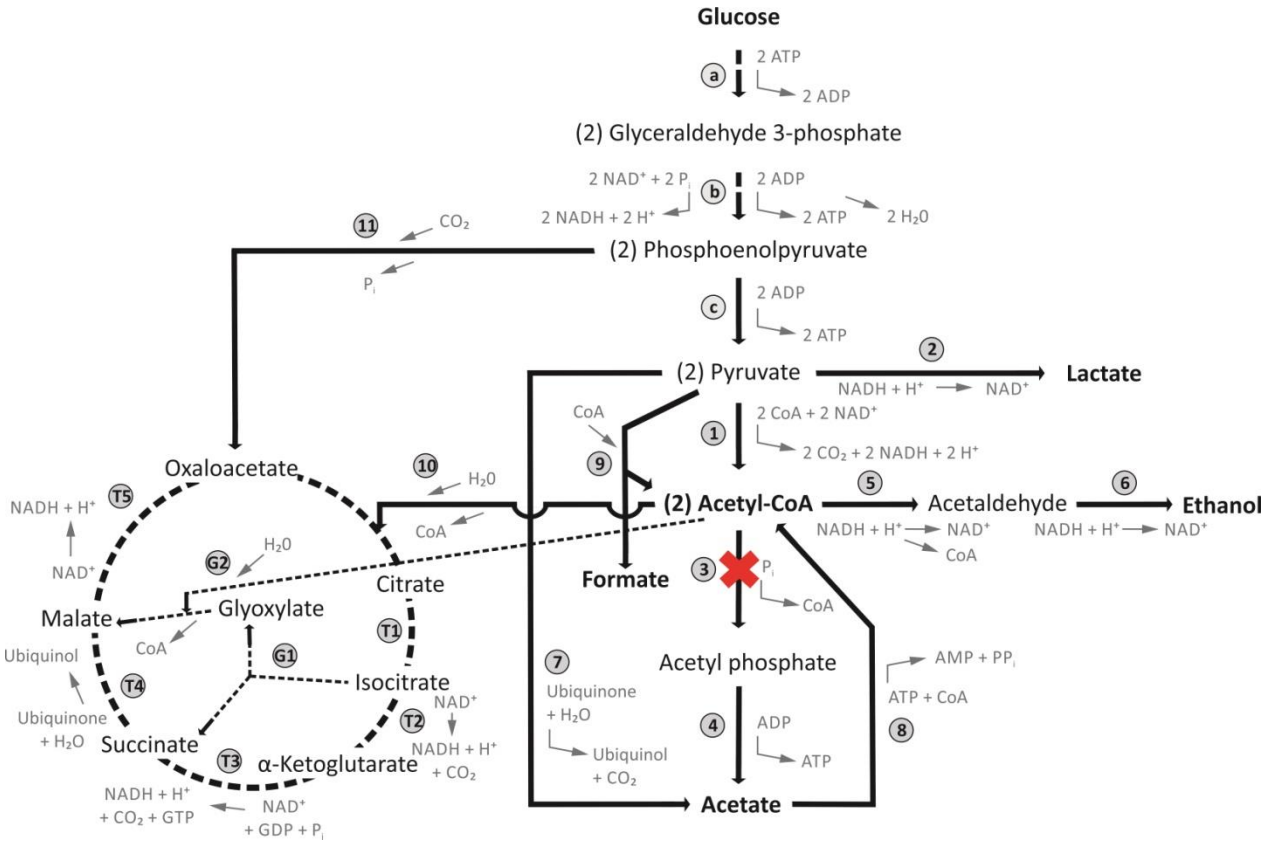

Figure 6-3: Central carbon metabolism of *E. coli*.
Adapted from [Jantama et al., 2008].
Circled numbers and letters refer to the enzymes employed:
1 pyruvate dehydrogenase complex (inactive in anaerobiosis), **2** D-lactate dehydrogenase, **3** phosphotransacetylase (**Pta**), **4** acetate kinase (**Ack**), **5** acetaldehyde dehydrogenase, **6** ethanol dehydrogenase, **7** pyruvate oxidase (**PoxB**), **8** acetyl-CoA synthetase (**Acs**), **9** pyruvate formate lyase (inactive in aerobiosis), **10** citrate synthase, **11** phosphoenolpyruvate carboxylase, **T1** aconitase, **T2** isocitrate dehydrogenase, **T3** α-ketoglutarate dehydrogenase & succinyl-CoA synthetase, **T4** succinate dehydrogenase & fumarase, **T5** malate dehydrogenase, **G1** isocitrate lyase, **G2** malate synthase.
Glycolysis (metabolism of glucose to pyruvate) is not presented in detail, but consists of the following enzymes: **a** hexokinase & glucose-6-phosphate isomerase & phosphofructokinase-1 & fructose-bisphosphate aldolase & triose-phosphate isomerase, **b** glyceraldehyde 3-phosphate dehydrogenase & phosphoglycerate kinase & phosphoglycerate mutase & enolase, **c** pyruvate kinase.
Substrate-to-product stoichiometry is not shown for reaction 2, 3, 5, 7, 9, 10, 11, G2.
Red cross marks the position of pta knockout in the *E. coli* metabolism.

Acetate production by *E. coli* during aerobic growth is considered a major problem for the success of microbial production processes [Bernal et al., 2016; Shimizu et al., 1988]. Acetate is known to inhibit cell growth [Luli and Strohl, 1990; Roe et al., 1998; Shimizu et al., 1988] and protein production [Aristidou et al., 1995; Jensen and Carlsen, 1990; Kim and Cha, 2003; Kim et al., 2015b] (see also discussion in 6.2, page 128), but it is also a competitor for the isopropanol precursor acetyl-CoA (see Figure 2-5, page 23). Bioreactor experiments with isopropanol-producing *E. coli* evinced that acetate is the major product in this scale (see 6.3, page 132). Acetate formation strongly correlated with cell growth and mostly ceased in stationary phase. The utilized *E. coli* DH5α belongs to the high acetate-producing K-12 strains (see 6.1, page 119). Thus, decreasing the acetate production capability of this strain seems mandatory to increase the carbon flux to isopropanol production. In 5.6.1 (page 109), objective was to eliminate the major acetate synthesis pathway Pta-Ack in *E. coli* DH5α by disruption of the pta gene via Red®/ET®

recombination (4.2.2.8). In 5.6.2 (page 112), influence of the pta knockout on isopropanol production was investigated for the first time.

The pta knockout strain *E. coli* DH5αΔpta did not produce acetate during exponential growth in MM plus glucose, in contrast to the strain with intact pta (Figure 5-32, page 111). Basal acetate concentration of 0.06 g L^{-1} in the medium of *E. coli* DH5αΔpta was probably the result of inoculation with the preculture, because it was already present at the beginning of the cultivation. As a consequence of pta disruption, mutated cells should be unable to produce a functional Pta. Introduction and subsequent removal of the FRT cassette by FLPe recombinase (Figure 4-2, page 56) excised a 426 bp pta gene fragment (see Table A-4, page 186 for DNA sequence of pta gene), only leaving behind a single 34 bp FRT site (including a stop codon) as a footprint. Expression of the disrupted gene should generate a truncated 218 aa Pta-variant (213 aa of Pta and 5 aa of FRT site). Full size Pta comprises 714 aa and is composed of three domains, of which the C-terminal one is involved in binding of the substrate and associated with catalytic activity [Campos-Bermudez et al., 2010]. Therefore, it can be assumed that omission of amino acid residues 214-714 leads to an inoperative enzyme, as confirmed by the missing acetate production by *E. coli* DH5αΔpta in exponential phase. Acetate production for *E. coli* DH5αΔpta was only observed in response to the glucose pulse (0.16 g L^{-1} at t = 8 h). Decreasing acetate concentration in the medium of the non-mutated strain at t = 8 h indicates that it consumed acetate at this point. The glucose pulse was applied to trigger a cellular response to the presence of a high glucose concentration. Differential response to the glucose pulse suggests a change in metabolic activity for the Pta-deficient strain. The low-level acetate synthesis by *E. coli* DH5αΔpta can be explained by activation of the PoxB as an alternative way for acetate excretion from pyruvate (Figure 6-3, circled number 7). Decrease of acetate concentration in the medium of non-mutated cells could be associated with acid re-uptake via the action of the Pta-Ack pathway [Xu et al., 1999]. Depending on the extracellular acetate concentration, *E. coli* was found to consume acetate even in the presense of excess glucose [Enjalbert et al., 2017]. Pta disruption eliminates the possibility of re-assimilating acetate in this way. In literature, Δpta strains were found to excrete pyruvate, glutamate and especially lactate instead of acetate in exponential phase [Chang et al., 1999; Kakuda et al., 1994]. Production of other metabolites cannot be ruled out for *E. coli* DH5αΔpta, because they were not measured in this case.

An influence of pta knockout on the central carbon metabolism of *E. coli* can be concluded from the lower growth rate of *E. coli* DH5αΔpta compared to the non-mutated strain (μ_{max} = 0.3 vs. 0.5 h^{-1}, Figure 5-32, page 111). Compromised growth is an often described phenomenon for cells with disrupted acetate synthesis genes. All Δpta strains created by Chang et al., Hahm et al. and Kakuda et al. displayed a lower maximal growth rate compared to the respective wildtype strains [Chang et al., 1999; Hahm et al., 1994; Kakuda et al., 1994]. Chang et al. hypothesized that growth reduction was caused by an accumulation of pyruvate/acetyl-CoA due to a high carbon influx that exceeded the required amount for biomass synthesis. The authors showed that introduction of the PHB synthesis genes from *C. necator* were able to channel the precursor metabolites and to restore growth and diminish by-product formation in the Pta-deficient cells [Chang et al., 1999].

Reduction of aerobic acetate overflow by metabolic engineering has been attempted by various scientists. The most straight-forward approach, which was also applied in this work, aims at deletion of one or more genes involved in acetate synthesis. A reverse strategy utilizes overexpression of acs to generate a strain with increased acetate assimilation capacity [Lin et al., 2006]. Another strategy is concerned with achieving a balance between glucose uptake and metabolic capacity by decreasing the glucose consumption rate of *E. coli*. Inactivation of the phosphotransferase system (PTS), principal and

highly efficient mechanism for glucose internalization and phosphorylation, led to an 80% acetate reduction in batch cultivation, but also to a considerably decreased growth rate of only 60% of the parent strain [Siguenza et al., 1999]. Overexpression of Mlc („making large colonies“), a transcription regulator for PTS, decreased glucose consumption without compromising growth, resulting in 50% reduced acetate production and an increased yield of a recombinant model protein [Cho et al., 2005]. A fourth approach concentrated on optimization of the TCA cycle by either upregulating TCA cycle genes or decreasing the excess NADH that inhibits the TCA cycle via enzymatic conversion by an NADH oxidase. The first strategy resulted in an almost 50% reduced acetate formation and a 22% higher CO_2 release, while maintaining high growth and glucose consumption rates [Veit et al., 2007]. The latter approach only prevented acetate production, when combined with gene deletions of arcA and/or iclR, coding for transcriptional respiration and glyoxylate shunt gene regulators [Liu et al., 2017; Vemuri et al., 2006]. The glyoxylate shunt (G1 & G2 in Figure 6-3, page 145) converts isocitrate to glyoxylate and succinate by isocitrate lyase (Icl, EC 4.1.3.1) and subsequently glyoxylate and acetyl-CoA to malate and CoA by malate synthase (MalS, EC 2.3.3.9), thus bypassing the NAD^+-consuming reactions of the TCA cycle, recycling CoA and reducing the carbon flux to acetyl-CoA [Holms, 1986].

Utilization of *E. coli* DH5αΔpta for isopropanol production in 10 L bioreactor scale resulted in 2-6 times increased isopropanol concentrations as well as drastically decreased acetate formation for *E. coli* DH5αΔpta_1E (0.2 g L^{-1} after 24 h) (see Figure 5-33, page 112) and *E. coli* DH5αΔpta_1C (no acetate after 24 h) (Figure 5-37, page 116) compared to their Pta-intact equivalents. Table 6-12 shows a side-by-side comparison of growth, glucose consumption and isopropanol formation parameters of the four strains after 24 h.

Table 6-12: Growth, glucose consumption and isopropanol formation parameters of *E. coli* DH5α_1E, *E. coli* DH5αΔpta_1E, *E. coli* DH5α_1C and *E. coli* DH5αΔpta_1C after 24 h in LB plus feed with glucose in 10 L bioreactor scale.

Parameters were calculated according to section 4.2.4.3 (page 66).

x_{max}… maximal cell dry weight, μ_{max}… maximal growth rate, P_S… volumetric substrate consumption rate, Q_S… specific substrate consumption rate (biomass-related), p_{max}… product concentration, $Y_{P/X}$… product yield (biomass-related), $Y_{P/S}$… product yield (from substrate), P_P... volumetric productivity

E. coli strain	x_{max} [g L^{-1}]	μ_{max} [h^{-1}]	P_S [g L^{-1} h^{-1}]	Q_S [g g^{-1} biomass h^{-1}]	p_{max} [g L^{-1}]	$Y_{P/X}$ [g g^{-1} biomass]	$Y_{P/S}$ [mol%][a]	P_P [g L^{-1} h^{-1}]
1E	4.0	0.6	0.808	0.204	0.88	0.227	13.4	0.036
Δpta_1E	3.4	0.5	1.574	0.467	1.94	0.608	15.8	0.083
1C	2.7	0.5	0.842	0.312	0.39	0.150	5.5	0.015
Δpta_1C	2.4	0.5	1.412	0.590	2.39	1.065	20.3	0.095

[a] For calculation purposes, glucose is considered the sole carbon source in the medium.

A reduction in growth rate could not be observed for the knockout strains. But both displayed a decreased maximal cell dry weight x_{max} and almost doubled volumetric and biomass-related glucose consumption rates P_S and Q_S. This indicates that pta disruption caused an increased carbon flux, which was not directed to acetate production or biomass formation, but rather (at least in part) to synthesis of the desired product. Interestingly, isopropanol formation started much earlier (t = 4.5-6 h) for the Pta-deficient strains than for their counterparts with intact Pta (t = 8-9 h). This might also be the result of decreased degradation and/or higher solubility of the first cascade enzymes, Act-StrepII (1E) and Act-StrepII (1C), as depicted in Table 6-13 (summary of Figure 5-19, page 97 and Figure 5-34, page 113 and Figure 5-16, page 94 and Figure 5-38, page 118).

Table 6-13: Production of isopropanol pathway enzymes in *E. coli* DH5α_1E, *E. coli* DH5αΔpta_1E, *E. coli* DH5α_1C and *E. coli* DH5αΔpta_1C in LB with glucose as carbon source in 10 L bioreactor scale.
S… soluble production, (S)… weak soluble production, IB… inclusion bodies (only), (IB)… weak inclusion bodies (only), D… potential degradation, (D)… weak potential degradation, (-)… no degradation

E. coli strain	Growth phase	Act-StrepII (1E or 1C)		Acct-His_{10} (2e)	Adc-FLAG (3c)	Idh-c-Myc (4c)
1E	Exponential	IB	D	n.d.	n.d.	IB
	Stationary	(S)	D	n.d.	n.d.	(S)
Δpta_1E	Exponential	(IB)	(-)	(S)	**S**	IB
	Stationary	**S**	(-)	**S**	**S**	**S**
1C	Exponential	**S**	(D)	**S**	(S)	(IB)
	Stationary	**S**	D	**S**	(S)	(S)
Δpta_1C	Exponential	**S**	(-)	**S**	**S**	IB
	Stationary	**S**	(D)	**S**	**S**	**S**

n.d…. not determined

Overall, solubility of the isopropanol pathway enzymes was increased in the knockout strains, especially for the third and fourth enzyme, Adc-FLAG (3c) and Idh-c-Myc (4c) in stationary phase. The strain with the highest isopropanol formation parameters, *E. coli* DH5αΔpta_1C, featured soluble presence of all four cascade enzymes already in late exponential/early stationary phase (t = 9 h) (Figure 5-38, page 118).

Determination of oxygen uptake rate (OUR) and carbon dioxide production rate (CPR) for *E. coli* DH5αΔpta_1E revealed that metabolic activity of the cells stayed high for up to 15 h of cultivation (Figure 5-36, page 115). This yields important information about the possible duration of a stationary phase production process. Isopropanol synthesis can continue well beyond the exponential phase (compare Figure 6-2, page 138) and production without growth would be beneficial to achieve high substrate-related yield $Y_{P/S}$. Timed supply of fresh nutrients, according to the O_2 and CO_2 measurements in exhaust gas, might be able to sustain cell metabolism and lead to prolonged isopropanol production. Calculation of the respiratory quotient (RQ) evinced an imbalance of respiratory activity in mid-exponential phase (Figure 5-36 right, page 115), when RQ was highest and well above 1 (RQ = 2.1). RQ is the ratio of CO_2 produced to O_2 consumed, calculated mole per mole, and a measure for the respiratory activity of the cells [Royce, 1992] as well as an indicator for the substrate consumed. Complete oxidation of glucose by respiration yields an RQ = 1 by Equation 6-1:

Equation 6-1 $$C_6H_{12}O_6 + 6\ O_2 \rightarrow 6\ CO_2 + 6\ H_2O\ .$$

An RQ of 1 was observed during the last 17 h of cultivation at μ ~0. RQ values below and above 1 indicate the accumulation of a metabolite and its consumption [Andersen and von Meyenburg, 1980]. RQ values for *E. coli* DH5αΔpta_1E can only be seen as approximations to the real values, because online measurements were conducted in 2 h intervals for 1.5 h, missing those periods when gasstripping was turned on. O_2/CO_2 monitoring over the whole cultivation period for all four strains would enable a more complete evaluation and comparison of their respiratory activities and uncover detailed metabolic changes induced by pta disruption.

Acetate reduction or elimination to improve biotechnological processes using *E. coli* has been performed by several researchers, either by knockout of an acetate synthesis pathway [Bauer et al., 1990; Centeno-Leija et al., 2014; Dittrich et al., 2005; Hahm et al., 1994; Kang et al., 2009; Kim et al., 2015b] or transcriptional regulators [Liu et al., 2017], by employment of an antisense RNA strategy [Kim and Cha,

2003] or by process monitoring/control [Akesson et al., 1999] with varying results for recombinant protein or metabolite formation. But this work presents the first approach for optimization of selective isopropanol production by disruption of an acetate-generating pathway in *E. coli*. In the following, a carbon mass balance is presented, displaying the carbon yield of isopropanol, biomass, CO_2 and other metabolites from glucose for isopropanol-producing *E. coli* strains with intact or non-functional Pta in 10 L bioreactor scale. Figure 6-4 gives an overview of the C-mols of glucose (100%) being converted into the C-mols of products by *E. coli* DH5α_1E, *E. coli* DH5αΔpta_1E, *E. coli* DH5α_1C and *E. coli* DH5αΔpta_1C after 24 h.

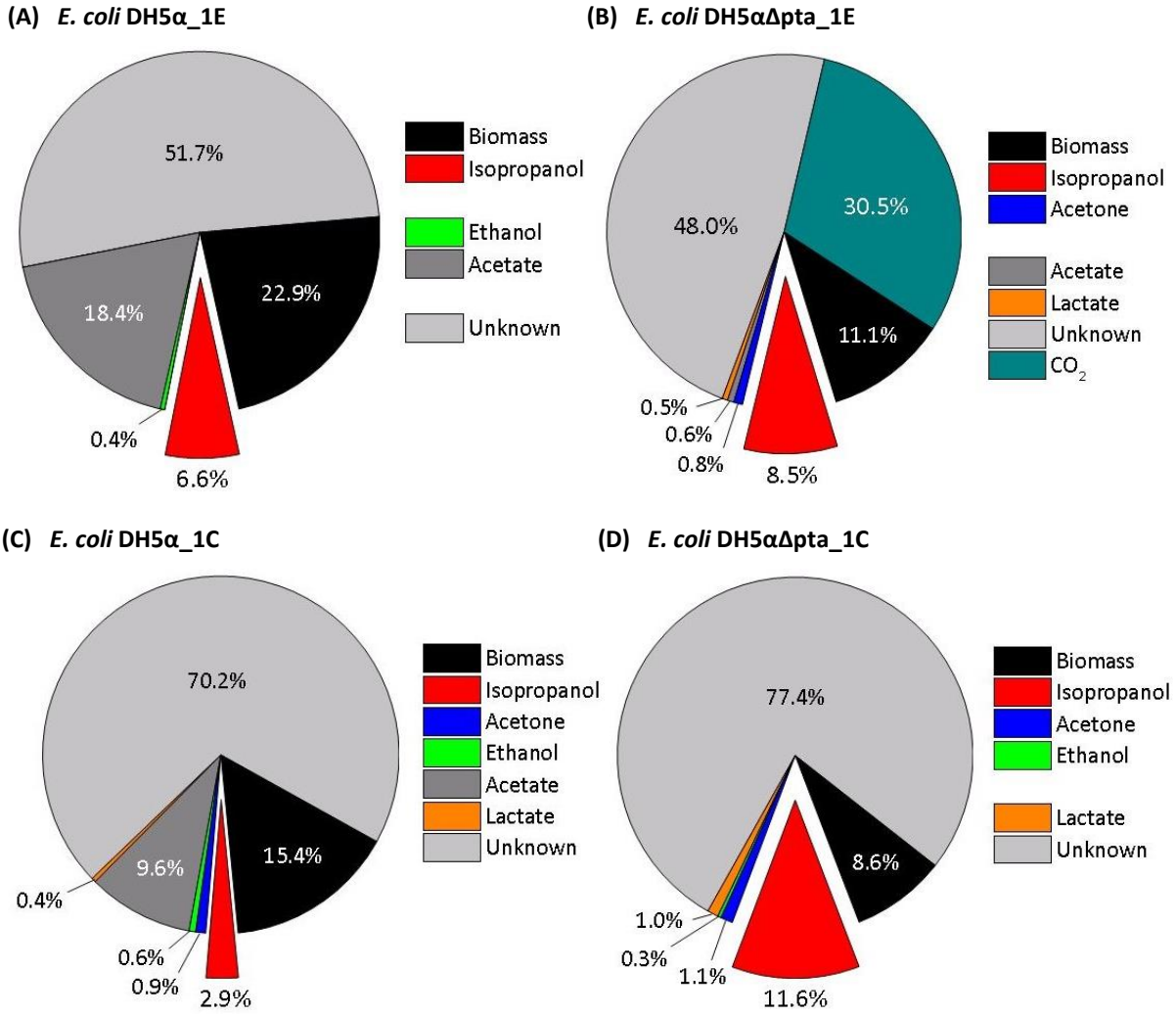

Figure 6-4: Carbon mass balances – Conversion efficiencies of *E. coli* DH5α_1E (A), *E. coli* DH5αΔpta_1E (B), *E. coli* DH5α_1C (C) and *E. coli* DH5αΔpta_1C (D) after 24 h in LB plus feed with glucose in 10 L bioreactor scale.
Online measurement of O_2 and CO_2 in reactor exhaust gas (4.2.3.8) of *E. coli* DH5αΔpta_1E was performed in a 2 h interval for 1.5 h, while gasstripping was turned off. Bacterial CO_2 production was calculated according to Equation 4-7. Gasstripping results for *E. coli* DH5αΔpta_1E were not included. Percentage of conversion was calculated according to Equation 6-2.

Technically, a nearly complete material balance can only be made for *E. coli* DH5αΔpta_1E, because here, online measurement of O_2 and CO_2 as well as gasstripping was performed over (at least parts of) the whole cultivation period. Other potentially generated and excreted metabolites like formate, succinate, malate and pyruvate were not measured. Therefore, the mass balances presented here have to be

viewed with regard to incompleteness. Mass balances were calculated in C-mol, according to Equation 6-2,

Equation 6-2 $$\boldsymbol{Conversion\ efficiency}\ [\%] = \frac{\boldsymbol{Product}\ [\boldsymbol{C-mol}]}{\boldsymbol{Educt}\ [\boldsymbol{C-mol}]} \cdot \mathbf{100}\ ,$$

stating the educt carbons (glucose) entering the bioreactor as well as the product carbons (biomass, isopropanol, acetone, ethanol, acetate, lactate, CO_2) generated in the bioreactor.

Most evident is the large portion of unknown products derived from glucose, ranging between 48.0-77.4%, which might be associated with non-measured metabolites, CO_2 generation or stripped products. For *E. coli* DH5αΔpta_1E, detected stripped metabolites (not included in Figure 6-4) can be assigned to ~1.0% of the converted products (compare to Figure 5-35, page 114). CO_2 holds a product share of 30.5% after 24 h, assumed that detection was exhaustive. Maximum theoretical isopropanol yield from glucose is 100 mol% or ~0.33 g g^{-1}. Ideal conversion of 6 C-mol glucose (1 mol, 100%) is coupled to the formation of 3 C-mol isopropanol (1 mol, 50% conversion efficiency) and the release of 3 C-mol CO_2 (3 mol, 50% conversion efficiency). Thus, the maximum theoretical conversion efficiency for isopropanol from glucose is 50%. *E. coli* DH5αΔpta_1E converted 8.5% glucose to isopropanol after 24 h, which would yield 8.5% CO_2 in an ideal case. In reality, CO_2 generation was 30.5%, due to biomass synthesis, maintenance [Holms, 1996] and other metabolic processes, and might be even higher, due to incomplete CO_2 measurements. Exhaust gas measurements for CO_2 and O_2 could be distorted by losses, due to the intermittent sampling patterns (interrupted by gasstripping) and/or by the use of long, non-gas-tight tubings to connect the exhaust gas line to the measurement device. The carbon mass balance cannot be considered as self-contained, due to the visible gap between the consumed glucose and the total known generated products. Further quantitative metabolic network profiling [Shen et al., 2016] and metabolic flux analysis (MFA) with ^{13}C-labeled glucose [Gonzalez et al., 2017; Long et al., 2016; McAtee et al., 2015] will be necessary to follow the carbon flux inside *E. coli* and eventually close the carbon gap identified in this work.

Disruption of pta increased the isopropanol conversion efficiency of *E. coli* DH5αΔpta_1E by 1.9% to 8.5% and of DH5αΔpta_1C by 8.7% to 11.6%, while acetate conversion efficiency was decreased by 17.8% to 0.6% and by 9.6% to zero. Share of biomass conversion was also lowered by ~7-12% for the knockout strains in comparison to their Pta-intact counterparts. Of the measured and excreted metabolites, only lactate conversion was slightly increased by 0.5-0.6%, while ethanol conversion was even decreased by 0.3-0.4%. Highest isopropanol conversion efficiency of 11.6% was achieved by *E. coli* DH5αΔpta_1C after 24 h cultivation (20.3 mol%, 0.07 g g^{-1}), constituting approximately one fifth of the maximum theoretical isopropanol yield from glucose. This illustrates that elimination of a competing metabolic pathway was successfully able to optimize selective isopropanol synthesis by engineered *E. coli*.

6.6 Thermodynamic and Kinetic Considerations on Isopropanol Production by Engineered *E. coli*

Enzymatic cascades benefit from a balanced metabolite flux through all conversion stages. Unbalanced substrate supply by slow or fast conversion, creates bottlenecks in the metabolite flow, which lead to a decreased catalytic efficiency of the whole cascade [Tamano, 2014]. In addition, insolubility of one or more enzymes as well as insufficient cofactor availability or the presence of inhibitors can decidedly affect enzyme activity [Lee et al., 2013; Rosano and Ceccarelli, 2014]. Also, presence of a competing pathway reduces precursor supply and diminishes formation of the desired product. In this work, some of these problems were addressed to optimize isopropanol production by recombinant *E. coli*. In the following, thermodynamic and kinetic considerations are presented, contributing to a more comprehensive understanding of the enzymatic isopropanol cascade.

Enzymes are biological catalysts that accelerate chemical reactions, i.e. they increase the rate of a reaction by lowering the activation energy. The velocity of a reaction then mostly depends on the catalytic properties (i.e. the kinetic parameters) of the enzyme, while spontaneity of the reaction depends on the energy states of educts (substrates) and products. A spontaneous or exergonic (energy-releasing) reaction will only occur if it increases the entropy, meaning that the educts harbor more free energy than the products, according to Equation 6-3 [Berg et al., 2007]:

Equation 6-3 $$\Delta \boldsymbol{G}^\circ = \Delta \boldsymbol{H}^\circ - \boldsymbol{T} \cdot \Delta \boldsymbol{S}^\circ \,,$$

with ΔG° = change of Gibbs free energy [J], ΔH° = change of enthalpy [J], T = temperature [K], ΔS° = change of entropy [J K^{-1}].

By the release of energy as heat, the system approaches a desired lower energy state, with equilibrium being the lowest energy state possible. Gibbs free energy G° serves as a measure to determine the released or consumed energy during a reaction. The change of Gibbs free energy ΔG° provides information about the spontaneity and the direction of the reaction. A negative ΔG° denotes a spontaneous or exergonic reaction, while a positive ΔG° indicates an endergonic reaction, which requires an energy input in order to take place, because the products have a higher free energy state than the educts. Also exergonic reactions must overcome the activation energy to proceed, a barrier which can be lowered by enzymes. The standard free energy change or standard transformed Gibbs energy of a reaction $\Delta_r G'^\circ$ depicts the amount of energy released or consumed under specified conditions of temperature, pressure, ionic strength and pH, and can be calculated for an enzymatic reaction from the concentration-based apparent equilibrium constant K_c', according to Equation 6-4 [Berg et al., 2007]:

Equation 6-4 $$\Delta_r \boldsymbol{G}'^\circ = -\boldsymbol{RT} \cdot \boldsymbol{ln}\, \boldsymbol{K_c}' \,,$$

with $\Delta_r G'^\circ$ = standard transformed Gibbs energy of a reaction [kJ mol^{-1}] at specified conditions of temperature, pressure, ionic strength and pH, R = ideal gas constant [J K^{-1} mol^{-1}], T = temperature [K], K_c' = apparent equilibrium constant (concentration-based).

To enable a thermodynamic assessment of the enzymatic reactions involved in this work, Table 6-14 lists K_c' and derived $\Delta_r G'^\circ$ values for the isopropanol pathway as well as for the competing Pta-Ack pathway.

Table 6-14: Thermodynamics of the isopropanol and acetate pathway reactions.
Unless otherwise stated, $\Delta_rG'°$ is calculated from K_c' according to Equation 6-4. K_c' reflects *in vitro* conditions.

Enzyme	Reaction	K_c'	$\Delta_rG'°$[kJ mol^{-1}]
Act	Acetyl-CoA + Acetyl-CoA ↔ Acetoacetyl-CoA + CoA	0.00002[a b]	27.4
Acct	Acetoacetyl-CoA + Acetate ↔ Acetoacetate + Acetyl-CoA	7.69231[a c]	-5.1
Adc	Acetoacetate → Acetone + CO_2	(irreversible reaction)	
Idh	Acetone + NADPH ↔ Isopropanol + $NADP^+$	0.03938[d]	8.0[d]
Total			**30.3**
Pta	Acetyl-CoA + P_i ↔ Acetyl phosphate + CoA	0.00750[a e]	12.1
Ack	Acetyl phosphate + ADP ↔ Acetate + ATP	342.46575[a f]	-14.5
Total			**-2.4**

K_c'… apparent equilibrium constant (concentration-based), $\Delta_rG'°$… standard transformed Gibbs energy of a reaction at specified conditions of temperature, pressure, ionic strength and pH, [a] according to [Goldberg and Tewari, 1994], [b] at pH 7.0, 25 °C and $MgCl_2$, [c] at pH 8.1, 25 °C and 0.005 mol L^{-1} $MgCl_2$, [d] calculated according to [Latendresse et al., 2012] at pH 7.3, [e] at pH 7.6 and 27 °C, [f] at pH 7.4, 25 °C and 0.2 mol L^{-1} $MgCl_2$

Summed up $\Delta_rG'°$ suggests that the isopropanol route is thermodynamically less favorable than the Pta-Ack pathway (irreversible reaction of Adc not considered). Two of the four isopropanol-associated enzymes, Act and Idh, favor the reverse reaction, yielding an endergonic net reaction for isopropanol synthesis. This might explain why recombinant *E. coli* with intact Pta preferentially channel acetyl-CoA into acetate rather than isopropanol production. It is reasonable to assume that Act is a bottleneck of the isopropanol cascade due to the high $\Delta_rG'°$ for condensation of two acetyl-CoA molecules [Wiesenborn et al., 1988]. In addition, Michaelis constant K_M for acetyl-CoA is ~10fold higher for Act (Table 5-1, page 72) in comparison to the K_M of Pta (K_M = 0.045 mM) [Campos-Bermudez et al., 2010]. In glucose-grown *E. coli*, the total cellular pool of acetyl-CoA ranges between 0.305 and 0.610 mM in exponential phase [Bennett et al., 2009; Chohnan et al., 1998]. If all acetyl-CoA was available for metabolite production (no TCA cycle activity), Act would only operate slightly above its half-maximal velocity, while Pta would already be working at full speed. Although the first acetate pathway reaction is endergonic, the thermodynamically favorable second reaction pulls the substrates into acetate formation. In addition, Ack catalyzes the synthesis of ATP, creating energy for the cell. Advantage of the isopropanol pathway is the presence of the third reaction, which is irreversible due to the release of CO_2 (no equilibrium), forcing the reaction to the product (acetone) side. Unfortunately, the reaction velocity of Adc is limited due to the relatively high K_M of 4.1-8 mM for acetoacetate (Table 5-3, page 73). The exergonic second reaction via Acct only proceeds if sufficient amounts of acetoacetyl-CoA are delivered by the first reaction and if intracellular acetate concentrations are high enough to meet the relatively high K_M of 53 mM (*E. coli* variant) or 1200 mM (*C. acetobutylicum* variant) (Table 5-2, page 73) for the second substrate. Availability of sufficient amounts of cofactor might present an additional obstacle for the Idh-catalyzed reaction (K_M for NADPH = 0.02 mM; Table 5-4, page 74). Cellular NADPH concentration for glucose-growing *E. coli* was determined to be 0.12 mM [Bennett et al., 2009], while stationary phase concentration can be assumed to be much lower due to downregulation of the NADPH-recycling pentose phosphate pathway [Chubukov and Sauer, 2014]. Potential solutions to these problems (e.g. application of isoenzymes with lower K_M; NADPH regeneration; shift of cofactor preference) were already discussed in 6.1 (page 119).

In an ideal stoichiometric scenario, with a conversion of 1 mol glucose to 1 mol isopropanol, as specified in Table 6-15, cellular requirements would demand the recycling of 2 mol ADP, 4 mol NAD^+, 1 mol CoA and 1 mol NADPH in addition to availability of acetate for a sustained Acct reaction.

Table 6-15: Ideal stoichiometric balance of the recombinant isopropanol pathway in *E. coli* (aerobic).
Biomass generation is not considered.

Pathway	Educts	Products
Glycolysis	Glucose[a] + 2 ADP + 2 P_i + 2 NAD^+	2 Pyruvate[b] + 2 NADH + 2 H^+ + 2 ATP + 2 H_2O
	2 Pyruvate[b] + 2 CoA + 2 NAD^+	2 Acetyl-CoA[c] + 2 CO_2 + 2 NADH + 2 H^+
Isopropanol	2 Acetyl-CoA[c]	Acetoacetyl-CoA[d] + CoA
	Acetoacetyl-CoA[d] + Acetate[e]	Acetoacetate[f] + Acetyl-CoA[c]
	Acetoacetate[f]	Acetone[g] + CO_2
	Acetone[g] + NADPH + H^+	Isopropanol[h] + $NADP^+$
Summary	**Glucose[a] + 2 ADP + 2 P_i + 4 NAD^+ + CoA + Acetate[e] + NADPH + H^+**	**Isopropanol[h] + 4 NADH + 4 H^+ + 2 ATP + 2 H_2O + Acetyl-CoA[c] + $NADP^+$ + 3 CO_2**

[a] $C_6H_{12}O_6$, [b] $C_3H_4O_3$, [c] $C_{23}H_{38}N_7O_{17}P_3S$, [d] $C_{25}H_{40}N_7O_{18}P_3S$, [e] $C_2H_4O_2$, [f] $C_4H_6O_3$, [g] C_3H_6O, [h] C_3H_8O

Harmonization of *E. coli* metabolism could be approached by overproduction of enzymes like e.g. PntAB (*E. coli* transhydrogenase, EC 1.6.1.5), which catalyze the energy-dependent transhydrogenation from NADH to $NADP^+$, yielding NADPH. Applicability of PntAB was shown by Cui et al., who achieved an increase in intracellular NADPH concentration as well as a 40% higher production of the desired product shikimic acid in recombinant *E. coli* [Cui et al., 2014]. An increase of the acetyl-CoA pool [Krivoruchko et al., 2015], e.g. by overproduction of acetyl-CoA-generating Acs [Leonard et al., 2007; Lin et al., 2006], in a Pta-deficient strain and/or elimination of other acetyl-CoA- or pyruvate-consuming reactions, e.g. by disruption of D-lactate dehydrogenase (EC 1.1.1.28), acetaldehyde dehydrogenase (EC 1.2.1.10) and ethanol dehydrogenase (EC 1.1.1.1) [Park et al., 2012; Zhu et al., 2011] or formate C-acetyltransferase (EC 2.3.1.54) [Atsumi et al., 2008; Causey et al., 2004; Ohno et al., 2013], could further stimulate isopropanol synthesis.

7 Summary

The overall aim of this work was optimization of selective isopropanol production by engineered *E. coli*. Isopropanol-producing *E. coli* strains were constructed by implementation of a 4-step enzymatic cascade for isopropanol synthesis (acetyl-CoA acetyltransferase = Act = 1, acetate CoA-transferase = Acct = 2, acetoacetate decarboxylase = Adc = 3, isopropanol dehydrogenase = Idh = 4) from acetyl-CoA, based on the biosynthesis pathway in *C. beijerinckii*. The genes were selected according to the known catalytic properties and performance of published and most commonly deployed isoenzymes. Due to the suggested crucial function of the first cascade enzyme, an *E. coli* (= E) and a *C. acetobutylicum* (= C) variant of Act were both tested for isopropanol production in *E. coli* DH5α and JM109. All genes were optimized for codon usage and GC content of *E. coli*. Rational design of the expression construct comprised choice of a suitably small vector (pHSG299), selection marker (kanamycin) and regulatory and auxiliary elements (tac promoter for each gene, CER sequence, rrnB T1 terminator). Employment of C-terminal peptide tags allowed tracking of the isopropanol pathway enzymes for the first time to investigate protein solubility and stability.

Isopropanol production of the four resulting strains, *E. coli* DH5α_1E, *E. coli* DH5α_1C, *E. coli* JM109_1E and *E. coli* JM109_1C, was evaluated in 100 mL shake flask scale to identify the best gene combination, *E. coli* host and induction temperature. Highest isopropanol concentration was achieved with *E. coli* DH5α_1C at an induction temperature of 37 °C. The strain produced 4.4 g L^{-1} isopropanol within 24 h, which is 48% higher than JM109_1C with the same gene combination. Both strains produced drastically less isopropanol at 24 °C (DH5α_1C: 0.8 g L^{-1}; JM109_1C: 0.6 g L^{-1}). The choice of isopropanol pathway genes displayed the strongest effect on the production result. Strains with the Act variant of *E. coli*, DH5α_1E and JM109_1E, did not generate isopropanol at 37 °C. At 24 °C, only *E. coli* DH5α_1E was able to produce 0.02 g L^{-1} in 24 h. WB analyses indicated that hampered isopropanol synthesis could be attributed to missing/minimal soluble production and degradation of the first enzyme, Act-StrepII (1E). Acetate was detected as a major by-product of *E. coli*. Its decreased production in strains with higher isopropanol formation capacity suggested a competition between the isopropanol and acetate biosynthesis pathway.

Scale-up of isopropanol production by recombinant *E. coli* to 10 L bioreactor scale was first demonstrated in this work. Application of a pulsed glucose fed-batch strategy and conditions identified as most suitable in shake flask resulted in a deviating strain performance. The best producer in small scale, *E. coli* DH5α_1C, generated only 0.4 g L^{-1} in 24 h, while DH5α_1E was able to produce 0.9 g L^{-1} isopropanol. Generally, isopropanol concentrations were considerably decreased compared to shake flask scale (0.9 vs. 4.4 g L^{-1}), while acetate was the major product in bioreactor scale (1.9-3.7 g L^{-1}). This could be associated with weak and/or insoluble production of the isopropanol pathway enzymes Act-StrepII (1C), Adc-FLAG (3c) and Idh-c-Myc (4c), especially in earlier stages of cultivation. Also, degradation of the crucial first cascade enzyme, Act-StrepII (1E), was confirmed by MALDI-TOF/TOF MS.

A lignocellulose hydrolysate from beech wood (BWH) was investigated as an alternative carbon source for isopropanol production. Shake flask experiments with *E. coli* DH5α_1C and BWH, instead of pure glucose, resulted in impaired isopropanol formation (100% BWH: no isopropanol in 24 h, 75% BWH:

0.5 g L^{-1}, 50% BWH: 1.8 g L^{-1}, pure glucose: 4.4 g L^{-1}), decreased glucose consumption (100% BWH: 0.3 g, 75% BWH: 0.4 g, 50% BWH: 0.5 g, pure glucose: 1.6 g) and increased acetate production (100% BWH: 2.0 g L^{-1}, 75% BWH: 1.6 g L^{-1}, 50% BWH: 0.6 g L^{-1}, pure glucose: 0.3 g L^{-1}). BWH-contained acetate and concomitant pH decrease in the medium were assumed to be responsible for this effect. In contrast, utilization of BWH as feed solution for *E. coli* DH5α_1E in 10 L bioreactor scale, after glucose was used in the initial batch phase, did not compromise isopropanol synthesis. In fact, final isopropanol concentration after 24 h was slightly increased in comparison to feeding with pure glucose (1.2 vs. 0.9 g L^{-1}), probably due to the increased solubility of Act-StrepII (1E) and Idh-c-Myc (4c). For the first time, a lignocellulose hydrolysate was successfully employed as carbon source for isopropanol production in a pH-controlled environment.

Gasstripping was assessed for *in situ* isopropanol separation and recovery in 10 L bioreactor scale. In a first setup, the bioreactor exhaust gas was directed to two gas washing bottles (GWB). Stripping of a cell-free model solution containing 3 g L^{-1} isopropanol effectively removed ~10% of isopropanol from the bioreactor within 4 h, confirming that this setup could be used to alleviate isopropanol toxicity during production. When gasstripping with GWB was performed in a 10 L bioreactor cultivation of *E. coli* DH5α_1E, a simultaneous transfer of isopropanol, acetone and ethanol was observed. Gasstripping led to a mixture of recovered products, which required further purification. Also, strong acetone evaporation caused depletion of the direct isopropanol precursor. With the GWB setup, the total amount of captured products could be increased by 35-66% (isopropanol: 10.64 vs. 17.65 g in 54 h, acetone: 0.81 vs. 1.12 g, ethanol: 0.82 vs. 1.11 g). The extent of volatile product evaporation during a standard bioreactor cultivation at 37 °C (without active gasstripping) was evaluated by application of a second setup. Use of a condensation trap (CT) and liquid nitrogen to freeze the condenser-cooled gas efflux displayed that product “loss” occured via aeration. Product loss by “unintended gasstripping” amounted to 9-18% after 30 h (isopropanol: 20.21 vs. 22.43 g, acetone: 1.00 vs. 1.18 g, ethanol: 0.77 vs. 0.84 g), indicating that product recovery should be an integral part of the aerobic isopropanol production process.

For the first time, selective isopropanol synthesis by *E. coli* was optimized by elimination of a competing metabolic pathway. Disruption of the major acetate biosynthesis pathway Pta-Ack by knockout of the phosphotransacetylase (pta) gene in *E. coli* DH5α resulted in a strain with drastically decreased acetate formation in exponential phase (DH5αΔpta: 0.2 g L^{-1} after 8 h, DH5α: 1.4 g L^{-1}). In 10 L scale, acetate production was successfully suppressed (DH5αΔpta_1E: 0.2 g L^{-1}, DH5αΔpta_1C: 0.0 g L^{-1} in 24 h), while isopropanol production was increased by a factor of 2-6 compared to the Pta-intact equivalent strains (0.9 vs. 1.9 g L^{-1} for DH5αΔpta_1E, 0.4 vs. 2.4 g L^{-1} for DH5αΔpta_1C). WB analyses displayed that solubility of Adc-FLAG (3c) and Idh-c-Myc (4c) was increased and degradation of Act-StrepII (1E)/(1C) was reduced in the knockout strains. Highest isopropanol yield in 10 L bioreactor scale was achieved by *E. coli* DH5αΔpta_1C (20.3 mol%, 0.07 g g^{-1} in 24 h), constituting one fifth of the maximum theoretical isopropanol yield from glucose.

8 Outlook

Clostridial solvent production for biofuels and chemical building blocks has been under investigation for more than a century, but despite proven industrial applicability, the bio-manufacturing processes from renewable resources still lack economic competitiveness with petroleum-based chemical processes. In the present work, *E. coli* has been evaluated as an alternative, recombinant host for isopropanol synthesis, providing the advantages of fast growth in aerobic conditions, flexible metabolism, genetically amenable genome and the variety of engineering tools available as well as its capability to utilize a broad range of carbon sources. Nevertheless, isopropanol production by *E. coli* is afflicted with its own unique challenges, some of which were identified and addressed in this thesis.

Engineering of the host strain itself offers potential for improvement, but also might constitute a tedious task. As successfully demonstrated by pta knockout, disruption of competing metabolic pathways can increase the carbon flux towards isopropanol production. Elimination of other acetyl-CoA- or pyruvate-consuming reactions like lactate, ethanol, formate or succinate/malate synthesis might prove beneficial for isopropanol production. In addition, disruption of the pyruvate-scavenging and acetate-producing PoxB may prove advantageous for prolonged stationary phase cultivation, despite its pronounced detrimental effect on cell growth [Dittrich et al., 2005]. In this case, implementation of a conditional knockout ("metabolic toggle switch"), as performed by Soma et al. with a cell density-dependent regulatory system, could be a potent un-coupling strategy to ensure sufficient bacterial growth with subsequent blockage and re-direction of the carbon flux to the desired product [Soma and Hanai, 2015]. Increasing the precursor acetyl-CoA pool by overexpression of the ATP-dependent Acs [Leonard et al., 2007; Lin et al., 2006] or ATP-independent pyruvate dehydrogenase from *Enterococcus faecalis* (Pdh, EC 1.2.4.1) [Kozak et al., 2014] are further means to enhance isopropanol production. Employment of an acetate-tapping enzyme like Acs in a Pta-deficient strain might appear contradictory. But if process design involves feeding of an acetate-containing lignocellulose hydrolysate like BWH as carbon source, introduction of an acetate-consuming pathway can be useful to avoid acetate accumulation, especially if the Pta-Ack pathway is barred. Harmonization of cellular metabolism comprises a more comprehensive approach than single knockout or overexpression strategies. As derived from stoichiometry, isopropanol formation from glucose requires the recycling of 2 mol ADP, 4 mol NAD^+, 1 mol CoA, 1 mol NADPH and the availability of acetate. Thoughtful coupling of enzymatic reactions like e.g. NADPH-generating PntAB or G6PDH, which provide one or more of these molecules, might ensure a more balanced metabolism for a sustained production. Tracking of the carbon flux inside *E. coli* by quantitative metabolic network profiling and metabolic flux analysis (MFA) will aid in deciphering cellular needs and metabolic constraints and also identify other potential "futile" pathways. Multiple, genomic integration of the isopropanol cascade genes into *E. coli* by CRISPR/Cas9 can be attempted to create a stable production strain.

Optimization of the isopropanol synthesis cascade by enzyme engineering or isoenzyme substitution seems evident from the results presented in this work. The crucial role of Act and its thermodynamically unfavorable acetyl-CoA condensation reaction requires a performance improvement of the first enzyme. Although Act degradation and insolubility could be diminished by pta knockout, the enzyme still seems unable to fully divert the carbon flux to isopropanol synthesis. Substitution of Act with an isoenzyme

featuring a lower K_M for acetyl-CoA (e.g. Acat1 gene product of *Rattus norvegicus*, K_M = 0.006 mM) [Duncombe and Frerman, 1976; Huth et al., 1974; Wiesenborn et al., 1988] might allow the reaction to proceed at high velocity when less substrate is available. In addition, Act could be engineered towards insensitivity to its inhibitor CoA (released by TCA cycle enzymes), as performed by Mann and Lutke-Eversloh by exchange of 3 amino acids, to increase its activity in exponential phase [Mann and Lutke-Eversloh, 2013]. Alternatively, employment of *Synechococcus elongatus* acetyl-CoA carboxylase (Acc) and *Streptomyces* sp. acetoacetyl-CoA synthase (NphT7) instead of Act could circumvent the unfavorable acetyl-CoA condensation due to application of an ATP-driven and an irreversible CO_2-releasing reaction [Lan and Liao, 2012]. The need to increase the functionality of the fourth pathway enzyme was affirmed by detection of acetone accumulation in the medium and by acetone evaporation during gasstripping experiments. The acetone-converting Idh-c-Myc (4c) not only displayed insolubility in shake flask and bioreactor experiments at 37 °C (although this problem was alleviated by pta knockout), but also requires NADPH as a cofactor. NADPH availability in stationary phase cells is theorized to be an order of magnitude lower than during exponential phase [Chubukov and Sauer, 2014]. Insolubility could be counteracted by decreasing the induction temperature to 24 °C, which was not tested in bioreactor experiments of this work. Also, co-production of chaperones like GroEL/GroES could increase solubility and activity of Idh and the other pathway enzymes [Marc et al., 2017], although the extra metabolic burden of gene expression must be taken into account. Switching cofactor preference from NADPH to NADH by amino acid substitution within the cofactor binding domain, as suggested by Korkhin et al., might be beneficial for sustained isopropanol production in stationary phase [Korkhin et al., 1998]. The thus created possibility for NAD^+ recycling may also improve the glycolytic flux due to its need for a re-oxidized cofactor. In addition, cofactor exchange may offer a higher metabolic flexibility under anaerobic or microaerobic conditions, when absence or limitation of oxygen triggers the formation of e.g. ethanol and lactate in response to low NAD^+ concentrations. Application of microaerobic conditions not only increased 1-butanol productivity in recombinant *E. coli* by a factor of 22 (calculated from [Atsumi et al., 2008]). Microaerobiosis also improved the performance of acetone-producing *E. coli* strains by a factor of 3 (master thesis by Anita May "*Entwicklung und Optimierung einer Prozessstrategie zur Produktion von Aceton mit* Escherichia coli *DH5α*", 2016, and personal communication with K. Patzsch of Fraunhofer CBP). The strains were derived from Idh-deletion experiments in the course of this work (master thesis by Benjamin Schrank "*Untersuchungen zur Produktion von Aceton und Isopropanol mit* Escherichia coli", 2015). Employment of an isoenzyme with a lower K_M for acetone and a higher catalytic efficiency than Idh (e.g. ADH1 gene product of *Entamoeba histolytica*, K_M = 0.02 mM, k_{cat}/K_M = 3790 s^{-1} mM^{-1}) [Ismaiel et al., 1993; Kumar et al., 1992] might increase the conversion efficiency of the fourth isopropanol synthesis step. Enzyme activity tests in recombinant cell extracts with substrate supplementation would allow rapid comparison of alternative cascades as well as identification of further enzymatic bottlenecks.

Rational process design offers a way to influence isopropanol productivity by process monitoring and control/adjustment of process variables. Application of a pH-adjustable, aerated miniature scale parallel reactor (e.g. Eppendorf DASGIP Parallel Bioreactor Systems) is recommended for rapid testing of potential candidate strains and scale-up conditions (pH, aeration rate etc.). A more sophisticated and automated feeding strategy, combined with complete online monitoring of O_2 consumption and CO_2 release to determine the cellular respiratory capacity, needs to be developed to balance substrate uptake and production, to ensure complete use of the available carbon source and to prevent accumulation of hydrolysate-associated inhibitors. Timed supply of nutrients might allow prolonged isopropanol production in stationary phase and increase substrate-related yield. Optimization of the gasstripping device by size adjustment of the receptive equipment or by installation of a condenser with

higher capacity is required to ensure complete re-capturing of the evaporating products. Utilization of electrodes for online measurement of alcohols in the exhaust gas can aid in determination of product "loss" and development of an appropriate stripping device. Application of constitutive promoters for each isopropanol pathway gene could facilitate the production process and eliminate the need for a costly inducer. Medium optimization or simple application of BWH in combination with MM could enable the use of a defined medium to achieve higher cell densities and to decrease the production costs.

Isopropanol tolerance of *E. coli* could be increased by classical methods like serial strain adaptation to higher stressor concentrations [Seregina et al., 2012] or random mutagenesis in combination with more advanced methods like genome shuffling to accelerate the evolutionary process [de Gerando et al., 2016; Guan et al., 2017; Zhang et al., 2002]. Rational approaches like identification and overexpression or regulation of genes involved in general stress response, membrane modification and efflux systems might to allow prolonged alcohol exposure and could potentially increase isopropanol production [Dunlop, 2011; Dunlop et al., 2011; Gonzalez et al., 2003; Okochi et al., 2007; Reyes et al., 2011; Woodruff et al., 2013; Zingaro and Papoutsakis, 2013].

Evaluation of other feedstocks for lignocellulose hydrolysate production could broaden the range of available carbon sources and offer flexibility of renewable supply. Fast-growing plants and endemic waste materials could be tested for a favorable sugar/lignin ratio and applicability as microbial substrates using pretreatment methods, that aim at energy- and cost-efficient conservation of sugars with less residues, while minimizing the inhibitor content [Taherzadeh and Karimi, 2008]. To name one example, cotton-based waste from textile industry might be an interesting resource due to its global abundance (10 billion kg in 2013, [NCC, 2014]) and the low lignin (~1% of dry mass), but high cellulose content (~94%) of cotton seed fibres [Fan et al., 2009; Saini et al., 2015; Timell, 1967]. The parallel use of multiple sugars is a desirable property of the production strain, because most hydrolysates not only contain glucose, but also other hexoses (e.g. mannose, galactose) and pentoses. Most microorganisms are inflicted with carbon catabolite repression (CCR), i.e. they exhibit a specific hierarchy for monosaccharide utilization, when exposed to a mixture of sugars. *E. coli* prefers metabolizing glucose, while enzymes for transport/metabolism of typical pentoses derived from lignocellulose hydrolysates (e.g. xylose, arabinose) are repressed [Vinuselvi et al., 2012]. Strain engineering strategies might involve relaxation of CCR and increasing the sugar uptake rate by manipulation of glucose metabolism [Yao et al., 2011] or transporters [Dien et al., 2002; Hernandez-Montalvo et al., 2001; Nichols et al., 2001]. But those measures often entail impairment of bacterial growth and require further investigation. A holistic approach, combining "pretreatment" and production, would be strain engineering for degradation of (at least parts of) the lignocellulosic material (e.g. cellulose) and subsequent synthesis of the desired product to reduce pretreatment-associated costs [la Grange et al., 2010]. Research on "simultaneous saccharification and fermentation" was performed for ABE-producing *Clostridia* [Mingardon et al., 2011; Mingardon et al., 2005] and certain yeasts [Den Haan et al., 2007; Hong et al., 2007; van Rooyen et al., 2005; Voronovsky et al., 2009] with varying degrees of success. *E. coli* was engineered for utilization of cellobiose [Rutter and Chen, 2014; Su et al., 1989; Vinuselvi and Lee, 2011], but application was mostly limited to ethanologenic strains [Shin et al., 2014]. First steps into synthesis of other valuable products by cellobiose-metabolizing *E. coli* were performed by Soma et al., who enabled cellobiose hydrolyzation by a cell surface-anchored cellulase for subsequent generation of isopropanol [Soma et al., 2012]. With regard to the plethora of polysaccharides in lignocellulose, the recalcitrance of the material and the resulting amount of strain engineering required, there is still a long way to go until consolidated bioprocessing with *E. coli* in a single bioreactor can be realized.

References

Abdehagh, N., Tezel, F. H. and Thibault, J. (2014). “Separation techniques in butanol production: Challenges and developments.” *Biomass & Bioenergy,* **60**, 222-246.

Abdel-Hamid, A. M., Attwood, M. M. and Guest, J. R. (2001). “Pyruvate oxidase contributes to the aerobic growth efficiency of Escherichia coli.” *Microbiology Society,* **147**, 1483-1498.

Ahmed, I., Ross, R. A., Mathur, V. K. and Chesbro, W. R. (1988). “Growth rate dependence of solventogenesis and solvents produced by Clostridium beijerinckii.” *Applied Microbiology and Biotechnology,* **28**, 182-187.

Akesson, M., Karlsson, E. N., Hagander, P., Axelsson, J. P. and Tocaj, A. (1999). “On-line detection of acetate formation in Escherichia coli cultures using dissolved oxygen responses to feed transients.” *Biotechnology and Bioengineering,* **64**, 590-598.

Aleklett, K., Hook, M., Jakobsson, K., Lardelli, M., Snowden, S. and Soderbergh, B. (2010). “The Peak of the Oil Age - Analyzing the world oil production Reference Scenario in World Energy Outlook 2008.” *Energy Policy,* **38**, 1398-1414.

Almeida, J. R. M., Modig, T., Petersson, A., Hahn-Hagerdal, B., Liden, G. and Gorwa-Grauslund, M. F. (2007). “Increased tolerance and conversion of inhibitors in lignocellulosic hydrolysates by Saccharomyces cerevisiae.” *Journal of Chemical Technology and Biotechnology,* **82**, 340-349.

Andersen, K. B. and von Meyenburg, K. (1980). “Are growth rates of Escherichia coli in batch cultures limited by respiration?” *Journal of Bacteriology,* **144**, 114-23.

Ando, S., Arai, I., Kiyoto, K. and Hanai, S. (1986). “Identification of aromatic monomers in steam-exploded poplar and their influences on ethanol fermentation by saccharomyces cerevisiae.” *Journal of Fermentation Technology,* **64**, 567-570.

Angov, E. (2011). “Codon usage: Nature's roadmap to expression and folding of proteins.” *Biotechnology journal,* **6**, 650-659.

Aristidou, A. A., San, K. Y. and Bennett, G. N. (1995). “Metabolic engineering of Escherichia coli to enhance recombinant protein production through acetate reduction.” *Biotechnology Progress,* **11**, 475-478.

Atsumi, S., Cann, A. F., Connor, M. R., Shen, C. R., Smith, K. M., Brynildsen, M. P., Chou, K. J. Y., Hanai, T. and Liao, J. C. (2008). “Metabolic engineering of Escherichia coli for 1-butanol production.” *Metabolic Engineering,* **10**, 305-311.

Baneyx, F. and Mujacic, M. (2004). “Recombinant protein folding and misfolding in Escherichia coli.” *Nature Biotechnology,* **22**, 1399-1408.

Bankar, S. B., Jurgens, G., Survase, S. A., Ojamo, H. and Granstrom, T. (2014). “Enhanced isopropanol-butanol-ethanol (IBE) production in immobilized column reactor using modified Clostridium acetobutylicum DSM792.” *Fuel,* **136**, 226-232.

Bauer, K. A., Benbassat, A., Dawson, M., Delapuente, V. T. and Neway, J. O. (1990). “Improved expression of human interleukin-2 in high-cell-density fermenter cultures of Escherichia coli K-12 by a phosphotransacetylase mutant.” *Applied and Environmental Microbiology,* **56**, 1296-1302.

Bennett, B. D., Kimball, E. H., Gao, M., Osterhout, R., Van Dien, S. J. and Rabinowitz, J. D. (2009). “Absolute metabolite concentrations and implied enzyme active site occupancy in Escherichia coli.” *Nature Chemical Biology,* **5**, 593-599.

Bentley, W. E., Mirjalili, N., Andersen, D. C., Davis, R. H. and Kompala, D. S. (1990). “Plasmid-encoded protein: the principal factor in the "metabolic burden" associated with recombinant bacteria.” *Biotechnology and Bioengineering,* **35**, 668-81.

Berg, J. M., Tymoczko, J. L. and Stryer, L. (2007). "Biochemie." 6th ed., Elsevier GmbH, München.

Bermejo, L. L., Welker, N. E. and Papoutsakis, E. T. (1998). "Expression of Clostridium acetobutylicum ATCC 824 genes in Escherichia coli for acetone production and acetate detoxification." *Applied and Environmental Microbiology,* **64**, 1079-1085.

Bernal, V., Castano-Cerezo, S. and Canovas, M. (2016). "Acetate metabolism regulation in Escherichia coli: carbon overflow, pathogenicity, and beyond." *Applied Microbiology and Biotechnology,* **100**, 8985-9001.

Bernardi, G. and Cordonnier, C. (1965). "Mechanism of degradation of DNA by endonuclease I from Escherichia coli." *Journal of Molecular Biology,* **11**, 141-3.

Bleicher, K. and Winter, J. (1991). "Purification and properties of F420-dependent and NADP+-dependent alcohol dehydrogenases of Methanogenium liminatans and Methanobacterium palustre, specific for secondary alcohols." *European Journal of Biochemistry,* **200**, 43-51.

Boopathy, R., Bokang, H. and Daniels, L. (1993). "Biotransformation of furfural and 5-hydroxymethyl furfural by enteric bacteria." *Journal of Industrial Microbiology & Biotechnology,* **11**, 147-50.

BP. (2016). "BP Statistical Review of World Energy." London, UK.

Bryant, F. R. (1988). "Construction of a recombinase-deficient mutant recA protein that retains single-stranded DNA-dependent ATPase activity." *Journal of Biological Chemistry,* **263**, 8716-23.

Burdette, D. S., Vieille, C. and Zeikus, J. G. (1996). "Cloning and expression of the gene encoding the Thermoanaerobacter ethanolicus 39E secondary-alcohol dehydrogenase and biochemical characterization of the enzyme." *Biochemical Journal,* **316**, 115-122.

Campos-Bermudez, V. A., Bologna, F. P., Andreo, C. S. and Drincovich, M. F. (2010). "Functional dissection of Escherichia coli phosphotransacetylase structural domains and analysis of key compounds involved in activity regulation." *Febs Journal,* **277**, 1957-1966.

Carvalheiro, F., Duarte, L. C. and Girio, F. M. (2008). "Hemicellulose biorefineries: a review on biomass pretreatments." *Journal of Scientific & Industrial Research,* **67**, 849-864.

Carvalho, H. and Meneghini, R. (2008). "Increased expression and purification of soluble iron-regulatory protein 1 from Escherichia coli co-expressing chaperonins GroES and GroEL." *Brazilian Journal of Medical and Biological Research,* **41**, 270-276.

Causey, T. B., Shanmugam, K. T., Yomano, L. P. and Ingram, L. O. (2004). "Engineering Escherichia coli for efficient conversion of glucose to pyruvate." *Proceedings of the National Academy of Sciences of the United States of America,* **101**, 2235-2240.

Centeno-Leija, S., Huerta-Beristain, G., Giles-Gomez, M., Bolivar, F., Gosset, G. and Martinez, A. (2014). "Improving poly-3-hydroxybutyrate production in Escherichia coli by combining the increase in the NADPH pool and acetyl-CoA availability." *Antonie Van Leeuwenhoek International Journal of General and Molecular Microbiology,* **105**, 687-696.

Ceresana. (2014). "Market Study: Propylene." Konstanz, Germany.

Chang, D. E., Shin, S., Rhee, J. S. and Pan, J. G. (1999). "Acetate metabolism in a pta mutant of Escherichia coli W3110: Importance of maintaining acetyl coenzyme a flux for growth and survival." *Journal of Bacteriology,* **181**, 6656-6663.

Chang, Y. Y., Wang, A. Y. and Cronan, J. E., Jr. (1994). "Expression of Escherichia coli pyruvate oxidase (PoxB) depends on the sigma factor encoded by the rpoS(katF) gene." *Molecular Microbiology,* **11**, 1019-28.

Chemie.de. "2-Propanol." http://www.chemie.de/lexikon/2-Propanol.html. 01.11.2017.

Cho, S., Shin, D., Ji, G. E., Heu, S. and Ryu, S. (2005). "High-level recombinant protein production by overexpression of Mlc in Escherichia coli." *Journal of Biotechnology,* **119**, 197-203.

Chohnan, S., Izawa, H., Nishihara, H. and Takamura, Y. (1998). "Changes in size of intracellular pools of coenzyme A and its thioesters in Escherichia coli K-12 cells to various carbon sources and stresses." *Bioscience, Biotechnology, and Biochemistry,* **62**, 1122-1128.

Chubukov, V. and Sauer, U. (2014). "Environmental dependence of stationary phase metabolism in Bacillus subtilis and Escherichia coli." *Applied and Environmental Microbiology,* **80**, 2901-2909, 10 pp.

Claassen, P. A. M., Budde, M. A. W. and Lopez-Contreras, A. M. (2000). "Acetone, butanol and ethanol production from domestic organic waste by solventogenic clostridia." *Journal of Molecular Microbiology and Biotechnology,* **2**, 39-44.

Clomburg, J. M. and Gonzalez, R. (2010). "Biofuel production in Escherichia coli: the role of metabolic engineering and synthetic biology." *Applied Microbiology and Biotechnology,* **86**, 419-434.

Collas, F., Kuit, W., Clement, B., Marchal, R., Lopez-Contreras, A. M. and Monot, F. (2012). "Simultaneous production of isopropanol, butanol, ethanol and 2,3-butanediol by Clostridium acetobutylicum ATCC 824 engineered strains." *AMB Express,* **2**, 45.

Crabtree, H. G. (1929). "Observations on the carbohydrate metabolism of tumors." *Biochemical Journal,* **23**, 536-45.

Crawford, D. L. and Crawford, R. L. (1976). "Microbial degradation of lignocellulose: the lignin component." *Applied and Environmental Microbiology,* **31**, 714-17.

Cui, Y. Y., Ling, C., Zhang, Y. Y., Huang, J. and Liu, J. Z. (2014). "Production of shikimic acid from Escherichia coli through chemically inducible chromosomal evolution and cofactor metabolic engineering." *Microbial Cell Factories,* **13**.

Dai, Z., Dong, H., Zhu, Y., Zhang, Y., Li, Y. and Ma, Y. (2012). "Introducing a single secondary alcohol dehydrogenase into butanol-tolerant Clostridium acetobutylicum Rh8 switches ABE fermentation to high level IBE fermentation." *Biotechnology for Biofuels,* **5**, 44.

Davies, R. (1943). "Studies on the acetone-butanol fermentation: 4. Acetoacetic acid decarboxylase of Cl. acetobutylicum (BY)." *The Biochemical Journal,* **37**, 230-8.

DDBST. "Saturated Vapor Pressure - Calculation by Antoine Equation." http://ddbonline.ddbst.de/AntoineCalculation/AntoineCalculationCGI.exe. 01.11.2017.

De Deken, R. H. (1966). "Crabtree effect: a regulatory system in yeast." *Journal of General Microbiology,* **44**, 149-156.

de Gerando, H. M., Fayolle-Guichard, F., Rudant, L., Millah, S. K., Monot, F., Ferreira, N. L. and Lopez-Contreras, A. M. (2016). "Improving isopropanol tolerance and production of Clostridium beijerinckii DSM 6423 by random mutagenesis and genome shuffling." *Applied Microbiology and Biotechnology,* **100**, 5427-5436.

de Gerando, H. M., Lopez-Contreras, A. M., Wasels, F., Bisson, A., Clement, B., Bidard, F., Jourdier, E. and Lopes, F. N. (2018). "Genome and transcriptome of the natural isopropanol producer Clostridium beijerinckii DSM6423." *Bmc Genomics,* **19**, 242.

De Graef, M. R., Alexeeva, S., Snoep, J. L. and Teixeira de Mattos, M. J. (1999). "The steady-state internal redox state (NADH/NAD) reflects the external redox state and is correlated with catabolic adaptation in Escherichia coli." *Journal of Bacteriology,* **181**, 2351-2357.

Deboer, H. A., Comstock, L. J. and Vasser, M. (1983). "The tac promoter - a functional hybrid derived from the trp and lac promoters." *Proceedings of the National Academy of Sciences of the United States of America-Biological Sciences,* **80**, 21-25.

Delmer, D. P. and Amor, Y. (1995). "Cellulose biosynthesis." *Plant Cell,* **7**, 987-1000.

Den Haan, R., Rose, S. H., Lynd, L. R. and van Zyl, W. H. (2007). "Hydrolysis and fermentation of amorphous cellulose by recombinant Saccharomyces cerevisiae." *Metabolic Engineering,* **9**, 87-94.

Desai, R. P. and Papoutsakis, E. T. (1999). "Antisense RNA strategies for metabolic engineering of Clostridium acetobutylicum." *Applied and Environmental Microbiology,* **65**, 936-945.

Dhamdhere, G. and Zgurskaya, H. I. (2010). "Metabolic shutdown in Escherichia coli cells lacking the outer membrane channel TolC." *Molecular Microbiology,* **77**, 743-54.

Dien, B. S., Nichols, N. N. and Bothast, R. J. (2002). "Fermentation of sugar mixtures using Escherichia coli catabolite repression mutants engineered for production of L-lactic acid." *Journal of Industrial Microbiology & Biotechnology,* **29**, 221-227.

Dittrich, C. R., Vadali, R. V., Bennett, G. N. and Sant, K. Y. (2005). "Redistribution of metabolic fluxes in the central aerobic metabolic pathway of E. coli mutant strains with deletion of the ackA-pta and poxB pathways for the synthesis of isoamyl acetate." *Biotechnology Progress,* **21**, 627-631.

Donovan, R. S., Robinson, C. W. and Glick, B. R. (1996). "Review: Optimizing inducer and culture conditions for expression of foreign proteins under the control of the lac promoter." *Journal of Industrial Microbiology,* **16**, 145-154.

Drissen, R. E. T., Maas, R. H. W., Tramper, J. and Beeftink, H. H. (2009). "Modelling ethanol production from cellulose: separate hydrolysis and fermentation versus simultaneous saccharification and fermentation." *Biocatalysis and Biotransformation,* **27**, 27-35.

Duncombe, G. R. and Frerman, F. E. (1976). "Molecular and catalytic properties of the Acetoacetyl-Coenzyme A Thiolase of Escherichia coli." *Archives of Biochemistry and Biophysics,* **176**, 159-170.

Dunlop, A. P. (1948). "Furfural formation and behavior." *Industrial and Engineering Chemistry,* **40**, 204-209.

Dunlop, M. J. (2011). "Engineering microbes for tolerance to next-generation biofuels." *Biotechnology for Biofuels,* **4**.

Dunlop, M. J., Dossani, Z. Y., Szmidt, H. L., Chu, H. C., Lee, T. S., Keasling, J. D., Hadi, M. Z. and Mukhopadhyay, A. (2011). "Engineering microbial biofuel tolerance and export using efflux pumps." *Molecular Systems Biology,* **7**.

Durre, P. (1998). "New insights and novel developments in clostridial acetone/butanol/isopropanol fermentation." *Applied Microbiology and Biotechnology,* **49**, 639-648.

Dusseaux, S., Croux, C., Soucaille, P. and Meynial-Salles, I. (2013). "Metabolic engineering of Clostridium acetobutylicum ATCC 824 for the high-yield production of a biofuel composed of an isopropanol/butanol/ethanol mixture." *Metabolic Engineering,* **18**, 1-8.

Eiteman, M. A. and Altman, E. (2006). "Overcoming acetate in Escherichia coli recombinant protein fermentations." *Trends in Biotechnology,* **24**, 530-536.

EMBL-EBI. "Clustal Omega." http://www.ebi.ac.uk/Tools/msa/clustalo/. 01.11.2017.

EndMemo. "DNA/RNA GC Content Calculator " http://www.endmemo.com/bio/gc.php. 01.11.2017.

Enjalbert, B., Millard, P., Dinclaux, M., Portais, J. C. and Letisse, F. (2017). "Acetate fluxes in Escherichia coli are determined by the thermodynamic control of the Pta-AckA pathway." *Scientific Reports,* **7**.

Ennis, B. M., Qureshi, N. and Maddox, I. S. (1987). "In-line toxic product removal during solvent production by continuous fermentation using immobilized Clostridium acetobutylicum." *Enzyme and Microbial Technology,* **9**, 672-675.

Ensley, B., McHugh, J. J. and Barton, L. L. (1975). "Effect of carbon sources on formation of alpha-amylase and glucoamylase by Clostridium acetobutylicum." *Journal of General and Applied Microbiology,* **21**, 51-59.

Essalem, M. E. E. and Mitchell, W. J. (2016). "Identification of a glucose-mannose phosphotransferase system in Clostridium beijerinckii." *Fems Microbiology Letters,* **363**.

Ezeji, T. and Blaschek, H. P. (2008). "Fermentation of dried distillers' grains and solubles (DDGS) hydrolysates to solvents and value-added products by solventogenic clostridia." *Bioresource Technology,* **99**, 5232-5242.

Ezeji, T., Milne, C., Price, N. D. and Blaschek, H. P. (2010). "Achievements and perspectives to overcome the poor solvent resistance in acetone and butanol-producing microorganisms." *Applied Microbiology and Biotechnology,* **85**, 1697-1712.

Ezeji, T. C., Qureshi, N. and Blaschek, H. P. (2004). "Butanol fermentation research: Upstream and downstream manipulations." *The Chemical Record,* **4**, 305-314.

Fan, L., Shi, W.-J., Hu, W.-R., Hao, X.-Y., Wang, D.-M., Yuan, H. and Yan, H.-Y. (2009). "Molecular and biochemical evidence for phenylpropanoid synthesis and presence of wall-linked phenolics in cotton fibers." *Journal of Integrative Plant Biology,* **51**, 626-637.

Feigenbaum, J. and Schulz, H. (1975). "Thiolases of Escherichia coli: Purification and chain length specificities." *Journal of Bacteriology,* **122**, 407-411.

Forsberg, C. W., Donaldson, L. and Gibbins, L. N. (1987). "Metabolism of rhamnose and other sugars by strains of Clostridium acetobutylicum and other Clostridium species." *Canadian Journal of Microbiology,* **33**, 21-26.

Fox, A. R., Soto, G., Mozzicafreddo, M., Garcia, A. N., Cuccioloni, M., Angeletti, M., Salerno, J. C. and Ayub, N. D. (2014). "Understanding the function of bacterial and eukaryotic thiolases II by integrating evolutionary and functional approaches." *Gene,* **533**, 5-10.

Fox, D. K. and Roseman, S. (1986). "Isolation and characterization of homogeneous acetate kinase from Salmonella typhimurium and Escherichia coli." *Journal of Biological Chemistry,* **261**, 13487-97.

Fridovich, I. (1963). "Inhibition of acetoacetic decarboxylase by anions - Hofmeister lyotropic series." *Journal of Biological Chemistry,* **238**, 592-&.

Gefen, G., Anbar, M., Morag, E., Lamed, R. and Bayer, E. A. (2012). "Enhanced cellulose degradation by targeted integration of a cohesin-fused beta-glucosidase into the Clostridium thermocellum cellulosome." *Proceedings of the National Academy of Sciences of the United States of America,* **109**, 10298-10303.

George, H. A. and Chen, J. S. (1983). "Acidic conditions are not obligatory for onset of butanol formation by Clostridium beijerinckii (synonym, C. butylicum)." *Applied and Environmental Microbiology,* **46**, 321-7.

Gerischer, U. and Durre, P. (1990). "Cloning, sequencing, and molecular analysis of the acetoacetate decarboxylase gene region from Clostridium acetobutylicum." *Journal of Bacteriology,* **172**, 6907-6918.

Girbal, L. and Soucaille, P. (1998). "Regulation of solvent production in Clostridium acetobutylicum." *Trends in Biotechnology,* **16**, 11-16.

Glascock, C. B. and Weickert, M. J. (1998). "Using chromosomal lacIQ1 to control expression of genes on high-copy-number plasmids in Escherichia coli." *Gene,* **223**, 221-31.

Goldberg, R. N. and Tewari, Y. B. (1994). "Thermodynamics of enzyme-catalyzed reactions: Part 2. Transferases." *Journal of Physical and Chemical Reference Data,* **23**, 547-617.

Gonen, C., Gungormusler, M. and Azbar, N. (2013). "Continuous Production of 1,3-Propanediol Using Waste Glycerol with Clostridium beijerinckii NRRL B-593 Immobilized on Glass Beads and Glass Rushing Rings." *Chemical and Biochemical Engineering Quarterly,* **27**, 227-234.

Gonzalez, J. E., Long, C. P. and Antoniewicz, M. R. (2017). "Comprehensive analysis of glucose and xylose metabolism in Escherichia coli under aerobic and anaerobic conditions by C-13 metabolic flux analysis." *Metabolic Engineering,* **39**, 9-18.

Gonzalez, R., Tao, H., Purvis, J. E., York, S. W., Shanmugam, K. T. and Ingram, L. O. (2003). "Gene array-based identification of changes that contribute to ethanol tolerance in ethanologenic Escherichia coli: comparison of KO11 (parent) to LY01 (resistant mutant)." *Biotechnology Progress,* **19**, 612-623.

Grethlein, H. E. (1985). "The effect of pore size distribution on the rate of enzymic hydrolysis of cellulosic substrates." *Bio/Technology,* **3**, 155-60.

Groot, W. J., Vanderlans, R. and Luyben, K. (1992). "Technologies for butanol recovery integrated with fermentations." *Process Biochemistry,* **27**, 61-75.

Grousseau, E., Lu, J., Gorret, N., Guillouet, S. E. and Sinskey, A. J. (2014). "Isopropanol production with engineered Cupriavidus necator as bioproduction platform." *Applied Microbiology and Biotechnology,* **98**, 4277-90.

Gruber, A. R., Lorenz, R., Bernhart, S. H., Neuboeck, R. and Hofacker, I. L. (2008). "The Vienna RNA Websuite." *Nucleic Acids Research,* **36**, W70-W74.

Guan, N., Li, J., Shin, H.-d., Du, G., Chen, J. and Liu, L. (2017). "Microbial response to environmental stresses: from fundamental mechanisms to practical applications." *Applied Microbiology and Biotechnology,* **101**, 3991-4008.

Guruprasad, K., Reddy, B. V. B. and Pandit, M. W. (1990). "Correlation between stability of a protein and its dipeptide composition: a novel approach for predicting in vivo stability of a protein from its primary sequence." *Protein Engineering,* **4**, 155-61.

Gutierrez, T., Buszko, M. L., Ingram, L. O. and Preston, J. F. (2002). "Reduction of furfural to furfuryl alcohol by ethanologenic strains of bacteria and its effect on ethanol production from xylose." *Applied Biochemistry and Biotechnology,* **98**, 327-340.

Guzman, L. M., Belin, D., Carson, M. J. and Beckwith, J. (1995). "Tight regulation, modulation, and high-level expression by vectors containing the arabinose P(BAD) promoter." *Journal of Bacteriology,* **177**, 4121-4130.

Haapalainen, A. M., Merilainen, G. and Wierenga, R. K. (2006). "The thiolase superfamily: condensing enzymes with diverse reaction specificities." *Trends in Biochemical Sciences,* **31**, 64-71.

Hahm, D. H., Pan, J. and Rhee, J. S. (1994). "Characterization and evaluation of a pta (phosphotransacetylase) negative mutant of Escherichia coli HB101 as production host of foreign lipase " *Applied Microbiology and Biotechnology,* **42**, 100-107.

Hanahan, D. (1983). "Studies on transformation of Escherichia coli with plasmids." *Journal of Molecular Biology,* **166**, 557-80.

Hanai, T., Atsumi, S. and Liao, J. C. (2007). "Engineered synthetic pathway for isopropanol production in Escherichia coli." *Applied and Environmental Microbiology,* **73**, 7814-7818.

Harris, L. M., Desai, R. P., Welker, N. E. and Papoutsakis, E. T. (2000). "Characterization of recombinant strains of the Clostridium acetobutylicum butyrate kinase inactivation mutant: Need for new phenomenological models for solventogenesis and butanol inhibition?" *Biotechnology and Bioengineering,* **67**, 1-11.

Hartmanis, M. G. N., Klason, T. and Gatenbeck, S. (1984). "Uptake and activation of acetate and butyrate in Clostridium acetobutylicum." *Applied Microbiology and Biotechnology,* **20**, 66-71.

Heap, J. T., Pennington, O. J., Cartman, S. T., Carter, G. P. and Minton, N. P. (2007). "The ClosTron: A universal gene knock-out system for the genus Clostridium." *Journal of Microbiological Methods,* **70**, 452-464.

Heckly, R. J. (1978). "Preservation of microorganisms." *Advances in Applied Microbiology,* **24**, 1-53.

Heider, J. (2001). "A new family of CoA-transferases." *Febs Letters,* **509**, 345-349.

Hernandez-Montalvo, V., Valle, F., Bolivar, F. and Gosset, G. (2001). "Characterization of sugar mixtures utilization by an Escherichia coli mutant devoid of the phosphotransferase system." *Applied Microbiology and Biotechnology,* **57**, 186-191.

Hirokawa, Y., Suzuki, I. and Hanai, T. (2015). "Optimization of isopropanol production by engineered cyanobacteria with a synthetic metabolic pathway." *Journal of Bioscience and Bioengineering,* **119**, 585-590.

Hiu, S. F., Zhu, C. X., Yan, R. T. and Chen, J. S. (1987). "Butanol-Ethanol Dehydrogenase and Butanol-Ethanol-Isopropanol Dehydrogenase: Different Alcohol Dehydrogenases in Two Strains of Clostridium beijerinckii (Clostridium butylicum)." *Applied and Environmental Microbiology,* **53**, 697-703.

Ho, M. C., Menetret, J. F., Tsuruta, H. and Allen, K. N. (2009). "The origin of the electrostatic perturbation in acetoacetate decarboxylase." *Nature,* **459**, 393-U107.

Holms, H. (1996). "Flux analysis and control of the central metabolic pathways in Escherichia coli." *Fems Microbiology Reviews,* **19**, 85-116.

Holms, W. H. (1986). "Evolution of the glyoxylate bypass in Escherichia coli - an hypothesis which suggests an alternative to the Krebs cycle." *Fems Microbiology Letters,* **34**, 123-7.

Holstein, S. A. and Hohl, R. J. (2004). "Isoprenoids: Remarkable diversity of form and function." *Lipids,* **39**, 293-309.

Hong, J., Wang, Y., Kumagai, H. and Tamaki, H. (2007). "Construction of thermotolerant yeast expressing thermostable cellulase genes." *Journal of Biotechnology,* **130**, 114-123.

Horinouchi, T., Sakai, A., Kotani, H., Tanabe, K. and Furusawa, C. (2017). "Improvement of isopropanol tolerance of Escherichia coli using adaptive laboratory evolution and omics technologies." *Journal of Biotechnology,* **255**, 47-56.

Huang, H., Liu, H. and Gan, Y. R. (2010). "Genetic modification of critical enzymes and involved genes in butanol biosynthesis from biomass." *Biotechnology Advances,* **28**, 651-657.

Hubbert, M. K. (1949). "Energy from fossil fuels." *Science,* **109**, 103-109.

Huth, W., Dierich, C., Von Oeynhausen, V. and Seubert, W. (1974). "Multiple mitochondrial forms of acetoacetyl-CoA thiolase in rat liver. Possible regulatory role in ketogenesis." *Biochemical and Biophysical Research Communications,* **56**, 1069-77.

ICIS. “Isopropanol (IPA) Uses and Market Data.” http://www.icis.com/resources/news/2007/11/05/9076020/isopropanol-ipa-uses-and-market-data/. 01.11.2017.

IDT. “OligoAnalyzer 3.1.” https://eu.idtdna.com/calc/analyzer. 01.11.2017.

IEA. (2008). “World Energy Outlook.” International Energy Agency. Paris, France.

IEA. (2014). “Bio-based Chemicals - Value Added Products from Biorefineries.” International Energy Agency - Task 42 Biorefinery. Paris, France.

Ikura, K., Kokubu, T., Natsuka, S., Ichikawa, A., Adachi, M., Nishihara, K., Yanagi, H. and Utsumi, S. (2002). “Co-overexpression of folding modulators improves the solubility of the recombinant guinea pig liver transglutaminase expressed in Escherichia coli.” *Preparative Biochemistry & Biotechnology,* **32**, 189-205.

Ingram, L. O. (1976). “Adaptation of membrane lipids to alcohols.” *Journal of Bacteriology,* **125**, 670-8.

Inokuma, K., Liao, J. C., Okamoto, M. and Hanai, T. (2010). “Improvement of isopropanol production by metabolically engineered Escherichia coli using gas stripping.” *Journal of Bioscience and Bioengineering,* **110**, 696-701.

IRENA. (2014). “REmap 2030.” International Renewable Energy Agency, Abu Dhabi, United Arab Emirates.

Ismaiel, A. A., Zhu, C. X., Colby, G. D. and Chen, J. S. (1993). “Purification and characterization of a primary-secondary alcohol dehydrogenase from 2 strains of Clostridium beijerinckii.” *Journal of Bacteriology,* **175**, 5097-5105.

Isobe, K. and Wakao, N. (2003). “Thermostable NAD(+)-dependent (R)-specific secondary alcohol dehydrogenase from cholesterol-utilizing Burkholderia sp AIU 652.” *Journal of Bioscience and Bioengineering,* **96**, 387-393.

Ithayaraja, M., Janardan, N., Wierenga, R. K., Savithri, H. S. and Murthy, M. R. N. (2016). “Crystal structure of a thiolase from Escherichia coli at 1.8 Å resolution.” *Acta Crystallographica, Section F: Structural Biology Communications,* **72**, 534-544.

Jana, S. and Deb, J. K. (2005). “Strategies for efficient production of heterologous proteins in Escherichia coli.” *Applied Microbiology and Biotechnology,* **67**, 289-298.

Jang, Y. S., Malaviya, A., Lee, J., Im, J. A., Lee, S. Y., Eom, M. H., Cho, J. H. and Seung, D. Y. (2013). “Metabolic engineering of Clostridium acetobutylicum for the enhanced production of isopropanol-butanol-ethanol fuel mixture.” *Biotechnology Progress,* **29**, 1083-1088.

Jantama, K., Haupt, M. J., Svoronos, S. A., Zhang, X., Moore, J. C., Shanmugam, K. T. and Ingram, L. O. (2008). “Combining metabolic engineering and metabolic evolution to develop nonrecombinant strains of Escherichia coli C that produce succinate and malate.” *Biotechnology and Bioengineering,* **99**, 1140-1153.

Jendrossek, D., Kruger, N. and Steinbuchel, A. (1990). “Characterization of alcohol dehydrogenase genes of derepressible wildtype Alcaligenes eutrophus H16 and constitutive mutants.” *Journal of Bacteriology,* **172**, 4844-4851.

Jenkins, L. S. and Nunn, W. D. (1987). “Regulation of the ato operon by the atoC gene in Escherichia coli.” *Journal of Bacteriology,* **169**, 2096-2102.

Jensen, E. B. and Carlsen, S. (1990). “Production of recombinant human growth-hormone in Escherichia coli - Expression of different precursors and physiological effects of glucose, acetate and salts.” *Biotechnology and Bioengineering,* **36**, 1-11.

Jiang, Y., Xu, C. M., Dong, F., Yang, Y. L., Jiang, W. H. and Yang, S. (2009). “Disruption of the acetoacetate decarboxylase gene in solvent-producing Clostridium acetobutylicum increases the butanol ratio.” *Metabolic Engineering,* **11**, 284-291.

Joensson, L. J., Alriksson, B. and Nilvebrant, N.-O. (2013). “Bioconversion of lignocellulose: inhibitors and detoxification.” *Biotechnology for Biofuels,* **6**, 16.

Jojima, T., Inui, M. and Yukawa, H. (2008). “Production of isopropanol by metabolically engineered Escherichia coli.” *Applied Microbiology and Biotechnology,* **77**, 1219-1224.

Jones, D. T. and Woods, D. R. (1986). “Acetone-butanol fermentation revisited.” *Microbiological Reviews,* **50**, 484-524.

Jungmeier, G. (2014). "The Biorefinery Fact Sheet." International Energy Agency - Task 42 Biorefinery. Paris, France.

Kakuda, H., Shiroishi, K., Hosono, K. and Ichihara, S. (1994). "Construction of pta-ack pathway deletion mutants of Escherichia coli and characteristric growth profiles of the mutants in a rich medium." *Bioscience Biotechnology and Biochemistry,* **58**, 2232-2235.

Kalapos, M. P. (2003). "On the mammalian acetone metabolism: from chemistry to clinical implications." *Biochimica Et Biophysica Acta-General Subjects,* **1621**, 122-139.

Kang, Z., Geng, Y. P., Xia, Y. Z., Kang, J. H. and Qi, Q. S. (2009). "Engineering Escherichia coli for an efficient aerobic fermentation platform." *Journal of Biotechnology,* **144**, 58-63.

Kiefhaber, T., Rudolph, R., Kohler, H. H. and Buchner, J. (1991). "Protein aggregation in vitro and in vivo: a quantitative model of the kinetic competition between folding and aggregation." *Bio/Technology,* **9**, 825-9.

Kim, J. Y. H. and Cha, H. J. (2003). "Down-regulation of acetate pathway through antisense strategy in Escherichia coli: Improved foreign protein production." *Biotechnology and Bioengineering,* **83**, 841-853.

Kim, S., Clomburg, J. M. and Gonzalez, R. (2015a). "Synthesis of medium-chain length (C6-C10) fuels and chemicals via β-oxidation reversal in Escherichia coli." *Journal of Industrial Microbiology & Biotechnology,* **42**, 465-475.

Kim, T.-S., Jung, H.-M., Kim, S.-Y., Zhang, L., Li, J., Sigdel, S., Park, J.-H., Haw, J.-R. and Lee, J.-K. (2015b). "Reduction of acetate and lactate contributed to enhancement of a recombinant protein production in E. coli BL21." *Journal of Microbiology and Biotechnology,* **25**, 1093-1100.

Kleifeld, O., Frenkel, A., Bogin, O., Eisenstein, M., Brumfeld, V., Burstein, Y. and Sagi, I. (2000). "Spectroscopic studies of inhibited alcohol dehydrogenase from Thermoanaerobacter brockii: Proposed structure for the catalytic intermediate state." *Biochemistry,* **39**, 7702-7711.

Kleifeld, O., Shi, S. P., Zarivach, R., Eisenstein, M. and Sagi, I. (2003). "The conserved Glu-60 residue in Thermoanaerobacter brockii alcohol dehydrogenase is not essential for catalysis." *Protein Science,* **12**, 468-479.

Klinke, H. B., Thomsen, A. B. and Ahring, B. K. (2004). "Inhibition of ethanol-producing yeast and bacteria by degradation products produced during pre-treatment of biomass." *Applied Microbiology and Biotechnology,* **66**, 10-26.

Knappe, J. and Sawers, G. (1990). "A radical-chemical route to acetyl-CoA: the anaerobically induced pyruvate formate-lyase system of Escherichia coli." *Fems Microbiology Reviews,* **75**, 383-98.

Koh, B. T., Nakashimada, U., Pfeiffer, M. and Yap, M. G. S. (1992). "Comparison of acetate inhibition on growth of host and recombinant Escherichia coli K-12 strains." *Biotechnology Letters,* **14**, 1115-1118.

Korkhin, Y., Kalb, A. J., Peretz, M., Bogin, O., Burstein, Y. and Frolow, F. (1998). "NADP-dependent bacterial alcohol dehydrogenases: Crystal structure, cofactor-binding and cofactor specificity of the ADHs of Clostridium beijerinckii and Thermoanaerobacter brockii." *Journal of Molecular Biology,* **278**, 967-981.

Korz, D. J., Rinas, U., Hellmuth, K., Sanders, E. A. and Deckwer, W. D. (1995). "Simple fed-batch technique for high cell density cultivation of Escherichia coli." *Journal of Biotechnology,* **39**, 59-65.

Kozak, B. U., van Rossum, H. M., Luttik, M. A. H., Akeroyd, M., Benjamin, K. R., Wu, L., de Vries, S., Daran, J.-M., Pronk, J. T. and van Maris, A. J. A. (2014). "Engineering acetyl coenzyme a supply: functional expression of a bacterial pyruvate dehydrogenase complex in the cytosol of Saccharomyces cerevisiae." *mBio,* **5**, e01696-14/1-e01696-14/12.

Krivoruchko, A., Zhang, Y. M., Siewers, V., Chen, Y. and Nielsen, J. (2015). "Microbial acetyl-CoA metabolism and metabolic engineering." *Metabolic Engineering,* **28**, 28-42.

Kumar, A., Shen, P. S., Descoteaux, S., Pohl, J., Bailey, G. and Samuelson, J. (1992). "Cloning and expression of an NADP+-dependent alcohol dehydrogenase gene of Entamoeba histolytica." *Proceedings of the National Academy of Sciences of the United States of America,* **89**, 10188-10192.

Kumar, P., Barrett, D. M., Delwiche, M. J. and Stroeve, P. (2009). "Methods for Pretreatment of Lignocellulosic Biomass for Efficient Hydrolysis and Biofuel Production." *Industrial & Engineering Chemistry Research,* **48**, 3713-3729.

Kusakabe, T., Tatsuke, T., Tsuruno, K., Hirokawa, Y., Atsumi, S., Liao, J. C. and Hanai, T. (2013). "Engineering a synthetic pathway in cyanobacteria for isopropanol production directly from carbon dioxide and light." *Metabolic Engineering,* **20**, 101-108.

Kyte, J. and Doolittle, R. F. (1982). "A simple method for displaying the hydropathic character of a protein." *Journal of Molecular Biology,* **157**, 105-32.

la Grange, D. C., den Haan, R. and van Zyl, W. H. (2010). "Engineering cellulolytic ability into bioprocessing organisms." *Applied Microbiology and Biotechnology,* **87**, 1195-1208.

Laemmli, U. K. (1970). "Cleavage of structural proteins during the assembly of the head of bacteriophage T4." *Nature (London, U. K.),* **227**, 680-685.

Lamed, R. J. and Zeikus, J. G. (1981). "Novel NADP-linked alcohol-aldehyde/ketone oxidoreductase in thermophilic ethanologenic bacteria." *Biochemical Journal,* **195**, 183-190.

Lan, E. I. and Liao, J. C. (2012). "ATP drives direct photosynthetic production of 1-butanol in cyanobacteria." *Proceedings of the National Academy of Sciences of the United States of America,* **109**, 6018-6023.

Larsson, S., Reimann, A., Nilvebrant, N. O. and Jonsson, L. J. (1999). "Comparison of different methods for the detoxification of lignocellulose hydrolyzates of spruce." *Applied Biochemistry and Biotechnology,* **77-9**, 91-103.

Latendresse, M., Malerich, J. P., Travers, M. and Karp, P. D. (2012). "Accurate Atom-Mapping Computation for Biochemical Reactions." *Journal of Chemical Information and Modeling,* **52**, 2970-2982.

Lee, H. V., Hamid, S. B. A. and Zain, S. K. (2014). "Conversion of lignocellulosic biomass to nanocellulose: structure and chemical process." *The Scientific World Journal*, 631013/1-631013/21.

Lee, J., Jang, Y. S., Choi, S. J., Im, J. A., Song, H., Cho, J. H., Seung, D. Y., Papoutsakis, E. T., Bennett, G. N. and Lee, S. Y. (2012a). "Metabolic Engineering of Clostridium acetobutylicum ATCC 824 for Isopropanol-Butanol-Ethanol Fermentation." *Applied and Environmental Microbiology,* **78**, 1416-1423.

Lee, S.-H., Yun, E. J., et al. (2016). "Biomass, strain engineering, and fermentation processes for butanol production by solventogenic clostridia." *Applied Microbiology and Biotechnology,* **100**, 8255-8271.

Lee, S., Nam, D., Jung, J. Y., Oh, M. K., Sang, B. I. and Mitchell, R. J. (2012b). "Identification of Escherichia coli biomarkers responsive to various lignin-hydrolysate compounds." *Bioresource Technology,* **114**, 450-456.

Lee, W. H., Kim, M. D., Jin, Y. S. and Seo, J. H. (2013). "Engineering of NADPH regenerators in Escherichia coli for enhanced biotransformation." *Applied Microbiology and Biotechnology,* **97**, 2761-2772.

Lehmann, D., Honicke, D., Ehrenreich, A., Schmidt, M., Weuster-Botz, D., Bahl, H. and Lutke-Eversloh, T. (2012). "Modifying the product pattern of Clostridium acetobutylicum." *Applied Microbiology and Biotechnology,* **94**, 743-754.

Lenz, T. G. and Moreira, A. R. (1980). "Economic evaluation of the acetone-butanol fermentation." *Industrial & Engineering Chemistry Product Research and Development,* **19**, 478-83.

Leonard, E., Lim, K.-H., Saw, P.-N. and Koffas, M. A. G. (2007). "Engineering central metabolic pathways for high-level flavonoid production in Escherichia coli." *Applied and Environmental Microbiology,* **73**, 3877-3886.

Liang, L. Y., Liu, R. M., Garst, A. D., Lee, T., Nogue, V. S. I., Beckham, G. T. and Gill, R. T. (2017). "CRISPR EnAbled Trackable genome Engineering for isopropanol production in Escherichia coli." *Metabolic Engineering,* **41**, 1-10.

Lin, H., Castro, N. M., Bennett, G. N. and San, K. Y. (2006). "Acetyl-CoA synthetase overexpression in Escherichia coli demonstrates more efficient acetate assimilation and lower acetate accumulation: a potential tool in metabolic engineering." *Applied Microbiology and Biotechnology,* **71**, 870-874.

Lin, Y. L. and Blaschek, H. P. (1983). "Butanol production by a butanol-tolerant strain of Clostridium acetobutylicum in extruded corn broth." *Applied and Environmental Microbiology,* **45**, 966-73.

Lin, Y. S., Wang, J., Wang, X. M. and Sun, X. H. (2011). "Optimization of butanol production from corn straw hydrolysate by Clostridium acetobutylicum using response surface method." *Chinese Science Bulletin,* **56**, 1422-1428.

Liu, M., Chen, H., Zhao, Z., Liu, H., Xian, M., Zhao, G. and Ding, Y. (2017). "Improving the production of acetyl-CoA-derived chemicals in Escherichia coli BL21(DE3) through iclR and arcA deletion." *BMC Microbiology,* **17**, 10.

Liu, T. J., Lin, L., Sun, Z. J., Hu, R. F. and Liu, S. J. (2010). "Bioethanol fermentation by recombinant E. coli FBR5 and its robust mutant FBHW using hot-water wood extract hydrolyzate as substrate." *Biotechnology Advances,* **28**, 602-608.

Long, C. P., Gonzalez, J. E., Sandoval, N. R. and Antoniewicz, M. R. (2016). "Characterization of physiological responses to 22 gene knockouts in Escherichia coli central carbon metabolism." *Metabolic Engineering,* **37**, 102-113.

Lopez-Soriano, F. J., Alemany, M. and Argiles, J. M. (1985). "Rat acetoacetic acid decarboxylase inhibition by acetone." *International Journal of Biochemistry,* **17**, 1271-1273.

Lopez-Soriano, F. J. and Argiles, J. M. (1986). "Rat acetoacetate decarboxylase - Its role in the disposal of 4C-ketone bodies by the fetus." *Hormone and Metabolic Research,* **18**, 446-449.

Luli, G. W. and Strohl, W. R. (1990). "Comparison of growth, acetate production, and acetate inhibition of *Escherichia coli* strains in batch and fed-batch fermentations." *Applied and Environmental Microbiology,* **56**, 1004-1011.

Lynnes, T., Pruss, B. M. and Samanta, P. (2013). "Acetate metabolism and Escherichia coli biofilm: new approaches to an old problem." *Fems Microbiology Letters,* **344**, 95-103.

Maddox, I. S., Steiner, E., Hirsch, S., Wessner, S., Gutierrez, N. A., Gapes, J. R. and Schuster, K. C. (2000). "The cause of "acid crash" and "acidogenic fermentations" duping the batch acetone-butanol-ethanol (ABE-) fermentation process." *Journal of Molecular Microbiology and Biotechnology,* **2**, 95-100.

Mann, M. S. and Lutke-Eversloh, T. (2013). "Thiolase engineering for enhanced butanol production in Clostridium acetobutylicum." *Biotechnology and Bioengineering,* **110**, 887-897.

Marblestone, J. G., Edavettal, S. C., Lim, Y., Lim, P., Zuo, X. and Butt, T. R. (2006). "Comparison of SUMO fusion technology with traditional gene fusion systems: Enhanced expression and solubility with SUMO." *Protein Science,* **15**, 182-189.

Marc, J., Grousseau, E., Lombard, E., Sinskey, A. J., Gorret, N. and Guillouet, S. E. (2017). "Over expression of GroESL in Cupriavidus necator for heterotrophic and autotrophic isopropanol production." *Metabolic Engineering,* **42**, 74-84.

Marques, J. C., Oh, I. K., Ly, D. C., Lamosa, P., Ventura, M. R., Miller, S. T. and Xavier, K. B. (2014). "LsrF, a coenzyme A-dependent thiolase, catalyzes the terminal step in processing the quorum sensing signal autoinducer-2." *Proceedings of the National Academy of Sciences of the United States of America,* **111**, 14235-14240.

Matar, S., Hatch, L. F. (2001). "Chemistry of Petrochemical Processes." 2nd ed., Elsevier Inc.

Mathews, S. L., Pawlak, J. and Grunden, A. M. (2015). "Bacterial biodegradation and bioconversion of industrial lignocellulosic streams." *Applied Microbiology and Biotechnology,* **99**, 2939-54.

May, A., Fischer, R.-J., Maria Thum, S., Schaffer, S., Verseck, S., Durre, P. and Bahl, H. (2013). "A modified pathway for the production of acetone in Escherichia coli." *Metabolic Engineering,* **15**, 218-25.

McAtee, A. G., Jazmin, L. J. and Young, J. D. (2015). "Application of isotope labeling experiments and C-13 flux analysis to enable rational pathway engineering." *Current Opinion in Biotechnology,* **36**, 50-56.

McMahon, M. and Mulcahy, P. (2002). "Bioaffinity purification of NADP(+)-dependent dehydrogenases: Studies with alcohol dehydrogenase from Thermoanaerobacter brockii." *Biotechnology and Bioengineering,* **77**, 517-527.

Meier, E. "European Beech." http://www.wood-database.com/european-beech/. 02.11.2017.

Mellmann, A., Lu, S., Karch, H., Xu, J.-g., Harmsen, D., Schmidt, M. A. and Bielaszewska, M. (2008). "Recycling of Shiga toxin 2 genes in sorbitol-fermenting enterohemorrhagic Escherichia coli O157:NM." *Applied and Environmental Microbiology,* **74**, 67-72.

Mermelstein, L. D., Welker, N. E., Bennett, G. N. and Papoutsakis, E. T. (1992). "Expression of cloned homologous fermentative genes in Clostridium acetobutylicum ATCC 824." *Bio-Technology,* **10**, 190-195.

Meyer, C. L. and Papoutsakis, E. T. (1989). "Increased levels of ATP and NADH are associated with increased solvent production in continuous cultures of Clostridium acetobutylicum." *Applied Microbiology and Biotechnology,* **30**, 450-459.

Miller, C. A., Ingmer, H. and Cohen, S. N. (1995). "Boundaries of the pSC101 Minimal Replicon Are Conditional." *Journal of Bacteriology,* **177**, 4865-4871.

Miller, E. N., Jarboe, L. R., Yomano, L. P., York, S. W., Shanmugam, K. T. and Ingram, L. O. (2009). "Silencing of NADPH-Dependent Oxidoreductase Genes (yqhD and dkgA) in Furfural-Resistant Ethanologenic Escherichia coli." *Applied and Environmental Microbiology,* **75**, 4315-4323.

Miller, R. G. and Sorrell, S. R. (2014). "The future of oil supply " *Philosophical Transactions of the Royal Society a-Mathematical Physical and Engineering Sciences,* **372**.

Mills, T. Y., Sandoval, N. R. and Gill, R. T. (2009). "Cellulosic hydrolysate toxicity and tolerance mechanisms in Escherichia coli." *Biotechnology for Biofuels,* **2**, No pp. given.

Mingardon, F., Chanal, A., Tardif, C. and Fierobe, H. P. (2011). "The Issue of Secretion in Heterologous Expression of Clostridium cellulolyticum Cellulase-Encoding Genes in Clostridium acetobutylicum ATCC 824." *Applied and Environmental Microbiology,* **77**, 2831-2838.

Mingardon, F., Perret, S., Belaich, A., Tardif, C., Belaich, J. P. and Fierobe, H. P. (2005). "Heterologous production, assembly, and secretion of a minicellulosome by Clostridium acetobutylicum ATCC 824." *Applied and Environmental Microbiology,* **71**, 1215-1222.

Mitchell, W. J., Albasheri, K. A. and Yazdanian, M. (1995). "Factors affecting utilization of carbohydrates by Clostridia." *Fems Microbiology Reviews,* **17**, 317-329.

Molgat, G. F., Donald, L. J. and Duckworth, H. W. (1992). "Chimeric allosteric citrate synthases: construction and properties of citrate synthases containing domains from two different enzymes." *Archives of Biochemistry and Biophysics,* **298**, 238-46.

Mollah, A. H. and Stuckey, D. C. (1993). "Feasibility of in situ gas stripping for continuous acetone-butanol fermentation by Clostridium acetobutylicum." *Enzyme and Microbial Technology,* **15**, 200-207.

Monod, J. (1949). "The growth of bacterial cultures." *Annual Review of Microbiology,* **3**, 371-94.

Monot, F., Engasser, J. M. and Petitdemange, H. (1984). "Influences of pH and undissociated butyric acid on the production of acetone and butanol in batch cultures of Clostridium acetobutylicum." *Applied Microbiology and Biotechnology,* **19**, 422-426.

Montenecourt, B. S. (1983). "Trichoderma reesei cellulases." *Trends in Biotechnology,* **1**, 156-61.

Mülhardt, C. (2013). "Der Experimentator Molekularbiologie/Genomics." 7th ed., Springer Spektrum, Berlin

Murphy, K. C. (2007). "The λ Gam Protein Inhibits RecBCD Binding to dsDNA Ends." *Journal of Molecular Biology,* **371**, 19-24.

Mussatto, S. I. and Roberto, I. C. (2004). "Alternatives for detoxification of diluted-acid lignocellulosic hydrolyzates for use in fermentative processes: a review." *Bioresource Technology,* **93**, 1-10.

Nair, R., Salvi, P., Banerjee, S., Raiker, V. A., Bandyopadhyay, S., Soorapaneni, S., Kotwal, P. and Padmanabhan, S. (2009). "Yeast extract mediated autoinduction of lacUV5 promoter: an insight." *New Biotechnology,* **26**, 282-288.

Nair, R. V. and Papoutsakis, E. T. (1994). "Expression of plasmid-encoded AAD in clostridium acetobutylicum M5 restores vigorous butanol production." *Journal of Bacteriology,* **176**, 5843-5846.

Nakajima, N., Ishihara, K., Tanabe, M., Matsubara, K. and Matsuura, Y. (1999). "Degradation of pectic substances by two pectate lyases from a human intestinal bacterium, Clostridium butyricum-beijerinckii group." *Journal of Bioscience and Bioengineering,* **88**, 331-333.

Nancib, N., Branlant, C. and Boudrant, J. (1991). "Metabolic roles of peptone and yeast extract for the culture of a recombinant strain of Escherichia coli." *Journal of Industrial Microbiology & Biotechnology,* **8**, 165-9.

NCC. (2014). "Cotton Supply and Demand." https://www.cotton.org/econ/cropinfo/supply-demand.cfm. 02.11.2017.

Nichols, N. N., Dien, B. S. and Bothast, R. J. (2001). "Use of catabolite repression mutants for fermentation of sugar mixtures to ethanol." *Applied Microbiology and Biotechnology,* **56**, 120-125.

Nicolaou, S. A., Gaida, S. M. and Papoutsakis, E. T. (2010). "A comparative view of metabolite and substrate stress and tolerance in microbial bioprocessing: From biofuels and chemicals, to biocatalysis and bioremediation." *Metabolic Engineering,* **12**, 307-331.

Nishihara, K., Kanemori, M., Kitagawa, M., Yanagi, H. and Yura, T. (1998). "Chaperone coexpression plasmids: Differential and synergistic roles of DnaK-DnaJ-GrpE and GroEL-GroES in assisting folding of an allergen of Japanese cedar pollen, Cryj2 in Escherichia coli." *Applied and Environmental Microbiology,* **64**, 1694-1699.

Nykanen, M., Saarelainen, R., Raudaskoski, M., Nevalainen, K. M. H. and Mikkonen, A. (1997). "Expression and secretion of barley cysteine endopeptidase B and cellobiohydrolase I in Trichoderma reesei." *Applied and Environmental Microbiology,* **63**, 4929-4937.

Ohno, S., Furusawa, C. and Shimizu, H. (2013). "In silico screening of triple reaction knockout Escherichia coli strains for overproduction of useful metabolites." *Journal of Bioscience and Bioengineering,* **115**, 221-228.

Okochi, M., Kurimoto, M., Shimizu, K. and Honda, H. (2007). "Increase of organic solvent tolerance by overexpression of manXYZ in Escherichia coli." *Applied Microbiology and Biotechnology,* **73**, 1394-1399.

Oksanen, T., Pere, J., Paavilainen, L., Buchert, J. and Viikari, L. (2000). "Treatment of recycled kraft pulps with Trichoderma reesei hemicellulases and cellulases." *Journal of Biotechnology,* **78**, 39-48.

Orosz, A., Boros, I. and Venetianer, P. (1991). "Analysis of the complex transcription termination region of the Escherichia coli rrnB gene." *European Journal of Biochemistry,* **201**, 653-9.

Outram, V., Lalander, C. A., Lee, J. G. M., Davies, E. T. and Harvey, A. P. (2017). "Applied in Situ Product Recovery in ABE Fermentation." *Biotechnology Progress,* **33**, 563-579.

Owen, N. A., Inderwildi, O. R. and King, D. A. (2010). "The status of conventional world oil reserves-Hype or cause for concern?" *Energy Policy,* **38**, 4743-4749.

Palmer, B. R. and Marinus, M. G. (1994). "The dam and dcm strains of Escherichia coli--a review." *Gene,* **143**, 1-12.

Palmqvist, E. and Hahn-Hagerdal, B. (2000a). "Fermentation of lignocellulosic hydrolysates. I: inhibition and detoxification." *Bioresource Technology,* **74**, 17-24.

Palmqvist, E. and Hahn-Hagerdal, B. (2000b). "Fermentation of lignocellulosic hydrolysates. II: inhibitors and mechanisms of inhibition." *Bioresource Technology,* **74**, 25-33.

Pampulha, M. E. and Loureiro-Dias, M. C. (1989). "Combined effect of acetic acid, pH and ethanol on intracellular pH of fermenting yeast." *Applied Microbiology and Biotechnology,* **31**, 547-50.

Panavas, T., Sanders, C. and Butt, T. R. (2009). "SUMO fusion technology for enhanced protein production in prokaryotic and eukaryotic expression systems." *Methods in Molecular Biology,* **497**, 303-317.

Park, C. H. and Geng, Q. H. (1992). "Simultaneous fermentation and separation in the ethanol and Abe fermentation." *Separation and Purification Methods,* **21**, 127-174.

Park, J., Rodriguez-Moya, M., Li, M., Pichersky, E., San, K.-Y. and Gonzalez, R. (2012). "Synthesis of methyl ketones by metabolically engineered Escherichia coli." *Journal of Industrial Microbiology & Biotechnology,* **39**, 1703-1712.

Pauli, G. and Overath, P. (1972). "Ato operon - a highly inducible system for acetoacetate and butyrate degradation in Escherichia coli." *European Journal of Biochemistry,* **29**, 553-&.

Pereira, D. A., Pinto, G. F. and Oestreicher, E. G. (1994). “Kinetic mechanism of the oxidation of 2-propanol catalyzed by Thermoanaerobium brockii alcohol dehydrogenase.” *Journal of Biotechnology,* **34**, 43-50.

Perez, J. M., Arenas, F. A., Pradenas, G. A., Sandoval, J. M. and Vasquez, C. C. (2008). “Escherichia coli YqhD Exhibits Aldehyde Reductase Activity and Protects from the Harmful Effect of Lipid Peroxidation-derived Aldehydes.” *Journal of Biological Chemistry,* **283**, 7346-7353.

Petersen, D. J., Cary, J. W., Vanderleyden, J. and Bennett, G. N. (1993). “Sequence and arrangement of genes encoding enzymes of the acetone-production pathway of Clostridium acetobutylicum ATCC 824.” *Gene,* **123**, 93-97.

Phue, J.-N. and Shiloach, J. (2004). “Transcription levels of key metabolic genes are the cause for different glucose utilization pathways in E. coli B (BL21) and E. coli K (JM109).” *Journal of Biotechnology,* **109**, 21-30.

Presnyak, V., Alhusaini, N., Chen, Y. H., Martin, S., Morris, N., Kline, N., Olson, S., Weinberg, D., Baker, K. E., Graveley, B. R. and Coller, J. (2015). “Codon Optimality Is a Major Determinant of mRNA Stability.” *Cell,* **160**, 1111-1124.

Qureshi, N. and Blaschek, H. P. (2001). “ABE production from corn: a recent economic evaluation.” *Journal of Industrial Microbiology & Biotechnology,* **27**, 292-297.

Qureshi, N., Saha, B. C., Dien, B., Hector, R. E. and Cotta, M. A. (2010a). “Production of butanol (a biofuel) from agricultural residues: Part I - Use of barley straw hydrolysate.” *Biomass & Bioenergy,* **34**, 559-565.

Qureshi, N., Saha, B. C., Hector, R. E., Dien, B., Hughes, S., Liu, S., Iten, L., Bowman, M. J., Sarath, G. and Cotta, M. A. (2010b). “Production of butanol (a biofuel) from agricultural residues: Part II - Use of corn stover and switchgrass hydrolysates.” *Biomass & Bioenergy,* **34**, 566-571.

Ramirez, D. M. and Bentley, W. E. (1993). “Enhancement of recombinant protein synthesis and stability via coordinated amino acid addition.” *Biotechnology and Bioengineering,* **41**, 557-65.

Rehm, H. (2016). "Der Experimentator Proteinbiochemie/Proteomics." 7th ed., Springer Spektrum, Berlin.

Reid, M. F. and Fewson, C. A. (1994). “Molecular Characterization of Microbial Alcohol Dehydrogenases.” *Critical Reviews in Microbiology,* **20**, 13-56.

Reyes, L. H., Almario, M. P. and Kao, K. C. (2011). “Genomic Library Screens for Genes Involved in n-Butanol Tolerance in Escherichia coli.” *Plos One,* **6**.

Reznikoff, W. S. (1992). “The lactose operon-controlling elements: a complex paradigm.” *Molecular Microbiology,* **6**, 2419-22.

Roe, A. J., McLaggan, D., Davidson, I., O'Byrne, C. and Booth, I. R. (1998). “Perturbation of anion balance during inhibition of growth of Escherichia coli by weak acids.” *Journal of Bacteriology,* **180**, 767-772.

Rosano, G. L. and Ceccarelli, E. A. (2014). “Recombinant protein expression in Escherichia coli: advances and challenges.” *Frontiers in microbiology,* **5**.

Royce, P. N. (1992). “Effect of changes in the pH and carbon dioxide evolution rate on the measured respiratory quotient of fermentations.” *Biotechnology and Bioengineering,* **40**, 1129-1138.

Rozen, S. “Primer3web 4.0.0.” http://primer3.ut.ee/. 01.11.2017.

Rozzell, J. D. and Benner, S. A. (1984). “Stereochemical imperative in enzymic decarboxylations. Stereochemical course of the decarboxylation catalyzed by acetoacetate decarboxylase.” *Journal of the American Chemical Society,* **106**, 4937-4941.

Rumbold, K., van Buijsen, H. J. J., Overkamp, K. M., van Groenestijn, J. W., Punt, P. J. and van der Werf, M. J. (2009). “Microbial production host selection for converting second-generation feedstocks into bioproducts.” *Microbial Cell Factories,* **8**.

Russell, J. B. (1992). “Another explanation for the toxicity of fermentation acids at low pH - anion accumulation versus uncoupling.” *Journal of Applied Bacteriology,* **73**, 363-370.

Rutter, C. and Chen, R. (2014). “Improved cellobiose utilization in E. coli by including both hydrolysis and phosphorolysis mechanisms.” *Biotechnology Letters,* **36**, 301-307.

Saha, B. and Cotta, M. A. (2012). "Ethanol production from lignocellulosic biomass by recombinant Escherichia coli strain FBR5." *Bioengineered,* **3**, 197-202.

Saini, J. K., Tewari, L. and Saini, R. (2015). "Lignocellulosic agriculture wastes as biomass feedstocks for second-generation bioethanol production: concepts and recent developments." *3 Biotech,* **5**, 337-353.

Schweizer, H. P. (2003). "Applications of the Saccharomyces cerevisiae Flp-FRT system in bacterial genetics." *Journal of Molecular Microbiology and Biotechnology,* **5**, 67-77.

Sears, K. D., Beelik, A., Casebier, R. L., Engen, R. J., Hamilton, J. K. and Hergert, H. L. (1971). "Southern pine prehydrolyzates. Characterization of polysaccharides and lignin fragments." *Journal of Polymer Science, Part C,* **36**, 425-43.

Seregina, T. A., Osipov, G. A., Shakulov, R. S. and Mironov, A. S. (2012). "Isolation and Phenotypic Characteristics of the Escherichia coli Butanol-Tolerant Mutants." *Microbiology,* **81**, 208-215.

Servinsky, M. D., Kiel, J. T., Dupuy, N. F. and Sund, C. J. (2010). "Transcriptional analysis of differential carbohydrate utilization by Clostridium acetobutylicum." *Microbiology Society,* **156**, 3478-3491.

Shen, Y., Fatemeh, T., Tang, L. H. and Cai, Z. W. (2016). "Quantitative metabolic network profiling of Escherichia coli: An overview of analytical methods for measurement of intracellular metabolites." *Trac-Trends in Analytical Chemistry,* **75**, 141-150.

Shiloach, J. and Fass, R. (2005). "Growing E. coli to high cell density - A historical perspective on method development." *Biotechnology Advances,* **23**, 345-357.

Shiloach, J., Kaufman, J., Guillard, A. S. and Fass, R. (1996). "Effect of glucose supply strategy on acetate accumulation, growth, and recombinant protein production by Escherichia coli BL21 (λDE3) and Escherichia coli JM109." *Biotechnology and Bioengineering,* **49**, 421-8.

Shiloach, J., Reshamwala, S., Noronha, S. B. and Negrete, A. (2010). "Analyzing metabolic variations in different bacterial strains, historical perspectives and current trends - example E. coli." *Current Opinion in Biotechnology,* **21**, 21-26.

Shimizu, N., Fukuzono, S., Fujimori, K., Nishimura, N. and Odawara, Y. (1988). "Fed-batch cultures of recombinant Escherichia coli with inhibitory substance concentration monitoring." *Journal of Fermentation Technology,* **66**, 187-91.

Shin, H. D., Wu, J. R. and Chen, R. (2014). "Comparative engineering of Escherichia coli for cellobiose utilization: Hydrolysis versus phosphorolysis." *Metabolic Engineering,* **24**, 9-17.

Shoaie, S., Karlsson, F., Mardinoglu, A., Nookaew, I., Bordel, S. and Nielsen, J. (2013). "Understanding the interactions between bacteria in the human gut through metabolic modeling." *Scientific Reports,* **3**, 2532.

SIB. "ProtParam." http://web.expasy.org/protparam/. 01.11.2017.

Siguenza, R., Flores, N., Hernandez, G., Martinez, A., Bolivar, F. and Valle, F. (1999). "Kinetic characterization in batch and continuous culture of Escherichia coli mutants affected in phosphoenolpyruvate metabolism: differences in acetic acid production." *World Journal of Microbiology & Biotechnology,* **15**, 587-592.

Sikkema, J., Debont, J. A. M. and Poolman, B. (1995). "Mechanisms of membrane toxicity of hydrocarbons." *Microbiological Reviews,* **59**, 201-222.

Soini, J., Ukkonen, K. and Neubauer, P. (2008). "High cell density media for Escherichia coli are generally designed for aerobic cultivations - consequences for large-scale bioprocesses and shake flask cultures." *Microbial Cell Factories,* **7**.

Soma, Y. and Hanai, T. (2015). "Self-induced metabolic state switching by a tunable cell density sensor for microbial isopropanol production." *Metabolic Engineering,* **30**, 7-15.

Soma, Y., Inokuma, K., Tanaka, T., Ogino, C., Kondo, A., Okamoto, M. and Hanai, T. (2012). "Direct isopropanol production from cellobiose by engineered Escherichia coli using a synthetic pathway and a cell surface display system." *Journal of Bioscience and Bioengineering,* **114**, 80-85.

Soma, Y., Tsuruno, K., Wada, M., Yokota, A. and Hanai, T. (2014). "Metabolic flux redirection from a central metabolic pathway toward a synthetic pathway using a metabolic toggle switch." *Metabolic Engineering,* **23**, 175-184.

Spaans, S. K., van, d. O. J., Kengen, S. W. M. and Weusthuis, R. A. (2015). "NADPH-generating systems in bacteria and archaea." *Frontiers in microbiology,* **6**, 742.

Sramek, S. J. and Frerman, F. E. (1975a). "Escherichia coli coenzyme A-Transferase - Kinetics, catalytic pathway and structure." *Archives of Biochemistry and Biophysics,* **171**, 27-35.

Sramek, S. J. and Frerman, F. E. (1975b). "Purification and properties of Escherichia coli coenzyme A-transferase." *Archives of Biochemistry and Biophysics,* **171**, 14-26.

Sramek, S. J. and Frerman, F. E. (1977). "Steady State kinetic mechanism of the Escherichia coli Coenzyme A Transferase." *Archives of Biochemistry and Biophysics,* **181**, 178-184.

Sramek, S. J., Frerman, F. E. and Adams, M. B. (1977a). "Sulfhydryl group reactivity in the Escherichia coli CoA transferase." *Archives of Biochemistry and Biophysics,* **181**, 516-524.

Sramek, S. J., Frerman, F. E., McCormick, D. J. and Duncombe, G. R. (1977b). "Substrate-induced conformational changes and half-sites reactivity in Escherichia coli CoA transferase." *Archives of Biochemistry and Biophysics,* **181**, 525-533.

Stewart, D. (2008). "Lignin as a base material for materials applications: Chemistry, application and economics." *Industrial Crops and Products,* **27**, 202-207.

Su, P., Delaney, S. F. and Rogers, P. L. (1989). "Cloning and expression of a β-glucosidase gene from Xanthomonas albilineans in Escherichia coli and Zymomonas mobilis." *Journal of Biotechnology,* **9**, 139-52.

Summers, D. K. and Sherratt, D. J. (1988). "Resolution of ColE1 dimers requires a DNA sequence implicated in the three-dimensional organization of the cer site." *EMBO Journal,* **7**, 851-8.

Sun, Y. and Cheng, J. Y. (2002). "Hydrolysis of lignocellulosic materials for ethanol production: a review." *Bioresource Technology,* **83**, 1-11.

Sun, Z., Chen, Y. X., Yang, C., Yang, S., Gu, Y. and Jiang, W. H. (2015). "A novel three-component system-based regulatory model for D-xylose sensing and transport in Clostridium beijerinckii." *Molecular Microbiology,* **95**, 576-589.

Survase, S. A., Jurgens, G., van Heiningen, A. and Granstrom, T. (2011). "Continuous production of isopropanol and butanol using Clostridium beijerinckii DSM 6423." *Applied Microbiology and Biotechnology,* **91**, 1305-1313.

Sutak, R., Hrdy, I., Dolezal, P., Cabala, R., Sedinova, M., Lewin, J., Harant, K., Muller, M. and Tachezy, J. (2012). "Secondary alcohol dehydrogenase catalyzes the reduction of exogenous acetone to 2-propanol in Trichomonas vaginalis." *Febs Journal,* **279**, 2768-2780.

Tagaki, W., Guthrie, J. P. and Westheimer, F. H. (1968). "Acetoacetate decarboxylase. Reaction with acetopyruvate." *Biochemistry,* **7**, 905-+.

Tagaki, W. and Westheimer, F. H. (1968). "Acetoacetate decarboxylase. Catalysis of hydrogen-deuterium exchange in acetone." *Biochemistry,* **7**, 901-+.

Taherzadeh, M. J. and Karimi, K. (2008). "Pretreatment of lignocellulosic wastes to improve ethanol and biogas production: A review." *International Journal of Molecular Sciences,* **9**, 1621-1651.

Takeshita, S., Sato, M., Toba, M., Masahashi, W. and Hashimotogotoh, T. (1987). "High-copy-number and low-copy-number plasmid vectors for LacZ-alpha complementation and chloramphenicol resistance or kanamycin resistance selection." *Gene,* **61**, 63-74.

Tamakawa, H., Mita, T., Yokoyama, A., Ikushima, S. and Yoshida, S. (2013). "Metabolic engineering of Candida utilis for isopropanol production." *Applied Microbiology and Biotechnology,* **97**, 6231-6239.

Tamano, K. (2014). "Enhancing microbial metabolite and enzyme production: current strategies and challenges." *Frontiers in microbiology,* **5**, 718.

TBI. "RNAfold." http://rna.tbi.univie.ac.at/cgi-bin/RNAWebSuite/RNAfold.cgi. 01.11.2017.

Terpe, K. (2003). "Overview of tag protein fusions: from molecular and biochemical fundamentals to commercial systems." *Applied Microbiology and Biotechnology,* **60**, 523-533.

Timell, T. E. (1967). "Recent progress in the chemistry of wood hemicelluloses." *Wood Science and Technology,* **1**, 45-70.

Torres, S., Pandey, A. and Castro, G. R. (2011). "Organic solvent adaptation of Gram positive bacteria: Applications and biotechnological potentials." *Biotechnology Advances,* **29**, 442-452.

Ulbricht, R. J., Northup, S. J. and Thomas, J. A. (1984). "A review of 5-hydroxymethylfurfural (HMF) in parenteral solutions." *Fundamental and Applied Toxicology,* **4**, 843-853.

UNFCCC. (2015). "Paris Agreement." United Nations Framework Convention on Climate Change. Paris, France.

van der Merwe, A. B., Cheng, H., Gorgens, J. F. and Knoetze, J. H. (2013). "Comparison of energy efficiency and economics of process designs for biobutanol production from sugarcane molasses." *Fuel,* **105**, 451-458.

van Rooyen, R., Hahn-Haegerdal, B., La Grange, D. C. and van Zyl, W. H. (2005). "Construction of cellobiose-growing and fermenting Saccharomyces cerevisiae strains." *Journal of Biotechnology,* **120**, 284-295.

Varshavsky, A. (1997). "The N-end rule pathway of protein degradation." *Genes Cells,* **2**, 13-28.

Veit, A., Polen, T. and Wendisch, V. F. (2007). "Global gene expression analysis of glucose overflow metabolism in Escherichia coli and reduction of aerobic acetate formation." *Applied Microbiology and Biotechnology,* **74**, 406-421.

Vemuri, G. N., Altman, E., Sangurdekar, D. P., Khodursky, A. B. and Eiteman, M. A. (2006). "Overflow metabolism in Escherichia coli during steady-state growth: Transcriptional regulation and effect of the redox ratio." *Applied and Environmental Microbiology,* **72**, 3653-3661.

Viegas, C. A. and Sa-Correia, I. (1991). "Activation of plasma membrane ATPase of Saccharomyces cerevisiae by octanoic acid." *Journal of General Microbiology,* **137**, 645-51.

Vinuselvi, P., Kim, M. K., Lee, S. K. and Ghim, C. M. (2012). "Rewiring carbon catabolite repression for microbial cell factory." *Bmb Reports,* **45**, 59-70.

Vinuselvi, P. and Lee, S. K. (2011). "Engineering Escherichia coli for efficient cellobiose utilization." *Applied Microbiology and Biotechnology,* **92**, 125-132.

Voronovsky, A. Y., Rohulya, O. V., Abbas, C. A. and Sibirny, A. A. (2009). "Development of strains of the thermotolerant yeast Hansenula polymorpha capable of alcoholic fermentation of starch and xylan." *Metabolic Engineering,* **11**, 234-242.

Wang, S. H., Zhang, Y. P., Dong, H. J., Mao, S. M., Zhu, Y., Wang, R. J., Luan, G. D. and Li, Y. (2011). "Formic Acid Triggers the "Acid Crash" of Acetone-Butanol-Ethanol Fermentation by Clostridium acetobutylicum." *Applied and Environmental Microbiology,* **77**, 1674-1680.

Weizmann, C. (1919). "Production of acetone and alcohol by bacteriological processes."

Welch, M., Villalobos, A., Gustafsson, C. and Minshull, J. (2009). "You're one in a googol: optimizing genes for protein expression." *Journal of the Royal Society Interface,* **6**.

Wiesenborn, D. P., Rudolph, F. B. and Papoutsakis, E. T. (1988). "Thiolase from Clostridium acetobutylicum ATCC 824 and its role in the synthesis of acids and solvents." *Applied and Environmental Microbiology,* **54**, 2717-2722.

Wiesenborn, D. P., Rudolph, F. B. and Papoutsakis, E. T. (1989). "Coenzyme-A transferase from Clostridium acetobutylicum ATCC 824 and its role in the uptake of acids." *Applied and Environmental Microbiology,* **55**, 323-329.

Wietzke, M. and Bahl, H. (2012). "The redox-sensing protein Rex, a transcriptional regulator of solventogenesis in Clostridium acetobutylicum." *Applied Microbiology and Biotechnology,* **96**, 749-761.

Wilks, J. C. and Slonczewski, J. L. (2007). "pH of the cytoplasm and periplasm of Escherichia coli: rapid measurement by green fluorescent protein fluorimetry." *Journal of Bacteriology,* **189**, 5601-5607.

Wilms, B., Hauck, A., Reuss, M., Syldatk, C., Mattes, R., Siemann, M. and Altenbuchner, J. (2001). "High-cell-density fermentation for production of L-N-carbamoylase using an expression system based on the Escherichia coli rhaBAD promoter." *Biotechnology and Bioengineering,* **73**, 95-103.

Wolfe, A. J. (2005). "The acetate switch." *Microbiology and Molecular Biology Reviews,* **69**, 12-+.

Woodruff, L. B. A., Pandhal, J., Ow, S. Y., Karimpour-Fard, A., Weiss, S. J., Wright, P. C. and Gill, R. T. (2013). "Genome-scale identification and characterization of ethanol tolerance genes in Escherichia coli." *Metabolic Engineering,* **15**, 124-133.

Woods, D. R. (1995). "The genetic engineering of microbial solvent production." *Trends in Biotechnology,* **13**, 259-264.

Xin, F. X., Chen, T. P., Jiang, Y. J., Dong, W. L., Zhang, W. M., Zhang, M., Wu, H., Ma, J. F. and Jiang, M. (2017). "Strategies for improved isopropanol-butanol production by a Clostridium strain from glucose and hemicellulose through consolidated bioprocessing." *Biotechnology for Biofuels,* **10**.

Xu, B., Jahic, M. and Enfors, S. O. (1999). "Modeling of overflow metabolism in batch and fed-batch cultures of Escherichia coli." *Biotechnology Progress,* **15**, 81-90.

Yang, J. L. and Yang, Y. (2012). "Plasmid size can affect the ability of Escherichia coli to produce high-quality plasmids." *Biotechnology Letters,* **34**, 2017-2022.

Yao, R. L., Hirose, Y., Sarkar, D., Nakahigashi, K., Ye, Q. and Shimizu, K. (2011). "Catabolic regulation analysis of Escherichia coli and its crp, mlc, mgsA, pgi and ptsG mutants." *Microbial Cell Factories,* **10**.

Ye, X. F., Morgenroth, E., Zhang, X. Y. and Finneran, K. T. (2011). "Anthrahydroquinone-2,6,-disulfonate (AH(2)QDS) increases hydrogen molar yield and xylose utilization in growing cultures of Clostridium beijerinckii." *Applied Microbiology and Biotechnology,* **92**, 855-864.

Zaldivar, J. and Ingram, L. O. (1999). "Effect of organic acids on the growth and fermentation of ethanologenic Escherichia coli LY01." *Biotechnology and Bioengineering,* **66**, 203-210.

Zaldivar, J., Martinez, A. and Ingram, L. O. (1999). "Effect of selected aldehydes on the growth and fermentation of ethanologenic Escherichia coli." *Biotechnology and Bioengineering,* **65**, 24-33.

Zhai, J., Cao, Q.-z. and Chang, W.-s. (2005). "Identification of E. coli K12 chromosomal insertion sites of bacteriophage ϕ297." *Journal of Medical Colleges of PLA,* **20**, 236-240.

Zhang, S. Z., Qu, C. Y., Huang, X. Y., Suo, Y. K., Liao, Z. P. and Wang, J. F. (2016). "Enhanced isopropanol and n-butanol production by supplying exogenous acetic acid via co-culturing two clostridium strains from cassava bagasse hydrolysate." *Journal of Industrial Microbiology & Biotechnology,* **43**, 915-925.

Zhang, Y.-X., Perry, K., Vinci, V. A., Powell, K., Stemmer, W. P. C. and del Cardalyre, S. B. (2002). "Genome shuffling leads to rapid phenotypic improvement in bacteria." *Nature,* **415**, 644-646.

Zhang, Y., Buchholz, F., Muyrers, J. P. P. and Stewart, A. F. (1998). "A new logic for DNA engineering using recombination in Escherichia coli." *Nature Genetics,* **20**, 123-128.

Zhou, J., Zhang, F. L., Meng, H. K., Zhang, Y. P. and Li, Y. (2016). "Introducing extra NADPH consumption ability significantly increases the photosynthetic efficiency and biomass production of cyanobacteria." *Metabolic Engineering,* **38**, 217-227.

Zhu, F., Zhong, X., Hu, M., Lu, L., Deng, Z. and Liu, T. (2014). "In vitro reconstitution of mevalonate pathway and targeted engineering of farnesene overproduction in Escherichia coli." *Biotechnology and Bioengineering,* **111**, 1396-1405.

Zhu, H., Gonzalez, R. and Bobik, T. A. (2011). "Coproduction of acetaldehyde and hydrogen during glucose fermentation by Escherichia coli." *Applied and Environmental Microbiology,* **77**, 6441-6450.

Zhuang, Z., Song, F., Martin, B. M. and Dunaway-Mariano, D. (2002). "The YbgC protein encoded by the ybgC gene of the tol-pal gene cluster of Haemophilus influenzae catalyzes acyl-coenzyme A thioester hydrolysis." *Febs Letters,* **516**, 161-163.

Zilberstein, D., Agmon, V., Schuldiner, S. and Padan, E. (1984). "Escherichia coli intracellular pH, membrane potential, and cell growth." *Journal of Bacteriology,* **158**, 246-52.

Zingaro, K. A. and Papoutsakis, E. T. (2013). "GroESL overexpression imparts Escherichia coli tolerance to i-, n-, and 2-butanol, 1,2,4-butanetriol and ethanol with complex and unpredictable patterns." *Metabolic Engineering,* **15**, 196-205.

Zondervan, E., Nawaz, M., de Haan, A. B., Woodley, J. M. and Gani, R. (2011). "Optimal design of a multi-product biorefinery system." *Computers & Chemical Engineering,* **35**, 1752-1766.

Zverlov, V. V. and Schwarz, W. H. (2008). "Bacterial cellulose hydrolysis in anaerobic environmental subsystems - Clostridium thermocellum and Clostridium stercorarium, thermophilic plant-fiber degraders." In: *Incredible Anaerobes: From Physiology to Genomics to Fuels* (Wiegel, J., Maier, R. J. and Adams, M. W. W., eds.), Blackwell Publishing, Oxford, 1125, 298-307.

A Appendix

A.1 DNA Sequences and Plasmid Maps

Table A-1: DNA sequence of pHSG299.
Size: 2673 bp. Source: Takara Korea Biomedical Inc. (Seoul, South Korea).
Isopropanol pathway genes were inserted via *Xba*I and *Acl*I restriction sites, removing the lac promoter including lac operator.
Legend: restriction site lac promoter lac operator kanamycin resistance gene pMB1 origin of replication.

```
   1  GAGGTCTGCC  TCGTGAAGAA  GGTGTTGCTG  ACTCATACCA  GGCCTGAATC  GCCCCATCAT
  61  CCAGCCAGAA  AGTGAGGGAG  CCACGGTTGA  TGAGAGCTTT  GTTGTAGGTG  GACCAGTTGG
 121  TGATTTTGAA  CTTTTGCTTT  GCCACGGAAC  GGTCTGCGTT  GTCGGGAAGA  TGCGTGATCT
 181  GATCCTTCAA  CTCAGCAAAA  GTTCGATTTA  TTCAACAAAG  CCACGTTGTG  TCTCAAAATC
 241  TCTGATGTTA  CATTGCACAA  GATAAAAATA  TATCATCATG  AACAATAAAA  CTGTCTGCTT
 301  ACATAAACAG  TAATACAAGG  GGTGTTATGA  GCCATATTCA  ACGGGAAACG  TCTTGCTCGA
 361  AGCCGCGATT  AAATTCCAAC  ATGGATGCTG  ATTTATATGG  GTATAAATGG  GCTCGCGATA
 421  ATGTCGGGCA  ATCAGGTGCG  ACAATCTATC  GATTGTATGG  GAAGCCCGAT  GCGCCAGAGT
 481  TGTTTCTGAA  ACATGGCAAA  GGTAGCGTTG  CCAATGATGT  TACAGATGAG  ATGGTCAGAC
 541  TAAACTGGCT  GACGGAATTT  ATGCCTCTTC  CGACCATCAA  GCATTTTATC  CGTACTCCTG
 601  ATGATGCATG  GTTACTCACC  ACTGCGATCC  CCGGGAAAAC  AGCATTCCAG  GTATTAGAAG
 661  AATATCCTGA  TTCAGGTGAA  AATATTGTTG  ATGCGCTGGC  AGTGTTCCTG  CGCCGGTTGC
 721  ATTCGATTCC  TGTTTGTAAT  TGTCCTTTTA  ACAGCGATCG  CGTATTTCGT  CTCGCTCAGG
 781  CGCAATCACG  AATGAATAAC  GGTTTGGTTG  ATGCGAGTGA  TTTTGATGAC  GAGCGTAATG
 841  GCTGGCCTGT  TGAACAAGTC  TGGAAAGAAA  TGCATAAGCT  TTTGCCATTC  TCACCGGATT
 901  CAGTCGTCAC  TCATGGTGAT  TTCTCACTTG  ATAACCTTAT  TTTTGACGAG  GGGAAATTAA
 961  TAGGTTGTAT  TGATGTTGGA  CGAGTCGGAA  TCGCAGACCG  ATACCAGGAT  CTTGCCATCC
1021  TATGGAACTG  CCTCGGTGAG  TTTTCTCCTT  CATTACAGAA  ACGGCTTTTT  CAAAAATATG
1081  GTATTGATAA  TCCTGATATG  AATAAATTGC  AGTTTCATTT  GATGCTCGAT  GAGTTTTTCT
1141  AATCAGAATT  GGTTAATTGG  TTGTAACACT  GGCAGAGCAT  TACGCTGACT  TGACGGGACG
1201  GCGGCTTTGT  TGAATAAATC  GCATTCGCCA  TTCAGGCTGC  GCAACTGTTG  GGAAGGGCGA
1261  TCGGTGCGGG  CCTCTTCGCT  ATTACGCCAG  CTGGCGAAAG  GGGGATGTGC  TGCAAGGCGA
1321  TTAAGTTGGG  TAACGCCAGG  GTTTTCCCAG  TCACGACGTT  GTAAAACGAC  GGCCAGTGAA
1381  TTCGAGCTCG  GTACCCGGGG  ATCCTCTAGA  GTCGACCTGC  AGGCATGCAA  GCTTGGCGTA
1441  ATCATGGTCA  TAGCTGTTTC  CTGTGTGAAA  TTGTTATCCG  CTCACAATTC  CACACAACAT
1501  ACGAGCCGGA  AGCATAAAGT  GTAAAGCCTG  GGGTGCCTAA  TGAGTGAGCT  AACTCACATT
1561  AATTGCGTTG  CGCTCACTGC  CCGCTTTCCA  GTCGGGAAAC  CTGTCGTGCC  AGCTGCATTA
1621  ATGAATCGGC  CAACGCGCGG  GGAGAGGCGG  TTTGCGTATT  GGGAACTTTT  GCTGAGTTGA
1681  AGGATCAGAT  CACGCATCTT  CCCGACAACG  CAGACCGTTC  CGTGGCAAAG  CAAAAGTTCA
1741  AAATCAGTAA  CCGTCAGTGC  CGATAAGTTC  AAAGTTAAAC  CTGGTGTTGA  TACCAACATT
1801  GAAACGTTGA  TCGAAAACGC  GCTGAAAAAC  GCTGCTGAAT  GTGCGAGCTT  CTTCCGCTTC
1861  CTCGCTCACT  GACTCGCTGC  GCTCGGTCGT  TCGGCTGCGG  CGAGCGGTAT  CAGCTCACTC
1921  AAAGGCGGTA  ATACGGTTAT  CCACAGAATC  AGGGGATAAC  GCAGGAAAGA  ACATGTGAGC
1981  AAAAGGCCAG  CAAAAGGCCA  GGAACCGTAA  AAAGGCCGCG  TTGCTGGCGT  TTTTCCATAG
```

```
2041  GCTCCGCCCC  CCTGACGAGC  ATCACAAAAA  TCGACGCTCA  AGTCAGAGGT  GGCGAAACCC
2101  GACAGGACTA  TAAAGATACC  AGGCGTTTCC  CCCTGGAAGC  TCCCTCGTGC  GCTCTCCTGT
2161  TCCGACCCTG  CCGCTTACCG  GATACCTGTC  CGCCTTTCTC  CCTTCGGGAA  GCGTGGCGCT
2221  TTCTCATAGC  TCACGCTGTA  GGTATCTCAG  TTCGGTGTAG  GTCGTTCGCT  CCAAGCTGGG
2281  CTGTGTGCAC  GAACCCCCCG  TTCAGCCCGA  CCGCTGCGCC  TTATCCGGTA  ACTATCGTCT
2341  TGAGTCCAAC  CCGGTAAGAC  ACGACTTATC  GCCACTGGCA  GCAGCCACTG  GTAACAGGAT
2401  TAGCAGAGCG  AGGTATGTAG  GCGGTGCTAC  AGAGTTCTTG  AAGTGGTGGC  CTAACTACGG
2461  CTACACTAGA  AGAACAGTAT  TTGGTATCTG  CGCTCTGCTG  AAGCCAGTTA  CCTTCGGAAA
2521  AAGAGTTGGT  AGCTCTTGAT  CCGGCAAACA  AACCACCGCT  GGTAGCGGTG  GTTTTTTTGT
2581  TTGCAAGCAG  CAGATTACGC  GCAGAAAAAA  AGGATCTCAA  GAAGATCCTT  TGATCTTTTC
2641  TACGGGGTCT  GACGCTCAGT  GGAACTCCGT  CGA
```

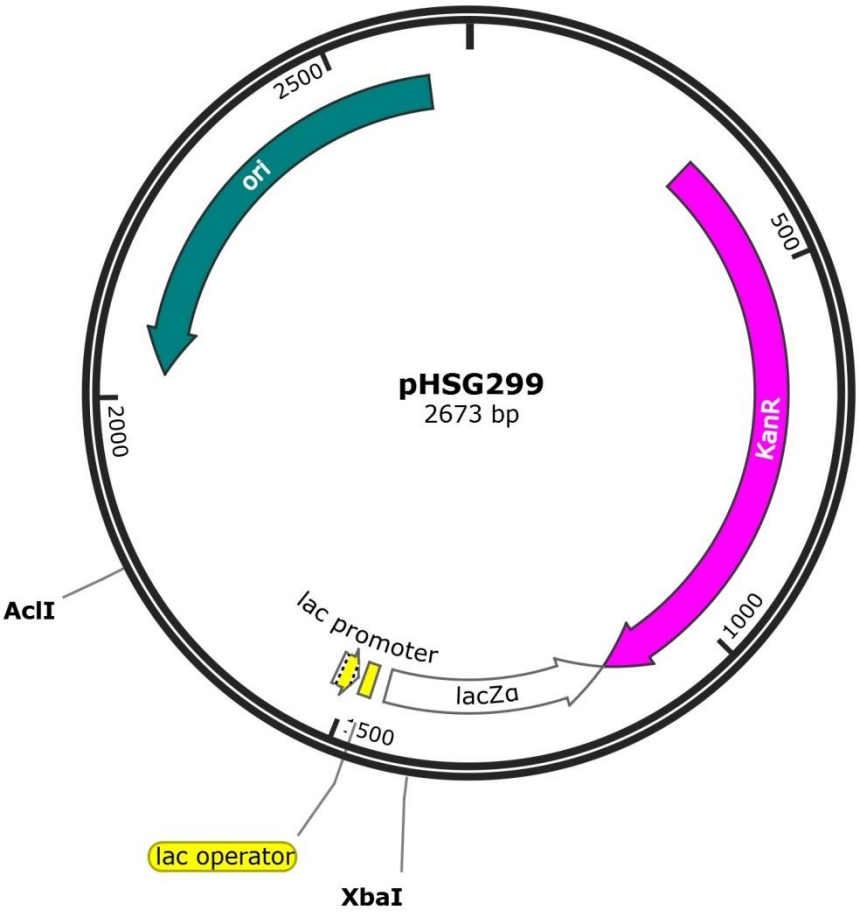

Figure A-1: Plasmid map of pHSG299.
Plasmid map was generated via SnapGene® Viewer 4.0.7 according to the DNA sequence provided by Takara Korea Biomedical Inc. (Seoul, South Korea).
Legend: KanR… kanamycin resistance gene ori… pMB1 origin of replication lacZα... α-peptide of β-galactosidase.

Table A-2: DNA sequence of pRK_ISO_1E2e3c4c.

Size: 2788 bp.

The original sequences of the isopropanol pathway genes were taken from GenBank® at National Center for Biotechnology Information (NCBI, U.S. National Library of Medicine, Bethesda, MD, USA). Protein Act (*E. coli* K-12 MG1655, EC number 2.3.1.9) is coded by gene atoB (AS: AAC75284.1), protein Acct (*E. coli* K-12 MG1655, EC number 2.8.3.8) by genes atoD (subunit α, AS: NP_416725.1) and atoA (subunit β, AS: NP_416726.1), protein Adc (*C. acetobutylicum* ATCC 824, EC number 4.1.1.4) by gene adc (AS: NP_149328.1) and protein Idh (*C. beijerinckii* NRRL B593, EC number 1.1.1.80) by gene adh (AS: AAA23199.2). DNA sequences were codon usage optimized and equipped each with an upstream tac promoter and a C-terminal peptide tag. Several suitable restriction sites were introduced for easy removal or insertion of DNA sequences. Optimization and gene synthesis was performed by DNA2.0 (Menlo Park, CA, USA). Subsequent cloning was done via *Xba*I and *Acl*I restriction sites into pHSG299 (Table A-1), removing the lac promoter including lac operator.

Legend: atoB atoD atoA adc adh
tac promoter lac operator ribosome binding site restriction site stop codon peptide tag
shared codon rrnB T1 terminator CER sequence kanamycin resistance gene pMB1 origin of replication.

```
   1 GAGGTCTGCC TCGTGAAGAA GGTGTTGCTG ACTCATACCA GGCCTGAATC GCCCCATCAT
  61 CCAGCCAGAA AGTGAGGGAG CCACGGTTGA TGAGAGCTTT GTTGTAGGTG GACCAGTTGG
 121 TGATTTTGAA CTTTTGCTTT GCCACGGAAC GGTCTGCGTT GTCGGGAAGA TGCGTGATCT
 181 GATCCTTCAA CTCAGCAAAA GTTCGATTTA TTCAACAAAG CCACGTTGTG TCTCAAAATC
 241 TCTGATGTTA CATTGCACAA GATAAAAATA TATCATCATG AACAATAAAA CTGTCTGCTT
 301 ACATAAACAG TAATACAAGG GGTGTTATGA GCCATATTCA ACGGGAAACG TCTTGCTCGA
 361 AGCCGCGATT AAATTCCAAC ATGGATGCTG ATTTATATGG GTATAAATGG GCTCGCGATA
 421 ATGTCGGGCA ATCAGGTGCG ACAATCTATC GATTGTATGG GAAGCCCGAT GCGCCAGAGT
 481 TGTTTCTGAA ACATGGCAAA GGTAGCGTTG CCAATGATGT TACAGATGAG ATGGTCAGAC
 541 TAAACTGGCT GACGGAATTT ATGCCTCTTC CGACCATCAA GCATTTTATC CGTACTCCTG
 601 ATGATGCATG GTTACTCACC ACTGCGATCC CCGGGAAAAC AGCATTCCAG GTATTAGAAG
 661 AATATCCTGA TTCAGGTGAA AATATTGTTG ATGCGCTGGC AGTGTTCCTG CGCCGGTTGC
 721 ATTCGATTCC TGTTTGTAAT TGTCCTTTTA ACAGCGATCG CGTATTTCGT CTCGCTCAGG
 781 CGCAATCACG AATGAATAAC GGTTTGGTTG ATGCGAGTGA TTTTGATGAC GAGCGTAATG
 841 GCTGGCCTGT TGAACAAGTC TGGAAAGAAA TGCATAAGCT TTTGCCATTC TCACCGGATT
 901 CAGTCGTCAC TCATGGTGAT TTCTCACTTG ATAACCTTAT TTTTGACGAG GGGAAATTAA
 961 TAGGTTGTAT TGATGTTGGA CGAGTCGGAA TCGCAGACCG ATACCAGGAT CTTGCCATCC
1021 TATGGAACTG CCTCGGTGAG TTTTCTCCTT CATTACAGAA ACGGCTTTTT CAAAAATATG
1081 GTATTGATAA TCCTGATATG AATAAATTGC AGTTTCATTT GATGCTCGAT GAGTTTTTCT
1141 AATCAGAATT GGTTAATTGG TTGTAACACT GGCAGAGCAT TACGCTGACT TGACGGGACG
1201 GCGGCTTTGT TGAATAAATC GCATTCGCCA TTCAGGCTGC GCAACTGTTG GGAAGGGCGA
1261 TCGGTGCGGG CCTCTTCGCT ATTACGCCAG CTGGCGAAAG GGGGATGTGC TGCAAGGCGA
1321 TTAAGTTGGG TAACGCCAGG GTTTTCCCAG TCACGACGTT GTAAAACGAC GGCCAGTGAA
1381 TTCGAGCTCG GTACCCGGGG ATCCTCTAGA GAGCTGTTGA CAATTAATCA TCGGCTCGTA
1441 TAATGTGTGG AATTGTGAGC GGATAACAAT TTCACACAGG AAACAGAATT CTGCTAGCAT
1501 GAAAAACTGT GTGATTGTCT CCGCTGTGCG TACCGCGATT GGTTCCTTTA ACGGTAGCTT
1561 GGCGTCCACG AGCGCGATCG ATCTGGGCGC CACGGTCATC AAAGCAGCGA TCGAGCGTGC
1621 AAAGATCGAC AGCCAGCATG TGGACGAAGT CATCATGGGC AACGTGCTGC AGGCCGGTCT
1681 GGGCCAGAAT CCGGCTCGCC AGGCGCTGCT GAAGAGCGGT CTGGCAGAAA CCGTTTGCGG
1741 CTTCACCGTT AACAAAGTTT GTGGTAGCGG TCTGAAGAGC GTCGCGTTGG CAGCGCAAGC
1801 CATTCAAGCG GGCCAGGCCC AGAGCATCGT GGCGGGTGGT ATGGAAAACA TGAGCCTGGC
1861 GCCGTACTTG CTGGATGCGA AGGCTCGTAG CGGTTACCGC TTGGGCGATG GTCAAGTGTA
1921 TGATGTTATT CTGCGTGACG GTCTTATGTG CGCTACGCAC GGCTACCACA TGGGCATCAC
1981 CGCGGAGAAT GTCGCGAAAG AGTATGGTAT TACCCGTGAA ATGCAGGATG AATTGGCGCT
2041 GCACAGCCAA CGTAAGGCTG CAGCCGCCAT CGAAAGCGGT GCCTTCACGG CCGAGATTGT
2101 TCCGGTTAAT GTCGTGACCC GTAAAAAGAC CTTTGTGTTC AGCCAAGACG AGTTTCCGAA
```

```
2161 GGCGAACAGC ACGGCAGAAG CGCTGGGTGC TCTGCGTCCG GCCTTCGACA AGGCTGGCAC
2221 TGTTACTGCG GGCAACGCGT CTGGCATCAA CGACGGTGCA GCAGCGCTGG TCATCATGGA
2281 AGAGTCAGCT GCACTGGCAG CGGGTCTGAC CCCACTGGCA CGCATCAAAA GCTACGCCTC
2341 TGGTGGCGTT CCTCCGGCCC TCATGGGTAT GGGTCCGGTG CCAGCAACGC AGAAAGCCCT
2401 GCAGCTGGCC GGTCTGCAAC TGGCGGACAT CGATCTGATC GAGGCAAATG AAGCGTTCGC
2461 AGCGCAATTT CTGGCGGTTG GTAAGAATCT GGGCTTTGAC AGCGAGAAAG TTAACGTAAA
2521 TGGTGGCGCG ATTGCTCTCG GCCACCCGAT TGGTGCGTCA GGTGCGCGCA TCCTGGTCAC
2581 CCTGCTGCAT GCAATGCAGG CCCGTGATAA AACCCTGGGT CTGGCAACGC TGTGCATTGG
2641 TGGCGGCCAA GGCATTGCAA TGGTGATTGA GCGCCTGAAT CCTAGGTGGA GCCATCCGCA
2701 GTTTGAAAAA TAACCTAGGT GAACGTCGCA TCAGGCAATG AATGCGAAAC CGCGGTGTAA
2761 ATAACGACAA AAATAAAATT GGCCGCTTCG GTCAGGGCCA ACTATTGCCT GAAAAAGGGT
2821 AACGATCCTC AGCGAGCTGT TGACAATTAA TCATCGGCTC GTATAATGTG TGGAATTGTG
2881 AGCGGATAAC AATTTCACAC AGGAAACAGA ATTCTCTCGA GATGAAAACG AAACTGATGA
2941 CTTTACAAGA TGCAACCGGC TTTTTCCGTG ATGGTATGAC CATTATGGTT GGTGGTTTCA
3001 TGGGCATCGG TACGCCAAGC CGCTTGGTGG AGGCATTGCT GGAATCTGGT GTGCGTGACT
3061 TGACTCTGAT CGCGAATGAT ACCGCGTTTG TGGACACGGG CATTGGTCCG CTGATTGTGA
3121 ACGGTCGTGT CCGCAAAGTG ATCGCGTCGC ATATCGGTAC CAATCCGGAA ACCGGCCGTC
3181 GTATGATCAG CGGTGAAATG GACGTTGTCC TGGTCCCGCA GGGCACCCTG ATTGAGCAGA
3241 TTCGCTGCGG CGGTGCTGGT CTTGGTGGCT TCCTGACGCC TACCGGCGTT GGCACCGTCG
3301 TGGAAGAGGG TAAGCAGACC CTGACGCTGG ACGGCAAGAC CTGGCTGCTG GAGCGTCCGC
3361 TGCGTGCTGA TCTGGCGCTG ATCCGTGCCC ACCGCTGTGA CACCCTGGGT AACCTGACGT
3421 ACCAACTGAG CGCGCGTAAT TTCAACCCGC TGATTGCCCT GGCGGCAGAT ATTACCCTGG
3481 TTGAGCCGGA TGAGCTGGTT GAAACGGGTG AGCTGCAACC GGACCACATC GTCACCCCTG
3541 GTGCCGTTAT CGACCACATC ATCGTTTCAC AGGAGAGCAA ATAATGGATG CCAAACAGCG
3601 TATTGCACGT CGCGTCGCCC AAGAATTGAG AGATGGTGAT ATCGTGAATC TGGGCATTGG
3661 CCTGCCGACG ATGGTCGCGA ATTACTTGCC GGAGGGTATC CATATTACCC TGCAAAGCGA
3721 AAACGGTTTT CTGGGTCTGG GTCCGGTCAC CACTGCGCAC CCGGACTTGG TTAATGCGGG
3781 TGGTCAACCT TGCGGTGTTC TGCCGGGTGC AGCTATGTTC GACTCCGCAA TGAGCTTTGC
3841 GTTAATCCGT GGCGGCCACA TTGATGCTTG TGTCCTGGGT GGCCTTCAGG TGGACGAGGA
3901 AGCGAACCTG GCGAACTGGG TGGTCCCGGG CAAGATGGTC CCGGGTATGG GTGGTGCTAT
3961 GGACCTGGTA ACCGGCAGCC GTAAGGTTAT CATTGCGATG GAGCACTGTG CGAAAGACGG
4021 CAGCGCAAAG ATCCTGCGCC GCTGCACGAT GCCGCTGACC GCCCAGCATG CAGTTCACAT
4081 GTTGGTGACC GAACTGGCCG TGTTTCGTTT CATTGATGGC AAAATGTGGC TGACGGAGAT
4141 CGCGGATGGC TGCGACCTGG CGACCGTGCG CGCCAAAACC GAGGCACGTT TCGAGGTTGC
4201 TGCAGACCTG AATACGCAGC GTGGTGACCT GTGGCGCGCC CATCATCACC ATCACCACCA
4261 TCATCACCAC TGAGGCGCGC CTAAACGTCG CATCAGGCAA TGAATGCGAA ACCGCGGTGT
4321 AAATAACGAC AAAAATAAAA TTCCAACTAT TGCCTGAAAA AGGGTAACGA TGTACAGAGC
4381 TGTTGACAAT TAATCATCGG CTCGTATAAT GTGTGGAATT GTGAGCGGAT AACAATTTCA
4441 CACAGGAAAC AGAATTCTTT AATTAAATGC TGAAAGATGA AGTTATCAAG CAAATTTCGA
4501 CCCCACTGAC CAGCCCGGCA TTCCCGCGTG GTCCATACAA GTTCCATAAT CGTGAATACT
4561 TTAACATTGT TTACCGTACG GACATGGATG CGCTGCGCAA GGTTGTTCCG GAGCCTTTGG
4621 AAATTGACGA GCCGTTAGTG CGCTTCGAGA TCATGGCCAT GCACGACACC AGCGGTCTGG
4681 GTTGCTACAC CGAGAGCGGC CAAGCGATCC CGGTGAGCTT CAACGGTGTC AAAGGTGATT
4741 ATCTGCACAT GATGTATCTG GATAACGAGC CAGCGATCGC GGTTGGTCGT GAACTGAGCG
4801 CTTATCCGAA AAAGCTGGGC TATCCGAAAC TGTTTGTGGA TTCTGATACC CTGGTGGGTA
4861 CCCTGGACTA TGGTAAACTG CGCGTGGCCA CGGCGACGAT GGGTTACAAA CATAAGGCGT
4921 TAGACGCGAA TGAAGCAAAG GATCAGATTT GTCGTCCGAA TTACATGCTG AAGATTATCC
```

```
4981 CGAACTACGA CGGCAGCCCG CGTATCTGCG AACTGATTAA TGCGAAGATT ACCGACGTTA
5041 CGGTCCACGA GGCATGGACT GGCCCGACCC GCCTGCAGTT GTTTGACCAT GCCATGGCTC
5101 CGCTGAACGA TCTGCCGGTG AAAGAGATTG TGAGCAGCTC CCACATCCTC GCCGACATTA
5161 TCCTGCCGCG TGCAGAGGTT ATCTATGACT ATCTGAAATG GCCGGCCGAT TATAAAGATG
5221 ATGATGATAA ATAAGGCCGG CCTGAACGTC GCATCAGGCA ATGAATGCGA AACCGCGGTG
5281 TAAATTTGGC CGCTTCGGTC AGGGCCAACT ATTGCCTGAA AAAGGGTAAC GATACTAGTG
5341 AGCTGTTGAC AATTAATCAT CGGCTCGTAT AATGTGTGGA ATTGTGAGCG GATAACAATT
5401 TCACACAGGA AACAGAATTC TACCGGTATG AAAGGTTTTG CAATGCTGGG CATCAATAAA
5461 CTGGGTTGGA TTGAGAAGGA ACGCCCGGTC GCGGGCAGCT ACGACGCGAT TGTTCGCCCG
5521 CTGGCAGTCA GCCCGTGCAC CAGCGATATC CACACGGTGT TCGAGGGTGC GCTGGGTGAT
5581 CGTAAAAACA TGATCCTGGG TCATGAGGCT GTGGGCGAAG TCGTGGAAGT TGGTTCCGAG
5641 GTTAAGGACT TTAAACCGGG TGATAGAGTT ATTGTCCCGT GCACGACCCC GGACTGGCGT
5701 TCTTTGGAAG TGCAAGCGGG TTTTCAGCAG CACTCCAATG GCATGTTGGC GGGCTGGAAA
5761 TTCAGCAATT TCAAAGACGG CGTGTTTGGC GAGTATTTCC ACGTTAATGA CGCGGATATG
5821 AACCTGGCAA TTCTGCCGAA AGATATGCCG CTGGAGAATG CGGTTATGAT TACGGACATG
5881 ATGACCACGG GTTTTCATGG CGCAGAACTG GCAGACATCC AAATGGGCAG CAGCGTTGTC
5941 GTCATCGGTA TCGGTGCGGT GGGCCTGATG GGTATCGCCG GTGCGAAACT GCGTGGTGCT
6001 GGTCGTATCA TCGGTGTCGG CAGCCGTCCG ATTTGCGTGG AGGCGGCCAA GTTCTACGGT
6061 GCCACCGACA TTCTGAACTA TAAGAATGGT CACATCGTTG ATCAGGTTAT GAAACTGACC
6121 AACGGTAAGG GCGTGGATCG TGTGATTATG GCTGGTGGTG GTAGCGAAAC CCTGTCTCAA
6181 GCCGTTTCCA TGGTCAAGCC AGGCGGCATT ATCAGCAACA TTAACTATCA TGGTTCGGGT
6241 GACGCACTGC TGATTCCGCG TGTTGAGTGG GGTTGTGGCA TGGCCCACAA AACTATTAAG
6301 GGCGGTCTGT GTCCGGGTGG TCGTCTGCGT GCGGAGATGC TGCGCGACAT GGTCGTATAC
6361 AACCGCGTTG ATCTGAGCAA GTTGGTGACC CATGTCTACC ACGGCTTCGA TCACATTGAG
6421 GAAGCGCTGC TGTTGATGAA GGATAAGCCG AAGGACCTGA TCAAAGCGGT GGTTATCTTG
6481 GGGCCCGAAC AGAAACTGAT TAGCGAAGAA GATCTGTAAG GGCCCTGAAT AAAACGAAAG
6541 GCTCAGTCGA AAGACTGGGC CTTTCGTTTT ATACGTCGCA TCAGGCAATG AATGCGAAAC
6601 CGCGGTGTAA ATAACGACAA AAATGGTCAG GGCCAACTAT TGCCTGAAAA AGGGTAACGA
6661 TATGGCCCTT CGCTGGGATG GTGAAACCAT GAAAAATGGC AGCTTCAGTG GATTAAGTGG
6721 GGGTAATGTG GCCTGTACCC TCTGGTTGCA TAGGTATTCA TACGGTTAAA ATTTATCAGG
6781 CGCGATCGCG GCAGTTTTTC GGGTGGTTTG TTGCCATTTT TACCTGTCTG CTGCCGTGAT
6841 CGCGCTGAAC GCGTTTTAGC GGTGCGTACA ATTAAGGGAT TATGGTAAAT CCACTTACTG
6901 TCTGCCCTCG TAGCCATAAC GTTGATCGAA AACGCGCTGA AAAACGCTGC TGAATGTGCG
6961 AGCTTCTTCC GCTTCCTCGC TCACTGACTC GCTGCGCTCG GTCGTTCGGC TGCGGCGAGC
7021 GGTATCAGCT CACTCAAAGG CGGTAATACG GTTATCCACA GAATCAGGGG ATAACGCAGG
7081 AAAGAACATG TGAGCAAAAG GCCAGCAAAA GGCCAGGAAC CGTAAAAAGG CCGCGTTGCT
7141 GGCGTTTTTC CATAGGCTCC GCCCCCCTGA CGAGCATCAC AAAAATCGAC GCTCAAGTCA
7201 GAGGTGGCGA AACCCGACAG GACTATAAAG ATACCAGGCG TTTCCCCCTG GAAGCTCCCT
7261 CGTGCGCTCT CCTGTTCCGA CCCTGCCGCT TACCGGATAC CTGTCCGCCT TTCTCCCTTC
7321 GGGAAGCGTG GCGCTTTCTC ATAGCTCACG CTGTAGGTAT CTCAGTTCGG TGTAGGTCGT
7381 TCGCTCCAAG CTGGGCTGTG TGCACGAACC CCCCGTTCAG CCCGACCGCT GCGCCTTATC
7441 CGGTAACTAT CGTCTTGAGT CCAACCCGGT AAGACACGAC TTATCGCCAC TGGCAGCAGC
7501 CACTGGTAAC AGGATTAGCA GAGCGAGGTA TGTAGGCGGT GCTACAGAGT TCTTGAAGTG
7561 GTGGCCTAAC TACGGCTACA CTAGAAGAAC AGTATTTGGT ATCTGCGCTC TGCTGAAGCC
7621 AGTTACCTTC GGAAAAAGAG TTGGTAGCTC TTGATCCGGC AAACAAACCA CCGCTGGTAG
7681 CGGTGGTTTT TTTGTTTGCA AGCAGCAGAT TACGCGCAGA AAAAAAGGAT CTCAAGAAGA
7741 TCCTTTGATC TTTTCTACGG GGTCTGACGC TCAGTGGAAC TCCGTCGA
```

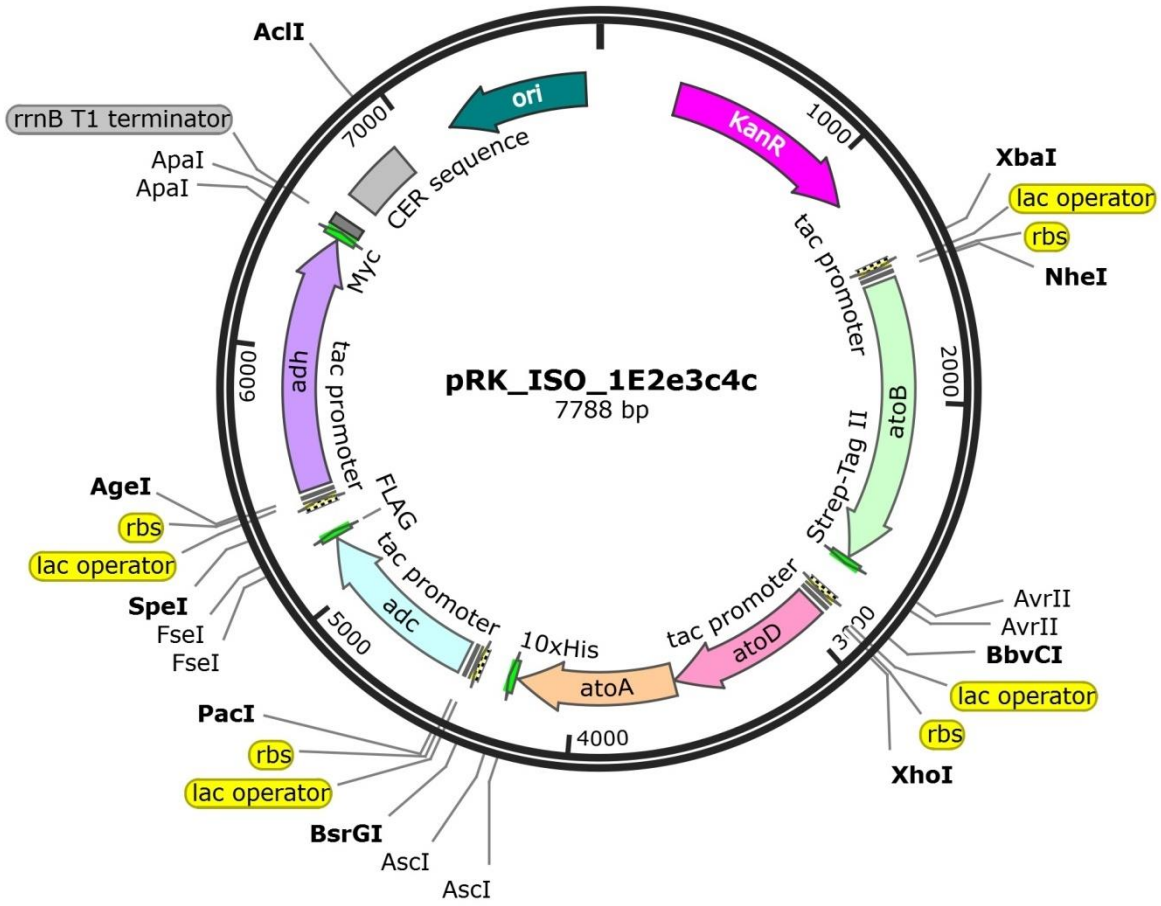

Figure A-2: Plasmid map of pRK_ISO_1E2e3c4c.
Plasmid map was generated via SnapGene® Viewer 4.0.7 according to the DNA sequence in Table A-2.
Legend: atoB... acetyl-CoA acetyltransferase gene, atoD/atoA... acetate CoA-transferase genes, adc... acetoacetate decarboxylase gene, adh... isopropanol dehydrogenase gene
rbs... ribosome binding site KanR... kanamycin resistance gene ori... pMB1 origin of replication.

Table A-3: DNA sequence of pRK_ISO_1C2e3c4c.

Size: 2782 bp.

The original sequences of the isopropanol pathway genes were taken from GenBank® at National Center for Biotechnology Information (NCBI, U.S. National Library of Medicine, Bethesda, MD, USA). Protein Act (*C. acetobutylicum* ATCC 824, EC number 2.3.1.9) is coded by gene thlA (AS: NP_349476.1), protein Acct (*E. coli* K-12 MG1655, EC number 2.8.3.8) by genes atoD (subunit α, AS: NP_416725.1) and atoA (subunit β, AS: NP_416726.1), protein Adc (*C. acetobutylicum* ATCC 824, EC number 4.1.1.4) by gene adc (AS: NP_149328.1) and protein Idh (*C. beijerinckii* NRRL B593, EC number 1.1.1.80) by gene adh (AS: AAA23199.2). DNA sequences were codon usage optimized and equipped each with an upstream tac promoter and a C-terminal peptide tag. Several suitable restriction sites were introduced for easy removal or insertion of DNA sequences. Optimization and gene synthesis of atoDA, adc and adh were performed by DNA2.0 (Menlo Park, CA, USA). Subsequent cloning was done via *Xba*I and *Acl*I restriction sites into pHSG299 (Table A-1), removing the lac promoter including lac operator. Codon usage optimization and synthesis of gene thlA was performed by Thermo Fisher Scientific - Life Technologies GmbH (Darmstadt, Germany). Insertion of thlA into pRK_ISO_1E2e3c4c was done after excision of atoB, resulting in pRK_ISO_1C2e3c4c.

Legend: thlA atoD atoA adc adh
tac promoter lac operator ribosome binding site restriction site stop codon peptide tag
shared codon rrnB T1 terminator CER sequence kanamycin resistance gene pMB1 origin of replication.

```
   1 GAGGTCTGCC TCGTGAAGAA GGTGTTGCTG ACTCATACCA GGCCTGAATC GCCCCATCAT
  61 CCAGCCAGAA AGTGAGGGAG CCACGGTTGA TGAGAGCTTT GTTGTAGGTG GACCAGTTGG
 121 TGATTTTGAA CTTTTGCTTT GCCACGGAAC GGTCTGCGTT GTCGGGAAGA TGCGTGATCT
 181 GATCCTTCAA CTCAGCAAAA GTTCGATTTA TTCAACAAAG CCACGTTGTG TCTCAAAATC
 241 TCTGATGTTA CATTGCACAA GATAAAAATA TATCATCATG AACAATAAAA CTGTCTGCTT
 301 ACATAAACAG TAATACAAGG GGTGTTATGA GCCATATTCA ACGGGAAACG TCTTGCTCGA
 361 AGCCGCGATT AAATTCCAAC ATGGATGCTG ATTTATATGG GTATAAATGG GCTCGCGATA
 421 ATGTCGGGCA ATCAGGTGCG ACAATCTATC GATTGTATGG GAAGCCCGAT GCGCCAGAGT
 481 TGTTTCTGAA ACATGGCAAA GGTAGCGTTG CCAATGATGT TACAGATGAG ATGGTCAGAC
 541 TAAACTGGCT GACGGAATTT ATGCCTCTTC CGACCATCAA GCATTTTATC CGTACTCCTG
 601 ATGATGCATG GTTACTCACC ACTGCGATCC CCGGGAAAAC AGCATTCCAG GTATTAGAAG
 661 AATATCCTGA TTCAGGTGAA AATATTGTTG ATGCGCTGGC AGTGTTCCTG CGCCGGTTGC
 721 ATTCGATTCC TGTTTGTAAT TGTCCTTTTA ACAGCGATCG CGTATTTCGT CTCGCTCAGG
 781 CGCAATCACG AATGAATAAC GGTTTGGTTG ATGCGAGTGA TTTTGATGAC GAGCGTAATG
 841 GCTGGCCTGT TGAACAAGTC TGGAAAGAAA TGCATAAGCT TTTGCCATTC TCACCGGATT
 901 CAGTCGTCAC TCATGGTGAT TTCTCACTTG ATAACCTTAT TTTTGACGAG GGGAAATTAA
 961 TAGGTTGTAT TGATGTTGGA CGAGTCGGAA TCGCAGACCG ATACCAGGAT CTTGCCATCC
1021 TATGGAACTG CCTCGGTGAG TTTTCTCCTT CATTACAGAA ACGGCTTTTT CAAAAATATG
1081 GTATTGATAA TCCTGATATG AATAAATTGC AGTTTCATTT GATGCTCGAT GAGTTTTTCT
1141 AATCAGAATT GGTTAATTGG TTGTAACACT GGCAGAGCAT TACGCTGACT TGACGGGACG
1201 GCGGCTTTGT TGAATAAATC GCATTCGCCA TTCAGGCTGC GCAACTGTTG GGAAGGGCGA
1261 TCGGTGCGGG CCTCTTCGCT ATTACGCCAG CTGGCGAAAG GGGGATGTGC TGCAAGGCGA
1321 TTAAGTTGGG TAACGCCAGG GTTTTCCCAG TCACGACGTT GTAAAACGAC GGCCAGTGAA
1381 TTCGAGCTCG GTACCCGGGG ATCCTCTAGA GAGCTGTTGA CAATTAATCA TCGGCTCGTA
1441 TAATGTGTGG AATTGTGAGC GGATAACAAT TTCACACAGG AAACAGAATT CTGCTAGCAT
1501 GAAAGAAGTT GTTATTGCAA GCGCAGTTCG TACCGCAATT GGTAGCTATG GTAAAAGCCT
1561 GAAAGATGTT CCGGCAGTTG ATCTGGGTGC AACCGCAATT AAAGAAGCAG TTAAAAAAGC
1621 CGGTATTAAA CCGGAAGATG TGAACGAAGT TATTCTGGGT AATGTTCTGC AGGCAGGTCT
1681 GGGTCAGAAT CCGGCACGTC AGGCAAGCTT TAAAGCAGGT CTGCCGGTTG AAATTCCGGC
1741 AATGACCATT AACAAAGTTT GTGGTAGCGG TCTGCGTACC GTTAGCCTGG CAGCACAGAT
1801 TATCAAAGCC GGTGATGCAG ATGTTATTAT TGCCGGTGGT ATGGAAAATA TGAGCCGTGC
1861 ACCGTATCTG GCAAATAATG CACGTTGGGG TTATCGTATG GGTAATGCCA AATTTGTGGA
1921 TGAGATGATT ACCGATGGTC TGTGGGATGC CTTTAACGAT TATCATATGG GTATTACCGC
1981 AGAGAATATT GCCGAACGTT GGAATATTAG CCGTGAAGAA CAGGATGAAT TTGCACTGGC
```

```
2041 AAGCCAGAAA AAAGCAGAAG AAGCAATTAA AAGCGGTCAG TTCAAAGATG AAATTGTGCC
2101 GGTTGTTATC AAAGGTCGTA AAGGTGAAAC CGTTGTTGAT ACCGATGAAC ATCCGCGTTT
2161 TGGTAGCACC ATTGAAGGTC TGGCAAAACT GAAACCGGCA TTCAAAAAAG ATGGCACCGT
2221 TACCGCAGGT AATGCAAGCG GTCTGAATGA TTGTGCAGCA GTTCTGGTTA TTATGAGCGC
2281 AGAAAAAGCA AAAGAACTGG GTGTTAAACC GCTGGCAAAA ATTGTGAGCT ATGGTAGTGC
2341 CGGTGTTGAT CCGGCAATTA TGGGTTATGG TCCGTTTTAT GCAACCAAAG CAGCAATTGA
2401 AAAAGCAGGT TGGACCGTTG ATGAACTGGA TCTGATTGAA AGCAATGAAG CATTTGCAGC
2461 ACAGAGCCTG GCAGTTGCAA AAGATCTGAA ATTCGATATG AATAAAGTGA ATGTGAATGG
2521 CGGTGCAATT GCCCTGGGTC ATCCGATTGG TGCAAGCGGT GCACGTATTC TGGTTACCCT
2581 GGTTCATGCA ATGCAGAAAC GTGATGCAAA AAAAGGTCTG GCCACCCTGT GTATTGGTGG
2641 TGGTCAGGGC ACCGCAATTC TGCTGGAAAA ATGTCCTAGG TGGAGCCATC CGCAGTTTGA
2701 AAAATAACCT AGGTGAACGT CGCATCAGGC AATGAATGCG AAACCGCGGT GTAAATAACG
2761 ACAAAAATAA AATTGGCCGC TTCGGTCAGG GCCAACTATT GCCTGAAAAA GGGTAACGAT
2821 CCTCAGCGAG CTGTTGACAA TTAATCATCG GCTCGTATAA TGTGTGGAAT TGTGAGCGGA
2881 TAACAATTTC ACACAGGAAA CAGAATTCTC TCGAGATGAA AACGAAACTG ATGACTTTAC
2941 AAGATGCAAC CGGCTTTTTC CGTGATGGTA TGACCATTAT GGTTGGTGGT TTCATGGGCA
3001 TCGGTACGCC AAGCCGCTTG GTGGAGGCAT TGCTGGAATC TGGTGTGCGT GACTTGACTC
3061 TGATCGCGAA TGATACCGCG TTTGTGGACA CGGGCATTGG TCCGCTGATT GTGAACGGTC
3121 GTGTCCGCAA AGTGATCGCG TCGCATATCG GTACCAATCC GGAAACCGGC CGTCGTATGA
3181 TCAGCGGTGA AATGGACGTT GTCCTGGTCC CGCAGGGCAC CCTGATTGAG CAGATTCGCT
3241 GCGGCGGTGC TGGTCTTGGT GGCTTCCTGA CGCCTACCGG CGTTGGCACC GTCGTGGAAG
3301 AGGGTAAGCA GACCCTGACG CTGGACGGCA AGACCTGGCT GCTGGAGCGT CCGCTGCGTG
3361 CTGATCTGGC GCTGATCCGT GCCCACCGCT GTGACACCCT GGGTAACCTG ACGTACCAAC
3421 TGAGCGCGCG TAATTTCAAC CCGCTGATTG CCCTGGCGGC AGATATTACC CTGGTTGAGC
3481 CGGATGAGCT GGTTGAAACG GGTGAGCTGC AACCGGACCA CATCGTCACC CCTGGTGCCG
3541 TTATCGACCA CATCATCGTT TCACAGGAGA GCAAATAATG GATGCCAAAC AGCGTATTGC
3601 ACGTCGCGTC GCCCAAGAAT TGAGAGATGG TGATATCGTG AATCTGGGCA TTGGCCTGCC
3661 GACGATGGTC GCGAATTACT TGCCGGAGGG TATCCATATT ACCCTGCAAA GCGAAAACGG
3721 TTTTCTGGGT CTGGGTCCGG TCACCACTGC GCACCCGGAC TTGGTTAATG CGGGTGGTCA
3781 ACCTTGCGGT GTTCTGCCGG GTGCAGCTAT GTTCGACTCC GCAATGAGCT TTGCGTTAAT
3841 CCGTGGCGGC CACATTGATG CTTGTGTCCT GGGTGGCCTT CAGGTGGACG AGGAAGCGAA
3901 CCTGGCGAAC TGGGTGGTCC CGGGCAAGAT GGTCCCGGGT ATGGGTGGTG CTATGGACCT
3961 GGTAACCGGC AGCCGTAAGG TTATCATTGC GATGGAGCAC TGTGCGAAAG ACGGCAGCGC
4021 AAAGATCCTG CGCCGCTGCA CGATGCCGCT GACCGCCCAG CATGCAGTTC ACATGTTGGT
4081 GACCGAACTG GCCGTGTTTC GTTTCATTGA TGGCAAAATG TGGCTGACGG AGATCGCGGA
4141 TGGCTGCGAC CTGGCGACCG TGCGCGCCAA AACCGAGGCA CGTTTCGAGG TTGCTGCAGA
4201 CCTGAATACG CAGCGTGGTG ACCTGTGGCG CGCCCATCAT CACCATCACC ACCATCATCA
4261 CCACTGAGGC GCGCCTAAAC GTCGCATCAG GCAATGAATG CGAAACCGCG GTGTAAATAA
4321 CGACAAAAAT AAAATTCCAA CTATTGCCTG AAAAAGGGTA ACGATGTACA GAGCTGTTGA
4381 CAATTAATCA TCGGCTCGTA TAATGTGTGG AATTGTGAGC GGATAACAAT TTCACACAGG
4441 AAACAGAATT CTTTAATTAA ATGCTGAAAG ATGAAGTTAT CAAGCAAATT TCGACCCCAC
4501 TGACCAGCCC GGCATTCCCG CGTGGTCCAT ACAAGTTCCA TAATCGTGAA TACTTTAACA
4561 TTGTTTACCG TACGGACATG GATGCGCTGC GCAAGGTTGT TCCGGAGCCT TTGGAAATTG
4621 ACGAGCCGTT AGTGCGCTTC GAGATCATGG CCATGCACGA CACCAGCGGT CTGGGTTGCT
4681 ACACCGAGAG CGGCCAAGCG ATCCCGGTGA GCTTCAACGG TGTCAAAGGT GATTATCTGC
4741 ACATGATGTA TCTGGATAAC GAGCCAGCGA TCGCGGTTGG TCGTGAACTG AGCGCTTATC
4801 CGAAAAAGCT GGGCTATCCG AAACTGTTTG TGGATTCTGA TACCCTGGTG GGTACCCTGG
```

```
4861 ACTATGGTAA ACTGCGCGTG GCCACGGCGA CGATGGGTTA CAAACATAAG GCGTTAGACG
4921 CGAATGAAGC AAAGGATCAG ATTTGTCGTC CGAATTACAT GCTGAAGATT ATCCCGAACT
4981 ACGACGGCAG CCCGCGTATC TGCGAACTGA TTAATGCGAA GATTACCGAC GTTACGGTCC
5041 ACGAGGCATG GACTGGCCCG ACCCGCCTGC AGTTGTTTGA CCATGCCATG GCTCCGCTGA
5101 ACGATCTGCC GGTGAAAGAG ATTGTGAGCA GCTCCCACAT CCTCGCCGAC ATTATCCTGC
5161 CGCGTGCAGA GGTTATCTAT GACTATCTGA AATGGCCGGC CGATTATAAA GATGATGATG
5221 ATAAATAAGG CCGGCCTGAA CGTCGCATCA GGCAATGAAT GCGAAACCGC GGTGTAAATT
5281 TGGCCGCTTC GGTCAGGGCC AACTATTGCC TGAAAAAGGG TAACGATACT AGTGAGCTGT
5341 TGACAATTAA TCATCGGCTC GTATAATGTG TGGAATTGTG AGCGGATAAC AATTTCACAC
5401 AGGAAACAGA ATTCTACCGG TATGAAAGGT TTTGCAATGC TGGGCATCAA TAAACTGGGT
5461 TGGATTGAGA AGGAACGCCC GGTCGCGGGC AGCTACGACG CGATTGTTCG CCCGCTGGCA
5521 GTCAGCCCGT GCACCAGCGA TATCCACACG GTGTTCGAGG GTGCGCTGGG TGATCGTAAA
5581 AACATGATCC TGGGTCATGA GGCTGTGGGC GAAGTCGTGG AAGTTGGTTC CGAGGTTAAG
5641 GACTTTAAAC CGGGTGATAG AGTTATTGTC CCGTGCACGA CCCCGGACTG GCGTTCTTTG
5701 GAAGTGCAAG CGGGTTTTCA GCAGCACTCC AATGGCATGT TGGCGGGCTG GAAATTCAGC
5761 AATTTCAAAG ACGGCGTGTT TGGCGAGTAT TTCCACGTTA ATGACGCGGA TATGAACCTG
5821 GCAATTCTGC CGAAAGATAT GCCGCTGGAG AATGCGGTTA TGATTACGGA CATGATGACC
5881 ACGGGTTTTC ATGGCGCAGA ACTGGCAGAC ATCCAAATGG GCAGCAGCGT TGTCGTCATC
5941 GGTATCGGTG CGGTGGGCCT GATGGGTATC GCCGGTGCGA AACTGCGTGG TGCTGGTCGT
6001 ATCATCGGTG TCGGCAGCCG TCCGATTTGC GTGGAGGCGG CCAAGTTCTA CGGTGCCACC
6061 GACATTCTGA ACTATAAGAA TGGTCACATC GTTGATCAGG TTATGAAACT GACCAACGGT
6121 AAGGGCGTGG ATCGTGTGAT TATGGCTGGT GGTGGTAGCG AAACCCTGTC TCAAGCCGTT
6181 TCCATGGTCA AGCCAGGCGG CATTATCAGC AACATTAACT ATCATGGTTC GGGTGACGCA
6241 CTGCTGATTC CGCGTGTTGA GTGGGGTTGT GGCATGGCCC ACAAAACTAT TAAGGGCGGT
6301 CTGTGTCCGG GTGGTCGTCT GCGTGCGGAG ATGCTGCGCG ACATGGTCGT ATACAACCGC
6361 GTTGATCTGA GCAAGTTGGT GACCCATGTC TACCACGGCT TCGATCACAT TGAGGAAGCG
6421 CTGCTGTTGA TGAAGGATAA GCCGAAGGAC CTGATCAAAG CGGTGGTTAT CTTGGGGCCC
6481 GAACAGAAAC TGATTAGCGA AGAAGATCTG TAAGGGCCCT GAATAAAACG AAAGGCTCAG
6541 TCGAAAGACT GGGCCTTTCG TTTTATACGT CGCATCAGGC AATGAATGCG AAACCGCGGT
6601 GTAAATAACG ACAAAAATGG TCAGGGCCAA CTATTGCCTG AAAAAGGGTA ACGATATGGC
6661 CCTTCGCTGG GATGGTGAAA CCATGAAAAA TGGCAGCTTC AGTGGATTAA GTGGGGGTAA
6721 TGTGGCCTGT ACCCTCTGGT TGCATAGGTA TTCATACGGT TAAAATTTAT CAGGCGCGAT
6781 CGCGGCAGTT TTTCGGGTGG TTTGTTGCCA TTTTTACCTG TCTGCTGCCG TGATCGCGCT
6841 GAACGCGTTT TAGCGGTGCG TACAATTAAG GGATTATGGT AAATCCACTT ACTGTCTGCC
6901 CTCGTAGCCA TAACGTTGAT CGAAAACGCG CTGAAAAACG CTGCTGAATG TGCGAGCTTC
6961 TTCCGCTTCC TCGCTCACTG ACTCGCTGCG CTCGGTCGTT CGGCTGCGGC GAGCGGTATC
7021 AGCTCACTCA AAGGCGGTAA TACGGTTATC CACAGAATCA GGGGATAACG CAGGAAAGAA
7081 CATGTGAGCA AAAGGCCAGC AAAAGGCCAG GAACCGTAAA AAGGCCGCGT TGCTGGCGTT
7141 TTTCCATAGG CTCCGCCCCC CTGACGAGCA TCACAAAAAT CGACGCTCAA GTCAGAGGTG
7201 GCGAAACCCG ACAGGACTAT AAAGATACCA GGCGTTTCCC CCTGGAAGCT CCCTCGTGCG
7261 CTCTCCTGTT CCGACCCTGC CGCTTACCGG ATACCTGTCC GCCTTTCTCC CTTCGGGAAG
7321 CGTGGCGCTT TCTCATAGCT CACGCTGTAG GTATCTCAGT TCGGTGTAGG TCGTTCGCTC
7381 CAAGCTGGGC TGTGTGCACG AACCCCCCGT TCAGCCCGAC CGCTGCGCCT TATCCGGTAA
7441 CTATCGTCTT GAGTCCAACC CGGTAAGACA CGACTTATCG CCACTGGCAG CAGCCACTGG
7501 TAACAGGATT AGCAGAGCGA GGTATGTAGG CGGTGCTACA GAGTTCTTGA AGTGGTGGCC
7561 TAACTACGGC TACACTAGAA GAACAGTATT TGGTATCTGC GCTCTGCTGA AGCCAGTTAC
7621 CTTCGGAAAA AGAGTTGGTA GCTCTTGATC CGGCAAACAA ACCACCGCTG GTAGCGGTGG
```

```
7681  TTTTTTTGTT  TGCAAGCAGC  AGATTACGCG  CAGAAAAAAA  GGATCTCAAG  AAGATCCTTT
7741  GATCTTTTCT  ACGGGGTCTG  ACGCTCAGTG  GAACTCCGTC  GA
```

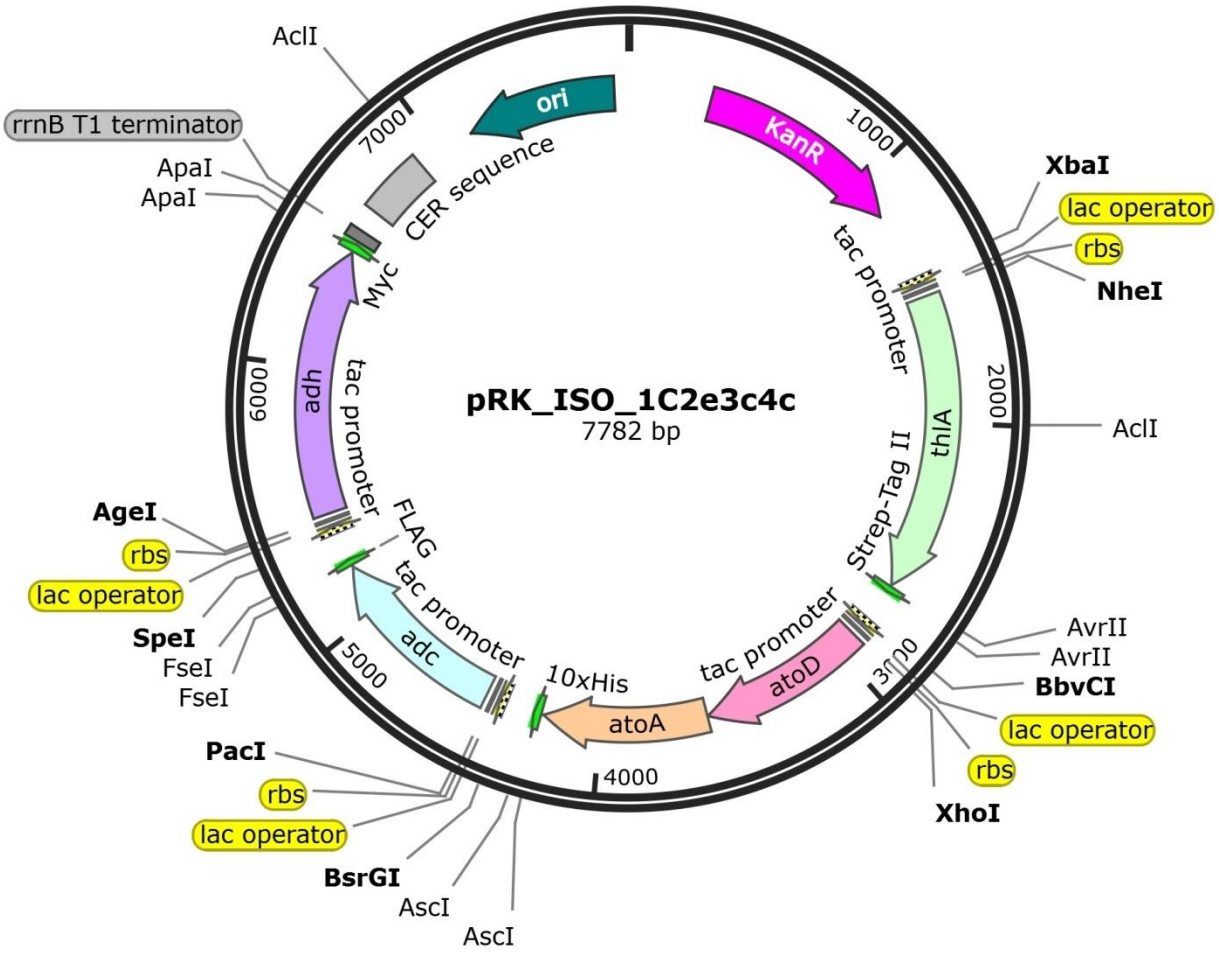

Figure A-3: Plasmid map of pRK_ISO_1C2e3c4c.
Plasmid map was generated via SnapGene® Viewer 4.0.7 according to the DNA sequence in Table A-3.
Legend: thlA... acetyl-CoA acetyltransferase gene, atoD/atoA… acetate CoA-transferase genes, adc… acetoacetate decarboxylase gene, adh… isopropanol dehydrogenase gene
rbs… ribosome binding site KanR… kanamycin resistance gene ori… pMB1 origin of replication.

Table A-4: DNA sequence of the pta gene (*E. coli*).

Size: 2145 bp.

Nucleotide sequence of pta was obtained GenBank® at National Center for Biotechnology Information (NCBI, U.S. National Library of Medicine, Bethesda, MD, USA) (AS: NC_000913.3, *E. coli* K-12 MG1655). Oligonucleotides for targeting the desired recombination site for pta disruption via Red®/ET® recombination (4.2.2.8) and for verification of Red®/ET® recombination mutants are listed in Table 4-10.

Legend:

Oligonucleotide target site for homologous recombination insertion site for FRT-PGK-gb2-neo-FRT cassette oligonucleotide target site for verification of mutants.

```
   1 GTGTCCCGTA TTATTATGCT GATCCCTACC GGAACCAGCG TCGGTCTGAC CAGCGTCAGC
  61 CTTGGCGTGA TCCGTGCAAT GGAACGCAAA GGCGTTCGTC TGAGCGTTTT CAAACCTATC
 121 GCTCAGCCGC GTACCGGTGG CGATGCGCCC GATCAGACTA CGACTATCGT GCGTGCGAAC
 181 TCTTCCACCA CGACGGCCGC TGAACCGCTG AAAATGAGCT ACGTTGAAGG TCTGCTTTCC
 241 AGCAATCAGA AAGATGTGCT GATGGAAGAG ATCGTCGCAA ACTACCACGC TAACACCAAA
 301 GACGCTGAAG TCGTTCTGGT TGAAGGTCTG GTCCCGACAC GTAAGCACCA GTTTGCCCAG
 361 TCTCTGAACT ACGAAATCGC TAAAACGCTG AATGCGGAAA TCGTCTTCGT TATGTCTCAG
 421 GGCACTGACA CCCCGGAACA GCTGAAAGAG CGTATCGAAC TGACCCGCAA CAGCTTCGGC
 481 GGTGCCAAAA ACACCAACAT CACCGGCGTT ATCGTTAACA AACTGAACGC ACCGGTTGAT
 541 GAACAGGGTC GTACTCGCCC GGATCTGTCC GAGATTTTCG ACGACTCTTC CAAAGCTAAA
 601 GTAAACAATG TTGATCCGGC GAAGCTGCAA GAATCCAGCC CGCTGCCGGT TCTCGGCGCT
 661 GTGCCGTGGA GCTTTGACCT GATCGCGACT CGTGCGATCG ATATGGCTCG CCACCTGAAT
 721 GCGACCATCA TCAACGAAGG CGACATCAAT ACTCGCCGCG TTAAATCCGT CACTTTCTGC
 781 GCACGCAGCA TTCCGCACAT GCTGGAGCAC TTCCGTGCCG GTTCTCTGCT GGTGACTTCC
 841 GCAGACCGTC CTGACGTGCT GGTGGCCGCT TGCCTGGCAG CCATGAACGG CGTAGAAATC
 901 GGTGCCCTGC TGCTGACTGG CGGTTACGAA ATGGACGCGC GCATTTCTAA ACTGTGCGAA
 961 CGTGCTTTCG CTACCGGCCT GCCGGTATTT ATGGTGAACA CCAACACCTG GCAGACCTCT
1021 CTGAGCCTGC AGAGCTTCAA CCTGGAAGTT CCGGTTGACG ATCACGAACG TATCGAGAAA
1081 GTTCAGGAAT ACGTTGCTAA CTACATCAAC GCTGACTGGA TCGAATCTCT GACTGCCACT
1141 TCTGAGCGCA GCCGTCGTCT GTCTCCGCCT GCGTTCCGTT ATCAGCTGAC TGAACTTGCG
1201 CGCAAAGCGG GCAAACGTAT CGTACTGCCG GAAGGTGACG AACCGCGTAC CGTTAAAGCA
1261 GCCGCTATCT GTGCTGAACG TGGTATCGCA ACTTGCGTAC TGCTGGGTAA TCCGGCAGAG
1321 ATCAACCGTG TTGCAGCGTC TCAGGGTGTA GAACTGGGTG CAGGGATTGA AATCGTTGAT
1381 CCAGAAGTGG TTCGCGAAAG CTATGTTGGT CGTCTGGTCG AACTGCGTAA GAACAAAGGC
1441 ATGACCGAAA CCGTTGCCCG CGAACAGCTG GAAGACAACG TGGTGCTCGG TACGCTGATG
1501 CTGGAACAGG ATGAAGTTGA TGGTCTGGTT TCCGGTGCTG TTCACACTAC CGCAAACACC
1561 ATCCGTCCGC CGCTGCAGCT GATCAAAACT GCACCGGGCA GCTCCCTGGT ATCTTCCGTG
1621 TTCTTCATGC TGCTGCCGGA ACAGGTTTAC GTTTACGGTG ACTGTGCGAT CAACCCGGAT
1681 CCGACCGCTG AACAGCTGGC AGAAATCGCG ATTCAGTCCG CTGATTCCGC TGCGGCCTTC
1741 GGTATCGAAC CGCGCGTTGC TATGCTCTCC TACTCCACCG GTACTTCTGG TGCAGGTAGC
1801 GACGTAGAAA AAGTTCGCGA AGCAACTCGT CTGGCGCAGG AAAAACGTCC TGACCTGATG
1861 ATCGACGGTC CGCTGCAGTA CGACGCTGCG GTAATGGCTG ACGTTGCGAA ATCCAAAGCG
1921 CCGAACTCTC CGGTTGCAGG TCGCGCTACC GTGTTCATCT TCCCGGATCT GAACACCGGT
1981 AACACCACCT ACAAAGCGGT ACAGCGTTCT GCCGACCTGA TCTCCATCGG GCCGATGCTG
2041 CAGGGTATGC GCAAGCCGGT TAACGACCTG TCCCGTGGCG CACTGGTTGA CGATATCGTC
2101 TACACCATCG CGCTGACTGC GATTCAGTCT GCACAGCAGC AGTAA
```

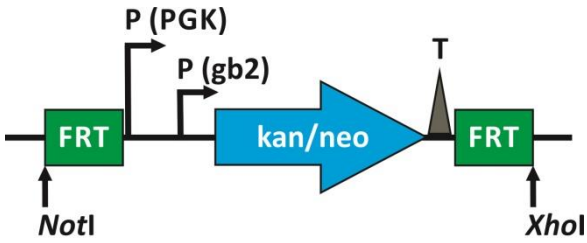

Figure A-4: Schematic presentation of FRT-PGK-gb2-neo-FRT cassette.
The FRT PGK-gb2-neo-FRT cassette encodes expression of the kanamycin resistance gene (kan) with a prokaryotic (gb2) promoter and expression of the neomycin resistance gene (neo) with a eukaryotic mouse phosphoglucokinase (PGK) promoter in *E. coli* and mammalian cells. FRT (FLP recombinase target) sites are later excised by FLP recombinase. For sequence details, see manufacturer's manual (Gene Bridges GmbH, Heidelberg, Germany).

A.2 Amino Acid Sequences and Enzyme Parameters

Table A-5: Amino acid sequence of Act-StrepII (1E).
Size: 404 aa (Act: 394 aa, StrepII: 8 aa).
Protein Act (*E. coli* K-12 MG1655, EC number 2.3.1.9) is coded by gene atoB (AS: AAC75284.1), which was codon usage optimized (DNA2.0, Menlo Park, CA, USA) and C-terminally fused to StrepII tag.
Legend: StrepII tag aa added by restriction site
Act… acetyl-CoA acetyltransferase, aa… amino acid(s)

```
  1 MKNCVIVSAV RTAIGSFNGS LASTSAIDLG ATVIKAAIER AKIDSQHVDE VIMGNVLQAG
 61 LGQNPARQAL LKSGLAETVC GFTVNKVCGS GLKSVALAAQ AIQAGQAQSI VAGGMENMSL
121 APYLLDAKAR SGYRLGDGQV YDVILRDGLM CATHGYHMGI TAENVAKEYG ITREMQDELA
181 LHSQRKAAAA IESGAFTAEI VPVNVVTRKK TFVFSQDEFP KANSTAEALG ALRPAFDKAG
241 TVTAGNASGI NDGAAALVIM EESAALAAGL TPLARIKSYA SGGVPPALMG MGPVPATQKA
301 LQLAGLQLAD IDLIEANEAF AAQFLAVGKN LGFDSEKVNV NGGAIALGHP IGASGARILV
361 TLLHAMQARD KTLGLATLCI GGGQGIAMVI ERLNPRWSHP QFEK
```

Table A-6: Parameters of Act-StrepII (1E) and Act (*E. coli*).
Parameters were calculated by ProtParam (4.1.13) according to the amino acid sequence (Table A-5). Protein half-life was estimated according to the amino acids present in the N-terminus [Varshavsky, 1997]. Stability was calculated according to the method described in [Guruprasad et al., 1990]. GRAVY sums all hydropathy values [Kyte and Doolittle, 1982] of the amino acids and divides them by the overall number of amino acids. Increasing positive score indicates increasing hydrophobicity.
MW of StrepII tag = 1058.1 Da, MW of StrepII tag plus aa added by restriction sites = 1311.4 Da.

Parameter	Act-StrepII (1E)	Act (*E. coli*)[c]
Number of amino acids	404	394
Molecular mass [Da]	41645.9	40352.4
Theoretical pI	7.05	6.61
Extinction coefficient	14690 [a]	9190 [a]
[L mol^{-1} cm^{-1}][d]	14440 [b]	8940 [b]
Cysteins	5	5
Half-life in *E. coli* [h]	>10	>10
Stability classification	stable	stable
GRAVY	0.210	0.268

pI… isoelectric point, GRAVY… grand average of hydropathicity, MW… molecular mass, aa… amino acid(s)
[a] assuming all cysteins form pairs, [b] assuming all cystein residues are reduced, [c] original enzyme in *E. coli*, [d] at 280 nm in H_2O.

Table A-7: Amino acid sequence of Act-StrepII (1C).
Size: 402 aa (Act: 392 aa, StrepII: 8 aa).
Protein Act (*C. acetobutylicum* ATCC 824, EC number 2.3.1.9) is coded by gene thlA (AS: NP_349476.1), which was codon usage optimized (Thermo Fisher Scientific - Life Technologies GmbH, Darmstadt, Germany) and C-terminally fused to StrepII tag.
Legend: StrepII tag aa added by restriction site
Act… acetyl-CoA acetyltransferase, aa… amino acid(s)

```
  1 MKEVVIASAV RTAIGSYGKS LKDVPAVDLG ATAIKEAVKK AGIKPEDVNE VILGNVLQAG
 61 LGQNPARQAS FKAGLPVEIP AMTINKVCGS GLRTVSLAAQ IIKAGDADVI IAGGMENMSR
121 APYLANNARW GYRMGNAKFV DEMITDGLWD AFNDYHMGIT AENIAERWNI SREEQDEFAL
181 ASQKKAEEAI KSGQFKDEIV PVVIKGRKGE TVVDTDEHPR FGSTIEGLAK LKPAFKKDGT
241 VTAGNASGLN DCAAVLVIMS AEKAKELGVK PLAKIVSYGS AGVDPAIMGY GPFYATKAAI
301 EKAGWTVDEL DLIESNEAFA AQSLAVAKDL KFDMNKVNVN GGAIALGHPI GASGARILVT
361 LVHAMQKRDA KKGLATLCIG GGQGTAILLE KCPRWSHPQF EK
```

Table A-8: Parameters of Act-StrepII (1C) and Act (*C. acetobutylicum)*.
Parameters were calculated by ProtParam (4.1.13) according to the amino acid sequence (Table A-7). Protein half-life was estimated according to the amino acids present in the N-terminus [Varshavsky, 1997]. Stability was calculated according to the method described in [Guruprasad et al., 1990]. GRAVY sums all hydropathy values [Kyte and Doolittle, 1982] of the amino acids and divides them by the overall number of amino acids. Increasing positive score indicates increasing hydrophobicity.
MW of StrepII tag = 1058.1 Da, MW of StrepII tag plus aa added by restriction sites = 1311.4 Da.

Parameter	Act-StrepII (1C)	Act (*C. acetobutylicum)*[c]
Number of amino acids	402	392
Molecular mass [Da]	42533.9	41240.5
Theoretical pI	7.62	6.92
Extinction coefficient	38180 [a]	32680 [a]
[L mol^{-1} cm^{-1}] [d]	37930 [b]	32430 [b]
Cysteins	4	4
Half-life in *E. coli* [h]	>10	>10
Stability classification	stable	stable
GRAVY	-0.056	-0.005

pI… isoelectric point, GRAVY… grand average of hydropathicity, MW… molecular mass, aa… amino acid(s)
[a] assuming all cysteins form pairs, [b] assuming all cystein residues are reduced, [c] original enzyme in *C. acetobutylicum*, [d] at 280 nm in H_2O.

Table A-9: Amino acid sequence of Acct-His$_{10}$ (2e) – subunit α & β.
Size: subunit α: 220 aa, subunit β: 216 aa, His$_{10}$: 10 aa.
Protein Acct (*E. coli* K-12 MG1655, EC number 2.8.3.8) is coded by genes atoD (subunit α, AS: NP_416725.1) and atoA (subunit β, AS: NP_416726.1), which were codon usage optimized (DNA2.0, Menlo Park, CA, USA). Subunit β was C-terminally fused to His$_{10}$ tag.
Legend: His$_{10}$ tag aa added by restriction site
Acct… acetate CoA-transferase, aa… amino acid(s)
Subunit α:

```
  1 MKTKLMTLQD ATGFFRDGMT IMVGGFMGIG TPSRLVEALL ESGVRDLTLI ANDTAFVDTG
 61 IGPLIVNGRV RKVIASHIGT NPETGRRMIS GEMDVVLVPQ GTLIEQIRCG GAGLGGFLTP
121 TGVGTVVEEG KQTLTLDGKT WLLERPLRAD LALIRAHRCD TLGNLTYQLS ARNFNPLIAL
181 AADITLVEPD ELVETGELQP DHIVTPGAVI DHIIVSQESK
```

Subunit β:

```
  1 MDAKQRIARR VAQELRDGDI VNLGIGLPTM VANYLPEGIH ITLQSENGFL GLGPVTTAHP
 61 DLVNAGGQPC GVLPGAAMFD SAMSFALIRG GHIDACVLGG LQVDEEANLA NWVVPGKMVP
121 GMGGAMDLVT GSRKVIIAME HCAKDGSAKI LRRCTMPLTA QHAVHMLVTE LAVFRFIDGK
181 MWLTEIADGC DLATVRAKTE ARFEVAADLN TQRGDLWRAH HHHHHHHHHH
```

Table A-10: Parameters of Acct-His$_{10}$ (2e) – subunit α & β and Acct (*E. coli*) – subunit β.
Parameters were calculated by ProtParam (4.1.13) according to the amino acid sequence (Table A-9). Protein half-life was estimated according to the amino acids present in the N-terminus [Varshavsky, 1997]. Stability was calculated according to the method described in [Guruprasad et al., 1990]. GRAVY sums all hydropathy values [Kyte and Doolittle, 1982] of the amino acids and divides them by the overall number of amino acids. Increasing positive score indicates increasing hydrophobicity.
MW of His$_{10}$ tag = 1389.4 Da, MW of His$_{10}$ tag plus aa added by restriction sites = 1802.9 Da.

Parameter	**Acct-His$_{10}$ (2e) – subunit α**	**Acct-His$_{10}$ (2e) – subunit β**	**Acct (*E. coli*) – subunit β[c]**
Number of amino acids	220	229	216
Molecular mass [Da]	23526.2	24744.5	22959.6
Theoretical pI	5.10	6.45	5.65
Extinction coefficient	7115 [a]	18240 [a]	12740 [a]
[L mol^{-1} cm^{-1}] [d]	6990 [b]	17990 [b]	12490 [b]
Cysteins	2	5	5
Half-life in *E. coli* [h]	>10	>10	>10
Stability classification	stable	unstable	unstable
GRAVY	0.155	0.007	0.172

pI… isoelectric point, GRAVY… grand average of hydropathicity, MW… molecular mass, aa… amino acid(s)
[a] assuming all cysteins form pairs, [b] assuming all cystein residues are reduced, [c] original enzyme in *E. coli*, [d] at 280 nm in H_2O.

Table A-11: Amino acid sequence of Adc-FLAG (3c).
Size: 255 aa (Adc: 244 aa, FLAG: 8 aa).
Protein Adc (*C. acetobutylicum* ATCC 824, EC number 4.1.1.4) is coded by gene adc (AS: NP_149328.1), which was codon usage optimized (DNA2.0, Menlo Park, CA, USA) and C-terminally fused to FLAG tag.
Legend: FLAG tag aa added by restriction site
Adc… acetoacetate decarboxylase, aa… amino acid(s)

```
  1 MLKDEVIKQI  STPLTSPAFP  RGPYKFHNRE  YFNIVYRTDM  DALRKVVPEP  LEIDEPLVRF
 61 EIMAMHDTSG  LGCYTESGQA  IPVSFNGVKG  DYLHMMYLDN  EPAIAVGREL  SAYPKKLGYP
121 KLFVDSDTLV  GTLDYGKLRV  ATATMGYKHK  ALDANEAKDQ  ICRPNYMLKI  IPNYDGSPRI
181 CELINAKITD  VTVHEAWTGP  TRLQLFDHAM  APLNDLPVKE  IVSSSHILAD  IILPRAEVIY
241 DYLKWPADYK  DDDDK
```

Table A-12: Parameters of Adc-FLAG (3c) and Adc (*C. acetobutylicum*).
Parameters were calculated by ProtParam (4.1.13) according to the amino acid sequence (Table A-11). Protein half-life was estimated according to the amino acids present in the N-terminus [Varshavsky, 1997]. Stability was calculated according to the method described in [Guruprasad et al., 1990]. GRAVY sums all hydropathy values [Kyte and Doolittle, 1982] of the amino acids and divides them by the overall number of amino acids. Increasing positive score indicates increasing hydrophobicity.
MW of FLAG tag = 1012.9 Da, MW of FLAG tag plus aa added by restriction sites = 1367.3 Da.

Parameter	Adc-FLAG (3c)	Adc (*C. acetobutylicum*)[c]
Number of amino acids	255	244
Molecular mass [Da]	28886.2	27536.8
Theoretical pI	5.39	5.81
Extinction coefficient	33475 [a]	26485 [a]
[L mol^{-1} cm^{-1}] [d]	33350 [b]	26360 [b]
Cysteins	3	3
Half-life in *E. coli* [h]	>10	>10
Stability classification	stable	stable
GRAVY	-0.291	-0.192

pI… isoelectric point, GRAVY… grand average of hydropathicity, MW… molecular mass, aa… amino acid(s)
[a] assuming all cysteins form pairs, [b] assuming all cystein residues are reduced, [c] original enzyme in *C. acetobutylicum*, [d] at 280 nm in H_2O.

Table A-13: Amino acid sequence of Idh-c-Myc (4c).
Size: 363 aa (Idh: 351 aa, c-Myc: 10 aa).
Protein Idh (*C. beijerinckii* NRRL B593, EC number 1.1.1.80) is coded by gene adh (AS: AAA23199.2), which was codon usage optimized (DNA2.0, Menlo Park, CA, USA) and C-terminally fused to c-Myc tag.
Legend: c-Myc tag aa added by restriction site
Idh… isopropanol dehydrogenase, aa… amino acid(s)

```
  1 MKGFAMLGIN  KLGWIEKERP  VAGSYDAIVR  PLAVSPCTSD  IHTVFEGALG  DRKNMILGHE
 61 AVGEVVEVGS  EVKDFKPGDR  VIVPCTTPDW  RSLEVQAGFQ  QHSNGMLAGW  KFSNFKDGVF
121 GEYFHVNDAD  MNLAILPKDM  PLENAVMITD  MMTTGFHGAE  LADIQMGSSV  VVIGIGAVGL
181 MGIAGAKLRG  AGRIIGVGSR  PICVEAAKFY  GATDILNYKN  GHIVDQVMKL  TNGKGVDRVI
241 MAGGGSETLS  QAVSMVKPGG  IISNINYHGS  GDALLIPRVE  WGCGMAHKTI  KGGLCPGGRL
301 RAEMLRDMVV  YNRVDLSKLV  THVYHGFDHI  EEALLLMKDK  PKDLIKAVVI  LGPEQKLISE
361 EDL
```

Table A-14: Parameters of Idh-c-Myc (4c) and Idh (*C. beijerinckii)*.

Parameters were calculated by ProtParam (4.1.13) according to the amino acid sequence (Table A-13). Protein half-life was estimated according to the amino acids present in the N-terminus [Varshavsky, 1997]. Stability was calculated according to the method described in [Guruprasad et al., 1990]. GRAVY sums all hydropathy values [Kyte and Doolittle, 1982] of the amino acids and divides them by the overall number of amino acids. Increasing positive score indicates increasing hydrophobicity.
MW of c-Myc tag = 1203.3 Da, MW of c-Myc tag plus aa added by restriction sites = 1357.4 Da.

Parameter	**Idh-c-Myc (4c)**	**Idh (*C. beijerinckii*)[c]**
Number of amino acids	363	351
Molecular mass [Da]	39055.3	37715.9
Theoretical pI	6.13	6.60
Extinction coefficient	32680 [a]	32680 [a]
[L mol^{-1} cm^{-1}] [d]	32430 [b]	32430 [b]
Cysteins	5	5
Half-life in *E. coli* [h]	>10	>10
Stability classification	stable	stable
GRAVY	0.078	0.115

pI… isoelectric point, GRAVY… grand average of hydropathicity, MW… molecular mass, aa… amino acid(s)
[a] assuming all cysteins form pairs, [b] assuming all cystein residues are reduced, [c] original enzyme in *C. beijerinckii*, [d] at 280 nm in H_2O.

A.3 Additional Result Figures

(A) Act-StrepII (1C) **(B) Acct-His_{10} (2e), Adc-FLAG (3c) & Idh-c-Myc (4c)**

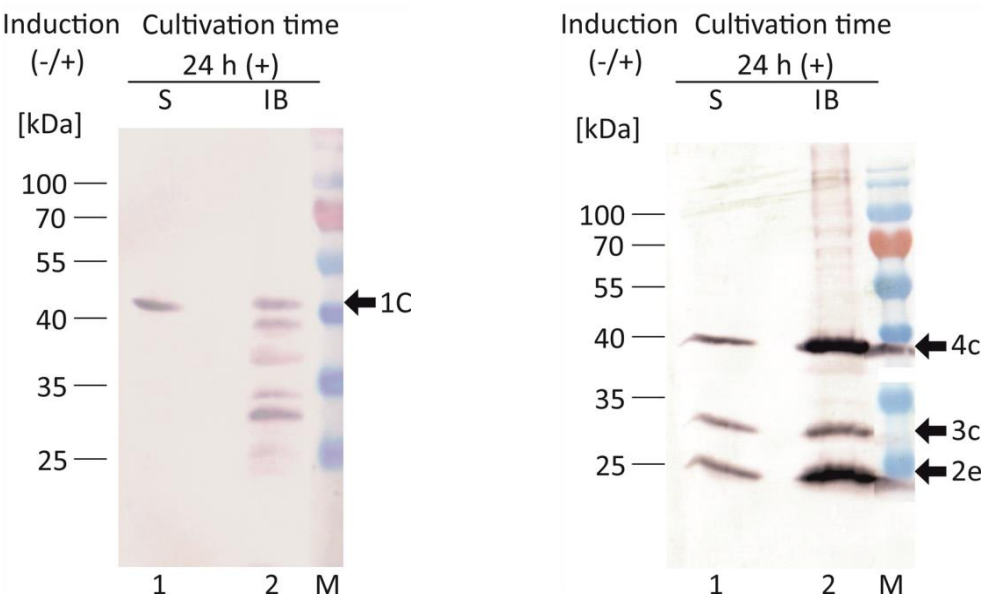

Figure A-5: Production of Act-StrepII (1C) (A), Acct-His_{10} (2e), Adc-FLAG (3c) and Idh-c-Myc (4c) (B) in *E. coli* DH5α_1C at 37 °C in 100 mL shake flask scale.

Recombinant *E. coli* DH5α were grown in 100 mL LB medium, 2% (w/v) glucose at 37 °C, 100 rpm. Induction was performed by addition of 0.1 mM IPTG at OD_{600} = 0.5 - 0.6. 1/OD samples were taken at intervals, lysed and divided into soluble and insoluble cell extract fraction (4.2.3.2). Extracts were separated by SDS-PAGE and Act-StrepII (1C) was visualized by WB with anti-StrepII®, Acct-His_{10} (2e) with anti-polyHistidine, Adc-FLAG (3c) with anti-FLAG® and Idh-c-Myc (4c) with anti-c-Myc and anti-Mouse IgG-conjugated alkaline phosphatase antibodies (dye: BCIP/NBT) (see Table 4-12 for antibodies).

Lanes with odd numbers display the soluble fraction (S), whereas lanes with even numbers display the insoluble fraction (IB) samples. Arrows indicate the detected proteins. Theoretical molecular protein masses were calculated using ProtParam: MW of Act-StrepII (1C) = 42.5 kDa, MW of Acct-His_{10} (2e) = 24.7 kDa, MW of Adc-FLAG (3c) = 28.9 kDa, MW of Idh-c-Myc (4c) = 39.0 kDa.

Act… acetyl-CoA acetyltransferase, Acct… acetate CoA-transferase, Adc… acetoacetate decarboxylase, Idh… isopropanol dehydrogenase

The original figures were kindly provided by B. Schrank.

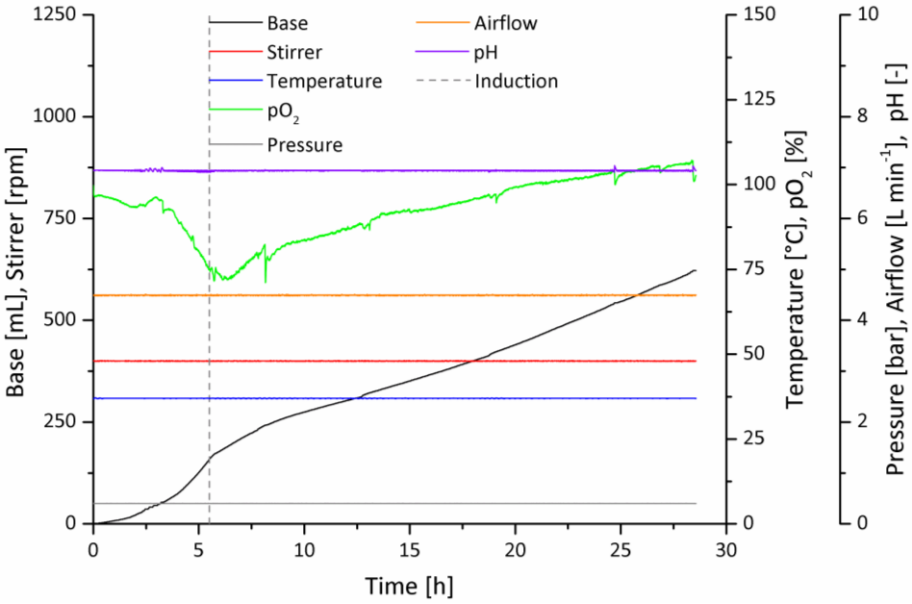

Figure A-6: Time course of control variables and base addition for *E. coli* DH5α_1E in LB plus 50% BWH/50% glucose feed in 10 L bioreactor scale.

Recombinant *E. coli* DH5α were cultivated in 10 L LB medium containing 2% (w/v) glucose. Pulsed feeding of a mixture consisting of 50% BWH and 50% pure glucose was applied when glucose concentration was below 10 g L^{-1}. Control variables were set to 37 °C, pH 7.0, 0.4 bar, 5 L air min^{-1}, 400 rpm (pO_2 > 25%). Induction was performed at OD_{600} ~6.0 with 0.1 mM IPTG.

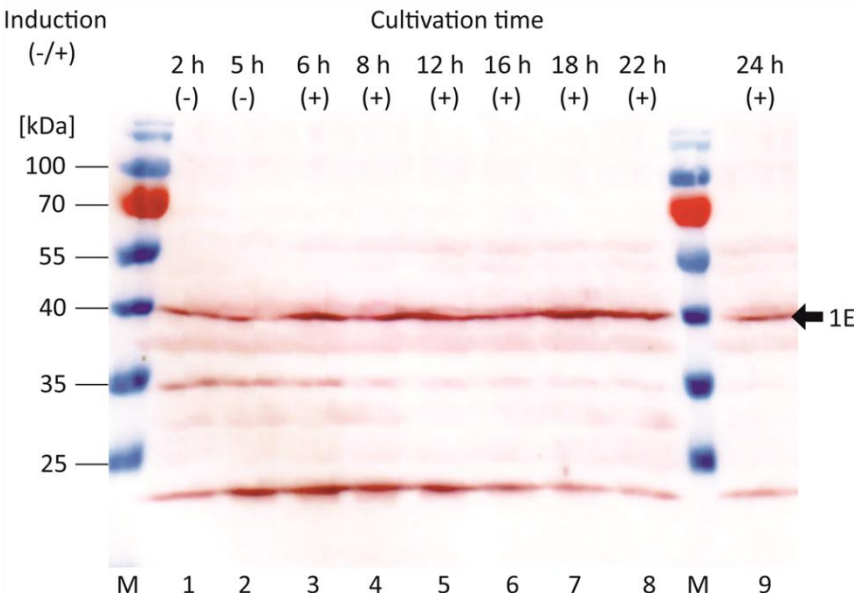

Figure A-7: Production of Act-StrepII (1E) in *E. coli* DH5α_1E in LB plus 50% BWH/50% glucose feed in 10 L bioreactor scale.

Recombinant *E. coli* DH5α were cultivated in 10 L LB medium containing 2% (w/v) glucose. Pulsed feeding of a mixture consisting of 50% BWH and 50% pure glucose was applied when glucose concentration was below 10 g L^{-1}. Control variables were set to 37 °C, pH 7.0, 0.4 bar, 5 L air min^{-1}, 400 rpm (pO_2 > 25%). Induction was performed at OD_{600} ~6.0 with 0.1 mM IPTG. 1/OD samples were taken at intervals and lysed. Extracts (TOTAL PROTEIN) were separated by SDS-PAGE and Act-StrepII (1E) was visualized by WB with anti-StrepII® and anti-Mouse IgG-conjugated alkaline phosphatase antibodies (dye: BCIP/NBT) (see Table 4-12 for antibodies).

Arrows indicate the detected proteins. Theoretical molecular protein masses were calculated using ProtParam: MW of Act-StrepII (1E) = 41.6 kDa.

Act… acetyl-CoA acetyltransferase

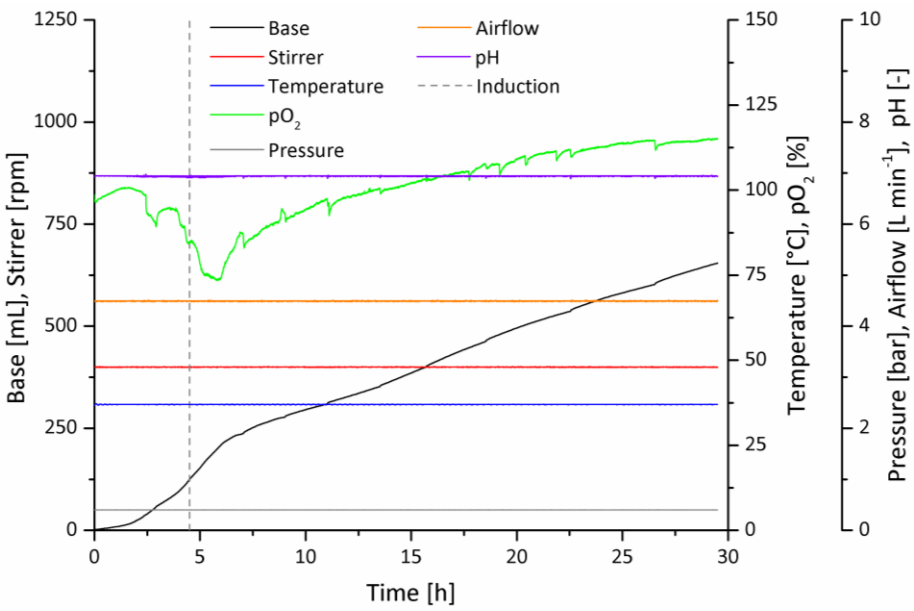

Figure A-8: Time course of control variables and base addition for *E. coli* DH5α_1E in LB plus 100% BWH feed in 10 L bioreactor scale.

Recombinant *E. coli* DH5α were cultivated in 10 L LB medium containing 2% (w/v) glucose. Pulsed feeding of 100% BWH was applied when glucose concentration was below 10 g L^{-1}. Control variables were set to 37 °C, pH 7.0, 0.4 bar, 5 L air min^{-1}, 400 rpm (pO_2 > 25%). Induction was performed at OD_{600} ~6.0 with 0.1 mM IPTG.

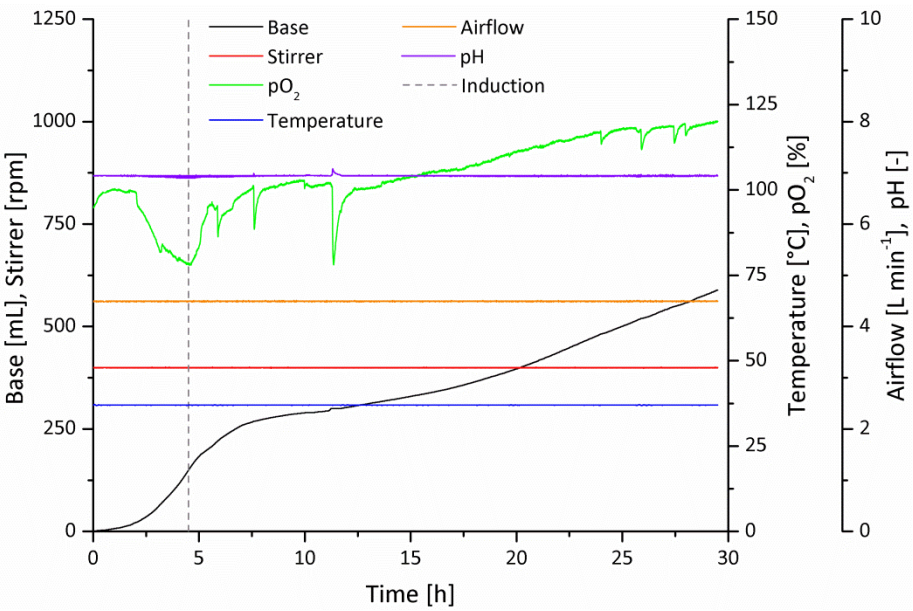

Figure A-9: Time course of control variables and base addition for *E. coli* DH5αΔpta_1E in LB plus glucose feed in 10 L bioreactor scale.

Recombinant *E. coli* DH5αΔpta were cultivated in 10 L LB medium containing 2% (w/v) glucose. Pulsed feeding of a 50% (w/v) glucose solution was applied when glucose concentration was below 10 g L^{-1}. Control variables were set to 37 °C, pH 7.0, 0.4 bar, 5 L air min^{-1}, 400 rpm (pO_2 > 25%). Induction was performed at OD_{600} ~6.0 with 0.1 mM IPTG.

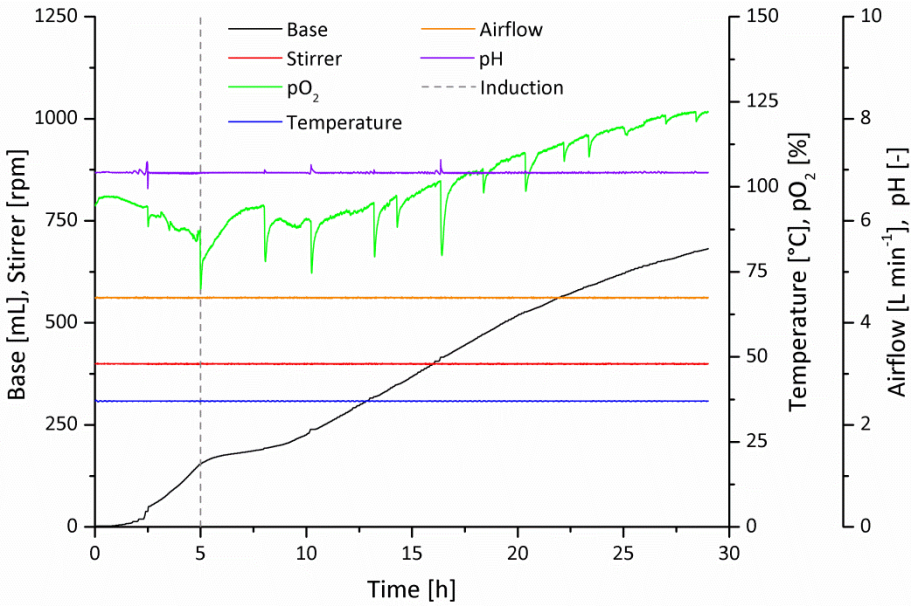

Figure A-10: Time course of control variables and base addition for *E. coli* DH5αΔpta_1C in LB plus glucose feed in 10 L bioreactor scale.

Recombinant *E. coli* DH5αΔpta were cultivated in 10 L LB medium containing 2% (w/v) glucose. Pulsed feeding of a 50% (w/v) glucose solution was applied when glucose concentration was below 10 g L^{-1}. Control variables were set to 37 °C, pH 7.0, 0.4 bar, 5 L air min^{-1}, 400 rpm (pO_2 > 25%). Induction was performed at OD_{600} ~6.0 with 0.1 mM IPTG.

Curriculum Vitae

Personal information

Name:	Ramona Engelhardt, née Konrad
Date of birth:	15th January 1982
Place of birth:	Bünde
Citizenship:	German
Marital status:	Married
Familial status:	One child
Email address:	Ramona.engelhardt@outlook.de

Academic and educational background

Jun 2016 - Dec 2019	Research associate at Martin Luther University (MLU) Halle-Wittenberg, Department of Downstream Processing (DoDP), headed by Prof. Dr. M. Pietzsch, EFRE-Project "*DESIGNER-Proteine – Entwicklung formaldehydfreier Bindemittel auf Proteinbasis"* (DESIGNER proteins – Development of protein-based, formaldehyde-free binders)
Apr 2013 - Oct 2015	Doctoral research associate at MLU Halle-Wittenberg, DoDP, headed by Prof. Dr. M. Pietzsch, BMBF Project "*Energieeffiziente Synthese von Olefinen aus den korrespondierenden Alkoholen*" (Energy-efficient synthesis of olefins from their corresponding alcohols), Leading-Edge Cluster "BioEconomy"
Oct 2009 - May 2012	Master of Science in Pharmaceutical Biotechnology at MLU Halle-Wittenberg, Final grade: 1.6 Master thesis "Function of the human membrane transporter-like protein CTL2" in the Department of Cell Culture, headed by PD Dr. M. Brandsch (Grade: 1.3)
Oct 2006 - Sep 2009	Bachelor of Science in Molecular Biotechnology at the University of Bielefeld, Final grade: 2.0 Bachelor thesis "Cloning of a heme tag into the plasmid pcDNA3.1 and expression studies in COS cells" in the Department of Cellular Genetics, headed by Prof. Dr. H. Ragg (Grade: 1.6)
Oct 2002 - Jun 2005	*Abitur* at *Westfalen-Kolleg* Bielefeld Final grade: 1.1
Aug 1998 - Jun 2001	Apprenticeship at *Stadtbibliothek* (municipal library) Bünde as "*Fachangestellte für Medien- und Informationsdienste, Fachrichtung Bibliothek*" (library assistant)
Oct 1992 - Jun 1998	Secondary education at *Gymnasium am Markt*, Bünde
Oct 1988 - Jun 1992	Primary education at *Grundschule* Bünde-Mitte

Research experience

Nov 2016 - Feb 2019	Scientific research consultant at MLU Halle-Wittenberg, DoDP, headed by Prof. Dr. M. Pietzsch, EFRE Project "*Optimierung von photosynthetischen Organismen mittels Metabolic Engineering*" (Optimization of photosynthetic organisms by Metabolic Engineering), Expertise: Molecular Biology, Genetic Engineering (CRISPR-Cas9)
Nov 2016 - Jan 2018	Scientific research consultant at MLU Halle-Wittenberg, DoDP, headed by Prof. Dr. M. Pietzsch, EFRE Project "*Entwicklung einer dermalen Trägerplattform zur Applikation von Tropoelastin*" (Development of a dermal carrier platform for application of tropoelastin), Expertise: Molecular Biology, Large-scale cultivation
Jun 2015 - Aug 2015	Pilot scale cultivations at Fraunhofer Center for Chemical-Biotechnological Processes (CBP; Leuna, Germany)
Nov 2015 - May 2016 & Oct 2012 - Mar 2013	Scientific research assistant at Martin Luther University Halle-Wittenberg, DoDP, headed by Prof. Dr. M. Pietzsch

Teaching experience

Supervision of practical courses "Basic lab course" and "Upstream Processing" (Master study course Pharmaceutical Biotechnology) and "*Arzneiformlehre II*" (Dosage forms II) (study course Pharmacy).
Supervision of master theses and project works.
Organization of orientation for incoming international students (Master study course Pharmaceutical Biotechnology).
Lectures on "Thesis/report writing" and "MS Excel" (Master study course Pharmaceutical Biotechnology).

Conference posters

Ramona Konrad, Martina Anwand, Tino Elter, Daniela Pufky-Heinrich, Markus Pietzsch: "Identification of bottlenecks in the *E. coli*-based synthesis of isopropanol from beech wood hydrolysates". BIOTRANS 2015, Vienna, Austria, TU Wien (Institute of Applied Synthetic Chemistry), July 2015.

Presentations

"*Mikrobielle Produktion von Grundchemikalien aus zuckerbasierten Rohstoffen*" (Microbial production of bulk chemicals from sugar-based feedstocks). BioEconomy Cluster BUSINESSTREFF „SILVA Exkursion - Rohstoff Zucker", Zeitz, Südzucker AG, November 2016.

(Signature)